

*Context dependent roles for p120-catenin in breast
cancer progression*

Ronald Cornelis Johannes Schackmann

ISBN: 978-90-8891-600-7

Printed by: Proefschriftmaken.nl, Uitgeverij BOXPress, 's-Hertogenbosch

Cover: A two-headed monster -known as p120- blocking the road to a PhD. A young scientist, carrying only a MSc degree. The yellow-brick road is comprised of an epithelial sheet of cells, losing contact and migrating to the right 'malignant' side. The monster is composed of a double helix –based on the original Watson and Crick model- flowing into p120 which is stitched onto a good (tumor suppressor, left) and an evil (oncogenic, right) head. A modified version of E-cadherin represents the monster's tail (for what is a monster without a tail?). Designed and created by Ron Schackmann. Special thanks to Stefanie de Poot, Martin Schackmann and Miranda van Amersfoort for critical input.

*Context dependent roles for p120-catenin in breast
cancer progression*

*Context-afhankelijke rollen van p120-catenine tijdens
borstkanker progressie*

(met een samenvatting in het Nederlands)

Proefschrift

ter verkrijging van de graad van doctor aan de Universiteit Utrecht op
gezag van de rector magnificus, prof. dr. G.J. van der Zwaan, ingevolge
het besluit van het college voor promoties in het openbaar te verdedigen
op donderdag 18 april 2013 des ochtends te 10.30 uur

door

Ronald Cornelis Johannes Schackmann

geboren op 15 juli 1984
te Amsterdam

Promotor: Prof. dr. R.H. Medema

Co-promotor: Dr. P.W.B. Derksen

Financial support for the printing of this thesis is gratefully acknowledged and was provided by Biospace lab. Dit proefschrift is verder mede gefinancierd door Stichting Proefdier en Maatschappij, ChipSoft BV, Biolegio en Roche.

Content

Chapter 1	General Introduction	7
Chapter 2	p120-catenin in Cancer; Models, Mechanisms, and Opportunities for Intervention	27
Chapter 3	Loss of p120-catenin Induces Metastatic Mammary Carcinoma through Induction of Anoikis Resistance and Sensitization of Growth Factor Receptor Signaling	37
Chapter 4	Cytosolic p120-catenin regulates growth of human and mouse metastatic lobular carcinoma through Rock1-mediated anoikis resistance	63
Chapter 5	Rock inhibition as a therapeutic alternative in the management of invasive lobular carcinoma	85
Chapter 6	Summary and Discussion	101
Addendum	References	110
	Nederlandse samenvatting	125
	Curriculum Vitae	127
	Publications	128
	Dankwoord	129



Chapter 1

General Introduction

Introduction

1. Breast cancer

With over 1.3 million new cases annually, breast cancer is the leading type of cancer among women of both the economically developing and developed countries. In addition, with roughly 450,000 deaths annually, breast cancer is the leading cause of cancer related death among women¹. Hereditary breast cancer -which accounts for roughly 5-10% of all breast cancers- is characterized by a germline mutation in one allele of a high penetrance susceptibility gene (such as BRCA1, BRCA2, STK11 TP53 or PTEN). Inactivation of the second allele of the tumor suppressor gene results in the early cancer predisposition². As opposed to hereditary disease, sporadic breast cancer tends to occur at a later stage in life, is strongly influenced by environmental factors and is caused by somatic rather than germline mutations. The arising mutations are mostly dominant activating or inactivating mutations, affecting genes such as TP53 and PTEN. However, the expression of these genes may also be altered as a result of non-mutational changes, for instance promoter hypermethylation.

Breast cancer presents with several stages of tumor development, ranging from the non-invasive atypical hyperplasia and carcinoma in situ to invasive carcinoma. However, whether all breast tumors go through the different stages in progression of the disease remains debated³⁻⁶. Epidemiological studies have shown that atypical hyperplasia and carcinoma in situ correlate with an increased chance of developing invasive carcinoma³. However, patients diagnosed with atypical hyperplasia in one breast, have equal risk of developing invasive breast cancer in either breast, suggesting that these lesions indicate a general increased risk rather than a direct precursor lesion of more aggressive disease⁷. Overall, this implies that atypical hyperplasia and carcinoma in situ are at least markers of an increased risk of developing invasive breast cancer⁷. The different stages of tumor development are further sub classified as being of either ductal or lobular subtype.

Invasive ductal and lobular breast carcinomas (IDC and ILC respectively) are the most common malignancies of the breast, accounting for roughly 80% and 10% of all invasive breast tumors respectively. The two tumor subtypes are distinguished based on their histology. IDC tends to form glandular structures resulting in palpable masses and calcification, whereas ILC presents with non-cohesive cells that invade the surrounding tissue in single-file, forming a highly diffuse growth pattern. As a result, lobular tumor types are difficult to detect by means of palpation and mammography⁸. Furthermore, ILC is more likely to present bilateral and with multifocality -possibly explained by the diffuse growth of ILC. The lack of cell-cell cohesion and increased invasive growth in ILCs is caused by the characteristic early loss of the metastasis suppressor E-cadherin -a key player in cell-cell adhesion^{9,10}. Although this suggests that ILC is more metastatic than IDC, the overall occurrence of metastatic disease is similar, resulting in comparable survival rates for both breast cancer subtypes¹¹⁻¹⁴. Treatment regimens are generally based on a number of criteria, namely tumor size, lymph node status, patient age, histological grade, proliferative index and expression of hormone (estrogen and progesteron) and growth factor receptors (such as EGFR and HER2/neu)¹⁵. The majority of ILCs (~80%) are estrogen receptor (ER) positive and therefore suitable for hormone therapy. Use of the ER antagonist tamoxifen or blocking intrinsic ER production via aromatase inhibitors have proven highly beneficial in reducing tumor recurrence, with a disease-free survival rate of 50%, roughly 7 years after primary treatment^{13,16}.

These criteria only provide limited information concerning the biology behind the different breast cancers. In recent years, genomic studies have established five breast cancer subtypes, Luminal A, Luminal B, HER2-enriched, Basal-like and normal breast-like^{17,18}. As methods for gene expression analysis improve, new breast cancer subtypes are likely to be determined, as recently shown for Claudin-low tumors^{19,20}.

The importance of these studies is demonstrated by Deisenroth et al²¹ who uncovered that luminal A-type ER+ tumors are often refractory to chemotherapy. By better defining the different breast cancer subtypes and investigating the misregulated signaling pathways, over-treatment can be prevented and novel treatment targets will be uncovered.

The treatment of breast cancer relies on surgery, radiation therapy and several systemic drugs, consisting of cytotoxic, hormone-based and immunotherapeutic agents. All of these drugs can be given before surgical resection to shrink the primary tumor (neoadjuvant), or in an adjuvant setting when systemic recurrence is predicted after surgical resection, or once metastatic disease occurs^{22, 23}. After treatment, over 30% of patients will relapse with metastatic disease within 3 to 10 years¹³. There are several explanations for relapse after initial treatment. First of all, it may be due to tumor heterogeneity, in which a small percentage of tumor cells is non-susceptible to initial treatment. Secondly, tumor cells may remain dormant at the site of dissemination during treatment but reacquire proliferative potential once the systemic treatment is halted. Lastly, tumor cells may acquire resistance to the original treatment for instance through receptor conversion and/or genomic instability^{13, 24-26}. Unfortunately, metastatic disease is often widespread, localized at inoperable sites and resistance to the primary therapeutics.

2. p120 catenin and the adherens junction; form and function

Epithelial junctions

Epithelial cells line the cavities and surfaces of nearly every organ and function as a protective barrier, preventing harmful substances from entering the circulation and at the same time selectively absorbing substances in for instance the intestine. Epithelial cells facilitate the initial detection and signaling of sensations such as taste and touch to neuronal cells. Furthermore, epithelial cells form the glandular structures capable of producing and excreting substances such as mucus and milk. Epithelia are defined as being single or multilayered sheets of highly polarized cells with a clear apical and basal side. In order to attain this epithelial morphology, the cells need to attach to their surroundings. This is accomplished through several types of junctions, ranging from focal adhesions and hemidesmosomes, which facilitate cell-matrix attachment, to desmosomes (macula adherens), tight- (zonula occludens), gap- (nexus) and adherens-junctions (AJ) (zonula adherens), which are required for cell-cell adhesion. However, the presence and importance of the different adhesion complexes is highly organ specific. Desomosomal and tight junctions, for instance, are most abundant in tissues that require more resistance to mechanical stress like the skin, or provide a barrier function such as the intestines^{27, 28}. The AJs, on the other hand, are crucial for initial intercellular adhesion, after which additional interactions such as tight junctions can be formed²⁹. Despite initial believes, AJs are highly dynamic, even in fully polarized and quiescent tissues. This allows for rapid adaptation to changes induced by for instance tissue damage³⁰.

Cadherins

Classical cadherins (here referred to as “cadherins”) are at the center of the AJ. Cadherins, first described as proteins of which the extracellular domain could decrease cell-cell adhesion in early mouse embryos (at the morula stage) in 1980³¹ were originally designated as Uvomorulin. Further research uncovered that expression of these cell-cell adhesion molecules was not limited to the early embryonic cells, and that adhesion was calcium (Ca²⁺)-dependent, which led to the designation Cadherin^{32, 33}. The cadherin family comprises several classical cadherins, including VE-cadherin (mainly expressed in vascular endothelial cells), N-cadherin (expressed in neuronal tissue) and the most widely expressed E-cadherin (the main epithelial cadherin, originally designated Uvomorulin)³⁴. Their extracellular

domain facilitates Ca^{2+} dependent homophilic interactions with other cadherins on neighboring cells. The cadherin cytoplasmic tail, however, directly interacts with p120-catenin -an interaction which is crucial for AJ stabilization³⁵ and membranous E-cadherin localization (discussed in detail below)- and with β -catenin. α -catenin interacts indirectly with cadherins, by associating with β -catenin. Combined, these three catenins are called the “core”-cadherin-catenin complex (Figure 3A).

p120-catenin a historic perspective

p120-catenin (p120) was originally identified as a substrate of constitutive active membranous viral v-Src tyrosine kinase, establishing p120 as a target in oncogenic transformation³⁶. Several years later, the 100-120 kDa protein was also found to be tyrosine phosphorylated upon ligand-induced stimulation of several growth factor receptors such as EGF and PDGF. This identified p120 as a substrate of both receptor and non-receptor tyrosine kinases in mitogen and oncogene driven phosphorylation^{37, 38}. In 1992, studies facilitated by the newly isolated p120 cDNA³⁹ uncovered the presence of four copies of the armadillo (ARM) repeat domain, originally identified in the *Drosophila* segment polarity armadillo (ARM) protein⁴⁰. Although structurally related, the ARM domains often do not share sequence identity between or even within a protein^{41, 42}. Although the ARM repeats in p120 only share 22% homology to those in β -catenin, they did hint at a possible association between p120 and E-cadherin³⁹. In 1994, p120 was indeed shown to interact directly with E-cadherin through the ARM repeats, after which the protein was designated p120-CAS (Cadherin-Associated Src Substrate). However, to avoid confusion with the similarly named p130-CAS (Crk-Associated Substrate)⁴³, p120-CAS was renamed to p120-catenin. Initially, skeptics feared cross-reaction between the novel p120 antibody and the -of similar kDa size- α and β catenin. Eventually, mapping and mutation of the E-cadherin-p120 interaction site offered the indisputable proof that p120 indeed associated directly with E-cadherin⁴⁴⁻⁴⁶.

p120 family members

p120 is a member of a subfamily of ARM-containing proteins that consists of δ -catenin, p0071 and ARVCF, which are highly related to p120 on a structural level.^{47, 48} δ -catenin is mainly expressed in neurons, where it facilitates a direct link between the adherens junction and the postsynaptic compartment, with an essential role in normal synaptic plasticity (reviewed in⁴⁹). ARVCF and p0071, on the other hand, are expressed in many tissues and display some level of redundancy towards p120. When overexpressed in the absence of p120, both proteins were shown capable of stabilizing E-cadherin expression^{35, 42, 50}. However, the physiological relevance of this redundancy is unclear, making it difficult to predict their ability to compensate for p120 loss in AJ stabilization. Interestingly, plakophilins 1-3 -which are more distantly related to p120- play a role in desmosome formation that is highly similar to the function of p120 in AJ stabilization⁵¹.

p120 general structure

The human p120-catenin gene CTNND1, located at chromosome 11q11, consists of 21 exons. Alternative splicing occurs for exons 18 (exon A), the nuclear export signal (NES) containing exon 20 (exon B) and the rarely expressed exon 11 (exon C). Four separate start codons located at residues 1, 55, 102 and 324 result in expression of the isoforms 1 through 4. The longest possible isoform -1ABC- is comprised of 968 amino acids. Structurally, the p120 protein contains a N-terminal coiled coil domain, only present in isoform 1. This region is followed by a regulatory domain harboring most of p120s tyrosine and serine/threonine phosphorylation sites. This domain is largely retained in both isoform 2 and 3. The beginning of the central Armadillo repeat domain contains the transcription start site of isoform 4. This domain consists

of 10 subsequent imperfect ARM domains, and harbors the rarely expressed exon C, located within ARM domain 6⁴². Finally, the C-terminal tail domain contains a couple of serine/threonine phosphorylation sites alongside the alternatively spliced exons A and exon B (Figure 1). p120 contains two nuclear localization signals, one located in the regulatory domain and one located within the sixth ARM repeat, although nuclear localization can occur in the absence of both domains.⁵²

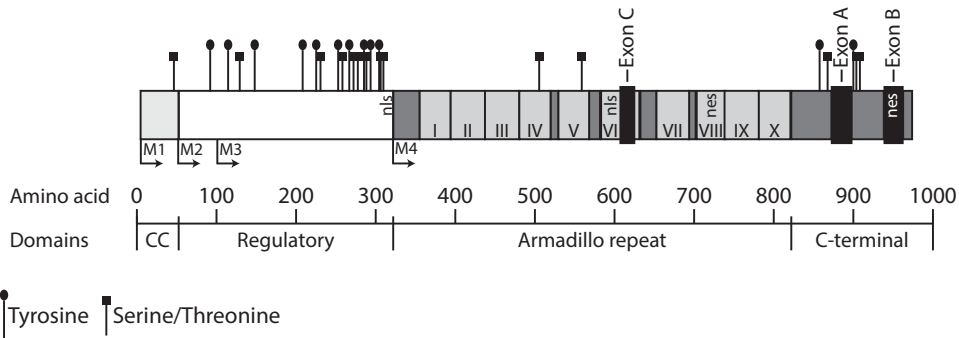


Figure 1
Schematic presentation of p120 structure. M1-4 designate locations of alternative start sites. Alternatively spliced exons A-C are indicated. Roman numbers indicate the 10 ARM repeats. The location of the validated identified Serine/Threonine and Tyrosine phosphorylation sites are depicted. nls: nuclear localization signal; nes: nuclear export signal; CC: coiled coil.

p120 isoform expression

Of the four main isoforms, 1 and 3 are the most commonly expressed, with often inclusion of exon A⁵³⁻⁵⁵. Expression of the isoforms is highly heterogeneous throughout different (mouse) tissues, with a preference of the long isoform 1 for more stable epithelial tissues such as the retina and lining of internal organs, whereas the shorter isoform 3 is preferentially expressed in epithelia with a more rapid turnover, such as the lining of the small intestine and bronchiolar epithelium⁵⁵. Furthermore, more motile mesenchymal-type cells such as fibroblasts and macrophages appear to preferentially express isoform 1^{42, 56}. Overall, isoform 1 is now referred to as the “mesenchymal”, and isoform 3 as the “epithelial” isoform, even though different p120 isoforms are often co-expressed in a balanced manner^{55, 57}.

p120 and the AJ

Formation of the AJ starts with the synthesis of E-cadherin, which immediately associates with β -catenin⁵⁸ resulting in transportation of E-cadherin to the cytoplasmic membrane⁵⁹. Here, p120 associates directly with E-cadherin, whereas α -catenin joins the complex through binding to β -catenin^{58, 60}. p120 is not required for proper translocation of E-cadherin, as E-cadherin mutants unable to bind p120 are still properly localized to the membrane^{45, 61} (Figure 2). However, association of p120 with cadherins does not always have to occur in close membranous proximity: in contrast to E-cadherin, N-cadherin already associates with p120 early during biosynthesis, whereas β -catenin association occurs later^{62, 63}. This clearly shows that different mechanisms are in play to control membranous localization of the AJ members.

Sole membrane localization of cadherins and catenins is insufficient to generate mature AJ, as this requires clustering of multiple cadherin-catenin complexes. So how does clustering occur? Cadherin molecules present on the plasma membrane do not spontaneously cluster for this so-called cis clustering is normally not energy-efficient.

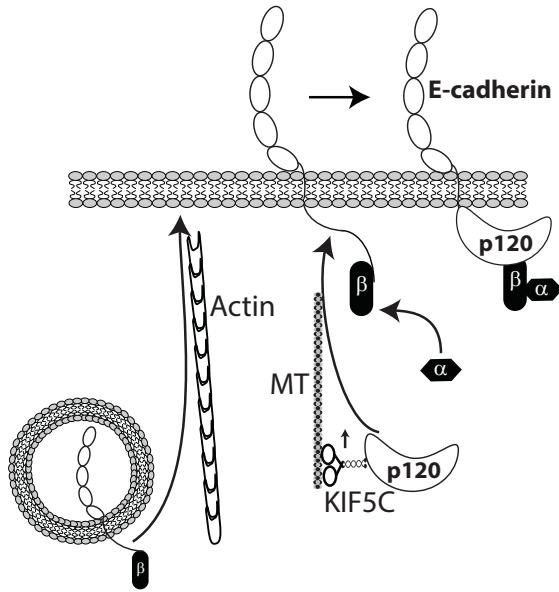


Figure 2

Model for membrane recruitment of the AJ complex members. Upon synthesis, E-cadherin is bound by β -catenin and targeted to the membrane via actin. Membrane targeting of p120 occurs through the plus-end-directed microtubule motor protein KIF5C. p120 and α -catenin associate with E-cadherin after membrane localization. MT: Microtubules; β : β -catenin; α : α -catenin; AJ: Adherens junction

(discussed below) ^{68, 69}. The recently solved p120 crystal structure -in complex with the E-cadherin juxtamembrane domain- has further unraveled which aminoacids are responsible in retaining the interaction between p120 and E-cadherin ⁶⁸.

In general, any of the four main p120 isoforms can stabilize the AJ as they all contain the ARM domain ⁷⁰. However, the efficiency of the different isoforms and the domains required for rescue are highly debated. For example, the colon carcinoma cell line SW48, showed most efficient AJ stabilization in the absence of the p120 N-terminal phosphorylation domain ⁶⁷. In sharp contrast, the human bronchial epithelial cell line (HBE) and human pulmonary giant cell carcinoma cell line H460 specifically showed dependency of AJ stability on the p120 N-terminal residues 1-54 to prevent migratory behavior and restore membranous E-cadherin. On the other hand, expression of isoform 3 resulted in increased migratory behavior, and did not rescue membranous E-cadherin expression ⁷¹. Although the presence of the ARM domain predicts that all p120 isoforms can interact with E-cadherin, their ability to stabilize membranous E-cadherin is apparently cell type specific and currently poorly understood. This is further complicated by the simultaneous expression of multiple p120 isoforms in many cell systems ^{55, 57}. Caution therefore has to be taken when combining results from different experimental systems to formulate an all-encompassing model.

Functional consequences of AJ maturation

As cells reach confluence in in vitro 2D cultures, they decrease or completely stop proliferating, similar to what is seen in vivo. Several events that remove cell-cell contacts, such as E-cadherin blocking antibodies or removal of extracellular Ca^{2+} relieve this inhibitory mechanism, resulting in re-activation of proliferation ⁷²⁻⁷⁴.

In contrast, Ca^{2+} dependent cell-cell trans interaction of cadherins is much more stable. This trans interaction decreases the flexibility of the cadherin molecule, allowing the low-affinity cis clustering to occur, required for the formation of mature AJs ⁶⁴⁻⁶⁶.

p120 instabilizing membranous cadherin expression

p120 plays a crucial role in regulating the stability of membranous cadherins. It was shown to directly associate with the juxtamembrane (membrane proximal) domain of E-cadherin ^{44, 46}. As mentioned previously, this interaction is facilitated through the p120 ARM domain, of which repeats 1-6 were shown to be crucial ^{67, 68}. This interaction results in masking of an endocytic motive and tyrosine residues Y755 and Y756 of E-cadherin, preventing E-cadherin degradation

Indeed the AJ is known to reduce the effect of EGF and other growth factors on cell proliferation⁷⁵. The mechanism behind this inhibition might involve mechanical restriction -where the AJs form a physical barrier, preventing the growth factor receptors from reaching their ligands due to their difference in apical and basolateral membrane localization respectively⁷⁶- or steric hindrance, where the AJs physically prevent either direct ligand binding or growth factor receptor dimerization⁷⁷. In processes such as wound healing, these mechanisms play an important role. Since tissue damage would abolish AJ integrity of cells at the edge of the wound, these cells would be sensitized to growth factors and proliferate, which is required for efficient wound healing.

AJ recycling and degradation

AJs are by no means static, and constant recycling occurs. A dileucine motive (LL 743-744) present in the juxtamembrane domain of E-cadherin was shown to be crucial for endocytosis. Mutation of this dileucine motive, which lies in the core p120 binding domain, not only prevents p120-binding, but also retains membranous E-cadherin in a similar manner as seen when clatherin-mediated endocytosis is chemically inhibited^{78, 79}. Endocytosis of E-cadherin can be affected by various proteins. For instance active Src -which is well known to cause junctional disruption- can activate the GTPase Rab5 to promote E-cadherin endocytosis by endosome fusion at the membrane⁸⁰. Furthermore, Src can also directly phosphorylate the tyrosine residues

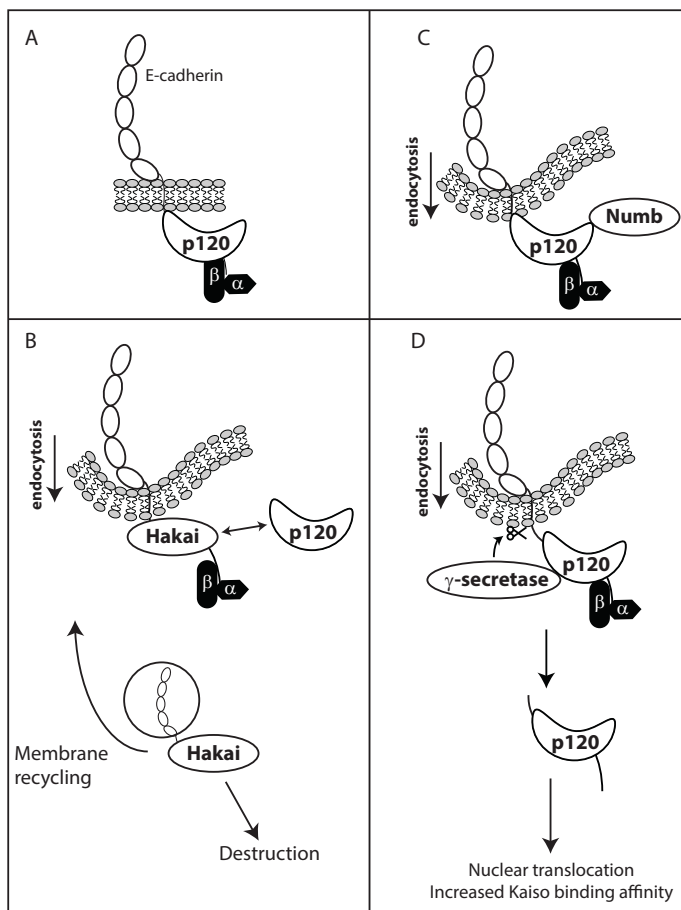


Figure 3
Mechanisms of AJ endocytosis. **A)** E-cadherin is retained at the membrane by p120. **B)** Hakai competes with p120 for association with E-cadherin. Upon binding, the AJ destabilizes and Hakai-mediated ubiquitination determines whether E-cadherin is targeted for lysosomal destruction or recycled to the membrane. **C)** External stimuli localize NUMB to the plasma membrane where it associates with p120 and facilitates endocytosis of E-cadherin still associated with p120. **D)** The γ -secretase complex associates with p120 and cleaves the C-terminal domain of E-cadherin. The p120-E-cadherin-tail complex can translocate to the nucleus and regulate Kaiso-mediated signaling. AJ: adherens junction; β : β -catenin; α : α -catenin

Y753 and Y754 (Y755/Y756 in ⁶⁸) of E-cadherin, which are normally masked by p120. This shifts the binding affinity of E-cadherin from p120 towards the E3 ubiquitin ligase Hakai ⁸⁰. Hakai then ubiquitinates E-cadherin, either at the membrane or soon after endocytosis, which determines whether E-cadherin is recycled to the membrane, or targeted for lysosomal destruction (Figure 3B) ⁸¹.

An alternative mechanism of AJ degradation is facilitated via the protein NUMB. NUMB is best known for its role in clathrin dependent endocytosis of for example Notch, growth factor receptors and certain integrins ^{82, 83}. NUMB can interact with the C-terminal region of p120, where it stimulates endocytosis of E-cadherin while still bound by p120. NUMB knockdown, or phosphorylation of NUMB through aPKC, preventing membrane targeting of NUMB, inhibit its endocytic ability ⁸⁴ (Figure 3C). However, NUMB can also associate directly with E-cadherin (at the same position where Hakai binds) when not bound by p120. Surprisingly, this interaction does not result in E-cadherin endocytosis, but rather inhibits apical translocation of E-cadherin, preventing AJ maturation. This was specifically shown in MDCK cells, where NUMB facilitates basal-lateral E-cadherin maintenance. Loss of NUMB results in apical E-cadherin accumulation and allows junction maturation ^{85, 86}. Although the exact mechanism of action remains unclear, in general NUMB appears to be a negative regulator of AJ formation (Figure 4).

E-cadherin stability is further regulated by presenilin ^{87, 88}, which is one of the four members of the transmembrane γ -secretase complex ⁸⁹. p120 recruits presenilin to the AJ, which can result in subsequent recruitment of the other γ -secretase members ^{90, 91}. The γ -secretase complex is capable of cleaving several transmembrane receptors including Notch and receptor tyrosine kinases ⁹², but has also been shown to cleave E-cadherin between residues 731 and 732, resulting in AJ disassembly ⁸⁸ (Figure 3D). The signaling required to assemble this complex and subsequently target its substrates is currently unknown. In general, γ -secretase mediated cleavage results in nuclear translocation of part of the cleaved receptor, often resulting in transcriptional regulation -as seen for Notch and ErbB4 signaling- ⁹². As discussed below, a similar event occurs upon γ -secretase mediated E-cadherin cleavage.

3. AJs and the cytoskeleton

Microtubules in AJ formation

Microtubules are cable-like structures present throughout the cell and function as a transportation highway, where kinesins are the motors that transport cargo specifically to either the microtubule plus or minus end ⁹³. Disruption of the microtubule network prevents AJs formation and stabilization ⁹⁴⁻⁹⁶. p120 directly associates with the plus-end directed microtubule motor KIF5C, facilitating membrane localization of p120 ⁹⁷ (Figure 2). In contrast to p120, the β -catenin-E-cadherin complex does not require microtubules to attain membrane localization ^{96, 98, 99}.

In addition to p120 localization, microtubules are crucial in clustering E-cadherin at sites of cell-cell contact. This is facilitated by lateral microtubules, which run from the basal to the apical cell membrane. It has been suggested that cadherin-catenin complexes along the membrane associate with PLEKHA7 through p120. This in turn recruits the motor protein KIFC3 which pulls the complex in apical direction until it encounters the microtubule end, where the cadherins cluster, and the AJ matures ¹⁰⁰ (Figure 4).

α -catenin; linking the AJ to the actin cytoskeleton

Although the exact means of interaction between the AJ and actin remains debated, an important role is played by α -catenin, which is bound to E-cadherin via β -catenin. Although α -catenin can directly interact with actin, this interaction is mutually exclusive with its ability to bind β -catenin ¹⁰¹⁻¹⁰³. Instead, α -catenin might facilitate actin binding through recruitment of other actin binding proteins such as EPLIN ¹⁰⁴,

α -actinin¹⁰⁵ or vinculin¹⁰⁶. Actual cross-talk between the AJ and actin was shown by inducing repeated extracellular torsion, via cadherin-coated beads, on cadherin molecules. This resulted in a conformational change of α -catenin facilitating recruitment of both EPLIN -an actin stabilizing protein- and vinculin - which links junctions to actin- to the AJ¹⁰⁷⁻¹⁰⁹ (Figure 5).

Even though this indicates how the AJ senses mechanical tension and signals to strengthen the actin cytoskeleton, the process of cell-cell adhesion is complicated by the plethora of cell-cell and cell-extracellular matrix adhesion complexes that often develop nearly simultaneous at the same location. Furthermore, intricate crosstalk between members of different types of adhesion complexes and non-discriminant protein functions Vinculin was for instance shown crucial for both focal adhesion and AJ interaction with actin- complicates the understanding of junction formation and maturation and leaves the question to what extent the different junction types require each other for formation.

AJs and the actin cytoskeleton

Regulation of actin dynamics is an important process in the formation and maturation of AJ. The RhoGTPases -Rho, Rac and Cdc42- are well known regulators of actin dynamics and -not surprisingly- play crucial roles in junction assembly¹¹⁰. During embryonic epithelial closure or wound healing, epithelial cells need to migrate into the open space in order to contact other epithelial cells and fuse the epithelial sheets to one another. This process can be mimicked in vitro by scratching an epithelial cell layer. This causes epithelial cells at the edge of the scratch wound to lack contact with other cells. In response, Rac1 driven protrusions are formed at the sides which lack contact and cells migrate into the wound¹¹¹. Once in contact with a neighbouring cell membrane, E-cadherin present in the protrusions leads to

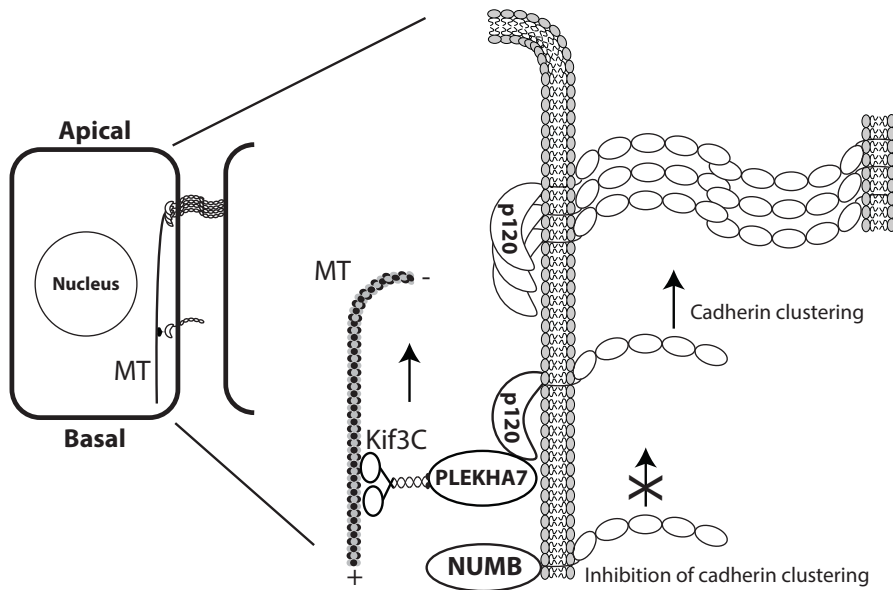


Figure 4

AJ clustering. AJ clustering. Overview of a polarized cell, depicting the basal and apical side and the formation of an AJ with a neighbouring cell (left side). E-cadherin molecules localized basally are targeted toward the apical side through association of p120 with PLEKHA7 and the motor protein Kif3c. The latter protein pulls E-cadherin along the lateral microtubules from the basal to the apical cell membrane to facilitate E-cadherin clustering and AJ formation (right side). Membranous E-cadherin can also be bound by NUMB, preventing cadherin clustering. MT: microtubule.

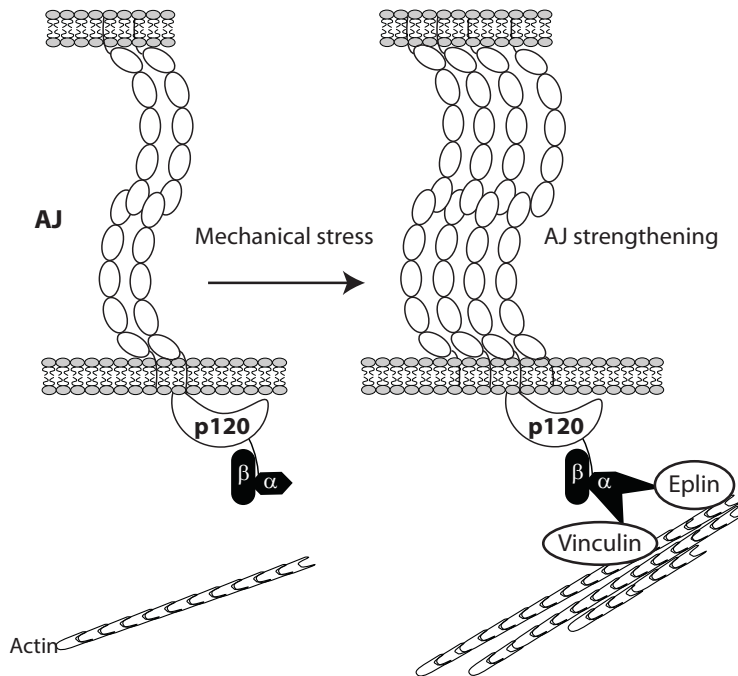


Figure 5
Induction of mechanical torsion strengthens the AJ and matures the actin cytoskeleton. Induction of torsion on E-cadherin induces a conformational change in α -catenin, resulting in the recruitment of several actin binding and modifying proteins, of which Vinculin and Eplln are depicted. As a result, cells become more resistant to mechanical forces.

trans homo-dimerization. This initial cell-cell cadherin contact causes further/local activation of Rac1, resulting in recruitment of several actin forming and stabilizing proteins, maturing the cytoskeleton^{112, 110, 113}. As the actin cytoskeleton matures, the initial AJs have a more stable basis to attach to. This stabilization causes a rapid diminishment of the active Rac1^{99, 114} and is followed by recruitment of the GTPase RhoA. The subsequent activation of its downstream effectors Rho Kinase (ROCK) 1 and 2 further stabilize the actin network by preventing activation of cofilin, an actin severing protein. Furthermore, Rock activates the actin-associated motor protein Myosin 2 through phosphorylation of its subunit myosin light chain (MLC)¹¹⁵. Although the mechanism remains unclear, active Myosin 2 somehow restricts E-cadherin membrane dynamics, which are required for E-cadherin clustering^{116, 117}. In addition, Myosin 2 facilitates contractile forces on the actin cytoskeleton and AJ, required for further junctional maturation and stabilization. Premature activation of RhoA -and the resulting contractile forces- will destabilize the maturing junctions^{34, 118} (Figure 6).

Over the past years, p120 has become known as an important regulator of the RhoGTPases, and thus crucial in mediating cellular actin dynamics. Not surprisingly, misregulation of p120 expression has severe effects on cell-cell contact and migration¹¹⁹.

p120, conflicting data on RhoA activity

Cytosolic p120

Originally, ectopically expressed p120 -which localizes in the cytosol- was shown to directly bind RhoA, in a manner that is mutually exclusive to E-cadherin binding, and which resulted in inhibition of RhoA activity as demonstrated by the formation of neuron-like branching in fibroblasts¹²⁰. It was postulated that cytosolic p120 functions as a RhoGDI, keeping RhoA in a GDP-bound inactive state. This binding ability requires the p120 N-terminal domain and probably the isoform 1 specific coiled-coil domain¹¹⁹. Furthermore, the presence of exon C in p120 disrupts the RhoA interaction^{56, 120}. Other studies have shown the branching phenotype

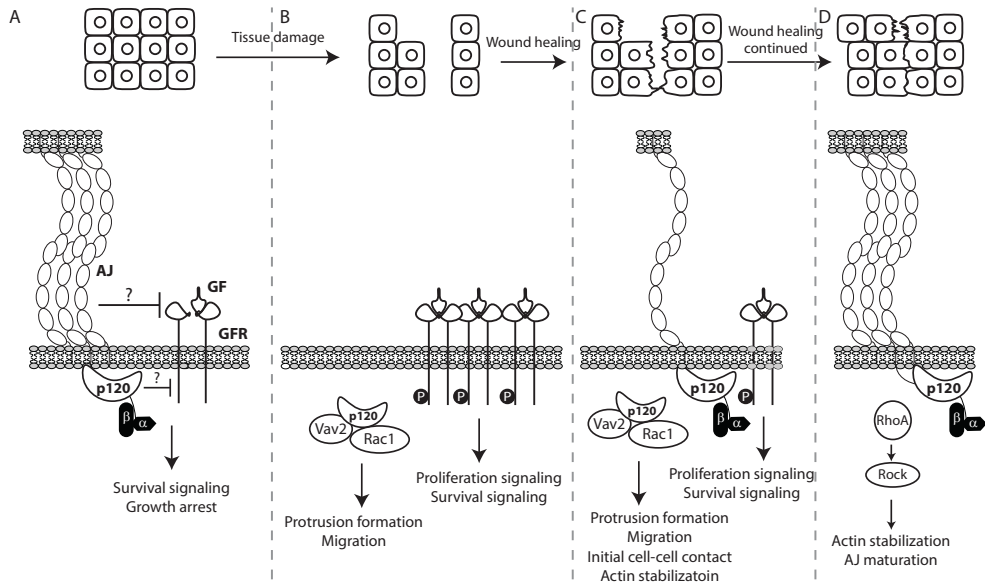


Figure 6

Repair of tissue damage. **A)** Under homeostasis, epithelial cells form a continuous sheet of cells (A upper figure). AJs are formed, and growth factor signalling is inhibited. Overall, growth is arrested (lower figure). **B)** Upon tissue damage, several epithelial cells lack proper cell-cell contact. At these sites, local Rac1 activation -for instance through cytosolic p120- stimulates protrusion formation. As AJs are lost, GFR signalling is no longer repressed. This results in stimulation of proliferation and survival. **C)** Cells start to migrate into the wound in order to restore the epithelial integrity. Upon initial cell-cell contact, Rac1 is further activated to stabilize actin and induce the initial E-cadherin interactions. **D)** Continued maturation of the junctions requires inactivation of Rac1 and activation of RhoA, which further induces actin stabilization and AJ maturation, resulting in restoration of the epithelial homeostasis. AJ: adherens junction; GFR: growth factor receptor; β: β-catenin; α: α-catenin; P: phosphorylation.

-indicative for RhoA inhibition- for all p120 isoforms, except isoform 4 and for splice variants expressing exon B, which harbors a nuclear export signal. Regardless of the mechanism behind RhoA inhibition, it has been suggested that cytosolic p120 -for instance due to loss of E-cadherin expression or a decreased affinity for E-cadherin- would as such induce migrational properties.

Conflict remains concerning the role of p120 in regulating RhoA activity. As shown in growth factor-stimulated epithelial keratinocytes, expression of p120 isoform 1 results in activation of RhoA and subsequent stimulation of migration¹²¹. This is rather surprising, as p120 isoform 1 was shown to inhibit RhoA activity, which is apparently surpassed when growth factors are stimulated. In further contrast, upon loss of E-cadherin and the subsequent cytosolic relocation of endogenous p120 (in mouse mammary epithelial tumor cells), no reduction in RhoA activity is observed, although overexpression of p120 in this system did induce the same branching phenotype^{57, 122}. However, no branching or RhoA inhibition occurred in endothelial cells overexpressing p120¹²³.

Membranous p120

Membranous p120 -which is bound to E-cadherin- was shown to recruit p190RhoGAP resulting in inhibition of RhoA. Furthermore, p120 was shown interact with PAK5 -a known inhibitor of RhoA activity- and could thus be important for balanced and localized RhoA activity¹²⁴. Another study showed that the binding of p120 to RhoA depends on Fyn and Src. Fyn phosphorylates the p120 regulatory domain at Y112, which inhibits interaction with RhoA, leaving RhoA GDP-bound and cytosolic. In

contrast, Src phosphorylation of p120 on Y217 and Y228 induces RhoA binding and rapid GTP loading¹²⁵. The mechanism behind this rapid RhoA activation is unknown, but could be caused by the presence of the G-protein Gα12. Gα12 can recruit several RhoGEFs capable of activating RhoA and was also shown to directly interact with p120. Gα12 associates both with E-cadherin-bound and cytosolic p120 and can override the inhibitory function of p120 on RhoA¹²⁶.

Loss of p120

Studies in invasive lung cancer cells showed that p120 silencing resulted in inactivation of RhoA (and increased Rac1 activity), promoting invasiveness^{127, 128}. However, loss of p120 does not necessarily affect the levels of GTP-bound RhoA (this thesis). Furthermore, even within a single cell type, the effect of p120 on RhoA activity is unclear, where overexpression of full-length p120 in mouse keratinocytes results in active RhoA¹²¹ and knockdown of p120 in mouse keratinocytes also results in active RhoA¹²⁹.

In conclusion, regulation of RhoA by p120 remains an incompletely understood

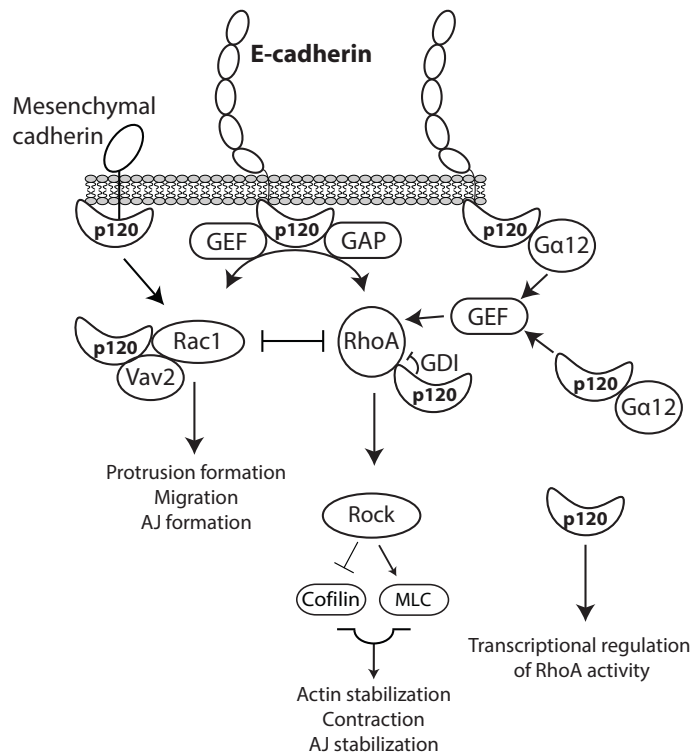


Figure 7

p120-mediated regulation of RhoA and Rac1 activity. Through binding to mesenchymal cadherins, p120 can facilitate activation of Rac1, and subsequent inactivation of RhoA. Bound to E-cadherin, p120 associates with multiple GEFs and GAPs which influence Rac1 and RhoA activity. Furthermore, p120 -both membrane bound and cytosolic- can directly associate with Gα12, which initiates multiple GEFs and facilitates activation of RhoA. Cytosolic p120 can bind both Rac1 and the GEF Vav2, inducing activation of Rac1, resulting in protrusion formation, migration and initial AJ formation. Cytosolic p120 also associates directly with RhoA in a GDI-like manner. Activation of RhoA and subsequent signaling through Rock induces actin stabilization -through inhibition of Cofilin- cell contraction -through activation of MLC- and AJ stabilization. p120 can also translocate to the nucleus and regulate RhoA activity by currently unknown transcriptional means. Overall, Rac1 and RhoA signaling are tightly balanced, and depending on the state the cell is in (for instance, migrating or inducing initial cell-cell contact) the balance can be shifted to either side.

mechanism which is likely cell type specific and sensitive to p120 (isoform) expression levels and localization. Clearly, p120 can regulate the activity of RhoA both positively and negatively although this is not obligatory (Figure 7).

p120 and Rac1 signaling

The RhoGTPase Rac1 is known to inhibit the activity of RhoA and vice versa¹³⁰. Given the effect of p120 on RhoA activity it is thus unsurprising that p120 also influences Rac1 activity. Whether or not Rac1 can directly interact with p120 is under debate. One study shows that Rac1 is unable to directly bind to p120. However the Rac1b splice isoform, often found upregulated in aggressive breast cancer¹³¹, was shown to directly interact with p120, and facilitated directed cell movement¹³². Furthermore, upon disruption of junctional stability, p120 was shown to associate with the GEF Vav2, which activates Rac1. This resulted in the localized formation of membrane protrusions and directed cell migration¹³³. Another study showed EGF-induced recruitment of Vav2 to the EGFR, also driving local Rac1 activation and protrusion formation¹³⁴. Because AJs are known to prevent ligand-induced EGFR signaling, this will only occur at sites where cell-cell contact is absent⁷⁵. Overall, all these observations fit with an important role for Rac1 activation at sites which lack proper cell-cell contact -such as at wound edges- in order to produce membrane protrusions and induce migration in an attempt to form AJs around the entire cell surface.

Alternatively, p120 can induce Rac1 activation by stabilizing mesenchymal cadherins such as Cadherin-11 and N-cadherin. p120 is crucial for stabilization of all cadherins, although the affinity of p120 is highest for the classical E-cadherin. Thus, upon loss of E-cadherin expression, p120 is free to stabilize the other cadherins. In contrast to E-cadherin, mesenchymal cadherins do not facilitate cell-cell junction formation.^{135, 136} Indeed, MDA-MB-231 cells, which lack E-cadherin, show increased stability of cadherin-11, and a similar effect is seen for N-cadherin in UMRC3 cells, which also lack E-cadherin¹³⁷. In both cell types, this leads to Rac1 activation and induces migration (Figure 7)

It is clear that the actin remodeling Rho family of GTPases is modulated by p120. Although many observations appear contradictory, they probably represent differences in cell-types studied or in the state the cell is in -be it in search of cell-cell contact, in the process of forming a novel AJ or at confluence where only AJ stabilization is required. Overall, Rac1 is required for initial cell-cell contact, and although the activity has to be decreased upon contact, membrane regions still lacking contact need to retain active Rac1. This is followed by activation of RhoA which is crucial for further junction maturation and stabilization¹³⁸ (Figure 7).

4. Nuclear p120

Nuclear localization of p120

As already mentioned, p120 contains two putative nuclear localization sequences. It remains unclear whether these sequences are required or whether the ARM domain suffices in facilitating nuclear targeting⁵². Several means by which p120 can attain nuclear localization have been uncovered. As discussed, the microtubule network is important in p120 membrane localization through interaction with kinesins. However, p120 can also directly bind to microtubules, an interaction which is mutually exclusive to its RhoGTPase and cadherin interaction^{97, 139}. Several serine residues (S538/S538/S587) located in the ARM domain of p120¹⁴⁰ are responsible for the p120-microtubule interaction. Disruption of the microtubule network using nocodazole results in a strong accumulation of nuclear p120. In contrast, stabilization of microtubules using taxol decreases nuclear p120.^{52, 97} Overall, this suggests that p120 is actively transported along microtubules by kinesins. The direct interaction with microtubules might be a safe-guard preventing cytosolic p120 from inadvertently going to the nucleus.

A possible intermediate in facilitating nuclear p120 localization is the Gli-similar protein Glis2. Glis2 can bind DNA, and acts as a transcriptional activator¹⁴¹. Upon binding the C-terminal domain of p120, Glis2 is cleaved which disrupts its DNA binding ability but leaves the nuclear localization capacity intact. Subsequently, Glis2 and p120 rapidly localize to the nucleus^{141, 142}. Interestingly, the interaction of p120 with Glis2 is prevented by binding of p120 to either cadherins or microtubules¹⁴² (Figure 8).

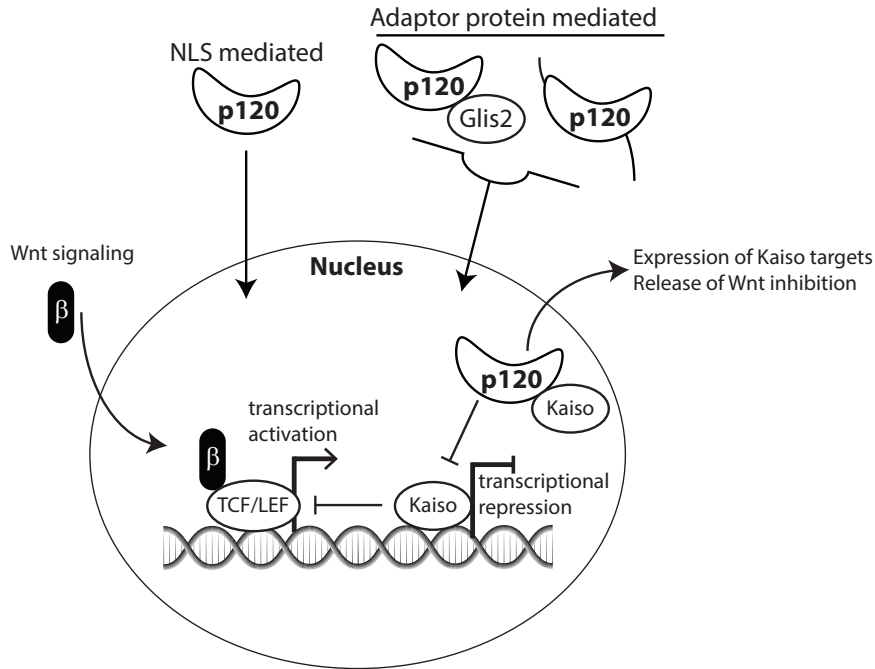


Figure 8

Transcriptional regulation through p120. Canonical Wnt signaling can induce stabilization and nuclear localization of β-catenin, where it associates with the TCF/LEF family of transcription regulators and drives transcription. Nuclear Kaiso represses expression of its target genes, and also sequesters TCF/LEF family members, preventing β-catenin-driven Canonical Wnt signaling. Nuclear localization of p120 can be attained through its NLS signaling sequences, or be mediated through additional adaptor proteins such as for instance Glis2 or the cytosolic domain of E-cadherin (as a result of E-cadherin cleavage by the γ-secretase complex, see Figure 3D). Nuclear p120 associates with Kaiso, relieving the transcriptional repression and resulting in expression of the Kaiso targets. Furthermore, p120 prevents Kaiso from inhibiting β-catenin-driven Wnt signaling. NLS: nuclear localization signal.

Finally, Dual specificity tyrosine-phosphorylation-regulated kinase 1A (Dyrk1A) -which is strongly associated with defects in neurological development (reviewed in¹⁴³)-, is capable of phosphorylating p120 isoform 1 at T47, facilitating nuclear localization.¹⁴⁴ Overall, these results suggest an important regulatory role for p120 in the nucleus.

Nuclear p120 modulates Kaiso functioning

Nuclear p120 can modulate gene expression through direct interaction with the transcriptional repressor Kaiso¹⁴⁵. Kaiso (ZTBT33) is a member of the POZ-ZF/BTB family of transcription factors that can bind to methylated DNA and/or a specific Kaiso binding sequence (TCCTGCNA)^{146, 147}. Several Kaiso target genes have been uncovered, such as MMP7, Siamois, CyclinD1 and the non-canonical Wnt11.

Expression of these genes are often found upregulated in cancer, suggesting that Kaiso-mediated transcriptional repression might have been lost^{148, 149}. Binding to Kaiso occurs through the p120 ARM domain and is thought to facilitate nuclear export of Kaiso and subsequent upregulation of the Kaiso target genes^{145, 150}.

As already briefly discussed above, γ -secretase is capable of cleaving the C-terminus of E-cadherin. This results in release of the cytoplasmic tail of E-cadherin, which retains its interaction with p120. The p120-bound E-cadherin fragment translocates to the nucleus where it relieves the Kaiso-mediated transcriptional repression. The presence of this E-cadherin fragment appears to enhance the ability of p120 to inhibit the Kaiso mediated repression¹⁵¹ (Figure 8).

Crosstalk between canonical Wnt signaling and p120

Canonical Wnt signaling is activated through binding of Wnt ligands to their respective receptors. The activated signaling cascade results in the expression of genes involved in cell proliferation and survival. Wnt signaling is crucial during normal development and wound healing, as is seen by the increased excretion of Wnt ligands in developing organs¹⁵² and in damaged (epithelial) tissue¹⁵³. Furthermore, misregulation of canonical Wnt signaling is often observed in several types of cancer (reviewed in^{154, 155}). Wnt signaling is facilitated by nuclear translocation of β -catenin, which can bind to the TCF/LEF family of transcription factors to promote gene expression. However, canonical Wnt signaling is inhibited by the presence of nuclear Kaiso, which sequesters the TCF/LEF family members (such as TCF3 and TCF4)^{156, 157}. Although β -catenin normally binds to E-cadherin at the plasma membrane, and cytosolic β -catenin is rapidly degraded by the tumor suppressor Adenomatous polyposis coli (APC), canonical Wnt signaling -for instance through mitogenic Wnt3a stimulation- facilitates disruption of the AJ and stabilization of β -catenin allowing nuclear localization^{156, 158, 159}. Wnt3a stimulation also increases the affinity of p120 towards Kaiso binding, stimulating nuclear export of Kaiso and relief of Kaiso-mediated transcriptional repression^{156, 158} (Figure 8).

Further regulation of canonical Wnt signaling by p120 is facilitated by delta-interacting protein A (DIPA, CCDC85B). p120 isoform 1 was found to interact with DIPA at the plasma membrane, although the majority of DIPA protein is localized in the nucleus¹⁶⁰. Nuclear DIPA competes with β -catenin for TCF4 binding, resulting in transcriptional repression of the canonical Wnt target genes¹⁶¹. Although the function of p120-bound DIPA is currently unknown, this interaction could encompass activation and nuclear targeting of DIPA, preventing unwanted Wnt signaling.

As described here, AJ stability facilitates several mechanisms which help to inhibit inappropriate canonical Wnt signaling. However, upon junctional disruption -for instance as a result of tissue wounding- Wnts are produced to stimulate wound healing^{162, 163}. Overall, it seems that p120 is an important regulator and mediator of both β -catenin driven canonical Wnt signaling and non-canonical Wnt signaling through Kaiso modulation. Although originally thought to be unrelated, there are clear indications of intricate cross-talk between these two pathways.

5. p120 expression and alternative splicing

Regulation of p120 expression

Due to the diverse functions and different splice variants of p120, transcriptional expression is likely to be tightly controlled. To date, several transcription factors that regulate p120 expression have been uncovered. The transcriptional repressor FOXC2, through direct binding to the p120 promoter, downregulates p120 in non-small cell lung cancer (NSCLC)¹⁶⁴. In breast, FOXC2 expression was found in metastatic murine cell lines and metastatic basal-like subtype of breast cancer¹⁶⁵. Unfortunately, this has never been studied in the context of p120 expression, but may mean that FOXC2 downregulates p120 in breast cancer. Furthermore,

the transcriptional repressor SP1, found in NSCLC cells, can also directly bind the promoter region of p120 and repress expression^{166, 167}. Finally, regulation of p120 protein expression is also determined by microRNA expression. microRNAs facilitate translational repression by binding to mRNAs and inhibiting translation. Since targeting occurs through imperfect complementation of the microRNA to the mRNA, requiring as little as 7 nucleotides, a single microRNA can target multiple mRNA sequences¹⁶⁸. Recently microRNA-197 was shown to downregulate p120 and disrupt junctional stability in pancreatic cancer cells¹⁶⁹. All the observed effects likely facilitate the induction of migrational properties caused by loss of AJ stability.

Alternative splicing of p120

Epithelial cells can transform toward mesenchymal cells in a process called epithelial to mesenchymal transition (EMT). EMT induction in MDCK cells through expression of the E-cadherin transcriptional repressors Snail, E47 or Slug, leads to a dramatic shift from mainly expressing p120 isoform 3 to an almost exclusive expression of isoform 1^{170, 171}. This shift is likely caused by the Epithelial Splicing Regulatory Protein (ESRP) 1 and 2, which are differentially expressed in epithelial as compared to mesenchymal cells. Knockdown of ESRP1/2 is known to result in a dramatic shift towards the “mesenchymal” p120 isoform 1 in epithelial PNT2 cells. Alternatively, overexpression of ESRP1 in the E-cadherin negative MDA-MB-231 cells shifted p120 isoform expression towards the epithelial isoform 3, strongly reducing isoform 1 expression¹⁷². Further comparison of these two model systems also show a strong shift in isoform expression of FGFR2, CD44 and ENAH^{172, 173}. Clearly, ESRP proteins are common targets of several EMT inducers. EMT driven by Snail, ZEB1 or TGF- β resulted in reduced ESRP1 expression.¹⁷⁴⁻¹⁷⁶

6. p120 phosphorylation, an unresolved matter

There is constant crosstalk between a multitude of different receptors and signaling molecules which facilitate for instance growth factor signaling, actin remodeling and AJ stability. In order to deal with constant changes in the environment, cells need to respond rapidly to internal and external mechanical forces and chemical signaling. Here, phosphorylation of tyrosine, serine and threonine residues plays a major role, as it can facilitate rapid changes in protein activity and protein binding affinity¹⁷⁷.

p120 phosphorylation

Large-scale proteomic projects have unveiled 68 phosphorylated sites in at least two separate screens, most of which have yet to be confirmed. (<http://www.phosphosite.org>). Thus far, 24 phosphorylation sites have been validated in p120 by means of site-directed mutagenesis or phosphor-specific antibodies (<http://www.phosphosite.org>), as depicted in Figure 1. The observed effects of p120 phosphorylation can thus far roughly be grouped into two categories: 1) affecting the ability of p120 to interact with RhoA, or 2) inducing nuclear translocation of p120 often as a result of decreased affinity for E-cadherin and increased Kaiso binding potential. In the first category, p120 phosphorylation at Y112 prevents association of membranous p120 with RhoA, whereas phosphorylation of S268 and S269 induce RhoA binding¹²⁵. In the second category, phosphorylation of T47, S268, S269 and S289 have been shown to decrease E-cadherin stability and to result in nuclear exclusion of Kaiso^{57, 124, 144, 156, 158, 178, 179}. Interestingly, phosphorylation of S288 by PAK5, a known inhibitor of RhoA, results in effects from both categories: it correlates with inhibition of RhoA^{57, 124} as well as nuclear translocation of p120 and subsequent removal of nuclear Kaiso^{178, 179}. As already suggested above, the regulation of RhoA activity might be through direct interaction with (phosphorylated) p120, or as a result of transcriptional events.

Association of p120 with Src family kinases

The members of the Src family of kinases are the main players in p120 tyrosine

phosphorylation. The best studied members of this family, Src¹⁸⁰, Yes¹⁸¹, Fyn¹⁸¹ and Fer¹⁸² can all interact with p120.

Conflicting results have been obtained on the effects of Src tyrosine kinase mediated phosphorylation of p120. On the one hand, this was shown to increase binding affinity towards E-cadherin^{183,184}, while other studies show decreased binding affinity¹⁸⁵⁻¹⁸⁷, or no effect on AJ stability at all¹⁸⁸. These discrepancies might be caused by differences in cell system, p120 isoform expression, means of Src activation and the state -being assembled, or already fully assembled- of AJ maturity. The latter is illustrated by Src being required at sites of newly formed junctions to regulate RhoGTPase activity and maturation of junctions^{189,190}, whereas Src activation can result in phosphorylation of β -catenin which results in disruption of mature junctions^{181,191}.

Similarly, Fer kinase directly associates with and phosphorylates p120¹⁸². This also results in phosphorylation of β catenin, causing disassembly of the AJ¹⁸¹. However, these signaling events are tightly balanced by the presence of several p120-binding phosphatases as discussed below.¹⁹²

Like Fer, Fyn kinase can directly associate with p120, induce β -catenin phosphorylation and junction disassembly. It is currently unknown whether Fyn can directly phosphorylate p120¹⁸¹. Finally, the kinase Yes, when activated by for instance Kras, can also directly associate with p120. Although the effects on junctional stability are unknown, Yes facilitates activation of Fyn and Fer, which in turn regulate AJ dynamics¹⁸¹.

Besides the Src family kinases, EGFR activation is likely to directly induce phosphorylation of p120, as stimulation results in Y228 phosphorylation in Src/Yes/Fyn negative mouse fibroblasts¹⁹³. As Fer has not been implicated in Y228 phosphorylation, the EGF receptor and other receptor tyrosine kinases are likely candidates to directly induce phosphorylation of p120.

p120 and dephosphatases

To date, three phosphatases have been identified to directly associate with p120, namely Dep-1 (ptprj, CD-148), SHP-1 (ptpn6) and RPTP μ (ptprm).

The amount of phosphorylated p120 tyrosine residues correlates with an increased affinity of p120 for the tyrosin phosphatase SHP-1.^{194,195} SHP-1 interaction decreases p120 phosphorylation but might also function to localize SHP-1 to AJs where it can de-phosphorylate closely associated proteins (such as AJ complex members and growth factor receptors). SHP-1 is by no means specific for phosphorylated p120, but instead recognizes sites specifically phosphorylated by Src¹⁹⁶. Not surprisingly, p120 isoform 4 binds least efficiently to SHP-1, as it lacks the phosphorylation domain. The presence of exon C also reduces SHP-1 association, probably because exon C decreases phosphorylation of p120 induced by EGF¹⁹⁷.

The transmembrane Density Enhanced Phosphatase-1 (Dep-1) is capable of binding p120 both in the presence and absence of a functional AJ. This interaction appears to be transient, and requires p120 to be phosphorylated. Dep-1 can also interact with several growth factor receptors^{198,199}, suggesting that p120 might function as a docking platform to facilitate localized dephosphorylation of growth factor receptors in the presence of stable AJs and facilitate the contact-induced inhibition of growth signaling.

The receptor protein-tyrosine phosphatase RPTP μ interacts specifically with membranous p120, where it de-phosphorylates tyrosine residues on p120 and β -catenin¹⁹⁹. Although the exact effects are unknown, this de-phosphorylation was shown to decrease cytosolic p120 localization in adipocytes²⁰⁰. In contrast to SHP-1 and Dep-1, RPTP μ already binds p120 in the absence of phosphorylation. This suggests that p120 may primarily be required for RPTP μ localization.

Due to close proximity of the AJ members and other membrane bound receptors, it cannot be excluded that additional kinases and phosphatases influence p120 by

binding to closely associated proteins ¹⁷⁷

In conclusion, the diverse functions that p120 fulfills are likely regulated by its phosphorylation status. Therefore, it would be interesting to uncover the pattern of phosphorylated sites on p120 under specific conditions -such as upon mitogenic stimulation of confluent versus sparsely plated cells, or at stages of initial junction formation. Once the specific phosphorylation patterns are uncovered, further investigation of the kinases, phosphatases and other p120-associated proteins will result in a better understanding of p120 phosphorylation and its role in various biological processes.

7. p120 binding partners; the orphans

Several additional p120 binding partners have been identified, although the biological relevance of the interactions often remains unknown. One of these proteins is the FERM-domain containing protein 5 (FRMD5). FRMD5 binds the C-terminal region of AJ associated p120. Knockdown of FRMD5 resulted in downregulation of E-cadherin expression and accelerated H1299 tumor outgrowth in vivo ²⁰¹.

Another interesting, but understudied p120-specific binding partner is hNanos1. hNanos1 expression is decreased in the presence of E-cadherin. Furthermore, overexpression of hNanos1 in DLD1 colorectal cells induces junctional disruption and cytoplasmic localization of p120 causing migration and invasion ²⁰². Overall hNanos1 appears to function as an EMT inducer, as also suggested by the inversely correlates of hNanos1 expression to E-cadherin expression.

Also, p120 can interact directly with the RhoA associated kinase Rock1. Loss of Rock1 appears to weaken but not completely disrupt junctions of A431 cells. Ca²⁺ switch experiments show co-localization of Rock1 with p120 during the reassembly of AJs, confirming its presence, at least in the initial junction formation. As already discussed, localized RhoA activity is required to generate stable AJs. Being a RhoA effector, the membrane association of Rock1 is most likely required to mediate the highly localized actin dynamics responsible for AJ assembly ^{203, 204}.

Finally, p120 has been linked to hemidesmosomes, by binding to the transmembrane protein BP180 (Type XVII Collagen). Hemidesmosomes are responsible for linking keratinocytes to the basement membrane, facilitating strong cell-extracellular matrix (ECM) binding ²⁰⁵. BP180 is a transmembrane protein that harbors a collagenous extracellular domain which interacts with laminins ²⁰⁵. Although the interaction appears specific for p120, and interestingly links p120 to a type of cell adhesion completely separate from cell-cell interactions, no additional experiments have thus far been performed to validate this interaction, or to uncover its functional consequences ^{206, 207}.

Outline of this thesis

We set out to determine which functions p120 plays in the development and progression of breast cancer. p120 has diverse roles in cell-cell adhesion, actin dynamics and transcriptional regulation. In chapter 2, the role of p120 in tumor progression is described, with specific focus on the p120 conditional mouse models currently available. Chapter 3 shows the implications of p120 loss in breast cancer development and uncovers p120 as a suppressor of metastasis driven by sensitized growth factor receptor signaling. Next, we describe the strong context dependent role p120 plays in breast cancer development upon E-cadherin loss. Here, cytosolic p120 is uncovered to be the driving force behind invasive lobular carcinoma by facilitating active Rho-Rock signaling. Chapter 5 describes the first steps in validating Rock as a promising druggable target in treating invasive lobular carcinoma. Finally, the findings and implications described in this thesis are discussed in chapter 6.



Chapter 2

p120-catenin in Cancer; Models, Mechanisms, and Opportunities for Intervention

Ron C.J. Schackmann, Milou Tenhagen, Robert A. H. van
de Ven and Patrick W.B. Derksen

To be submitted

Abstract

Functional inactivation of the adherens junction (AJ) is an established hallmark of cancer development and progression. p120-catenin (p120) has emerged as a key player in the regulation of tumor progression, because it regulates E-cadherin turnover and epithelial integrity, controls activity of RhoGTPases, and mediates gene transcription through interaction with Kaiso. Indeed, evidence is mounting that loss or aberrant localization of p120 may control the development and progression of several cancer types. Here we discuss past and present findings that implicate p120 in the regulation of cancer and highlight opportunities for clinical intervention.

p120 form and function

p120 (*CTNND1*) is a member of a subfamily of armadillo (ARM) repeat-containing proteins that consists of δ -catenin, p0071 and ARVCF⁴⁷. While δ -catenin is the only member that is mainly expressed in neurons⁴⁹, ARVCF and p0071 are expressed in many tissues sharing some of the signaling functions of p120⁵⁰. *CTNND1* contains multiple alternative start sites, resulting in four isoforms⁵³ of which the most well studied isoforms are the “mesenchymal” isoform 1 and “epithelial” isoform 3. Despite their nomenclature, isoform expression is not restricted to a specific cell type and may be expressed simultaneously⁵⁵. Isoforms may further differ through usage of three alternatively spliced exons, suggesting diverse and non-overlapping functions⁵⁶. Finally, the presence of multiple phosphorylation sites at the regulatory- (N-terminal) and C-terminal domain indicates that control of p120’s biological function is multi-layered and complex¹⁹².

p120 is best known for its ability to bind to and stabilize classical cadherins at the cell membrane (Fig. 1A)^{208, 209}. Removal of p120 by genetic means in cell lines results in rapid disassembly of the cadherin complex and subsequent proteasomal and lysosomal degradation³⁵. Although the exact details of the regulatory posttranslational events remain unclear, an attractive mechanism is the dissociation of p120 from E-cadherin through Src-mediated phosphorylation. In this scenario, tyrosine phosphorylation of p120 leads to binding of the Cbl-like protein Hakai to E-cadherin and subsequent ubiquitination and proteasomal degradation^{80, 210}. Another candidate for the regulation of E-cadherin turnover is Presenilin, a protein that can also bind and target the complex for proteolytic degradation⁸⁷. Although the mechanism awaits clarification, a common characteristic of Hakai and Presenilin seems that both proteins compete with p120 for binding to E-cadherin. In order to attain membranous localization, p120 binds kinesin heavy chains by means of its N-terminal regulatory region, or by directly binding to microtubules via the ARM repeat domain^{97, 139}. Once localized, direct interaction of the ARM repeats with the juxtamembrane domain of cadherins stabilizes the complex and results in the formation and maturation of intercellular adherens junctions⁴⁵.

A prominent mechanism for AJ integrity is the regulation of RhoGTPases by membrane-localized p120. At the junction, p120 can recruit p190RhoGAP, which will drive local Rac-dependent antagonism of Rho and subsequent AJ formation²¹¹. Alternatively, RhoA can be inactivated by Fyn-dependent phosphorylation of p120 on tyrosine residue 112 (Y112)¹²⁵. Upon cytosolic overexpression, p120 can act as a direct inhibitor of RhoA by functioning as a Rho Guanosine nucleotide Dissociation Inhibitor (GDI), or, indirectly through the RhoGEF Vav2^{42, 138}. Conversely, Src-mediated phosphorylation of p120 (Y217 and Y228) has been shown to result in activation of RhoA¹²⁵. Irrespective of the exact mechanism, it is clear that p120 is at the center of Rho GTPase control and the regulation of AJ dynamics.

In addition to its membrane-related and cytosolic functions, the presence of NLS and NES sequences render p120 capable of shuttling in and out of the nucleus^{52, 150}. Cytosolic/nuclear p120 can modulate gene expression through direct interaction with Kaiso¹⁴⁵. Kaiso (ZBT33) was identified as a transcriptional repressor and member of the POZ-ZF/BTB family of transcription factors that can bind to methylated DNA and/or a specific Kaiso binding sequence (*TCCTGCNA*)^{146, 147}. Binding of p120 to the zinc finger-containing region of Kaiso inhibits its DNA binding and relieves repression of transcriptional targets, which have been linked to Wnt-dependent developmental processes^{147, 148, 212}.

p120 has been strongly linked to tissue homeostasis. Due to the fact that germline *Ctnnd1* deletion results in embryonic lethality in mice, conditional mice have been generated that allow tissue-specific and inducible ablation. Conditional p120 loss

in the mammary and salivary glands using MMTV-Cre resulted in a block in acinar development and intraepithelial hyperplasia²¹³. Likewise, p120 knock-out in the skin resulted in epidermal hyperplasia that was accompanied by chronic inflammation without overt abnormalities in junctional integrity and epithelial barrier formation¹²⁹. Interestingly, while the epithelial lining of the gastro intestinal tract does not appear permissive for the induction of hyperplasia upon p120 loss, massive intestinal barrier defects and chronic inflammation were observed upon homozygous knockout of p120 using Villin-Cre driver mice²¹⁴. Given the overt barrier defects, studies were undertaken in the Reynolds lab using tamoxifen-inducible Villin promoters to drive stochastic Cre expression in the colon. Lowering the penetrance of p120 deletion resulted in hyperplasia and adenoma-type lesions²¹⁵. Although the phenotypic differential consequences are clearly influenced by the various Cre systems used, these results emphasize the markedly different effects of p120 loss, depending on the target organ and dosage of inactivation. In conclusion, a vast body of literature shows that p120 is the master regulator of E-cadherin stability and as such retains a gatekeeper role in the maintenance of epithelial homeostasis.

p120 as tumor suppressor

Loss of E-cadherin expression is an established hallmark of cancer progression²¹⁶. Because p120 controls turnover of classical cadherins, its loss has received increasing attention in the context of tumor development. In mice, ablation of p120 in keratinocytes resulted in inflammation, mitotic alterations and skin cancer through hyperactivation of RhoA and NF κ B²¹⁷. Concordantly, human squamous cell carcinomas (SCC) often show aberrant localization or absence of p120, accompanied by activity of inflammatory pathways^{217, 218}. Because mice devoid of p120 showed intact epidermal barrier formation, and SCC are often characterized by loss of p120 while retaining low-level membranous E-cadherin expression, it is likely that p120 family members may act functionally redundant in the skin.

Loss or downregulation of p120 is also a frequent event in SCC of the upper gastro intestinal (GI) tract and in colorectal adenocarcinomas^{219, 220}. In the epidermoid carcinoma cell line A431, RNAi-mediated knock-down of p120 led to a tyrosine phosphorylation-independent increase of collective migration and invasion in vitro²²¹. p120 knockdown was accompanied by a marked downregulation of P-cadherin and E-cadherin, corroborating the notion that AJ function and stability are governed by p120. Recently, Rustgi and co-workers showed that conditional p120 ablation in the upper GI tract using a L2-Cre driver resulted in tumor formation that was accompanied by NF κ B activation and dependent on the induction of inflammation²¹⁹. Even though the underlying transcriptional mechanisms remained elusive, the model clearly showed upregulation of proinflammatory cytokines such as GM-CSF, MCP-1 and CSL1 upon p120 deletion²¹⁹. Surprisingly, none of the aforementioned studies reported metastatic dissemination, which suggests that in these models redundancy or alternative modes of cell-cell interaction may prevent invasion and metastasis.

A recent intriguing finding from the Reynolds lab links loss of p120 to colon cancer. Using the aforementioned tamoxifen-inducible Villin-Cre system it was reported that while stochastic deletion of p120 was tolerated, all large adenomas that developed expressed p120 and showed upregulation of β -catenin, suggesting that limited p120 ablation may perhaps promote tumorigenesis by an indirect and non-cell autonomous mechanism²¹⁵. In such a scenario, loss of p120 induces production of cytokines and an influx of immune cells that drive chronic inflammation and subsequent cancer development. In contrast to skin and the upper GI tract, loss of p120 in the colon did not lead to activation of the NF κ B pathway, which again denotes tissue-specific differential responses upon p120 loss.

p120 expression and localization can be used to establish the differential diagnosis of

breast cancer. Whereas loss of E-cadherin and subsequent cytoplasmic localization of p120 are typical for Invasive Lobular Carcinoma (ILC), Invasive Ductal Carcinoma (IDC) usually retains membrane-localized E-cadherin and p120²²². However, several studies indicated that approximately 10% of all IDC cases show complete or partial loss of p120^{223, 224}. The fact that (i) p120 loss in IDC is not a common feature, (ii) inactivating mutations have not been reported, but (iii) loss of p120 correlated with disease progression^{224, 225}, implies that inactivation of the AJ through loss of p120 represents a late (epigenetic) event in invasive breast cancer. As it is still unclear what the consequences of p120 loss are during breast cancer progression, we induced conditional p120 loss in a non-invasive breast tumor model, based on WAP-Cre-mediated conditional inactivation of p53 (our unpublished data,²²⁶). Somatic inactivation of p120 resulted in the formation of metaplastic IDC that metastasized to lymph nodes and lungs, a functional consequence not observed in the aforementioned conditional mouse models in skin and the GI tract. However, comparable with results observed in the GI tract, we observed an influx of tumor-associated macrophages due to the production of proinflammatory cytokines in p120 null tumor cells (schackmann et al manuscript in preparation). A mechanistic basis for the acquisition of metastatic capacity in breast cancer may lie in the finding that inhibition of p120 expression in MCF7 resulted in anchorage independence through E-cadherin downregulation and subsequent activation of Rac and Ras²²⁷. In addition, our unpublished results indicate that Ras may be activated through the relief of growth factor receptor inhibition by E-cadherin (schackmann et al manuscript in preparation). Regardless the exact mechanism, it is clear that p120 controls the transition from a noninvasive to a metastatic breast cancer cell. An explanation for the tissue-specific differences may also reside in the fact that the two mammary epithelial cell types (*i.e.* luminal and myoepithelial cells) could display a differential dependency on p120 function, which may influence cellular (adhesive) responses in the absence of p120. Alternatively, because p120 family members do not appear to functionally compensate in the mammary gland²²⁸, and luminal mammary epithelia fails to express a redundant classical cadherin upon loss of E-cadherin^{226, 229}, p120 null cells can progress to invasive and metastatic cells.

In short, evidence is mounting that p120 acts a tumor suppressor (Fig. 1B); either in a classical setting or upon concomitant inactivation of an additional tumor suppressor. While the underlying transcriptional mechanism remains largely unknown and is most likely organ specific, a common denominator in the p120 knock-out models is the production of cytokines. This paracrine cue results in the influx of inflammatory cells and the formation of a microenvironment that is strongly linked to tumor development and progression²³⁰.

Oncogenic functions of p120

Mutational inactivation of E-cadherin has been causally linked to tumor development and progression^{9, 231-233}. Upon E-cadherin loss, and in contrast to β -catenin, p120 is not proteasomically degraded but resides in the cytosol and nucleus^{122, 171}. In E-cadherin negative breast and colon cancer cells, cytosolic p120 coincided with inhibition of RhoA and controlled tumor cell migration^{234, 235}. The link from p120 to Rho GTPase signaling was further demonstrated in E-cadherin positive MDCK cells. Here, RNAi-mediated p120 inhibition resulted in a Rac1 or Src-dependent acquisition of anchorage-independence, thereby unexpectedly positioning Rac upstream of p120²³⁶. In the E-cadherin negative breast cancer cell line MDA-MB-231, cytosolic p120 controlled migration and anchorage-independence through activation of the Rac-MAPkinase pathway^{137, 227}. Here, survival signals were provided by p120 through interaction and stabilization of Cadherin-11, which resulted in the activation of Rac, Ras and possibly PI3K²²⁷. Surprisingly, upon a cadherin switch from E-cadherin

to P-cadherin, ovarian and pancreatic cancer cells showed expression of cytosolic p120 that regulated a Rac-dependent activation of cell migration^{237, 238}. Using a mouse model based on mammary-specific conditional inactivation of E-cadherin and p53 we recently demonstrated an oncogenic role for p120 in ILC. Here, p120 enabled indirect activation of the Rho-Rock axis through binding and inhibition of the Rho antagonist myosin phosphatase Rho interacting protein (MRIP), thus promoting anchorage-independent tumor growth and metastasis¹²². These divergent findings exemplify that biochemical signals downstream of cytosolic p120 may be differentially regulated depending on cancer type and cellular context (Fig. 1C). They furthermore implicate that –while p120 exerts RhoGDI activity– its inhibition of Rho may depend on tissue type and the mode of E-cadherin inactivation. Furthermore, our unpublished observations extended our previous findings in ILC by showing that p120 also contributes to ILC etiology, since combined conditional inactivation of p120 in the mouse ILC model inhibited ILC development (Tenhagen *et al.* manuscript in preparation).

Do specific p120 isoforms influence cancer cell behavior? Several studies indicated that

expression of the ‘mesenchymal’ p120 isoform 1 significantly correlated to metastatic disease in lung, kidney and breast tumors^{224, 232, 239}. Experiments in cell lines indicated that whereas the short isoforms 3 and 4 did not control migration, isoform 1 facilitated inhibition of Rho and activation of Rac¹¹⁹. Moreover, recent data showed that upon integrin linkage, overexpression of the transcriptional repressor Zeppo1 controls downregulation of E-cadherin and a concomitant increase in p120 isoform 1 expression. This subsequently caused activation of Rac and inhibition of Rho, leading to increased migration of mammary epithelial cells and enhanced tumor growth and metastasis in a transplantation-based mouse model of breast cancer⁵⁴. Because several cancer types express more than one isotype simultaneously, it remains to be established how the p120 isoforms contribute to cancer growth and dissemination.

p120 can also bind and de-repress transcriptional repression of Kaiso. Expression studies indicated that localization of Kaiso is enigmatic and highly dependent on tumor type and physical context²⁴⁰. Notwithstanding the unclear role of p120-dependent regulation of Kaiso in tumor development and progression, several bona fide Kaiso targets (*e.g.* Wnt11, MMP7, Siamois, CyclinD1) have been strongly linked to cancer. Interestingly, Kaiso knockout mice are viable, fertile and neither showed an overt phenotype nor developed tumors²⁴¹. Moreover, ablation of Kaiso did not influence expression of the established target genes. Remarkably, when crossed onto tumor-prone *Apc*^{Min/+} mice, Kaiso loss delays tumor onset, which is surprising given the fact that Kaiso target genes are implicated in protumorigenic processes²⁴¹. A possible explanation for these unexpected results may be that Kaiso acts as a regulator of Wnt signaling in a synergistic manner either through interaction with TCF/LEFs or through coincidence of Kaiso targets with Wnt targets¹⁵⁷. Developmental studies by the McCrea lab suggested overlapping but functionally diverse roles for the regulation of Wnt targets by Kaiso and TCF/LEF²⁴², which may underlie the unanticipated results obtained in the *Apc*^{Min/+} mice. In human cancer, others and we have shown that nuclear Kaiso correlated with metastatic prostate cancer and high grade IDC, suggesting that nuclear Kaiso may exert oncogenic properties^{243, 244}. In contrast, cytosolic Kaiso expression is strongly linked to E-cadherin mutant breast cancer²⁴⁴, which would suggest a role for Kaiso target genes in ILC. Indeed, our unpublished results indicated that p120 controls ILC tumor growth through relief of Kaiso-dependent transcriptional repression of *Wnt11* (Van de Ven, Manuscript in preparation)

In summary, past and present data clearly implicate p120 in the regulation of cancer

development and progression (Fig. 1C). p120 is therefore unique because it can act as a tumor suppressor or oncogene. While the molecular events downstream of p120 may differ depending on context and tissue type, the phenotypic consequences are largely in conjunction with inactivation of the AJ. Mechanistically, p120 is a master regulator of RhoGTPases and –although the regulation remains unraveled– the de-repression of Kaiso targets and production of promalignant cytokines. Thus, p120 and its downstream effector pathways may hold promise as targets for the development of future therapeutic intervention strategies.

Future directions and clinical implications

Many aspects of p120 signaling remain unclear. How do specific isoforms, splice variants and the balance between them contribute to malignancy? To address these questions inducible and tightly controllable systems will have to be developed to comprehend the regulation of this delicate balance. Moreover, although phospho-specific antibodies have become available, little to none is currently known about the contribution of p120 phosphorylation to neoplastic transformation and progression. Another compromising problem is the fact that certain tissue types show functional redundancy while others do not, and the current lack of knowledge how this effects the activation of downstream effectors.

Over the past decade, p120 was linked to an increasing number of direct and indirect binding partners, ranging from regulators of cadherin stability to actin polymerization and microtubule dynamics. Although this further increases complexity of the problem faced, it may also provide an entry into the identification of additional drug targets to treat cancer.

Based on the models and mechanisms described here, evidence is mounting that p120 is a key player in tumor development and progression. Nonetheless, the contribution of p120 to malignancy seems variable, context dependent and tumor type specific. As a result and from a clinical point of view, design of an intervention strategy thus presents a problem. So far attention has been largely focused on aberrant activation of the Rho GTPases and their effector molecules. In ILC, we showed that pharmacological inhibition of Rock dramatically inhibited anchorage-independence, while IDC cells appear refractory to inhibition of Rock¹²². These findings illustrated that additional biomarkers will have to be employed to stratify whether and how a given tumor subtype may be permissive for inhibition of a specific oncogenic pathway. Also, recent data suggested that early mutational inactivation of E-cadherin in ILC resulted in differential activation of pathways downstream of cytosolic p120 as opposed to late epigenetic inactivation of E-cadherin in IDC¹²². Whereas pharmacological inhibitors of Rho and Rac have been widely used in an experimental setting, they still await entry into the clinical oncology arena. Here, the GTPase inhibitors may prove to be successful in the treatment of tumors fueled by signals downstream of and dependent on p120, provided treatment-eligible patients are correctly identified based on functional biomarkers. While inhibition of primary tumor growth and metastatic dissemination can be achieved using RNAi-mediated inhibition of p120, it still remains unclear if pharmacological inhibitors targeting downstream effectors will be equally successful. Given the recent advances made in the field of p120 cancer biology, the future holds promise for the development of clinical interventions to successfully treat p120-related cancer.

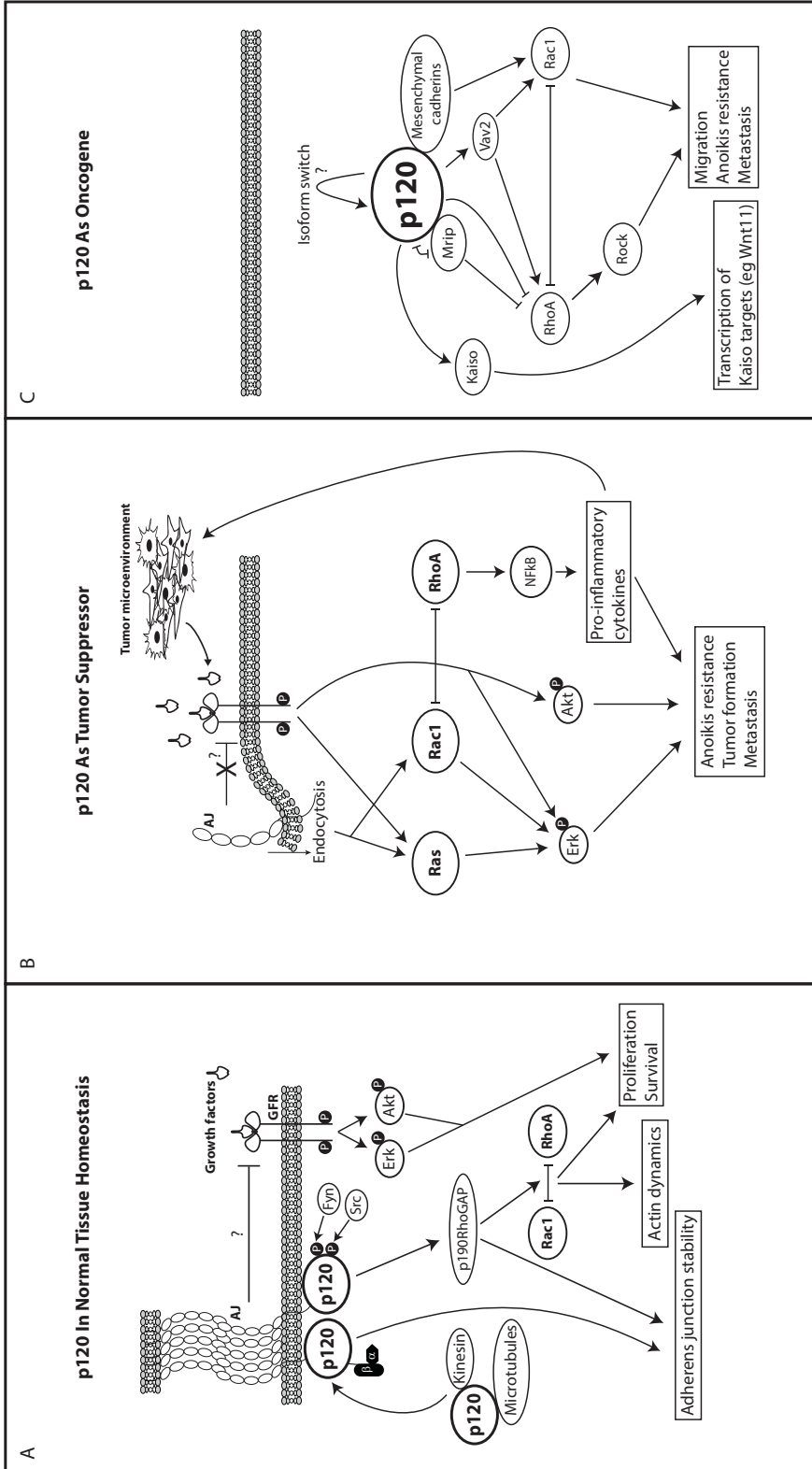


Figure 1

p120 at the core of cancer development and progression. p120 is the gatekeeper of epithelial homeostasis (**A**), which lies at the basis of its role as tumor suppressor (**B**) thereby triggering inflammation, anoikis resistance and tumor cell invasion. Upon functional inactivation of E-cadherin, p120 resides in the cytosol and nucleus (**C**) where it regulates cancer progression through regulation of the RhoGTPases, actin remodeling, and de-repression of Kaiso transcriptional repression. See text for further details. AJ, Adherens junction; GFR, Growth factor receptor.



Chapter 3

Loss of p120-catenin Induces Metastatic Mammary Carcinoma through Induction of Anoikis Resistance and Sensitization of Growth Factor Receptor Signaling

Ron C.J. Schackmann, Sjoerd Klarenbeek, Eva J. Vlug, Suzan Stelloo, Miranda van Amersfoort, Milou Tenhagen, Tanya M. Braumuller, Jeroen F. Vermeulen, Petra van der Groep, Ton Peeters, Elsken van der Wall, Paul J. van Diest, Jos Jonkers, Patrick W.B. Derksen

Under consideration; Cancer Research

Abstract

Metastatic breast cancer is the main cause of cancer-related death in women of the Western world. Besides antagonists targeting Her2 and the Estrogen receptor, there is currently no biochemical rationale for treatment of metastatic breast cancer. While loss of cell-cell adhesion is key to breast cancer progression, little is known about the underlying mechanisms that drive tumor invasion and metastasis. Here we show that somatic loss of p120-catenin (p120) in a mouse model of noninvasive mammary carcinoma results in formation of stromal-dense and metaplastic carcinomas that metastasized to lungs and lymph nodes. Loss of p120 in anchorage-dependent breast cancer cell lines strongly promotes anoikis resistance through hyper sensitization of growth factor receptor signaling. Interestingly, p120 deletion induces secretion of inflammatory cytokines, a feature that likely underlies the formation of the prometastatic microenvironment in p120 negative mammary carcinomas. Our model thus establishes a preclinical platform for the development of tailored intervention regimens that target growth factor receptor signals to treat p120-negative metastatic breast cancer.

Introduction

Adherens junctions (AJ) are required to maintain epithelial tissue integrity. They are established by homotypic interactions between E-cadherin molecules on neighboring cells, which in turn bind to cytosolic catenins that control linkage to and regulation of the microtubule and actin cytoskeleton²⁴⁵. Loss or temporal down regulation of E-cadherin is strongly linked to tumor development and progression in several cancer types²⁴⁶. In breast cancer, the timing of AJ inactivation has considerable impact on tumor etiology and cellular biochemistry. Whereas mutational inactivation of E-cadherin is an initiating and causal event in the development of invasive lobular carcinoma (ILC)^{9, 226, 232}, late epigenetic silencing may underlie the progression of invasive ductal carcinoma (IDC)²⁴⁷ in a process called epithelial to mesenchymal transition (EMT)²⁴⁸. Indeed, whereas translocation of p120-catenin (p120) upon E-cadherin inactivation controls Rock-dependent metastasis of ILC, IDC cells do not show dependency on this pathway^{122, 227}. Thus, p120 may play context-dependent roles in the development and progression of breast cancer.

Under physiological conditions, p120 binds to the intracellular juxtamembrane domain of E-cadherin²⁰⁸. Here, p120 controls E-cadherin stability and turnover in a process mediated by Hakai-dependent ubiquitination^{35, 45, 80}. We and others have shown that genetic ablation of E-cadherin or p120 in mouse mammary epithelial cells results in the induction of apoptosis, indicating that inactivation of AJ function is not tolerated in the mammary gland^{226, 228, 229, 249}. In contrast, genetic inactivation in other organ systems does not induce cell death, but instead induces impaired tissue homeostasis and hyperplasia^{129, 213, 250, 251}. Also, p120 inactivation in mice seems to result in inflammation, which may be caused by a loss of barrier function and the production of inflammatory chemo-attractants^{129, 213, 214}. Interestingly, recent data showed that p120 can function as a bona fide tumor suppressor in the upper gastro-intestinal tract. Here, somatic p120 inactivation induced the development of squamous cell carcinoma, which was accompanied by autocrine production of monocyte/macrophage attractants, thus promoting a proinvasive tumor microenvironment²¹⁹.

Several studies indicated that p120 may be lost or inactivated in approximately 10% of IDC breast cancer cases. Loss was defined as absence of expression in more than 10% of the tumor cells, and correlated to absence of progesterone receptor (PR) expression and poor prognosis^{223-225, 252, 253}. Here, we have analyzed p120 expression in a comprehensive set of invasive breast cancer samples and studied the consequences of somatic inactivation of p120 in mammary tumor development and progression in the context of p53 loss. Mammary-specific p120 loss in mice resulted in a switch from nonmetastatic to metastatic mammary carcinoma. Furthermore, inactivation of p120 resulted in anoikis resistance, which was exacerbated by a sensitization to growth factor receptor signaling due to inactivation of the AJ. Finally, we show that loss of p120 results in secretion of pro-inflammatory cytokines, which may promote formation of a prometastatic tumor microenvironment.

Results

Loss of p120 expression in invasive breast cancer

To extend previous findings on loss of p120 expression in breast cancer, we performed immunohistochemistry on a panel of 298 invasive ductal breast cancers and determined their clinicopathological variables (Table S1). Membranous p120 was scored (absent/low versus medium/high) in three independent tissue cores per tumor. Since we hypothesized that loss of p120 may be linked to increased tumor progression, we defined expression as absent/low if more than 10% of the tumor cells were negative for p120 (Figure S1), as has been used for E-cadherin²⁵⁴. Using these parameters, we observed that 34% of the IDC samples showed absent/low

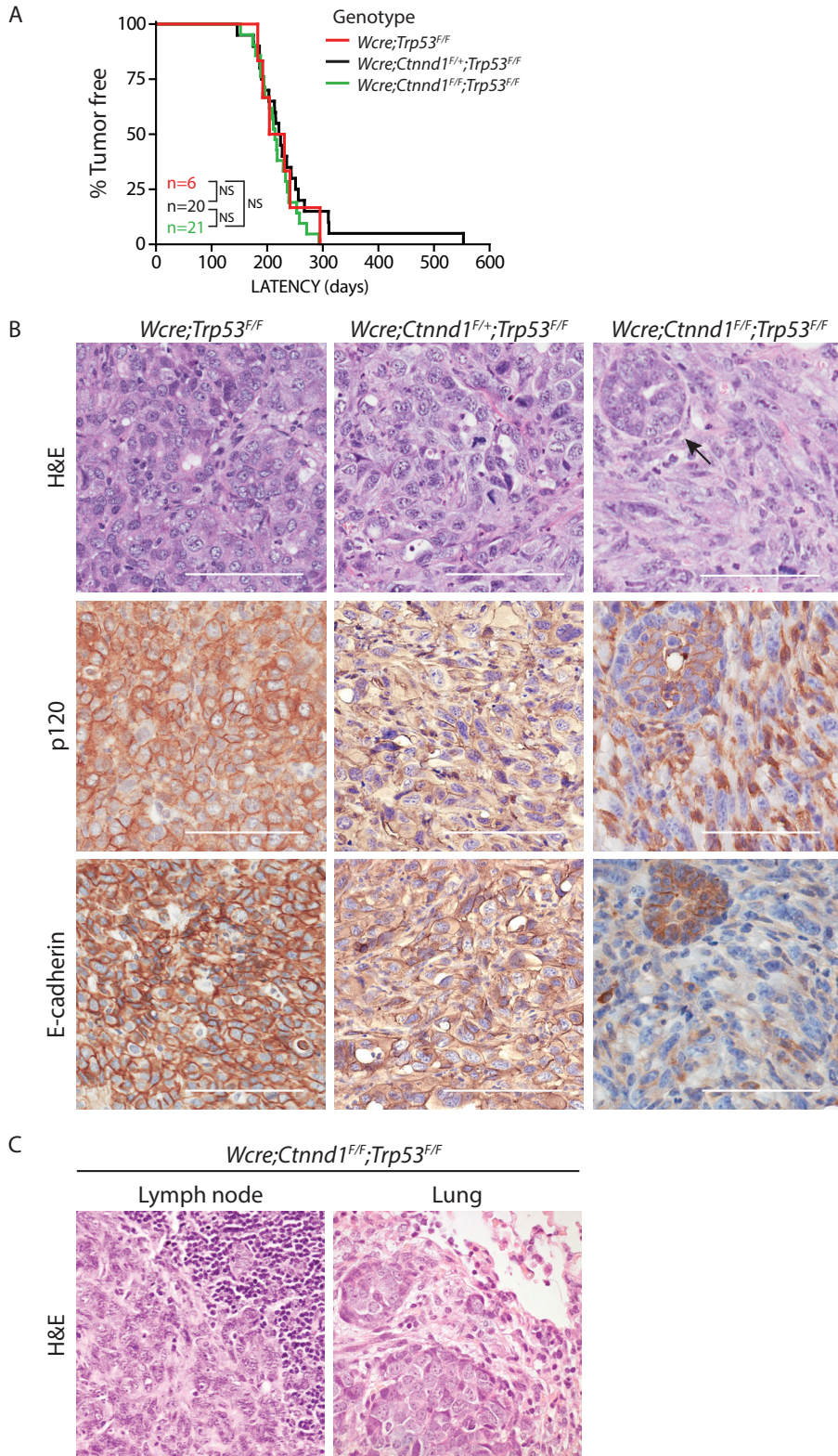


Figure 1

p120 is a metastasis suppressor in mammary carcinoma. **A)** Conditional mammary-specific inactivation of p120 does not influence tumor-free latency. Kaplan-Meier survival curves for Wcre;Trp53^{F/F} (red line) versus Wcre;Ctnd1^{F/+};Trp53^{F/F} (black line) versus Wcre;Ctnd1^{F/F};Trp53^{F/F} (green line). Mice were killed when tumors reached an average diameter of 10 mm. NS = not significant. **B and C)** Loss of p120 induces a switch from nonmetastatic to metastatic mammary carcinoma. **(B)** Histopathology of consecutive sections from mammary tumors derived from Wcre;Trp53^{F/F} (left panels), Wcre;Ctnd1^{F/+};Trp53^{F/F} (middle panels) and Wcre;Ctnd1^{F/F};Trp53^{F/F} (right panels). Shown are H&E staining and immunohistochemistry for p120 and E-cadherin. Arrow in right panels point to a pre-existent hyperplastic mammary duct. **(C)** Homozygous loss of p120 leads to metastasis. Examples of distant metastases from Wcre;Ctnd1^{F/F};Trp53^{F/F} female animals showing disseminated tumor cells in a lymph node (left) and lungs (right). Bars: 100 μ m.

p120 staining. Upon correlation of p120 expression levels to clinicopathological variables, a significant association was obtained between p120 loss, high tumor grade (p=0.007), mitotic index (MAI) (p=0.002) and overall absence of hormone receptor expression (p=0.039) (Table S2). Although p120 expression levels did not associate with tumor size, lymph node status or the other clinicopathological variables tested (Table S2), these data suggest that loss of p120 expression coincides with breast cancer aggressiveness.

Somatic inactivation of p120 results in the formation of metastatic mammary carcinoma

Functional inactivation of the AJ through somatic inactivation of E-cadherin is causal to the development of ILC²³². In E-cadherin mutant breast cancer, p120-catenin (p120) translocates to the cytosol where it exerts a key oncogenic role by regulating anchorage-independent tumor growth and metastasis¹²². To study the effect of p120 loss on tumor progression, we introduced a conditional p120 allele (Ctnd1^F;²¹³ onto the Wcre;Trp53^{F/F}²²⁶ noninvasive mammary carcinoma model, to produce Wcre;Ctnd1^{F/+};Trp53^{F/F} and Wcre;Ctnd1^{F/F};Trp53^{F/F} mice. To correct for differences in genetic background between the Ctnd1^F²¹³ and the Wcre;Trp53^{F/F} (FVB/N; 129P2/OlaHsd) mice, a control cohort was bred using Wcre;Ctnd1^{F/+};Trp53^{F/F} litter mates to produce Wcre;Trp53^{F/F} with a comparable mixed background. Next, females were monitored for spontaneous tumor development. In contrast to conditional inactivation of E-cadherin^{226, 232}, we observed that the median tumor-free latency (T₅₀) did not significantly change in either Wcre;Ctnd1^{F/+};Trp53^{F/F} (T₅₀=223 days) or Wcre;Ctnd1^{F/F};Trp53^{F/F} female mice (T₅₀=214 days) when compared to Wcre;Trp53^{F/F} females (T₅₀=218 days) (p=0.6057 and 0.4906 and respectively) (Figure 1A and Table 1). Mammary tumors from Wcre;Trp53^{F/F} females were morphologically typed as solid carcinomas and carcinosarcomas, with expansive growth, dense cellular sheets and irregular bundles of polygonal to plump spindle-shaped cells (Table 1). Tumors that developed in Wcre;Ctnd1^{F/+};Trp53^{F/F} and Wcre;Ctnd1^{F/F};Trp53^{F/F} females showed a shift from expansive to invasive growth as compared to Wcre;Trp53^{F/F} animals (p=0.053 and

Table 1. Mammary tumor spectrum of Wcre;Trp53^{F/F}, Wcre;Ctnd1^{F/+};Trp53^{F/F} and Wcre;Ctnd1^{F/F};Trp53^{F/F} female mice.

genotype	number of mice	median latency	metastasis	local invasion	AC	SC/CS	mILC
Wcre;Trp53 ^{F/F}	6	218	0 (0%)	0 (0%)	0 (0%)	6 (100%)	0 (0%)
Wcre;Ctnd1 ^{F/+} ;Trp53 ^{F/F}	20	223	1 (5%)	10 (50%)	1 (5%)	19 (95%)	1 (5%)
Wcre;Ctnd1 ^{F/F} ;Trp53 ^{F/F}	21	214	9 (43%)	14 (67%)	3 (14%)	18 (86%)	1 (5%)

In tumors composed of 2 separate histological types, both are counted separately. AC: adenocarcinoma: glandular-type mammary carcinoma. SC/CS: solid carcinoma/carcinosarcoma: tumor consisting of epithelial and mesenchymal cell types. mILC: mouse invasive lobular carcinoma.

$p=0.006$ respectively; Table 1). In contrast to somatic E-cadherin inactivation and the development of ILC, both heterozygous and homozygous loss of p120 resulted in metaplastic tumor cells displaying a spindle cell morphology, often expressing vimentin and focal expression of CK8, CK14, reminiscent of an EMT (Figure 1B, top panels and Table S3). Tumors developed with high incidence multifocally in different mammary glands and were characterized by a more abundant and dense stromal microenvironment. Mammary tumors from *Wcre;Ctnnd1^{F/+};Trp53^{F/F}* females did not show loss of heterozygosity of the *Ctnnd1* locus, as tumors expressed membrane-localized p120 and E-cadherin (Figure 1B middle panels and Table S3). Mammary tumors from *Wcre;Ctnnd1^{F/F};Trp53^{F/F}* females showed large cells with pleomorphic nuclei, coarsely clumped chromatin and sparse cytoplasm. As expected, all tumors from *Wcre;Ctnnd1^{F/F};Trp53^{F/F}* female mice lacked expression of membranous p120 and E-cadherin (Figure 1B right panels, Table 1, Table S3).

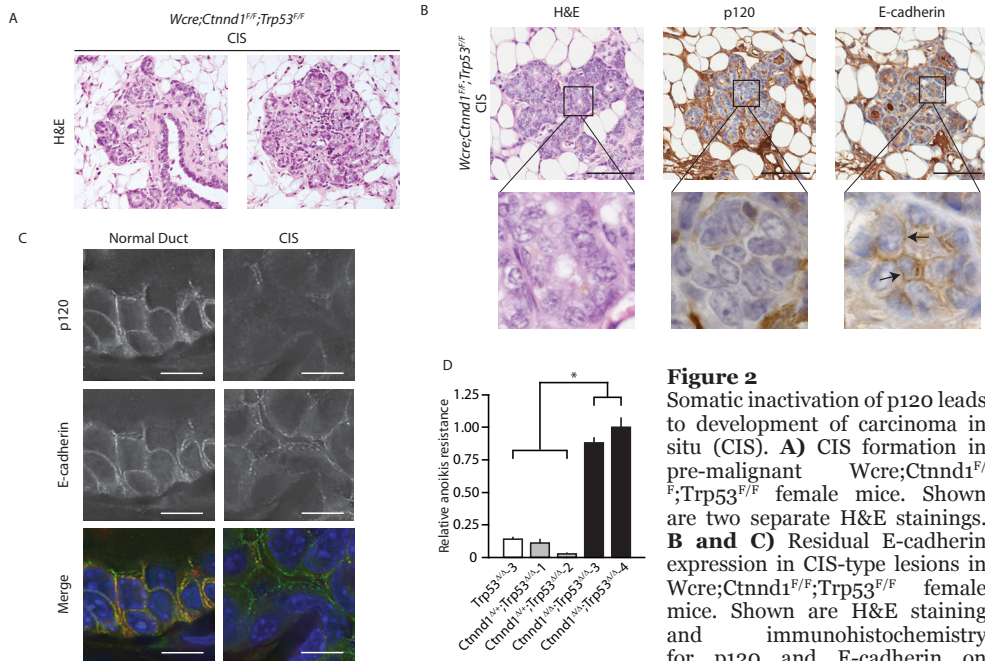
When compared to human breast cancer, the expansive tumors arising in *Wcre;Trp53^{F/F}* mice corresponded to well differentiated “luminal type” IDC, with low proliferation and little nuclear atypia. They predominantly express luminal CK8, showing little expression of basal CK14. Also, these tumors show a relatively good prognosis with infrequent formation of distant metastases. The highly infiltrative tumors arising in *Wcre;Ctnnd1^{F/F};Trp53^{F/F}* females, corresponded to poorly differentiated “basal type”, presenting phenotypic features resembling human metaplastic IDC, which are characterized by a high proliferation rate, strong nuclear atypia, expression of CK14 and vimentin, and poor prognosis with rapid onset of distant metastases.

Interestingly, and in contrast to dual somatic inactivation of E-cadherin and p53^{226, 232}, we observed abundant formation of precursor carcinoma in situ (CIS) lesions in tumor-free *Wcre;Ctnnd1^{F/F};Trp53^{F/F}* females (Figure 2A). CIS lesions showed loss of p120, but occasionally retained low levels of E-cadherin expression (Figure 2B and 2C), indicating that upon p120 inactivation residual E-cadherin remains expressed in a temporal manner, which may underlie the initial noninvasive nature of the CIS-type structures.

Next, we examined whether the acquisition of invasive behavior upon p120 ablation resulted in an increased metastatic rate. We observed a significant increase in tumor cell dissemination in *Wcre;Ctnnd1^{F/F};Trp53^{F/F}* versus *Wcre;Ctnnd1^{F/+};Trp53^{F/F}* and *Wcre;Trp53^{F/F}* female mice (both $p<0.05$; Table 1), a phenotype not observed in previously published models where inactivation was targeted to the gastro-intestinal tract or skin^{129, 213, 214, 219}. Metastases phenotypically resembled the primary tumor and localized to regional or distant lymph nodes and lungs (Figure 1C). Because tumor-free latency was identical in *Wcre;Ctnnd1^{F/+};Trp53^{F/F}* versus *Wcre;Ctnnd1^{F/F};Trp53^{F/F}* mice, but only *Wcre;Ctnnd1^{F/F};Trp53^{F/F}* showed metastatic dissemination, we generated primary cultures from both tumor models and assayed anoikis resistance, a hallmark of metastatic cells^{232, 255, 256}. In agreement with the *in vivo* metastatic behavior, we observed that tumor cells derived from *Wcre;Ctnnd1^{F/F};Trp53^{F/F}* female mice were anoikis resistant, while neither cells from *Wcre;Ctnnd1^{F/+};Trp53^{F/F}* nor *Wcre;Trp53^{F/F}* mammary tumors survived under these conditions (Figure 2D). These results suggest that homozygous inactivation of p120 is necessary for the acquisition of anchorage independence and subsequent dissemination of mammary tumor cells. In conclusion, we show that conditional loss of p120 induces a transition to highly invasive and metastatic mammary carcinoma.

Loss of p120 results in loss of the adherens junction, transition to a mesenchymal phenotype and anoikis resistance

Since we observed anoikis resistance in primary tumor cells derived from *Wcre;Ctnnd1^{F/F};Trp53^{F/F}* female mice (Figure 2D), we examined if p120 inactivation was causal to this anchorage-independent survival phenotype. To this end, we



made use of *Trp53^{Δ/Δ}* tumor cell lines previously generated from adenocarcinomas that developed in either *K14Cre;Trp53^{F/F}*¹²⁸ or *Wcre;Trp53^{F/F}* female mice²²⁶. Two independent *Trp53^{Δ/Δ}* cell lines were transduced using a doxycycline (Dox)-inducible lentiviral construct targeting p120 (p120-iKD). Dox administration resulted in a strong reduction of p120 protein expression (Figure 3A), which was accompanied by a decrease in both E-cadherin and β -catenin levels and a slight decrease in α -catenin protein expression (Figure S2A and S2B). Upon p120-iKD, cells lost their typical epithelial appearance and showed a transition towards a mesenchymal and motile phenotype (Figure S2F). To confirm the specificity of the RNAi sequence used, we reconstituted cells with a non-targetable p120 cDNA to near endogenous levels, which completely reverted the Dox-induced EMT phenotype (Figure S2E and S2F). We next cultured two independent *Trp53^{Δ/Δ};p120-iKD* cell lines in suspension and assayed anoikis resistance in the presence and absence of Dox. While the majority of untreated *Trp53^{Δ/Δ};p120-iKD* cells underwent anoikis, administration of Dox induced anoikis resistance (Figure 3B), which could be fully reverted upon expression of a non-targetable p120 construct (Figure 3B). To substantiate these findings, we employed two E-cadherin expressing and anchorage-dependent human breast cancer cell lines (T47D and MCF7) in which we performed knockdown of p120 and assayed anchorage independence. MCF7 was previously reported to acquire anchorage independence in soft agar upon constitutive p120 KD²²⁷. Indeed, as for the mouse mammary carcinoma cells, p120-iKD induced downregulation of the AJ members and functionally induced anoikis resistance (Figure S2C and S2D, Figure 3C and 3D). In conclusion, our data show that p120 knockdown results in loss of

AJ function, and suggests that this underlies acquisition of anoikis resistance. Since these features are well known hallmarks of malignancy²¹⁶, our findings suggest that loss of p120 may lead to metastasis through acquisition of anchorage independence.

Loss of p120 potentiates growth factor receptor signaling

Upon knockdown of p120 in MCF7, cells acquire Rac-dependent anchorage independent survival, which is probably due to relieve of E-cadherin-mediated inhibition of Ras²²⁷. While we could confirm that active Rac1 levels increased in MCF7 upon p120-iKD, we did not detect activation of Rac1 in Trp53^{Δ/Δ};p120-iKD or T47D;p120-iKD cells after Dox administration (Figure S3). Also, no changes were observed in the levels or activity of the other Rho family members RhoA and Cdc42 (Figure S3C), indicating that loss of p120 in these cell systems does not result in aberrant Rho GTPase activation.

Formation or functional disruption of AJs can affect epidermal growth factor receptor (EGFR) activity activity⁷⁵. Whether this effect results in activation or

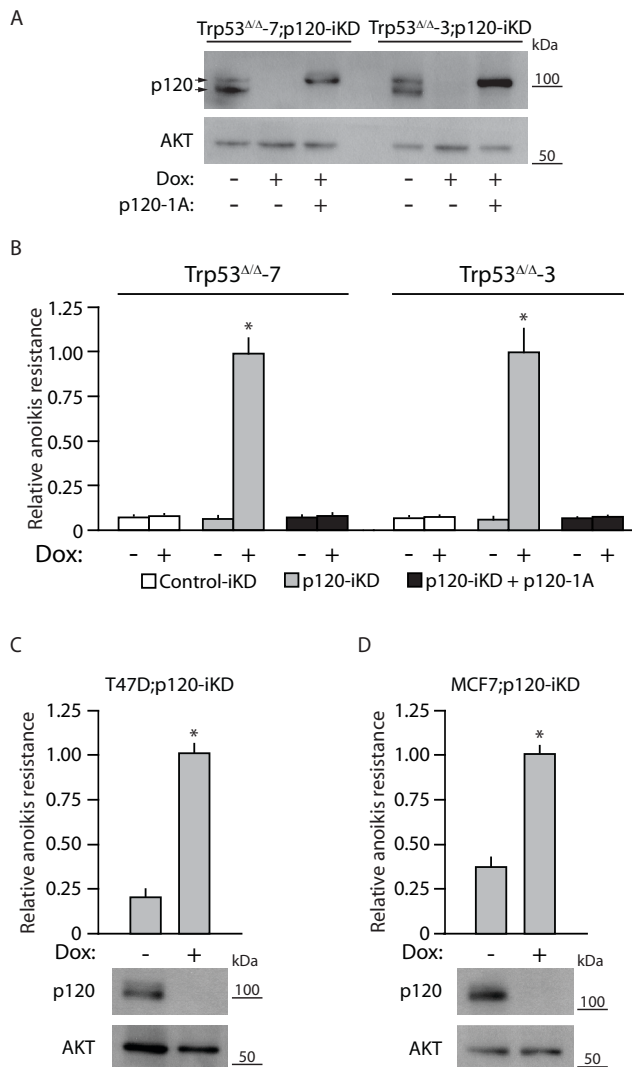


Figure 3

Loss of p120 results in anoikis resistance of E-cadherin expressing breast cancer cells. **A**) Two independent Trp53^{Δ/Δ} cell lines were transduced with viruses carrying Dox-inducible p120 shRNAs (p120-iKD) and a non-targetable p120 isoform1A (p120-1A). Shown is the extent of p120 knockdown and p120-1A expression levels. Arrows indicate p120 isoforms. AKT was used as a loading control. **B**) Trp53^{Δ/Δ};Control-iKD, p120-iKD and p120-1A expressing mammary carcinoma cells were cultured in the presence or absence of Dox for 4 days before subjecting cells to 4 days of anchorage independent culturing and subsequent anoikis resistance analysis using FACS. **C and D**) T47D (**C**) and MCF7 (**D**) were transduced with viruses carrying p120-iKD constructs targeting human p120, treated with Dox for 4 days and subjected to non-adherent culturing. Anoikis resistance was analyzed after 4 days. Lower panels show the extent of p120 knockdown (upper blot). AKT was used as loading control (lower blot). *= $p < 0.005$. Error bars represent standard deviation of triplicate experiments.

inhibition of EGFR, appears to be largely cell type dependent ^{77, 257}. Because p120 knockdown resulted in a loss of AJ formation through downregulation of E-cadherin, we wondered whether growth factor receptor (GFR) signaling was affected. To this end, we stimulated Dox-treated Trp53^{Δ/Δ};p120-iKD cells with EGF and assayed EGFR phosphorylation. While EGF stimulation in control-iKD cells induced a modest EGFR tyrosine phosphorylation, knockdown of p120 resulted in a 1.5 to 2.0 fold increased phosphorylation (Figure 4A, compare lanes 3 and 4; quantified in Figure 4B, non-stimulated in Figure S5A). In line with these findings, we observed that the downstream PI3K/AKT and MAPK pathways displayed a 3-5-fold increased EGF-induced phosphorylation upon knockdown of p120 (Figure 4A and 4B). Furthermore, EGF stimulation of MCF7;p120-iKD cells showed a similar increase in EGFR, AKT and MAPK phosphorylation upon knockdown of p120 (Figure 4C and 4D). The increased EGFR signaling following p120 knockdown was not due to increased EGFR levels or EGF binding at the plasma membrane (Figure 4A and Figure S5C). Also, p120 knockdown did not induce autocrine activation of growth factor receptor signaling in the presence of anchorage, as serum starvation did not result in activation of EGFR, AKT or MAPK (Figure S5A and S5B). To determine whether the sensitized GFR signaling was EGFR-specific, we also stimulated our cells with hepatocyte growth factor (HGF) to activate the receptor tyrosine kinase MET. In line with the effects on EGF-dependent signaling, we observed a marked increase of AKT and MAPK phosphorylation upon p120 knockdown and subsequent HGF treatment in mouse and human cells (Figure S4A-S4C), indicating that p120-controlled growth factor receptor signaling is a general mechanism. In conclusion, our data imply that loss of p120 leads to an increased sensitization of GFR signaling in breast cancer cells.

Since knockdown of p120 resulted in increased growth factor sensitization of pathways implicated in growth and survival, we used EGF stimulation to examine whether this mechanism could increase anchorage independent growth and survival of breast cancer cells. We therefore plated Trp53^{Δ/Δ};p120-iKD cells under anchorage-independent conditions and assayed anoikis resistance. In control cells, EGF stimulation neither induced proliferation nor mediated survival. However, addition of EGF led to an additional increase in anoikis resistance upon knockdown of p120 (Figure 4E). Although less prominent, EGF stimulation also induced a significant increase in anoikis resistance of MCF7;p120-iKD cells (Figure 4F). Because AJ-dependent relieve of GFR inhibition is not specific for a given receptor and MCF7 responds more prominent to HGF than EGF, we stimulated MCF7;p120-iKD cells with HGF. In line with the EGF-dependent findings in our mouse cell lines, we observed that activation of the MET receptor induced a prominent p120-dependent increase in anoikis resistance of MCF7 (Figure S4E). In conclusion, we find that loss of p120 enhances anoikis resistance through increased sensitization of GFR signaling pathways, a mechanism that may stimulate metastasis in p120 negative breast cancer.

Loss of p120 leads to a proinvasive microenvironment

Based on the prominent presence of stroma in the metaplastic p120 null mammary carcinomas and our finding that loss of p120 induces sensitization of GFR signaling, we examined a potential source of growth factors in metastatic tumors from Wcre;Ctnnd1^{F/F};Trp53^{F/F} female mice. Immunohistochemistry indeed revealed an abundant presence of vimentin-expressing cells surrounding p120 negative tumor cells (Figure 5A, middle panel). We next analyzed p120 negative carcinomas for influx of macrophages, a renowned source of EGF ²⁵⁸. p120 negative tumors from mouse and human samples contained a large macrophage-dense microenvironment (Figure 5A and 5B). Moreover, a combination of immunohistochemistry and RNA in situ hybridization revealed that the tumor-associated macrophages produced EGF

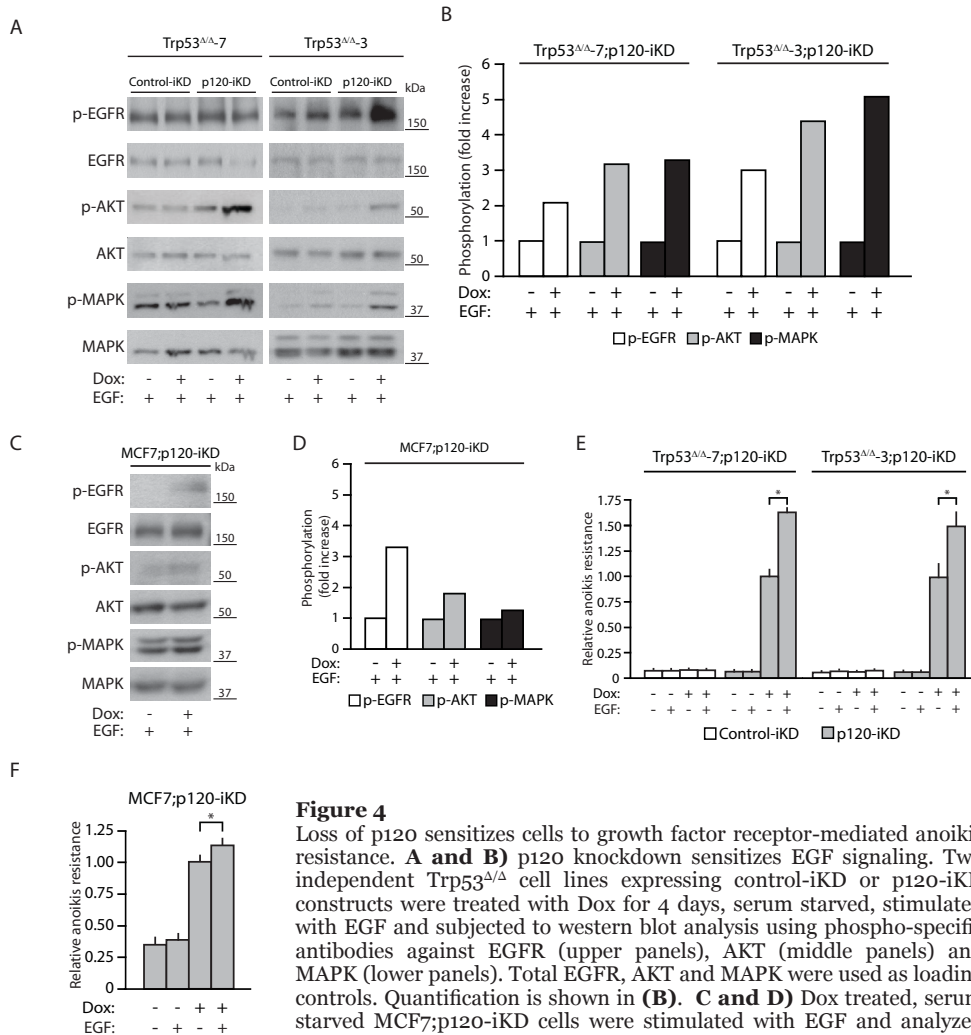


Figure 4

Loss of p120 sensitizes cells to growth factor receptor-mediated anoikis resistance. **A and B**) p120 knockdown sensitizes EGF signaling. Two independent Trp53^{ΔΔ} cell lines expressing control-iKD or p120-iKD constructs were treated with Dox for 4 days, serum starved, stimulated with EGF and subjected to western blot analysis using phospho-specific antibodies against EGFR (upper panels), AKT (middle panels) and MAPK (lower panels). Total EGFR, AKT and MAPK were used as loading controls. Quantification is shown in **(B)**. **C and D**) Dox treated, serum starved MCF7;p120-iKD cells were stimulated with EGF and analyzed as in **(A)**. Quantification is shown in **(D)**. **E**) EGF promotes anchorage independent survival upon p120 loss. Anoikis resistance was analyzed in

Trp53^{ΔΔ};p120-iKD cells in the presence or absence of EGF and Dox as indicated. Error bars represent the SD of triplicate experiments. **F**) EGF promotes anchorage independent survival upon p120 loss in human breast cancer cells. Anoikis resistance of MCF7;p120-iKD cells was assayed in the presence or absence of Dox and EGF as indicated. * = p < 0.05. Error bars represent the SD of triplicate experiments.

(Figure 5C), indicating that a paracrine source of GFR signals is present in the tumor microenvironment.

In the GI-tract and skin, p120 loss resulted in cytokine secretion and subsequent attraction of immune cells^{129, 214, 219}. To determine whether p120 loss would also control production of proinflammatory cytokines in breast cancer, we assayed culture supernatant from Trp53^{ΔΔ};p120-iKD cells and control Trp53^{ΔΔ} cells using an antibody-based cytokine array. Using these tools we observed that knockdown of p120 in Trp53^{ΔΔ} cells indeed increased secretion of numerous cytokines. Several of these are responsible for macrophage and lymphocyte attraction like MIP-3a²⁵⁹, IL-17F²⁶⁰ and CCL2²⁶¹ (Figure 5D), thus suggesting that p120 negative tumor cells are a paracrine source for the influx of inflammatory cells and subsequent formation of a prometastatic microenvironment.

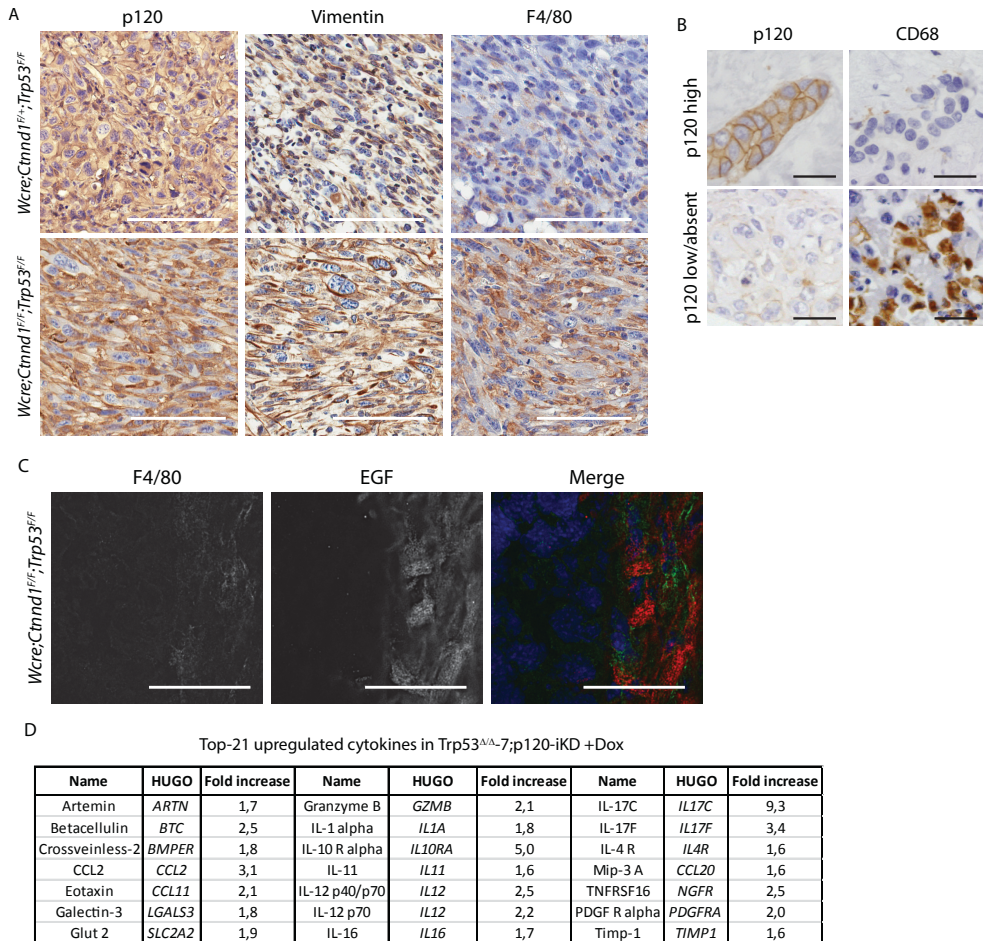


Figure 5

Loss of p120 induces cytokine production and leads to the development of a prometastatic tumor microenvironment. **A)** p120 deficient mammary tumors are characterized by an abundant tumor microenvironment. The presence of stromal cells/macrophages in Wcre;Ctnnd1^{F/+};Trp53^{F/F} (top panels) and Wcre;Ctnnd1^{F/F};Trp53^{F/F} (bottom panels) mouse mammary carcinomas were analyzed by immunohistochemistry. Shown are representative stainings for p120, Vimentin and F4/80. Bars: 100 μm. **B)** Human IDC samples were stained for p120 (left panels) and CD68 (right panels). Shown are representative examples of IDC expressing high p120 (upper panels) and low/absent p120 expression (lower panels). Bars 20μm. **C)** Macrophages produce EGF. Wcre;Ctnnd1^{F/F};Trp53^{F/F} tumors were stained for macrophages using immunofluorescence (green, left panel) and EGF mRNA using RNA in situ (red, middle panel). DNA was visualized using using DAPI (blue, right panel). Bars 20μm. **D)** Loss of p120 induces secretion of pro-inflammatory cytokines. Trp53^{ΔΔ-7};p120-iKD cells were treated with Dox for 4 days. Cells were re-plated and cultured for 4 additional days. The conditioned medium was analyzed for cytokine production using a biotin-label-based antibody array. Shown are the top-20 upregulated cytokines upon p120 knockdown. Fold increase indicates the relative increase in pixel intensity upon p120 knockdown.

In conclusion, we show that loss of p120 results in the production of cytokines that may control influx of macrophages and other stromal cells that can promote progression of p120 negative tumor cells through the induction of sensitized growth factor receptors signaling pathways.

Discussion

p120 loss leads to anoikis resistance and metastasis

In breast cancer, disruption of AJ complex formation through early mutational inactivation of E-cadherin leads to the development of ILC^{9, 226, 232}. Upon inactivation of E-cadherin, p120 translocates to the cytosol, where it functions as an oncogene controlling Rock-mediated anoikis resistance of ILC cells¹²². In contrast to ILC, most IDC cases retain expression of a functional AJ complex that may be inactivated through epigenetic mechanisms at later stages of breast cancer progression²⁴⁷. Interestingly, and in contrast to the salivary gland²¹³, gastro-intestinal tract^{214, 219}; dental enamel²⁵⁰; ocular tissue²⁵¹ and skin¹²⁹, somatic inactivation of p120 in the mammary gland is not tolerated²²⁸. These tissue-specific differences are further exemplified by the fact that p120 knockout in the upper gastro-intestinal tract resulted in the formation of invasive squamous esophageal carcinomas²¹⁹.

In order to determine a possible role for p120 during breast cancer progression we crossed the conditional p120 allele³⁵ onto the *Wcre;Trp53^{F/F}* mouse model of noninvasive breast cancer. Using this compound mouse model we observed that –while onset and incidence of primary tumor development was unaffected– homozygous p120 loss resulted in metastatic disease. Interestingly, metastatic spread was not reported in other conditional p120 tumor models^{129, 213, 214}. Metastatic spread of tumors from *Wcre;Trp53^{F/F}* and *Wcre;Ctnnd1^{F/+};Trp53^{F/F}* female mice was a rare event. Since E-cadherin remained expressed and derivative cell lines functionally displayed anchorage dependence, it indicated that E-cadherin expression may be the rate-limiting factor preventing initial tumor cell invasion and metastasis upon p120 loss. Supporting this assumption is our observation that E-cadherin is temporally retained on the cell surface upon p120 inactivation in preinvasive CIS-type lesions from *Wcre;Ctnnd1^{F/F};Trp53^{F/F}* mice. Also, we have shown previously that low E-cadherin expression levels are sufficient to induce anchorage dependency in anoikis resistant mILC cells^{226, 232}.

Interestingly, and in contrast to mutational E-cadherin loss, we observed that somatic p120 inactivation did not result in the formation of ILC, but instead resulted in metaplastic carcinoma. Differences may be explained by the fact that p120 plays a key oncogenic role in ILC progression through MRIP-dependent regulation of the Rho, Rock and the cytoskeleton^{122, 234}. Moreover, in contrast to E-cadherin inactivation, we did not observe metastases to typical ILC dissemination sites such as bone marrow and gastro-intestinal tract in the current p120 conditional knockout model. Finally, dual inactivation of p120 and p53 did not accelerate tumor development as seen for combined E-cadherin and p53 loss^{226, 232}. These phenotypic and functional differences between p120 and E-cadherin suggest that although the overall consequence is AJ inactivation and metastasis, p120 loss leads to a biochemically and functionally different breast cancer phenotype.

p120 loss sensitizes cells to growth factor receptor signaling

How does p120 loss regulate anoikis resistance? Our data indicate that p120 loss results in a decrease of E-cadherin dependent pro-apoptotic signals in the absence of anchorage, resulting in anoikis. In this scenario, heterozygous p120 loss will not result in metastasis, because residual membranous E-cadherin expression will induce anoikis in the cells that escape from the primary tumor. An additional scenario may be provided by GFR signaling. Membrane receptors can directly influence the activity of unrelated neighboring receptors^{262, 263}. Depending on cellular context, E-cadherin expression may influence EGFR activation^{77, 257}. Indeed, studies in gastric cancer showed that germ-line and somatic (in-frame deleterious) mutations in the E-cadherin extracellular domain lead to increased activation of EGFR signaling^{264, 265}. We show here that inactivation of the AJ through loss of p120 leads to increased sensitization of growth factor receptor signaling, a phenomenon that is

likely dependent on E-cadherin turnover. While it is still controversial whether this mechanism is ligand dependent, our data indicate that the growth factor receptor hypersensitivity upon p120 loss is not caused by upregulation of EGFR expression levels or increased EGF binding at the cell surface (Figure 4A and Figure S5C). Given our observation that E-cadherin-dependent inhibition of GFR signaling is not specific for a given receptor, it seems unlikely that specific posttranslational modifications regulate this process. Thus, although further research is needed to delineate the exact mechanism, we propose that increased sensitization of growth factor receptor signaling may be caused by a relief of direct or indirect mechanical restriction or steric hindrance between the AJ and growth factor receptors.

Loss of p120 results in a prometastatic microenvironment

While the precise nature of the influx of inflammatory cells may depend on the model system studied, several groups reported that p120 ablation may lead to inflammation^{129, 214, 219}. In line with this we found that loss of p120 results in the development of stromal dense and macrophage rich mammary tumors. Furthermore, we show that loss of p120 leads to secretion of several cytokines, which may control the recruitment of inflammatory cells (e.g. macrophages), that have been implicated in inflammation-associated cancer initiation and promotion²⁶⁶ and are correlated with poor prognosis in breast cancer^{267, 268}. Moreover, it has been well established that mammary tumor cells may instigate a paracrine loop that involves the production of chemoattractants and subsequent recruitment of EGF-producing macrophages, resulting in activation of prometastatic pathways in tumor cells^{269, 270}.

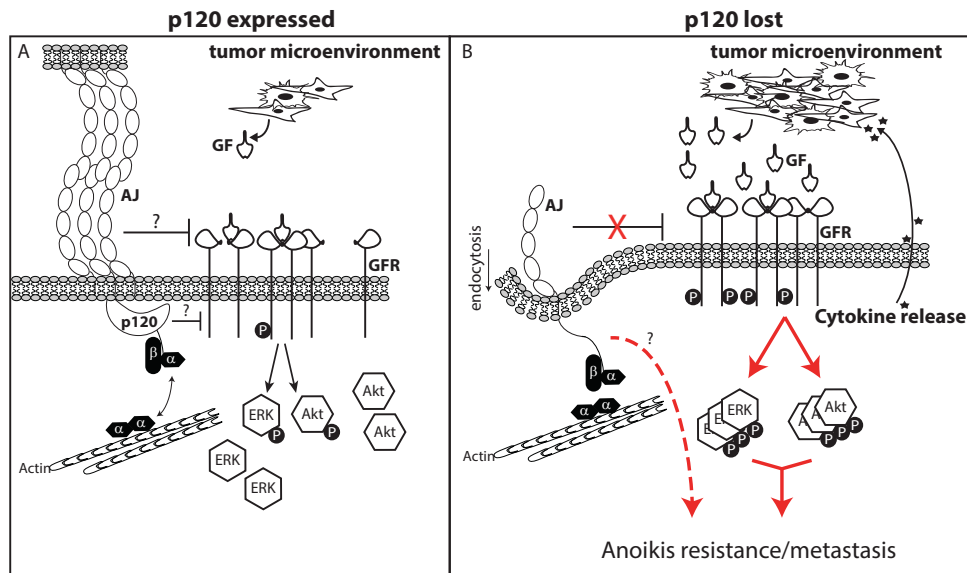


Figure 6

Model for p120 as a breast cancer metastasis suppressor. **A)** In the presence of p120, E-cadherin is stabilized at the plasma membrane leading to the formation of AJs. The AJ inhibits growth factor receptor (GFR) induced growth factor receptor (GFR) activation through currently unknown mechanisms. **B)** Upon loss of p120 the AJ is dismantled and E-cadherin and β -catenin are degraded. As a result, anoikis resistance is induced, and subsequently enhanced by hypersensitized GFR signaling due to the relief of E-cadherin-dependent GFR inhibition. In addition, loss of p120 induces cytokine secretion, resulting in stimulation of the tumor micro-environment. This may facilitate a paracrine loop that activates sensitized GFR signaling in p120 negative tumor cells. The exact mechanism behind this increased sensitization is currently unknown, but does not appear to involve increased growth factor receptor expression, autocrine growth factor receptor activation or increased growth factor binding.

In closing, we propose that p120 inactivation and subsequent E-cadherin loss is a late event in IDC tumor progression. To our knowledge, there have been no reports on mutational p120 inactivation in breast cancer. Although such mutations could have easily been missed using past sequencing techniques and the fact that p120 loss is often observed in only a small percentage of the tumor, CTNND1 mutations are most probably a rare event. Conversely, this could also indicate that p120 inactivation in IDC may be caused by epigenetic or other indirect mechanisms, as has been shown for E-cadherin²⁷¹⁻²⁷³. This, and because of the fact that homozygous p120 inactivation in mice does not induce the formation of mouse ILC, leads us to hypothesize that inactivation of p120 probably occurs during late progression of invasive breast cancer. While the exact mechanism that regulates p120 inactivation remains to be resolved, our data show that E-cadherin-dependent inhibition of GFR signaling is relieved upon inactivation of p120. As a consequence, anoikis resistant cells are sensitized to prometastatic growth factors. Since others and we show that p120 loss also facilitates concomitant formation of a prometastatic microenvironment, inactivation of p120 induces multiple hallmarks of metastatic cancer. A simplified model of our findings is presented in Figure 6. We think that our findings may have substantial clinical ramifications. In our model GFR signaling can be enhanced independent of growth factor receptor expression levels. Thus, our data imply that the mere presence of certain GFRs is of clinical importance, provided that breast cancer cells are p120 negative. Accordingly and depending on the GFRs expressed, patients suffering from p120-negative IDC may be eligible for treatment with GFR inhibitors targeting the expressed receptors. We have thus uncovered a tumor-promoting role for p120 in breast cancer progression that provides an alternate rationale for therapeutic intervention of p120 negative metastatic breast cancer.

Materials and Methods

Additional experimental procedures are described in detail in the Supplemental Experimental Procedures.

Patient material

298 cases of IDC were collected and histologically examined as described in the supplemental experimental procedures.

Antibodies, drugs and cytokine array

All antibodies, drugs and working dilutions are described in the supplemental experimental procedures. Biotin Label-based Mouse Antibody Array, was used according to the manufactures recommendations (RayBiotech AAM-BLM-1-4).

Mouse crossings and genotyping

Conditional p120 mice were crossed onto Wcre;Trp53^{F/F} animals. The resulting Wcre;Ctnnd1^{F/+};Trp53^{F/F} mice were subsequently used to generate Wcre;Trp53^{F/F} mice with a comparable mixed (C57/Bl-6 X FVB/N) background. Wcre;Trp53^{F/F}, Wcre;Ctnnd1^{F/+};Trp53^{F/F} and Wcre;Ctnnd1^{F/F};Trp53^{F/F} female mice were monitored for tumor development and euthanized when tumors reached a diameter of 1 cm. Age at death was used to generate tumor-free survival curves. For additional information, see the supplemental experimental procedures.

Plasmids

For stable knockdown of p120, previously described sequences were cloned into a Dox inducible lentiviral expression system¹²². For p120 reconstitution experiments a lentiviral p120-1A cDNA expression construct was generated as described in the

supplemental experimental procedures.

Virus production and Rho pulldown

Lentivirus production and transductions were done as described¹²². In short, 10^6 Cos-7 cells were seeded onto 10 cm petri dishes and transiently transfected after 24 hr with third-generation packaging constructs²⁷⁴ and the indicated viral construct using X-tremeGENE 9 reagent (Roche). Pulldown assays for GTP-loaded RhoGTP family members were performed as described^{122, 275}.

Cell culture

Mouse Trp53 Δ/Δ -7 (WP6) and Trp53 Δ/Δ -3 (KP6) cell lines were generated from primary tumors that developed in Wcre;Trp53 F/F and K14cre;Trp53 F/F female mice respectively. Cells were cultured as described²³². Human breast cancer cell lines T47D and MCF7 were cultured in DMEM·F12 (Invitrogen) containing 6% fetal calf serum, 100 IU/ml penicillin and 100 μ g/ml streptomycin.

Immunohistochemistry and fluorescence

Tissues and cells were isolated, fixed and stained as described in the supplemental experimental procedures. In situ hybridization–IHC double staining experiments were performed using labeled PCR products to identify EGF mRNA as described in the supplemental experimental procedures. Samples were analyzed using a DeltaVision RT system (Applied Precision), equipped with a CoolSnap HQ camera and SoftWorx software. Maximum projections were taken from a stack of deconvolved images.

Western blot

Western blotting was done as described²⁷⁶.

Anoikis resistance and FACS analysis

Anoikis resistance was analyzed by seeding cells under non-adherent conditions and analyzing cell viability using FACS analysis as described in the supplemental experimental procedures. To determine cellular EGF binding ability, 400 ng of Alexa Fluor 647 conjugated EGF (Invitrogen) was incubated with 1×10^5 trypsinized ice-cold cells in 100 μ l PBS. Cells were washed with PBS to remove unbound EGF-647 and subjected to FACS analysis.

Growth factor stimulation assays

Cells were seeded at 400,000 cells per 6-well in growth factor free medium for 4 hours, subsequently washed and serum-starved overnight. Next, cells were stimulated with EGF (5ng/ml; Sigma) or HGF (25ng/ml; R&D Systems) for 10 minutes. Cells were placed on ice and washed twice with ice-cold PBS containing Ca $^{2+}$ and Mg $^{2+}$, and directly lysed in lysis buffer.

Statistical Analyses

Statistical analyses were performed as described in the supplemental experimental procedures

Acknowledgements

We wish to thank Eva Schut-Kregel for excellent technical support. Participants of the MMM meeting and members of the Bos, Burgering, and Pathology labs are acknowledged for help and fruitful discussions. We are also indebted to the UMC Biobank. This work was supported by the UMC Cancer Center and a grant from the Netherlands Organization for Scientific Research (NWO-VIDI 917.96.318).

Supplemental experimental procedures

Patients

The study population was derived from the archives of the Departments of Pathology of the University Medical Center Utrecht, Utrecht, The Netherlands and comprised 298 cases of invasive ductal carcinoma (IDC) as described ²⁴⁴. Histological grade was assessed according to the Nottingham scheme, and mitotic activity index (MAI) was assessed as before ²⁷⁷. From representative donor paraffin blocks of the primary tumors, tissue microarrays were constructed as described ^{244, 278}. The use of anonymous or coded left over material for scientific purposes is part of the standard treatment contract with patients in The Netherlands ²⁷⁹. Ethical approval was not required.

Antibodies and drugs

The following antibodies were used: mouse anti-p120 (WB 1:2000, IF 1:500, IHC 1:500, BD Biosciences), TRITC-conjugated p120 (IF 1:150; BD Biosciences) mouse anti-E-cadherin (WB 1:2000, BD Biosciences), FITC-conjugated E-cadherin (IF 1:150; BD Biosciences), mouse anti-E-cadherin (IHC 1:200, clone 4A2C7, Zymed, Invitrogen), rat anti-cytokeratin (CK) 8 (Troma-1, IHC 1:125, DSHB products), rabbit anti-CK14 (IHC 1:10,000, BabCo), guinea pig anti-vimentin (IHC 1:400, RDI), rabbit anti-SMA (IHC 1:350, Lab Vision), Rat anti-mouse F4/80 (IHC 1:300, Serotec), Mouse anti- β -catenin (WB 1:2000, BD Biosciences), rabbit anti α E-catenin (WB 1:2000, Sigma) goat anti-AKT1 (C-20, WB 1:1000, Santa Cruz Biotechnology), rabbit anti pAKT1^{S473} (WB 1:1000, Cell Signaling), rabbit anti-ERK1 (C-16, WB 1:2000, Santa Cruz Biotechnology), rabbit anti p-MAPK (p44/42, WB 1:2000, Cell Signaling), mouse anti-RhoA (WB 1:250, Santa Cruz Biotechnology), mouse anti-Rac1 (WB 1:1000, Upstate), rabbit anti-Cdc42 (WB 1:250, Santa Cruz Biotechnology), rabbit anti EGFR (WB 1:500, Cell Signaling), rabbit anti p-EGFR^{T1068} (WB 1:1000, Cell Signaling), sheep anti-digoxigenin (Roche). Secondary antibodies: HRP-conjugated rabbit anti-goat, goat anti-mouse, (1:2000, Dako), HRP-conjugated goat anti-rabbit (1:2000, Cell Signaling), rabbit anti-sheep antibodies (DAKO), Alexa Fluor-561-conjugated anti-mouse antibodies (Molecular probes), goat anti-rat Alexa Fluor-488 (Invitrogen), goat anti-rabbit Alexa Fluor-555 (Invitrogen), biotin-conjugated anti-guinea pig (Jackson ImmunoResearch).

Mouse crossings and genotyping

p120 conditional mice containing *loxP* sites in intron 2 and 8 of *Ctnnd1*, (Black-swiss;129SvEvTac) ²¹³ were crossed onto the *Wcre;Trp53^{F/F}* mouse model (FVB/N;Ola129/sv) ^{226, 232}. From the offspring, cohorts of *Wcre;Ctnnd1^{F/+};Trp53^{F/F}* and *Wcre;Ctnnd1^{F/F};Trp53^{F/F}* mice were generated. The (*Wcre*);*Ctnnd1^{F/+};Trp53^{F/F}* mice were subsequently used to generate *Wcre;Trp53^{F/F}* mice to control for the introduction of Black-swiss;129SvEvTac genetic material. Mice were bred and maintained on a mixed background of (FVB/N;Ola129/sv). Genotyping was done by PCR as previously described for all alleles ^{213, 226}. Mice were monitored for the development of mammary tumors, which were detected by palpation. Mice were euthanized by CO₂ inhalation when mammary tumor size reached a diameter of 10mm. Full autopsies were performed to analyze tumor phenotypes and to detect metastases. Age at the time of euthanasia was used to generate the tumor-free survival curve.

Plasmids

For stable knockdown of p120, sequences directed against mouse (5' GCCAGAAGTGGTGC GAATA 3') and human (5' GCCAGAGGTGGTTCGGATA 3') p120 and a control siRNA sequence (5' TTCTCCGAACGTGTCACGTT 3') were

cloned into a Dox inducible lentiviral expression system as described¹²². For p120 reconstitution experiments, pEGFP-C1-p120-1A (gift from J.M. Daniel, McMaster University, Hamilton, Canada) was mutated by means of QuikChange XL site directed mutagenesis (Stratagene) using primers containing three silent mutations (forward: 5'AACTCTTATTTTCAGCCAGAAGTCGTCCGCATATACATTTCACTCCTTAAGG3', reverse: 5'CCTTAAGGAGTCAAATGTATATGCGGACGACTTCTGGCTGAAATAAGAGTT3'). *EcoRV* and *NheI* sites were added 5' and 3' of p120-1A, by means of Phusion PCR (Thermo Scientific) (forward: 5'AATTGATATCATGGACGACTCAGAGGTGGAGTCGAC3', reverse: 5'TTAAGCTAGCCTAAATCTTCTGCATCAAGGGTGTCCC3'). *EcoRV*-p120-1A-*NheI* was subsequently cloned into the lentiviral expression vector pLV.bc.puro (gift from C. Löwik, Leiden University Medical Center, Leiden, the Netherlands). pCMV-SPORT-EGF (open biosystems) was used as template to generate the DIG-labeled EGF probe by PCR. Primers: forward: 5' GGACTTGTGCCGGTCTCTGCC 3', reverse: 5' GCGCTCGAGTGGGACTTGGG 3'

Immunohistochemistry and fluorescence

Tissues were isolated, fixed in 4% formaldehyde for 48 hours, dehydrated, cut into 4µm sections and stained with hematoxylin and eosin. For single staining, fixed sections were rehydrated and incubated with primary antibodies. Endogenous peroxidases were blocked with 3% H₂O₂ and stained with biotin-conjugated secondary antibodies, followed by incubation with HRP-conjugated streptavidin-biotin complex (DAKO). Substrate was developed with DAB (DAKO). For immunofluorescence, fixed sections were rehydrated, boiled in citrate and incubated with primary antibodies overnight. Stainings were scored as described²⁴⁴. Cells were grown on cover slips and fixed in 1% paraformaldehyde/PBS for 10 minutes. Cells were permeabilized using 0.3% Triton-X100/PBS and subsequently blocked using 5% BSA (Roche). Samples were incubated with primary antibodies in 1% BSA for 60 minutes, followed by secondary antibodies for 30 minutes. DNA was stained with DAPI for 5 minutes (Molecular Probes) and cover slips were mounted onto object glasses using vectashield mounting medium (Vector laboratories).

In situ-hybridisation-IHC double staining was performed on freshly frozen tissue as described²⁸⁰. Slides were hybridized overnight with DIG-labeled EGF probe as described²⁸⁰. Subsequently, the slides were incubated with primary antibody F4/80. The EGF probe was detected with sheep anti-digoxigenin antibody (Roche) followed by a secondary rabbit anti-sheep antibody (DAKO). Alexa Fluor-555-conjugated goat anti-rabbit (Invitrogen) was used to detect DIG-labeled EGF probes.

Samples were analyzed using a DeltaVision RT system (Applied Precision) using a 40x, 63x and 100x lens at room temperature, equipped with a CoolSnap HQ camera and SoftWorx software. Maximum projections were taken from a stack of deconvolved images.

Anoikis resistance

Anoikis resistance was analyzed by seeding cells at a density of 20,000 cells per well (in 500 µl) in a 24-well ultra-low cluster polystyrene culture dish (Corning). After 4 days, cells were harvested and resuspended in 75µl of Annexin-V buffer supplemented with Annexin-V and Propidium Iodide. The percentage of anoikis resistant cells was determined as described²³². Anoikis resistant cells were defined as the Annexin-V and Propidium Iodide negative population. Relative no. of viable cells represents the number of cells analyzed at high flow speed for 30 seconds on an BD FACSCalibur.

Statistical Analyses

Statistical analyses were performed using GraphPad Prism 5 (GraphPad Software).

Analyses on human samples were performed as previously described (Vermeulen et al., 2012). For analysis of growth pattern and metastasis formation, Fisher's exact test was used. For metastasis-free survival analysis, the Log-Rank test was used. For anoikis assays, statistical significance was calculated using the Student's T-test (2-tailed), showing measurements of at least three independent experiments. Error bars in all experiments represent standard deviation of at least triplicate measurements. We considered p-values less than 0.05 as statistically significant.

Ethics Statement

All animal experiments were approved by the University Animal Experimental Committee, University Medical Center Utrecht. Use of anonymous or coded leftover material for scientific purposes is part of the standard treatment contract with patients in our hospitals.

Supplemental data

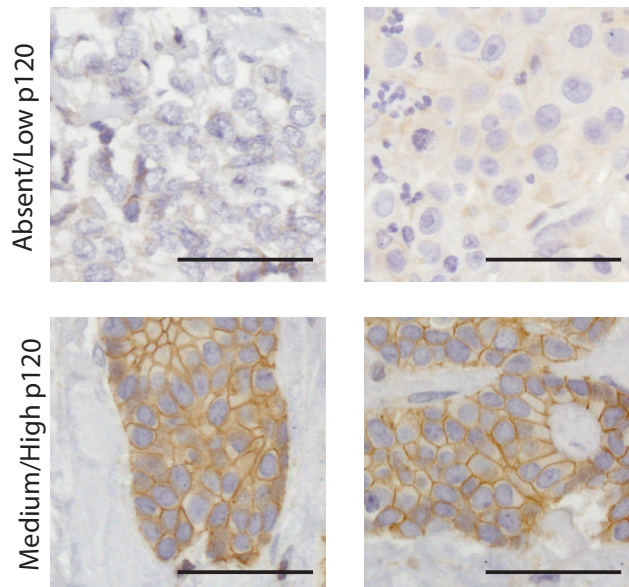


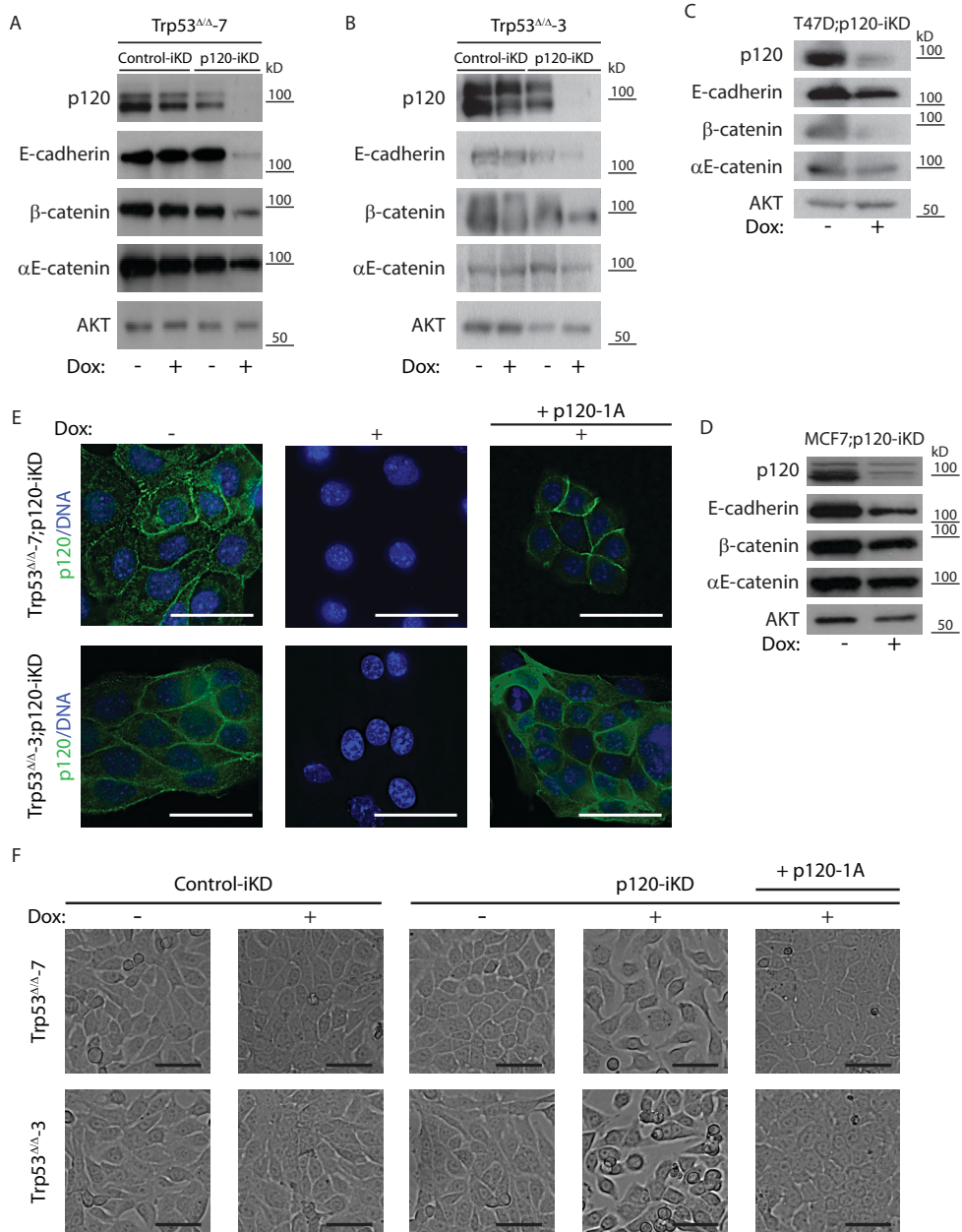
Figure S1
p120 expression levels in human IDC. A panel of 298 invasive ductal carcinomas was analyzed for p120 expression by immunohistochemistry. Shown are four representative stainings indicating different p120 expression levels. Bars 50µM.

3

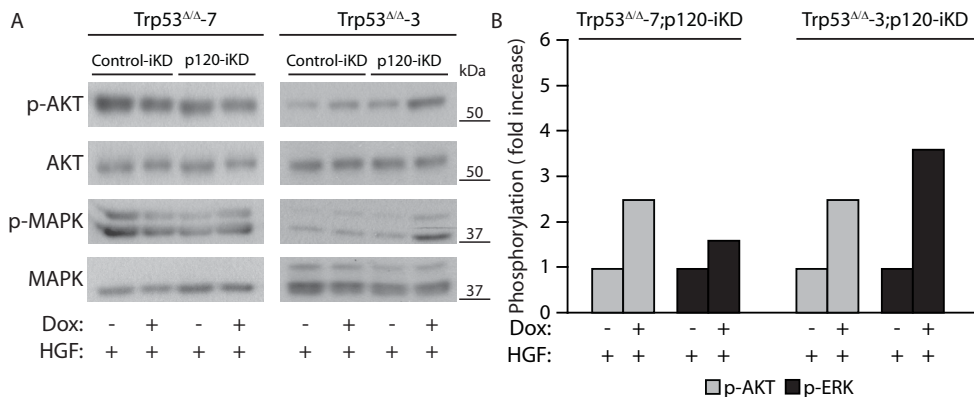
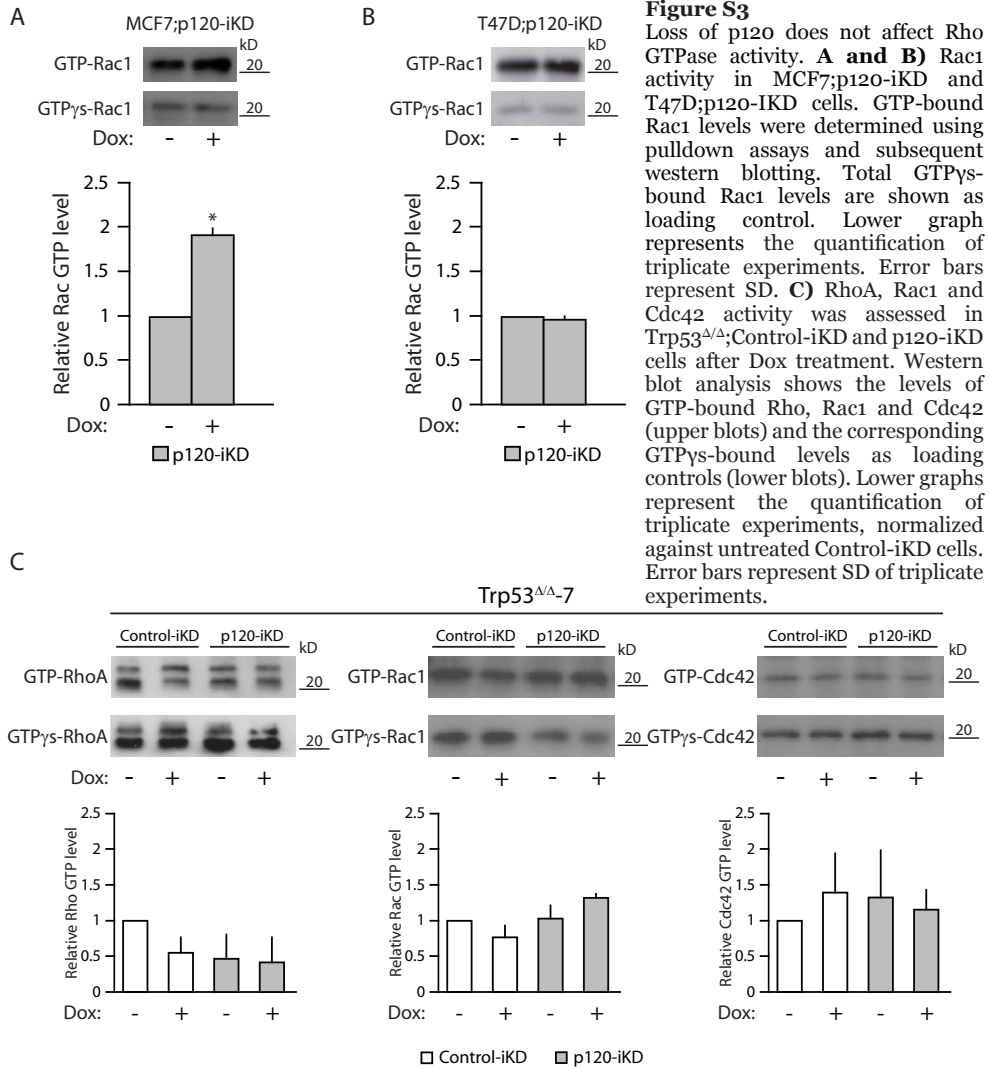
Table S1. Clinicopathological characteristics of 298 invasive ductal breast cancers studied for the expression of p120.

Feature	Grouping	N or value	%
Age (years)	Mean	60	
	Range	28 to 88	
Tumour size (cm)	≤2	139	46.6
	>2 and ≤5	136	45.6
	>5	18	6.0
	Not available	5	1.7
Histological Grade	1	55	18.5
	2	98	32.9
	3	143	48.0
	Not available	2	0.7
MAI (per 2mm ²)	≤ 12	135	45.3
	≥ 13	163	54.7
Lymph node status	Negative ^A	138	46.3
	Positive ^B	146	49.0
	Not available	14	4.7

(^A: negative = No or No(i+); ^B:positive = ≥N1mi (according to TNM 7th edition, 2010))

**Figure S2**

p120 knockdown decreases AJ member expression levels and disrupts cell-cell contact in breast cancer cells. **A-D**) Dox-treated and untreated Control-iKD and Trp53^{Δ/Δ};p120-iKD mouse mammary carcinoma cells (**A and B**) and human T47D;p120-iKD (**C**) and MCF7;p120-iKD cells (**D**) were subjected to western blot analysis, showing the effect of p120 knockdown on E-cadherin, β-catenin and αE-catenin expression levels. AKT was used as loading control. **E and F**) p120 controls epithelial integrity of mammary carcinoma cells. Trp53^{Δ/Δ};p120-iKD and Trp53^{Δ/Δ};p120-iKD cells expressing p120-1A were stained for p120 (green) to visualize knockdown and correct relocalization. DNA was visualized using DAPI (blue). Trp53^{Δ/Δ} cell lines expressing inducible control (Control-iKD) or Trp53^{Δ/Δ};p120-iKD and Trp53^{Δ/Δ};p120-iKD cells expressing p120-1A were grown in the absence or presence of Dox for 4 days. Pictures were taken using bright field microscopy to show epithelial monolayer integrity (**F**). Bars: 50 μm.



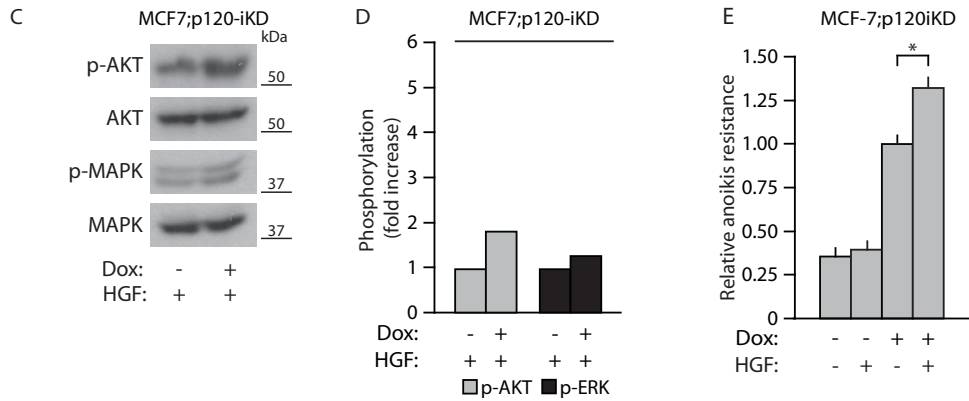


Figure S4

Loss of AJ integrity sensitizes cells to HGF signaling. **A and B**) p120 knockdown results in sensitization to HGF-induced signaling. Two independent $Trp53^{\Delta/\Delta}$ cell lines expressing Control-iKD or p120-iKD were treated with Dox for 4 days, serum starved, stimulated with HGF and subjected to western blot analysis for phosphorylated AKT and MAPK. Total AKT and MAPK were used as loading controls. Quantification is shown in **(B)**. **C and D**) MCF7;p120-iKD cells were cultured in the presence of Dox, serum starved, stimulated with HGF and subjected to western blot analysis as in **(A)**. Quantification is shown in **(D)**. **E**) HGF promotes anchorage independent survival upon p120 loss in human breast cancer cells. Dox-induced MCF7;p120-iKD cells were cultured in ultra-low cluster plates for 4 days in the presence or absence of Dox and HGF as indicated. *= $p < 0.05$. Error bars represent the SD of triplicate experiments.

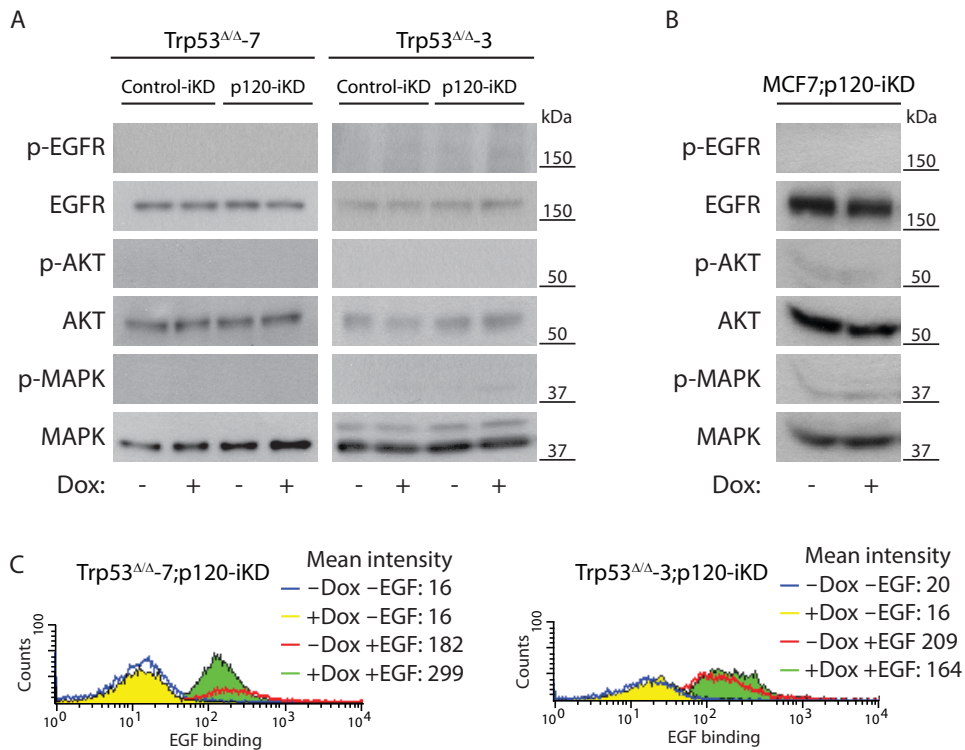


Figure S5

Loss of p120 and subsequent AJ inactivation does not result in activation of autocrine survival pathways or increased EGF binding. **A and B**) knockdown of p120 does not activate AKT or MAPK signaling under anchorage-dependent conditions. Two independent $Trp53^{\Delta/\Delta}$ cell lines **(A)** and MCF7 cells **(B)** expressing Control-iKD or p120-iKD constructs were serum starved, and subjected to western blot

analysis for phosphorylated EGFR (upper panels), AKT (middle panels) and MAPK (lower panels). Total EGFR, AKT and MAPK were used as loading controls. Note the absence of phosphorylation signal upon p120 knockdown. C) p120 knockdown does not increase quantitative EGF-binding. p120-iKD expressing Trp53^{2/Δ} cell lines were treated with Dox for 4 days, serum-starved and trypsinized. Ice-cold cells were incubated with or without Alexa647-conjugated EGF and subjected to FACS analysis.

Table S2. Correlation of p120 expression with clinicopathological and molecular features of invasive breast cancer.

Feature	N	p120 expression		
		Low N (%)	High N (%)	p-value
Histological grade				
1	55	13 (23.6)	42 (76.4)	
2	98	26 (26.5)	72 (73.5)	
3	143	61 (42.7)	82 (57.3)	0.007
MAI (per 2mm ²)				
≤ 12	135	33 (24.4)	102 (75.6)	
≥ 13	163	67 (41.1)	96 (58.9)	0.002
Tumour size (cm)				
≤2	139	43 (30.9)	96 (69.1)	
>2 and ≤5	136	47 (34.6)	89 (65.4)	
>5	18	6 (33.3)	12 (66.7)	0.814
Lymph node status				
Negative	138	43 (31.2)	95 (68.8)	
Positive	146	54 (37.0)	92 (63.0)	0.301
Perou / Sorlie classification				
Luminal	227	69 (30.4)	158 (69.6)	
HER2-driven	19	7 (36.8)	12 (63.2)	
Basal/TN	52	24 (46.2)	28 (53.8)	0.090
Hormonal receptors				
Positive	227	69 (30.4)	158 (69.6)	
Negative	71	31 (43.7)	40 (56.3)	0.039
ERα				
Negative	75	31 (41.3)	44 (58.7)	
Positive	223	69 (30.9)	154 (69.1)	0.099
PR				
Negative	135	53 (39.3)	82 (60.7)	
Positive	163	47 (28.8)	116 (71.2)	0.058
HER2				
Negative	259	88 (34.0)	171 (66.0)	
Positive	39	12 (30.8)	27 (69.2)	0.692
EGFR				
Negative	232	79 (34.1)	153 (65.9)	
Positive	64	21 (32.8)	43 (67.2)	0.853

Table S3. Immunohistochemistry of primary *Wcre;Ctnd1^{E/+};Trp53^{F/F}* and *Wcre;Ctnd1^{E/F};Trp53^{F/F}* mouse mammary tumors.

Genotype	Animal ID	Pathology ID	Diagnosis	p120	E-cadherin	CK8	CK14	Vimentin
<i>Wcre;Ctnd1^{E/+};Trp53^{F/F}</i>	771229	11SJK061	SC/CS, AC	+/-	+/-	+	+ (f)	+
	772032	11SJK012	SC/CS	+/-	+	+ (f)	+ (f)	+
	772034	10SJK267	SC/CS	+	+	+	+ (f)	+
	772036	11SJK026	SC/CS	+	+/-	+	+ (f)	+
	779779	11SJK034	SC/CS	+	+	-	+	+
	785919	11SJK052	SC/CS	+	+	+	+	-
	785920	11SJK155	SC/CS	+ (cyt)	+	-	+ (f)	+
	811561	11SJK139	SC/CS	+	+	+ (f)	+	+
	811563	11SJK159	SC/CS	+	+	+ (f)	+ (f)	+ (f)
	811576	11SJK152	SC/CS	+	+/-	+ (f)	+	+
<i>Wcre;Ctnd1^{E/F};Trp53^{F/F}</i>	634482	09DER002	SC/CS	nd	-	-	-	+
	634485	09DER009	SC/CS	nd	+/- (cyt)	+	nd	-
	653684	09DER014	SC/CS	-	-	+ (f)	+ (f)	+
	749675	10SJK247	SC/CS	-	+ (cyt)	-	+	+
	757516	10SJK246	SC/CS	-	+ (cyt)	+ (f)	+ (f)	+
	771213	11SJK003	SC/CS	-	+ (cyt)	-	+ (f)	+
	785921	11SJK067	SC/CS	-	+ (cyt)	+ (f)	+	+
	788323	11SJK054	SC/CS	-	+ (cyt)	+ (f)	+	+
	795701	11SJK053	SC/CS	-	+ (cyt)	+ (f)	+	+ (f)
	805081	11SJK157	AC	-	+/- (mem)	+	+ (f)	-
805082	11SJK173	SC/CS	-	+ (cyt)	-	+ (f)	+	
826536	11SJK170	SC/CS	-	+ (cyt)	-	+ (f)	+	

f=focal, cyt=cytosol, mem=membrane, CK8 and CK14 show a mixed but exclusive expression pattern.



Chapter 4

4

Cytosolic p120-catenin regulates growth of human and mouse metastatic lobular carcinoma through Rock1-mediated anoikis resistance

Ron C.J. Schackmann, Miranda van Amersfoort, Judith H.I. Haarhuis, Eva J. Vlug, Vincentius A. Halim, Jeanine M.L. Roodhart, Joost S. Vermaat, Emile E. Voest, Petra van der Groep, Paul J. van Diest, Jos Jonkers and Patrick W.B. Derksen

J Clin Invest. 2011 Aug;121(8):3176-88.

Abstract

Metastatic breast cancer is the major cause of cancer-related death amongst women of the Western world. Invasive carcinoma cells have acquired a decisive and key feature that allows them to counteract apoptotic signals in the absence of anchorage, enabling cell survival during invasion and dissemination. While loss of E-cadherin is a cardinal event in the development and progression of invasive lobular carcinoma (ILC), little is known about the underlying mechanisms that govern these processes. Using a mouse model of human ILC we show that cytosolic p120-catenin (p120) regulates tumor growth upon loss of E-cadherin through the induction of anoikis resistance. p120 confers anchorage independence by indirect activation of Rho-Rock signaling through interaction and inhibition of Mrip, an antagonist of Rho-Rock function. We show that primary human ILC samples express hallmarks of active Rock signaling and that Rock controls anoikis resistance of human ILC cells. Thus, we have linked loss of E-cadherin – an initiating event in ILC development – to Rho-Rock-mediated control of anchorage-independent survival. Since activation of Rho and Rock are strongly linked to cancer progression and susceptible to pharmacological inhibition, these insights may have significant clinical implications for the development of tailor-made intervention strategies to better treat invasive and metastatic lobular breast cancer.

Introduction

Breast cancer progression depends on the capacity of cells to invade, metastasize and colonize distant sites. Loss of tumor cell adhesion and subsequent anchorage-independent survival are crucial steps in this process. In breast cancer, invasive ductal carcinoma (IDC) often co-expresses E-cadherin, β -catenin and p120-catenin (p120) at the cell membrane in structures called adherens junctions (AJ)²⁸¹. During IDC tumor progression, AJ may be lost due to E-cadherin inactivation through epigenetic mechanisms resulting in an epithelial to mesenchymal transition (EMT), which is widely believed to mark the conversion to malignancy. In contrast, invasive lobular carcinoma (ILC) is characterized by loss or inactivation of E-cadherin at the initiating stages of tumor development, suggesting a difference in tumor etiology compared to IDC^{9, 232, 282}.

Catenins respond differentially to functional loss of E-cadherin. Unlike β -catenin, p120 is not degraded in human ILC, but instead accumulates in the cytoplasm and nucleus where it has been proposed to regulate processes that influence invasiveness²³⁴. While cytosolic p120 coincides with loss of E-cadherin in ILC, IDC shows a p120 expression pattern that seems unrelated to E-cadherin and β -catenin status, including complete loss of p120 expression in approximately 10% of the cases²²³. These characteristics have advocated p120 expression and localization as a decisive marker in the differential diagnosis between IDC and ILC²²². Abnormalities in p120 expression have been reported in a variety of tumors, ranging from complete loss of protein expression to accumulation²²⁵. Thus, depending on tumor type, p120 may play a role as an oncogene or exert tumor suppressor functions.

Cytoplasmic overexpression of p120 results in a branching phenotype as a consequence of inhibition of the small GTPase RhoA, probably through indirect activation of the other Rho family members, Rac1 and Cdc42¹²⁰. Here, p120 may function as a Rho-GDP dissociation inhibitor (GDI) by directly binding RhoA, leading to inhibition of stress fiber-mediated contractility, thus resulting in an increase in motility¹³⁸. Rho proteins not only regulate cell morphology, but also gene expression, cell proliferation and survival²⁸³. Key downstream effectors of Rho GTPase signaling are the Rho-associated kinases Rock1 and Rock2²⁸⁴ which regulate the actin cytoskeleton and cellular metabolism through phosphorylation of downstream effectors such as Cofilin²⁸⁵ and Myosin Light Chain (MLC)²⁸⁶. In cancer, activation or overexpression of Rho GTPases and downstream Rock signaling components correlates with invasion, angiogenesis and overall aggressiveness of tumors of the GI tract, testis and bladder²⁸⁷⁻²⁹⁰.

Myosin phosphatase Rho-interacting protein (Mrip; Mrip or p116^{RIP3}) is a ubiquitously expressed protein that was identified as a direct RhoA binding partner in mouse and human cells, resulting in inhibition of RhoA-mediated functions^{291, 292}. Mrip causes actin filament disassembly, probably by acting as a scaffold for multiple actin remodeling proteins like RhoA and myosin phosphatase and localizing them to actin filaments^{293, 294}.

Here, we have used well-defined mouse models of human ILC to show that loss of E-cadherin leads to translocation of p120 to the cytosol. In this setting, cytosolic p120 shows preferential binding to Mrip, an interaction that relieves the antagonistic effects of p120 and Mrip on the Rho-Rock signaling pathway. As a consequence, RhoA and downstream Rock1 signaling is active, resulting in anoikis resistance and in vivo tumor growth of metastatic lobular breast cancer.

Results

Somatic loss of E-cadherin leads to translocation of p120 to the cytosol

We have shown in a conditional mouse model of human ILC that loss of E-cadherin is causally related to the acquisition of anoikis resistance and subsequent metastasis

of mammary tumor cells²³². Using mouse ILC (mILC) as a model system, we set out to investigate the consequences of somatic loss of E-cadherin to the adherens junction complex members. First, we analyzed the expression and localization of β -catenin and activity of canonical Wnt signaling. In agreement with previous studies^{295, 296} we show that somatic inactivation of E-cadherin does not induce accumulation of β -catenin and subsequent activation of canonical Wnt signaling in mILC (Supplementary Information Figure S1).

Since cytoplasmic p120 expression can be used as a decisive tool in the differential

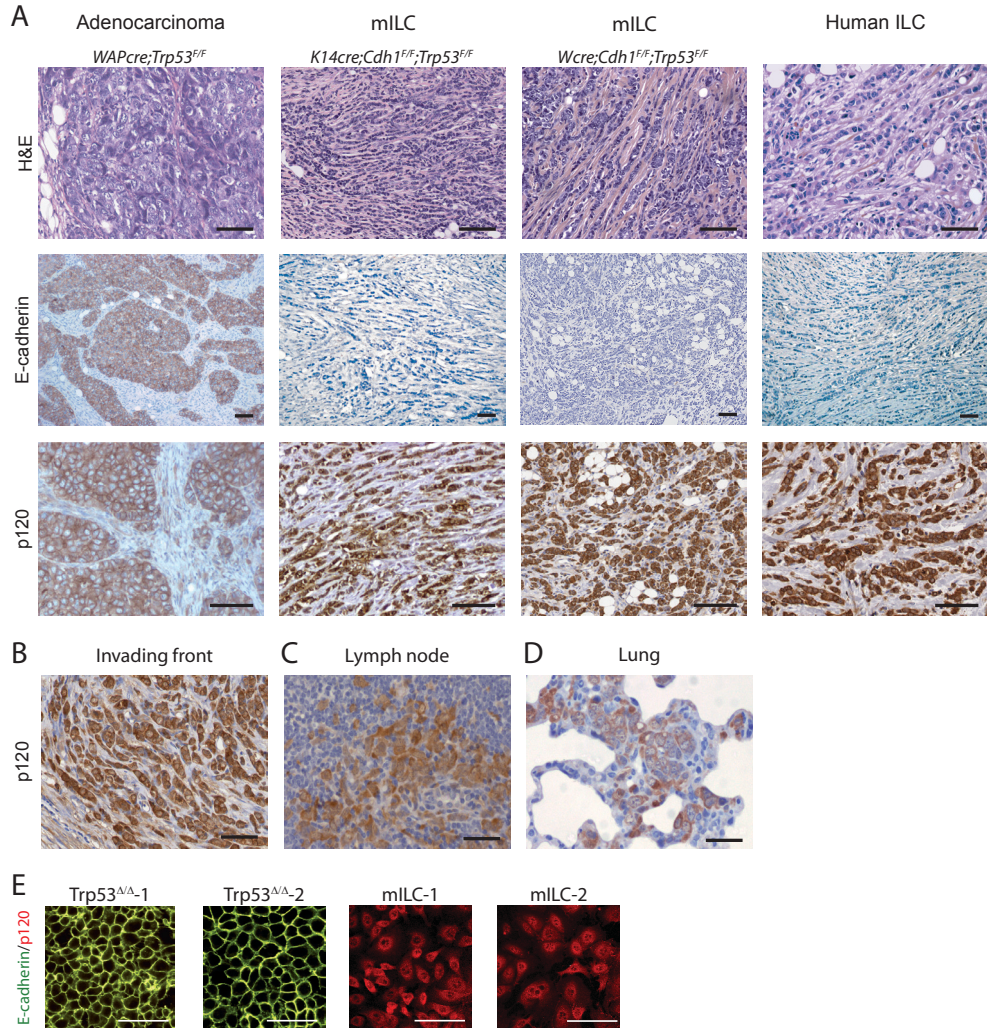


Figure 1

Loss of E-cadherin results in translocation of p120 to the cytosol. **A**) Comparative histochemistry on mammary tumors derived from *Wcre;Trp53^{F/F}* (left panels; adenocarcinoma), *K14cre;Cdh1^{F/F};Trp53^{F/F}* (middle left panels; mouse ILC) and *Wcre;Cdh1^{F/F};Trp53^{F/F}* female mice (middle right panels; mouse ILC) and a classical human ILC sample (right panels). Shown are H&E stainings and immune histochemistry for E-cadherin and p120. Note the striking resemblance of p120 localization in human and mouse ILC. **B-D**) p120 translocation is retained during metastasis of mILC. Invasive cells from a primary mILC (**B**) and examples of distant metastatic mILC in a caudal lymph node (**C**) and lungs (**D**). All samples shown are from *Wcre;Cdh1^{F/F};Trp53^{F/F}* female mice. **E**) Cytosolic localization of p120 in mILC cell lines. *Trp53^{ΔΔ}* (left panels) and mILC cell lines (right panels) were stained for E-cadherin (green) and p120 (red). Bars, 30 μ m.

diagnosis between IDC and ILC, and has been shown to correlate with invasiveness and metastatic capacity,^{222,234,294} we closely examined p120 expression in mILC. Using immune histochemistry, we observed that p120 expression was indeed retained in primary mammary tumors from the *K14cre;Cdh1^F;Trp53^F*²³² and *Wcre;Cdh1^F;Trp53^F*²²⁶ mouse models. While E-cadherin-expressing benign adenocarcinomas showed distinct membrane-localized p120, mILC samples exclusively displayed cytosolic p120, identical to their human analogue (Figure 1A, compare p120 staining of left panel to right panels). Immune histochemistry also revealed that cytosolic expression of p120 was retained in mILC cells that had invaded surrounding mammary tissue (Figure 1B) and in metastatic cells that had colonized a caudal lymph node and the lungs (Figure 1C and D). In mILC cell lines (n=8) p120 also localized to the cytosol (right panels, Figure 1E). Loss of E-cadherin did not result in accumulation of p120, as determined by western blotting and expression profiling of primary tumors and their cell line derivatives (data not shown). Based on molecular weight, we detected concomitant expression of p120 isoforms 1 and 3 in E-cadherin proficient (*Trp53^{Δ/Δ}*) and mILC cell lines (Figure 2B and data not shown).

p120 regulates anoikis resistance of mILC cells

Loss of a functional AJ is a key event that leads to anchorage-independency of mILC cells²³². As p120 is translocated to the cytosol in mILC, we wondered whether it contributed to the regulation of anoikis resistance. To test this, we cloned a previously published siRNA against mouse p120³⁵ into a lentiviral system and established knock-down of both p120 isoforms upon transduction (Figure 2A), which did not inhibit anchorage-dependent proliferation or viability of these cell lines (Figure 2A right graph). By growing cells in suspension and assaying apoptosis we have found a near-perfect correlation between anoikis resistance and *in vivo* metastasis²³², a parallel we did not observe using growth in soft agar (data not shown). Interestingly, anoikis resistance was significantly inhibited upon p120 knock-down in three independent mILC cell lines (Figure 2A left graph), suggesting that p120 facilitates anchorage independent survival. A control shRNA vector targeting human p120 (containing three mismatches compared to the mouse sequence) did neither affect anoikis resistance, nor did it influence anchorage-dependent growth. To determine whether the p120-controlled anoikis resistance also contributes to tumor growth *in vivo*, we performed orthotopic transplantations of luciferase-expressing mILC-1 cells in which p120 was genetically silenced. p120 knock-down in mILC-1 cells resulted in a robust inhibition of tumor growth, implicating that inhibition of anoikis resistance prevented colonization and subsequent outgrowth (Figure 2B). Also, p120 knock-down prevented lung metastasis, whereas control shRNA mILC-1 cells readily metastasized (Figure 2C). These findings indicate that p120 controls the regulation of mILC tumor growth through acquisition of anoikis resistance.

p120 controls activation of Rho-Rock signaling in mILC

Overexpression of p120 has been shown to inhibit the activation of RhoA, possibly by functioning as a RhoGDI, or alternatively, through Vav-2-mediated activation of Rac1^{120,138}. To analyze whether cytosolic p120 regulates RhoA in our system, we assessed actin polymerization, an indirect but functional read-out of active Rho-Rock signaling, in three independent mILC cell lines. Surprisingly, we detected abundant stress fibers using phalloidin staining, which could be substantiated by GTP pulldown assays and western blotting for RhoA (Supplementary Information Figure S2A and B). Furthermore, we observed phosphorylation of Cofilin, which could be specifically inhibited upon administration of the Rock inhibitors Y-27632 or hydroxy (OH-) fasudil (Supplementary Information Figure S2C). We therefore conclude that Rho-Rock signaling is active in the presence of endogenous cytosolic p120 in mILC.

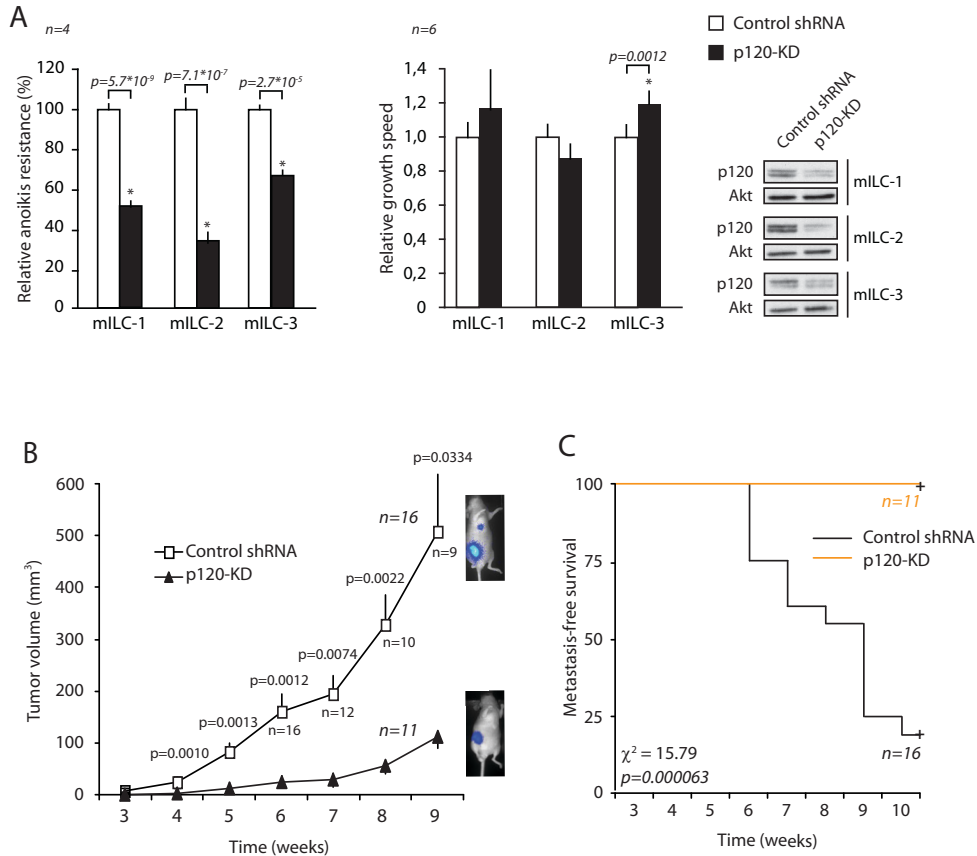


Figure 2

p120 controls mILC anoikis resistance and tumor growth. **A**) p120 regulates context-dependent survival of mILC in vitro. Cells were transduced with viruses carrying mouse p120 shRNAs and grown for four days in the absence (left graph) and presence (right graph) of anchorage, after which anoikis resistance (left) and growth speed (right) were analyzed. Western blotting for p120 is shown to depict the extent of shRNA KD in three independent mILC cell lines. Akt was used as a loading control. Error bars represent standard deviation of triplicate measurements. **B**) Inhibition of p120 reduces mILC growth in vivo. Luciferase-expressing mILC control-shRNA (open squares) or p120-KD cells (filled triangles) were orthotopically transplanted into recipient mice and tumor volume was measured longitudinally. Error bars represent standard error of the mean. **C**) Shown is a Kaplan-Meier metastasis-free survival plot of the mice shown in Figure B, orthotopically transplanted with either mILC-1 control-shRNA (black line) or p120-KD cells (orange line). Recipient animals were followed in time and sacrificed when bioluminescence was detected in the lungs (>500 counts). The controls in B and C represent the same control group as depicted in Figure 5C and D.

Given the fact that RhoGDI function has been attributed to p120, we determined the effect of p120 overexpression on our cells. Only upon induction of high levels of p120 overexpression, mILC cells showed a ‘branching’ phenotype (Supplementary Information Figure S3), which is strongly linked to a p120-mediated inactivation of RhoA¹²⁰. We therefore conclude that mILC cells –depending on the level of exogenous overexpression– conform to the notion that cytosolic p120 may inhibit RhoA.

Next, we set out to determine whether p120 directly affects RhoA and downstream signaling via Rock. Hereto we performed a stable knock-down of p120 and tested the effect on actin polymerization. F-actin was clearly re-organized (Figure 3A; left versus middle panel) and showed a marked reduction in stress fiber formation that was identical to that seen in Rock1 knock-down mILC-1 cells, which we used as a

control (Figure 3A; right panel). These results imply that p120 regulates the actin cytoskeleton, possibly through modulation of Rho and Rock. Despite the effect on the actin remodeling, we did not observe an effect of p120 knock-down on GTP-bound RhoA (Figure 3B), indicating that in mILC p120 does not directly regulate the activity of RhoA. Next, we analyzed Rho-Rock signaling, by probing the phosphorylation status of the two prominent downstream Rock targets Cofilin and MLC upon inhibition of p120. In line with the observed effects on actin depolymerization, we observed a reduction in phosphorylated Cofilin and MLC, which was similar to the inhibition seen in Rock1- knock-down (KD) mILC-1 cells (Figure 3C), suggesting that p120 may regulate anoikis resistance through targets downstream of Rho and Rock. To substantiate the notion that p120 exerts its effect due to its cytosolic localization, we restored p120 to the cell membrane by lentiviral reconstitution of E-cadherin. As expected, relocalization of endogenous p120 resulted in a reduction of phosphorylated MLC (Supplementary Information Figure S4A-D). To uncouple E-cadherin-controlled cell-cell adhesion from the p120-mediated and localization-dependent regulation of Rock signaling, we cloned a lentiviral version of a fusion construct in which the extracellular domain of E-cadherin was replaced by that of the IL2 receptor ²⁹⁷, and transduced mILC-1 cells. Indeed, upon expression of the IL2R-Ecad-cyto fusion protein we observed an inhibition of Rock signaling independent of homotypic adherens junction formation (Supplementary Information Figure S4D). Moreover, these results were functionally substantiated by a decrease in anoikis resistance upon relocalization of p120, using both wild-type E-cadherin and the IL2R-Ecad-cyto fusion (Supplementary Information Figure S4E). Taken together, we conclude that localization of p120 regulates Rock-mediated anoikis resistance in mILC.

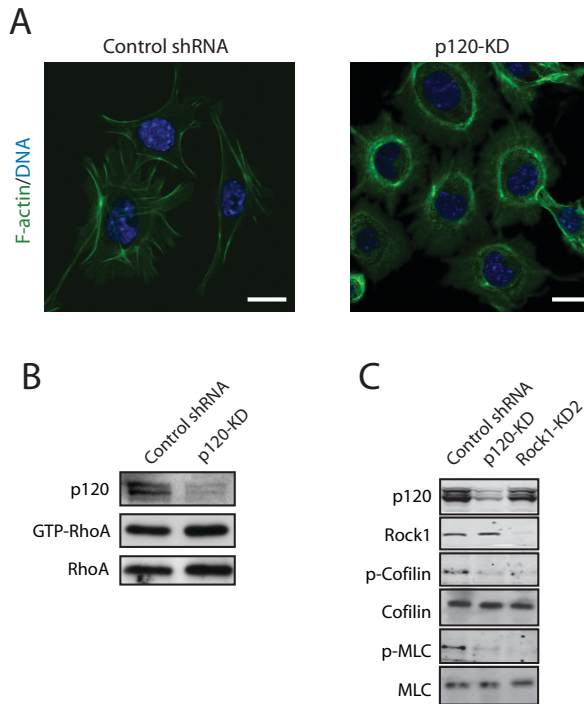


Figure 3

p120 controls activation of Rock signaling in mILC. **A**) p120 controls actin polymerization. Control shRNA (left panel) and p120-KD mILC-1 cells (middle panel) were stained for Filamentous (F)-actin using Alexa-488 conjugated phalloidin (green). Rock1-KD2 mILC-1 cells (right panel) were used as a positive control for actin depolymerization. DNA was visualized using DAPI (blue). Bars, 5 μ m. **B**) Inhibition of p120 does not affect RhoA activity. GST-Rhotekin pull-down assays

were performed on lysates from control shRNA or p120-KD cells and blotted for GTP-bound RhoA and total RhoA. A representative experiment of three is shown. **C**) Rock signaling is regulated by p120. Western blot analysis showing the inhibitory effect of p120 KD on phosphorylation of the downstream Rock effectors Cofilin and MLC. Total Cofilin and MLC are shown as loading controls. Rock1-KD2 mILC-1 cells were used as a positive control for inhibition of Cofilin and MLC phosphorylation.

Cytoplasmic p120 controls Rho-Rock signaling through binding of Mrip

In light of the fact that p120 has been described as a RhoGDI¹²⁰, we set out to identify possible intermediates that would explain active Rho-Rock signaling in the presence of cytosolic p120. To this end, we performed immune precipitations (IP) on endogenous p120 from mILC-1 and Trp53^{Δ/Δ}-2 cells and performed mass spectrometry (MS) on the differential p120 binding partners in mILC cells (Figure 4A). From the resulting data, we identified myosin phosphatase Rho-interacting protein (Mrip), an antagonist of Rho function as a prominent hit (mascot score of 1702). We could substantiate the p120-Mrip interaction upon exogenous expression of hemagglutinin (HA)-tagged Mrip into mILC-1 cells and subsequent co-IP using antibodies against HA (Figure 4B). Moreover, we confirmed our MS data by demonstrating the interaction of the endogenous proteins by co-IP and subsequent western blot analysis (Figure 4C). In conclusion, these biochemical data demonstrate that p120 interacts with Mrip in mILC.

Since Mrip has been shown to exert inhibitory effects on Rho function, and p120 can act as a modulator of Rho-Rock signals, we hypothesized that the interaction between cytosolic p120 and Mrip may impede their inhibitory effects downstream of Rho. If so, overexpression of Mrip should lead to inhibition of Rock signaling in mILC cells. Indeed, lentiviral-mediated overexpression of HA-tagged Mrip in mILC-1 cells resulted in decreased phosphorylation levels of MLC and a reduction in stress fibers (Figure 4D). Subsequent western blotting confirmed these findings as we observed a marked reduction of phosphorylated levels of Cofilin and MLC (Figure 4E). To test the functional consequences of these findings, we transduced mILC-1 cells with HA-tagged Mrip using an increasing multiplicity of infection (Figure 4F). Upon transfer to anchorage-independence we indeed observed that anoikis resistance of mILC cells was gradually decreased with increasing protein levels of Mrip (Figure 4F; left graph). Overexpression of Mrip also reduced anchorage-dependent growth (Figure 4F; right graph), implicating that proximal interference of actin polymerization is not tolerated in the presence of anchorage. Next we set out to test whether inhibition of Mrip would lead to decreased Rock signaling, since both p120 and Mrip can antagonize the Rho-Rock axis. Using stable shRNA-mediated knock-down of Mrip, we observed that Mrip inhibition is not tolerated and results in cell death, independent of cellular context (data not shown and Figure 4G). Since inhibition of p120 or overexpression of Mrip resulted in a decrease of Rock signaling and subsequent anoikis resistance, we reasoned that simultaneous inhibition of p120 and Mrip should restore active Rock signaling and re-establish anoikis resistance. To investigate this, we generated mILC-1 cells carrying a doxycycline (dox)-inducible p120 shRNA construct (p120-KD^{dox}) and transduced these cells with a constitutive Mrip-shRNA-expressing construct (p120-KD^{dox}; Mrip-KD). As expected, culturing p120-KD^{dox}; Mrip-KD cells in the absence of dox resulted in massive cell death (Figure 4G). However, dox-inducible inhibition of p120 fully rescued anoikis resistance in the context of Mrip knock down (Figure 4G). In agreement with these findings we observed that simultaneous knock-down of p120 and Mrip restored Rock signaling activity (Figure 4H). Our data therefore indicate that Rho-Rock signaling is active due to the p120-Mrip interaction, thereby promoting anoikis resistance. Moreover, they imply specificity for the p120 and Mrip siRNA sequences, since inducible inhibition of p120 results in a full reversal of the anoikis phenotype upon knock-down of Mrip.

Rock controls anoikis resistance and in vivo tumor growth of mILC

As Rho and Rock are refractory to pharmacological inhibition, we set out to test whether inhibition of this pathway could influence anoikis resistance of mILC. Inhibition of Rho using C3 transferase or Rock using Y-27632 or OH-fasudil reduced anoikis resistance of mILC cells, whereas identical concentrations had no

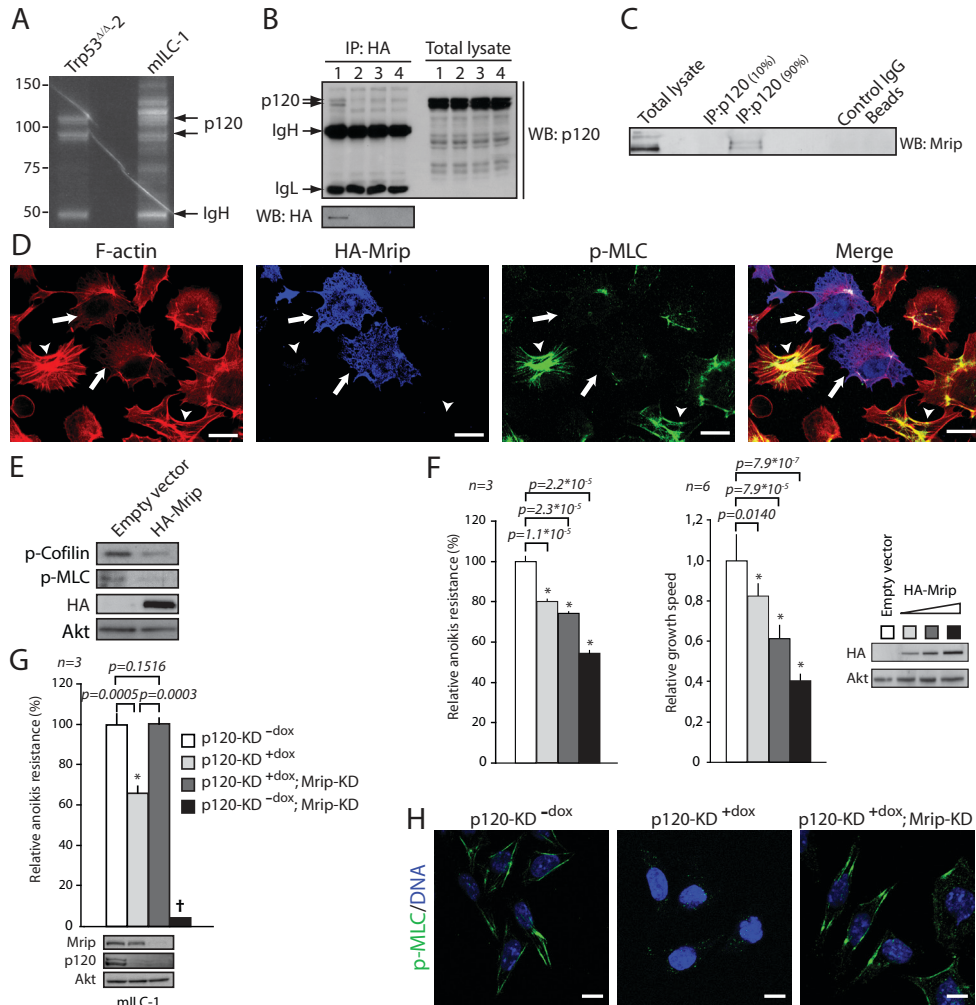


Figure 4

Interaction between p120 and Mrip facilitates Rock-dependent anoikis resistance. **A-C**) p120 interacts with Mrip. **A**) p120 was IPed from Trp53^{Δ/Δ-2} and mILC-1 cells and differential bands were analyzed using mass spectrometry. IgH=Immune globulin heavy chain. **B**) mILC-1 cells were transfected with HA-Mrip, co-IPed using anti-HA antibodies and blotted for p120 (upper panel, left side). (1), Empty vector (2), No vector (3), No transfection (4). Total cell-lysates (TL) were blotted for p120 as input control (upper panel, right side). Lower panel shows HA-Mrip expression. IgL=Ig light chain. **C**) Endogenous p120 was IPed from mILC-1 cells, western blotted and stained for Mrip. Also shown are IgG and beads-only controls. **D** and **E**) Mrip overexpression inhibits Rock signaling. **D**) HA-Mrip-transduced mILC-1 cells were mixed with empty-vector-transduced cells and stained for F-actin (red), HA (blue) and phospho-MLC (green). Transduced cells (arrows), control cells (arrowheads). Bars, 5 μm. **E**) HA-Mrip-transduced cells were assayed for phospho-Cofilin, phospho-MLC and Akt (loading control). **F**) Overexpression of HA-Mrip reduces anoikis resistance and growth of mILC. mILC-1 cells were transfected with HA-Mrip using increasing viral titers, assayed for anoikis resistance (left graph) and growth speed (right graph). Western blotting shows expression levels of HA-Mrip and loading controls (Akt). **G** and **H**) Concomitant knockdown of p120 and Mrip rescues anoikis resistance through restoration of Rock signaling. mILC-1 cells containing dox-inducible shRNA sequences targeting p120 and constitutive Mrip shRNAs were assayed for anoikis resistance (**G**). Activity of Rock signaling was assessed by staining for phospho-MLC (green) Bars, 5 μm (**H**).

inhibitory effects on anchorage-dependent growth (Supplementary Information Figure S2D and Figure 5A). To extend these findings, we tested whether genetic

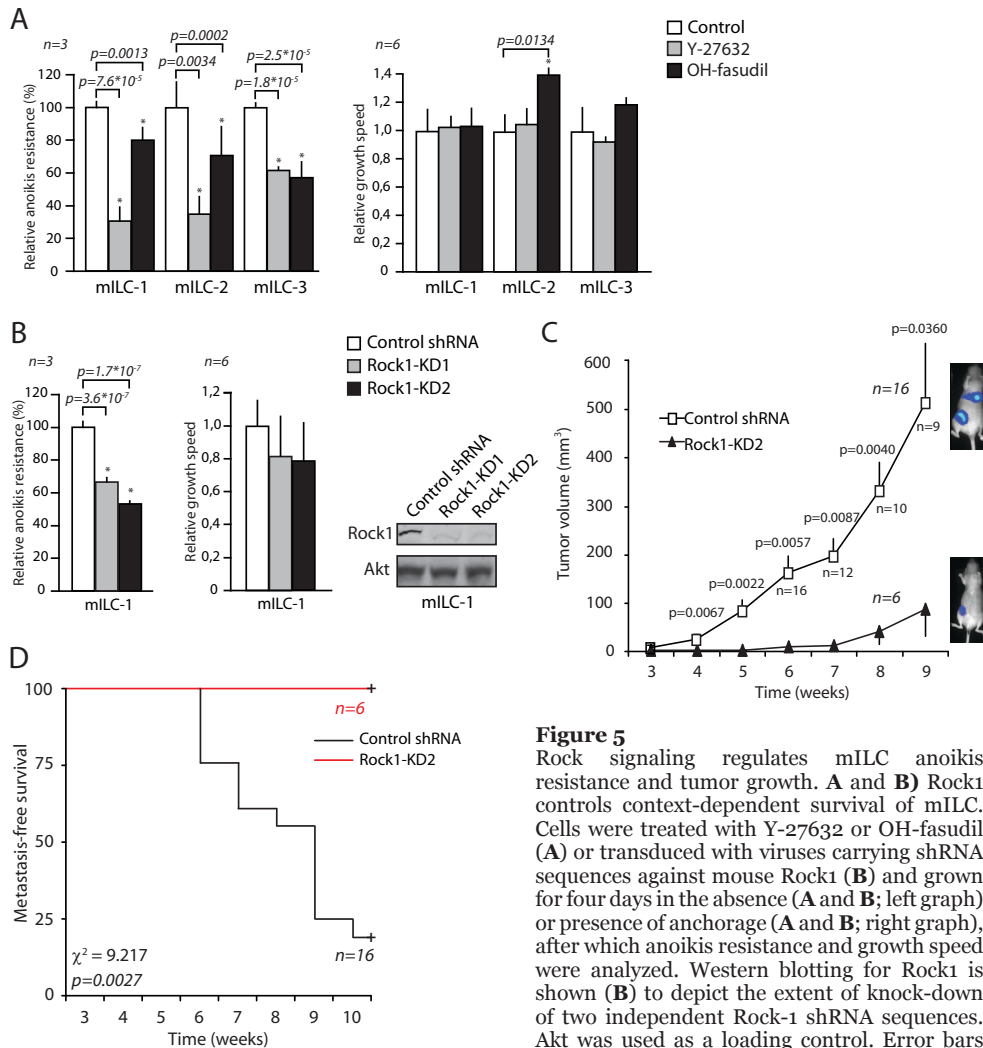


Figure 5

Rock signaling regulates mILC anoikis resistance and tumor growth. **A** and **B**) Rock1 controls context-dependent survival of mILC. Cells were treated with Y-27632 or OH-fasudil (**A**) or transduced with viruses carrying shRNA sequences against mouse Rock1 (**B**) and grown for four days in the absence (**A** and **B**; left graph) or presence of anchorage (**A** and **B**; right graph), after which anoikis resistance and growth speed were analyzed. Western blotting for Rock1 is shown (**B**) to depict the extent of knock-down of two independent Rock-1 shRNA sequences. Akt was used as a loading control. Error bars represent the standard deviation of triplicate measurements. **C**) Inhibition of Rock1 reduces mILC tumor growth. Luciferase-expressing mILC-1 control shRNA (open squares) or Rock1-KD2 cells (filled triangles) were orthotopically transplanted into recipient mice and tumor volume was measured longitudinally. Error bars represent standard error of the mean. **D**) Mice transplanted with either mILC-1 control-shRNA (black line) or Rock1-KD2 cells (red line) were followed in time using bioluminescence to detect metastasis. Shown is a Kaplan-Meier metastasis-free survival plot upon knock-down of Rock1 in mILC-1 cells. Mice were sacrificed when bioluminescence (>500 counts) was detected in the lungs. The controls in **C** and **D** represent the same control group as depicted in Figure 2B and C.

inhibition of Rock1 would result in inhibition of anoikis resistance. Indeed, using two independent shRNAs we observed a strong reduction of anoikis resistance, whereas anchorage-dependent growth was not significantly affected (Figure 5B). To validate these observations in vivo, we orthotopically transplanted Rock1-KD mILC-1 cells in recipient female animals and followed tumor growth and dissemination longitudinally. Similar to the effects seen upon transplantation of p120-KD cells, we observed a retardation of tumor growth compared to control animals (Figure 5C). Moreover, Rock-mediated inhibition of tumor growth also prevented mILC lung metastasis (Figure 5D).

Together, these data illustrate the importance of Rho-Rock signaling in the regulation of mILC anoikis resistance and in vivo tumor growth.

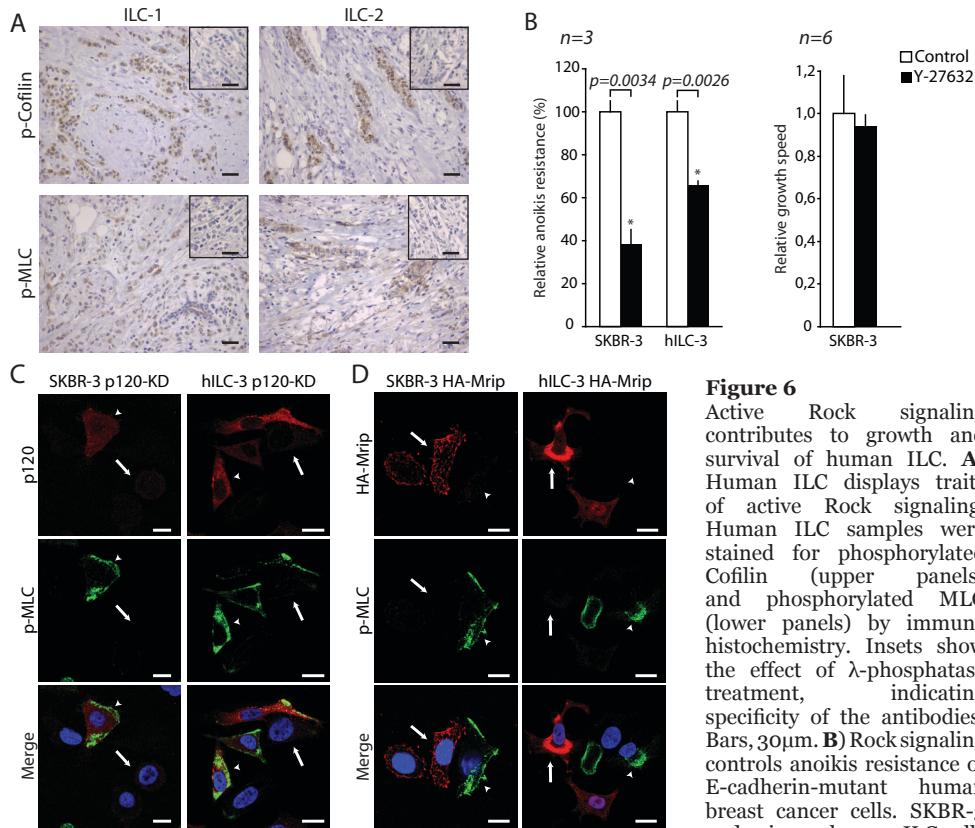
Rock signaling controls anoikis resistance in human ILC

Because findings from our mouse models of human ILC show an important role for Rock signaling in context-dependent tumor growth, we wondered whether this also holds true for its human counterpart. To test this, we started to investigate this by using immune histochemistry on primary ILC tumor tissues. As in mILC, we detected mutual expression of phosphorylated Cofilin and phosphorylated MLC in the majority of human ILC samples (13 of 17 and 11 of 17 respectively) (Figure 6A). When we compared the extent of phosphorylated Cofilin in IDC versus ILC, we found a significant increase from 46% (n=91;IDC) to 77% (n=17;ILC) respectively (Pearson exact χ^2 two-sided; $p < 0.01$), strengthening the notion that activation of Rock may be a feature of ILC. To address whether the activation of Rock has functional implications for ILC survival, we tested the effect of Rock inhibition on anoikis resistance of an E-cadherin mutant, luminal-type cell line (SKBR-3) and on primary human ILC cells derived from pleural effusion fluids (hILC-3). As in our mouse model, we observed that Y-27632 induced a significant decrease in anoikis resistance of SKBR-3 and hILC-3 cells (Figure 6B). Anchorage-dependent growth of SKBR-3 was not affected by Y-27632 (Figure 6B), which is in agreement with data obtained in our mILC lines. In concordance with our findings in mILC, we also observed an inhibition of anoikis resistance when SKBR-3 was treated with C3 and OH-Fasudil (Supplementary Information Figure S5). Because hILC-3 does not proliferate under adherent culture conditions (data not shown), we could not assess anchorage-dependent growth. To confirm that p120 regulates Rock signaling analogous to our mouse model, we transduced SKBR-3 and hILC-3 cells with lentiviruses expressing p120 shRNA and probed for phospho-MLC. Indeed, p120 knock-down resulted in an inhibition of MLC phosphorylation (Figure 6C). Moreover, transduction of HA-tagged Mrip resulted in reduced levels of phospho-MLC (Figure 6D), suggesting that human ILC also functionally depends on the p120-Mrip interaction for activation of Rock signals. In conclusion, our findings confirm that human ILC depends on active Rock signals for the regulation of anchorage-independence. Furthermore, they corroborate our finding that the p120-Mrip interaction facilitates active Rock signaling, which is required for anchorage-independent survival.

Discussion

Clinically, p120 localization can be used as a determinant in the differential diagnosis between ductal and lobular tumor types²²². While cytosolic p120 coincides with E-cadherin loss in ILC, IDC shows an expression pattern that seems unrelated to E-cadherin and β -catenin status, including complete loss of p120 expression in approximately 10% of the cases²²³. Since early loss of E-cadherin is causal to ILC formation, we think this evokes biochemical signals that differ from inactivation of E-cadherin during later stages.

Our data demonstrate that cytosolic p120 exerts oncogenic properties that become eminent in the absence of anchorage. We show that upon loss of E-cadherin, p120 translocates to the cytosol where it can bind the inhibitor of Rho function Mrip, thereby presenting novel insight on how p120 may facilitate anoikis resistance through indirect activation of the Rho-Rock signaling pathway. Several lines of evidence concur with the notion that p120 plays an important role in regulating anchorage-independence of cancer cells. For instance, it was recently shown that p120 controls growth in soft agar of E-cadherin-expressing MDCK cells, which rely on overexpression of exogenous dominant active oncogenes such as Src or Rac for anchorage-independence. Interestingly, p120 knock-down in Src or Rac-



absence of anchorage and treated with 10 μ M Y-27632. After four days anoikis resistance was determined. Error bars represent standard deviation of triplicate measurements. **C)** Loss of cytosolic p120 causes decreased MLC phosphorylation in human ILC. SKBR-3 (left panel) and primary hILC-3 cells (right panel) were transduced with viruses carrying shRNA sequences against human p120. Cells were stained for DNA using DAPI (blue), p120 (red) and p-MLC (green). Arrowheads indicate nontransduced cells, arrows show transduced p120-KD cells; note the reduction in phosphorylated MLC upon p120 KD. Bars, 5 μ m. **D)** Overexpression of HA-Mrip causes decreased MLC phosphorylation in human ILC. SKBR-3 (left panel) and hILC-3 cells (right panel) were transduced with viruses carrying HA-tagged Mrip. Cells were stained for DNA using DAPI (blue), HA (red) and p-MLC (green). Arrows indicated HA-Mrip expressing cells, arrowheads show nontransduced cells. Bars, 5 μ m.

transformed MDCK cells inhibited anchorage independent growth in soft agar, an effect that could be rescued by Rock inhibition using Y-27632²³⁶. Furthermore, recent data showed that in MDA-MB-231 (MM231; a human IDC cell line in which E-cadherin is silenced by methylation), p120 also controls anchorage-independence although in these cells, it is controlled by a Rac1-dependent activation of the MAPK pathway. Here, it was hypothesized that E-cadherin loss during tumor progression may relieve the negative regulation of Ras through p120-dependent activation of Rac in a cell type-specific manner²²⁷. Since it is assumed that active Rac counterbalances the activity of Rho¹³⁰, these findings imply that under these settings and in these cell types, active Rho-Rock signaling does not induce anchorage-independence. As expected, when cultured in the absence of anchorage and treated with Y-27632, MM231 cells did not show decreased anoikis resistance (data not shown). Moreover, Rac signaling does not appear to be the driver of anoikis resistance of mILC because dominant-negative-RacN17 or the Rac inhibitor NSC-23766 did not influence anchorage-independent survival of mILC (data not shown). Moreover, we have no

indication that p120 interacts with Cadherin-11 in mILC based on our Mass Spec analyses, clearly indicating the differences in model systems studied. We have refrained from using soft agar as a substrate for the anoikis experiments because it does not provide predictive value for in vivo metastasis when using our mouse cell lines. An explanation for this could reside in the fact that soft agar often contains denatured collagen, which is known to trigger binding of $\alpha 5\beta 1$ and αv integrins and subsequent activation of Rac through exposed RGD binding²⁹⁸⁻³⁰⁰. It is still unclear how Rho is activated in ILC. Given our finding that inhibition of p120 and Rock leads to context-dependent effects on tumor cell survival, we think that upon transition to anchorage independence, cells undergo morphological changes that may activate Rho and its downstream targets³⁰¹. Alternatively, the activation of Rho in ILC may also be triggered by (autocrine) activation of receptor-mediated signaling^{128, 302, 303}. We anticipate that the level and mode of activation may be different in the context of Rho-mediated induction of apoptosis, that can be triggered by strong exogenous cues, such as LPA and ethanol^{304, 305}. Interestingly, Rock signaling can also be activated upon induction of apoptosis. In this scenario, activation of caspases promote Rho-independent cleavage and constitutive activation of Rock1, leading to membrane blebbing and disruption of nuclear integrity.³⁰⁶⁻³⁰⁸ In contrast, human ILC and mouse ILC (Cdh1 Δ/Δ ;Trp53 Δ/Δ) control anoikis resistance by continuous activation of Rho-dependent Rock signaling (Supplementary Figure 2). We therefore think that the difference in functional outcome as a result of actin-myosin contractility during apoptosis may either be due to differences in the level of Rock1 activation or that activation of Rock1 by apoptosis-inducing cues (such as FasL or a combination of TNF α and cycloheximide) may confer modulation of additional pathways that facilitate membrane blebbing and relocalization of fragmented DNA into apoptotic bodies. Finally, while our data evidently show that cytosolic p120 regulates Rock signals and subsequent anoikis resistance in mILC, we cannot exclude the possibility that loss of p53 may affect Rock signaling when concomitantly inactivated with E-cadherin. Regardless the exact mechanism, it is clear that signaling events downstream of p120 show differences based on context and cell-type.

We show that in contrast to benign E-cadherin expressing Trp53 Δ/Δ cells, the p120-Mrip interaction is apparent in metastatic E-cadherin-deficient (mILC) cells, where it provides a rationale for the manifestation of active RhoA in the presence of cytosolic p120. It furthermore offers an explanation for the cell-type specific differences regarding the activation of pathways downstream of p120. We anticipate that at least two mechanisms could account for the presence of active Rho-Rock signaling in ILC. First, binding of p120 to Mrip may render p120 incapable of exerting its established Rho modulating function. Unfortunately we could not verify this option due to severe cell death upon Mrip knock-down, which could be either caused by a strong inhibition of actin dynamics, or an artificial hyper activation of the Rock pathway. Second, we rationalize that the p120-Mrip interactions may prevent Mrip from inhibition of downstream Rho signals^{292, 294, 309}, thus promoting anoikis resistance.

In conclusion, our data establishes a functional link between early loss of E-cadherin, cytosolic translocation of p120, and subsequent Rock-mediated regulation of anchorage-independent tumor growth of ILC. Using our mouse models of human ILC, we have detected active Rho-Rock signaling in the presence of endogenous cytosolic p120 as a consequence of the interaction of cytosolic p120 with Mrip. Since both p120 and Mrip display Rho-Rock-inhibitory functions, it provides an alternative and novel mechanism for the regulation of anoikis resistance in metastatic breast cancer. In the presence of anchorage, the p120-mediated activation of Rho and Rock will be overridden by ECM-mediated integrin crosslinking, which will provide potent outside-in survival signals. Upon the transition to anchorage-independence, the integrin-mediated survival signals are lost and because cytosolic p120 binds to Mrip, Rock signaling remains active and thus drives anoikis resistance. A schematic

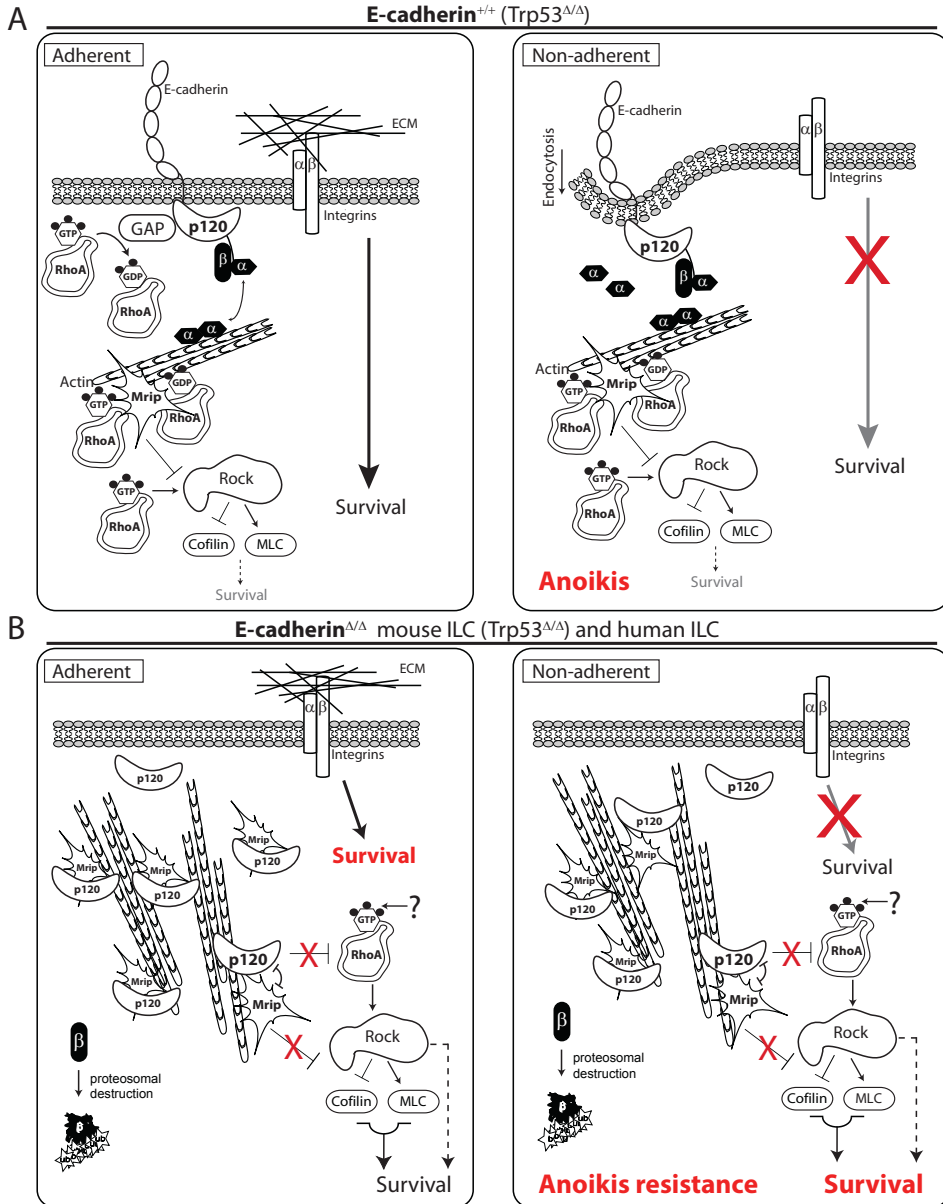


Figure 7

Model for the p120-mediated regulation of anoikis resistance in ILC upon loss of E-cadherin. **A**) Under benign conditions and in the presence of a functional adherens junction, Rho levels and cellular survival mechanisms are balanced through a fine-tuned equilibrium of protein interactions and signaling pathways (left panel). When cells are deprived of extra cellular matrix (ECM)-integrin interactions, a potent outside-in survival signal is impeded, resulting in anoikis because of a lack of compensatory survival mechanisms (right panel). **B**) Upon early mutational inactivation of E-cadherin in human ILC and mouse ILC ($Cdh1^{\Delta/\Delta}; Trp53^{\Delta/\Delta}$), the adherens junction is disassembled, resulting in proteasomal degradation of β -catenin. More important, p120 translocates to the cytosol where it binds Mrip, an antagonist of Rho-Rock function. Since p120 has RhoGDI functions, this interaction will alleviate the inhibitory functions of both p120 and Mrip, leading to active Rho-Rock signaling by an unknown mechanism. Although activation of Rho and Rock may have a positive effect on cellular survival in the presence of ECM, these signals will be overridden by powerful integrin-mediated survival cues (left panel). However, when ILC cells transfer to anchorage-independence, the survival signals that emanate from Rho and Rock will rescue the cells, leading to anoikis resistance of ILC (right panel).

working model showing the effects of p120 delocalization, the consequences on downstream Rho-Rock signaling and subsequent anoikis resistance is depicted in Figure 7. Our model favors a mechanism whereby during ILC tumor etiology, endogenous p120 has reached an equilibrium with Mrip in such a manner that the net result is an active Rho-Rock signaling pathway that regulates anchorage-independent tumor growth. Because Rock signaling is active in the majority of ILC, and Rock is susceptible to pharmacological inhibition, we reason that the context-dependent manner by which this pathway regulates tumor cell survival, provides a window of opportunity for the design of novel clinical intervention strategies. We foresee that inhibition of Rock may be combined with conventional chemotherapy to better treat ILC in the metastatic setting.

Methods

Cell culture, antibodies and inhibitors

Mouse mILC-1 ($Cdh1^{\Delta/\Delta}; Trp53^{\Delta/\Delta}$) and $Trp53^{\Delta/\Delta}$ cell lines were derived from primary tumors that developed in $K14cre; Cdh1^{F/F}; Trp53^{F/F}$ and $K14cre; Trp53^{F/F}$ female mice respectively²³². Cell lines mILC-2 and mILC-3 were generated from primary mammary tumors from $Wcre; Cdh1^{F/F}; Trp53^{F/F}$ female mice²²⁶. Cells were cultured as described²³². Human breast cancer cell line SKBR-3 was cultured in DMEM-F12 (Invitrogen) containing 6% fetal calf serum, 100 IU/ml penicillin and 100 μ g/ml streptomycin. Human primary ILC material was obtained from pleural effusion fluids from a female patient suffering from metastatic ILC. Mononuclear cells were isolated by Ficoll-Paque gradient centrifugation. Purity of the clinical sample was >90%, based on the co-expression of epithelial cytokeratins and estrogen receptor. Recombinant Wnt3a was kindly provided by R. Nusse (Howard Hughes Medical Institute, Stanford University, USA) The following antibodies were used: mouse anti-p120 (610133 BD Biosciences), TRITC-conjugated p120 (610137 BD Biosciences), mouse anti-E-cadherin (610182 BD Biosciences), mouse anti- β -catenin (610154 BD Biosciences), mouse anti-dephospho β -catenin (ALX-804-259 Alexis Biochemicals), mouse anti-Rock1 (611136 BD Biosciences), mouse anti-RhoA (SC-418 Santa Cruz Biotechnology), goat anti-Akt1 (C-20; SC-1618 Santa Cruz Biotechnology), rabbit anti-Erk1 (C-16; SC-93 Santa Cruz Biotechnology), rabbit anti-phospho cofilin (Ser3 77g2; 3313), rabbit anti-phospho-MLC2 (Ser19; 3671), rabbit anti-cofilin (3312), rabbit anti-MLC2 (3672) (all Cell Signaling Technology), mouse anti-HA (12-CA5; a kind gift from B. Burgering; UMC Utrecht, the Netherlands); rabbit anti-HA (HA11 16B12; MMS-101R; Covance), rabbit anti-Mrip (a kind gift from W. Moolenaar; Netherlands Cancer Institute, Amsterdam, the Netherlands); Alexa Fluor-488 and Alexa Fluor-633 conjugated phalloidin (both Invitrogen). Secondary antibodies: Alexa Fluor-488, 561 and 633-conjugated anti-mouse and anti-rabbit antibodies (Molecular probes). The following inhibitors were used: Y-27632 (Sigma); 10 μ M all assays, Hydroxy Fasudil (Sigma) (60 μ M), and cell-permeable C3-transferase (Cytoskeleton); 0.02 μ g/ml (mouse cell lines), 0.0025 μ g/ml (human cell lines).

Immune histochemistry and fluorescence

Tissues were isolated and fixed in 4% formaldehyde for 48 hours. Tissues were dehydrated, cut into 4 μ m sections and stained with hematoxylin and eosin. For single staining, fixed sections were rehydrated and incubated with primary antibodies. Endogenous peroxidases were blocked with 3% H_2O_2 and stained with biotin-conjugated secondary antibodies, followed by incubation with HRP-conjugated streptavidin-biotin complex (DAKO). Substrate was developed with DAB (DAKO). For immune fluorescence, cells were grown on cover slips and fixed in 1% paraformaldehyde/PBS for 10 minutes. Cells were permeabilized using 0.3% Triton-X100/PBS and subsequently blocked using 5% BSA (Roche). Cover slips

were incubated with primary antibodies in 1% BSA for 60 minutes. Then, cells were incubated in 1% BSA with secondary antibodies for 30 minutes. DNA was stained with DAPI for 5 minutes (Molecular Probes) and cover slips were mounted onto object glasses using vectashield mounting medium (Vector laboratories). Cells were analyzed by confocal laser microscopy using a Zeiss LSM510 META (Carl Zeiss).

Constructs, viral production and transduction

For stable knock-down of p120, we cloned sequences directed against mouse (5' GCCAGAAGTGGTGC GAATA 3') and human (5' GCCAGAGGTGGTTCGGATA 3') p120 that were described³⁵. Mrip RNAi sequence (5' GAGCAAGTGTTCAGAACTGC 3') was derived from²⁹⁴. RNAi sequences against mouse Rock1 (1:5' TGTCGAAGATGCCATGTTA 3' 2: 5' GACCTTCAAGCACGAATTA 3') were derived from an ON-TARGET SMARTpool (Dharmacon), synthesized as shRNA sequences with *Bgl*II/*Cla*I and *Xho*I overhangs, and cloned into pSUPER³¹⁰. Next, the H1 polymerase promoter-shRNA sequence cassette was removed with enzymes *Bgl*II/*Cla*I and *Eco*RI, and ligated into the lentiviral vector pLVTHM³¹¹. J. Collard (Netherlands Cancer Institute, Amsterdam, the Netherlands) provided the GST-RBD plasmid. H. Clevers (Hubrecht Institute, Utrecht, The Netherlands) provided the β -catenin (*Cttnb1*) expression plasmid. HA-tagged Mrip was provided in pCDNA3 by W. Moolenaar (Netherlands Cancer Institute, Amsterdam, the Netherlands)²⁹¹. *Mlu*I and *Nhe*I sites were added 5' and 3' respectively by means of phusion PCR. *Mlu*I-HA-Mrip-*Nhe*I was subsequently cloned into the lentiviral expression vector pLV.bc.puro (a kind gift from C. Löwik; LUMC, Leiden, the Netherlands). The pCDNA3.IL2R-hEcadTail construct (a kind gift from A. Yap; University of Queensland, Brisbane, Australia) was digested with enzymes *Eco*RV/*Xba*I to excise the IL2R-Ecadherin fusion, which was subsequently cloned into the lentiviral expression vector pLV.bc.puro yielding pLV.IL2R-hEcadTail.puro (IL2R-Ecad-cyto). p120-1A (*Ctnd1*) was released from pEGFP-p1201A (a kind gift from J. Daniel, McMaster University, Ontario, Canada) by PCR using Phusion taq polymerase and cloned into *Eco*RV-digested pCDNA3.1(+) (Invitrogen). The pmCherry-H2B expression plasmid was a kind gift from S. Lens (UMC Utrecht, the Netherlands). The inducible RNAi system was obtained from TaconicArtemis (TaconicArtemis, Köln, Germany). Oligo's were designed as follows: *Bbs*I-shRNA-*Xho*I and cloned *Bbs*I/*Xho*I into the pH1tet-flex transfer vector. The HitetO-shRNA cassette was amplified by means PCR using Phusion DNA polymerase and primers with *Pac*I sites. The resulting product was digested with *Pac*I and cloned into FH1tUTG³¹². Lentiviral particles were produced in Cos-7 cells using third-generation packaging constructs²⁷⁴. Supernatant containing viral particles was harvested 48 hours after transfection, passed through a 45 μ m filter and concentrated 10 to 150-fold by centrifugation (175,000g; 150 min). mILC cells were transduced overnight in the presence of 4 μ g/ml polybrene (Sigma). Doxycyclin-inducible cell lines were treated with 0.1 μ g/ml doxycycline for 4 days, which was refreshed every 2 days.

Wnt signaling reporter assay

Analysis of canonical Wnt signaling done using Wnt reporter assays as described³¹³.

Anoikis resistance and colony formation assay

For determination of anoikis resistance, cells were plated and cultured in the absence of EGF and Insulin at a density of 100,000 or 20,000 cells per well in a 6 or 24-well ultra-low cluster polystyrene culture dish (Corning) respectively. After 4 days, cells were harvested and the percentage of anoikis resistant cells was determined by staining with FITC or APC-conjugated Annexin-V (IQ Products) and ToPro-3 (Molecular Probes) and analyzed by FACS. Anoikis resistant cells were defined as the Annexin-V and ToPro-3 negative population. For quantification of growth under

adherent conditions, cells were plated at a density of 20,000 cells in a 24-well culture plate (Corning) and cultured in the absence of EGF and Insulin for 4 days. Cells were subsequently fixed with 100% methanol, stained using 0.2% crystal violet (Sigma) and washed with water to remove nonincorporated dye. Incorporated crystal violet was eluted using acetic acid 10% (v/v) and quantified with a spectrophotometer at 560nm (Biorad).

Rho pull down, Immune precipitation, western blotting and mass spectrometry

Cells were lysed in 500 μ l buffer containing 0.5% NP-40, 50 mM Tris-Cl; pH 7.4, 150 mM NaCl, 5 mM MgCl₂, 10% glycerol (all Sigma) and protease inhibitors (leupeptin 10 μ g/ml; apoptin 10 μ g/ml; PMSF 1 μ g/ml) (Roche). Next, Rho-GTP was isolated from the lysates using the Rho Binding Domain (RBD) of the human Rhotekin protein²⁷⁵ fused to glutathione-S-transferase GST (residues 7-89) and coupled to glutathione agarose beads (Sigma). Cells were grown to 80% confluence, washed twice with calcium-containing PBS and directly lysed in lysis buffer containing 50mM Tris-Cl (1M pH 8.0), 1mM EDTA, 150mM NaCl (Riedel-de Haën), 5mM NaF (Fluka), 1% NP40, 2mM NaVO₃ and 1 tablet/50ml Complete (Roche). Lysates were pre-cleared using protein A/G agarose beads (Millipore). Supernatant was incubated with antibodies for 16 hr at 4°C and protein A/G beads were added to pull down the complexes. After removal of the unbound fraction, the beads were extensively washed, boiled for 5 min in sample buffer, and western blotted. For phosphorylation assays, cells were lysed directly in buffer containing 50 mM Tris-Cl (pH 6.8), 0.5% β -mercaptoethanol, 2% SDS, 0.005% bromophenolblue and 10% glycerol (all Sigma). Samples were heated for 5 min. at 100°C, and proteins were separated using standard PAGE protocols and blotting as described²⁷⁶. Protein extracts p120-immune-precipitated from mILC-1 and Trp53 ^{Δ/Δ} cells were subjected to SDS-PAGENUPAGE 4-12% gradient gel (Invitrogen). Protein bands were stained using SYPRO Ruby (Invitrogen) and visualized under UV light. mILC-1 and Trp53 ^{Δ/Δ} lanes were compared and differentially expressed bands were cut. Peptides were extracted with 10% formic acid (BDH) and subjected to nanoscale liquid chromatography tandem mass spectrometry (nanoLC-MS/MS) analysis, performed on an Agilent 1100 HPLC system (Agilent technologies) connected to an LTQ Linear Ion Trap Mass Spectrometer combined with an Orbitrap (ThermoFisher)³¹⁴. Spectra were searched against the IPI (International Protein Index) mouse database using Mascot software version 2.2.0 (www.matrixscience.com). Peptides with mascot score >35 were considered for further analysis.

Orthotopic transplantations

Recipient female nude mice (Hsd:Athymic Nude-Foxn1^{nu}; Harlan) were anaesthetized with IsoFlo (isoflurane; Le Vet Pharma). The 4th (inguinal) mammary gland was exposed and approximately 10,000 luciferase-expressing mILC cells were injected using a 10 μ l Hamilton syringe. 100 μ l (0.03mg/ml) Temgesic (Buprenorphine) was injected subcutaneous as analgesic treatment. After a recovery period of two weeks, mice were anaesthetized with IsoFlo, injected ip with 225 μ g/g body weight *n*-luciferin (potassium salt; Biosynth AG) and imaged on a Biospace ϕ bioluminescence imager (Biospace Lab). Tumor development was measured using a digital caliper (Mitutoyo) on a weekly basis. Mice were sacrificed when tumor volume reached >500 mm³, or if mice presented detectable lung metastases using bioluminescence.

All animal experiments were performed in accordance with the guidelines of the University Animal Experimental Committee, University Medical Center Utrecht, The Netherlands.

Statistical Analyses

For colony formation and anoikis assays, statistical significance was calculated using the Student's T-test (2-tailed), showing measurements of at least three independent experiments. Statistical significance of the genetic inhibition experiments in mice was calculated using the Mann Whitney test, error bars represent standard error of the mean. Error bars in all other experiments represent standard deviation of at least triplicate measurements. For metastasis-free survival analysis, the Log-Rank test was used. We considered p-values of $p < 0.05$ as statistically significant.

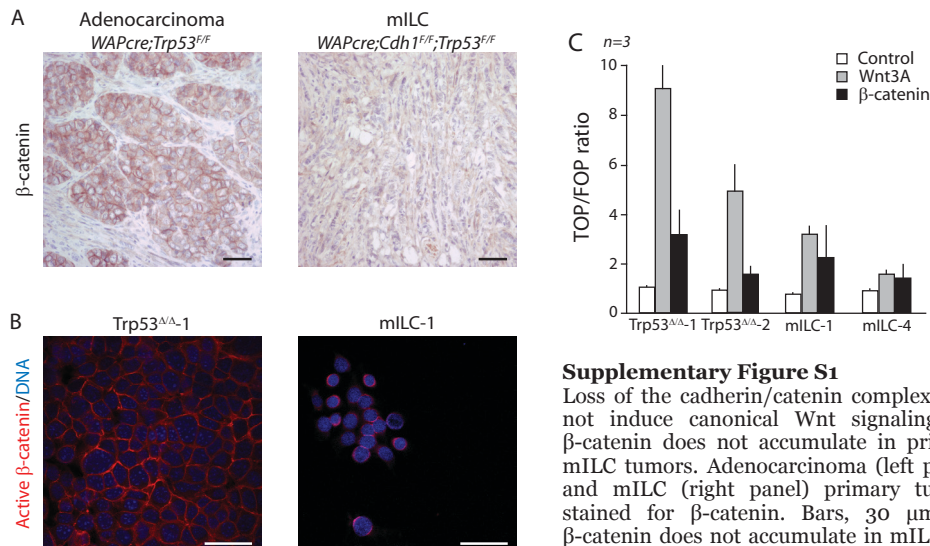
Acknowledgements:

We wish to thank W. Moolenaar for the HA-tagged Mrip expression construct and Mrip antibodies. We express our gratitude to J. Hendriksen, A. Jaspers and M. Vromans for excellent technical support. Members of the Kranenburg, van Rheeën, and Experimental Oncology lab are acknowledged, for help and fruitful discussions. We thank J. Collard for providing the GST-RBD plasmid, R. Nusse for recombinant Wnt3a, H. Clevers for providing the β -catenin expression plasmid, A. Yap for the IL2R-hEcadTail fusion construct, S. Lens for the pmCherry-H2B construct and J. Daniel for the pEGFP-p1201A construct. The Biomolecular Mass Spectrometry and Proteomics group at Utrecht University is acknowledged for support, and J. de Rooij and D. Pirone are acknowledged for critical review of the manuscript. We are also indebted to the animal facility and the UMC biobank. This work was supported by the UMC Cancer Center, grants from the Netherlands Organization for Scientific Research (NWO-VENI 016.056.135 to PWBD, NWO-VIDI 917.96.318 to PWBD and NWO-VIDI 917.36.347 to JJ), the Dutch Cancer Society (NKI 2006-3486 to JJ) and Pink Ribbon.

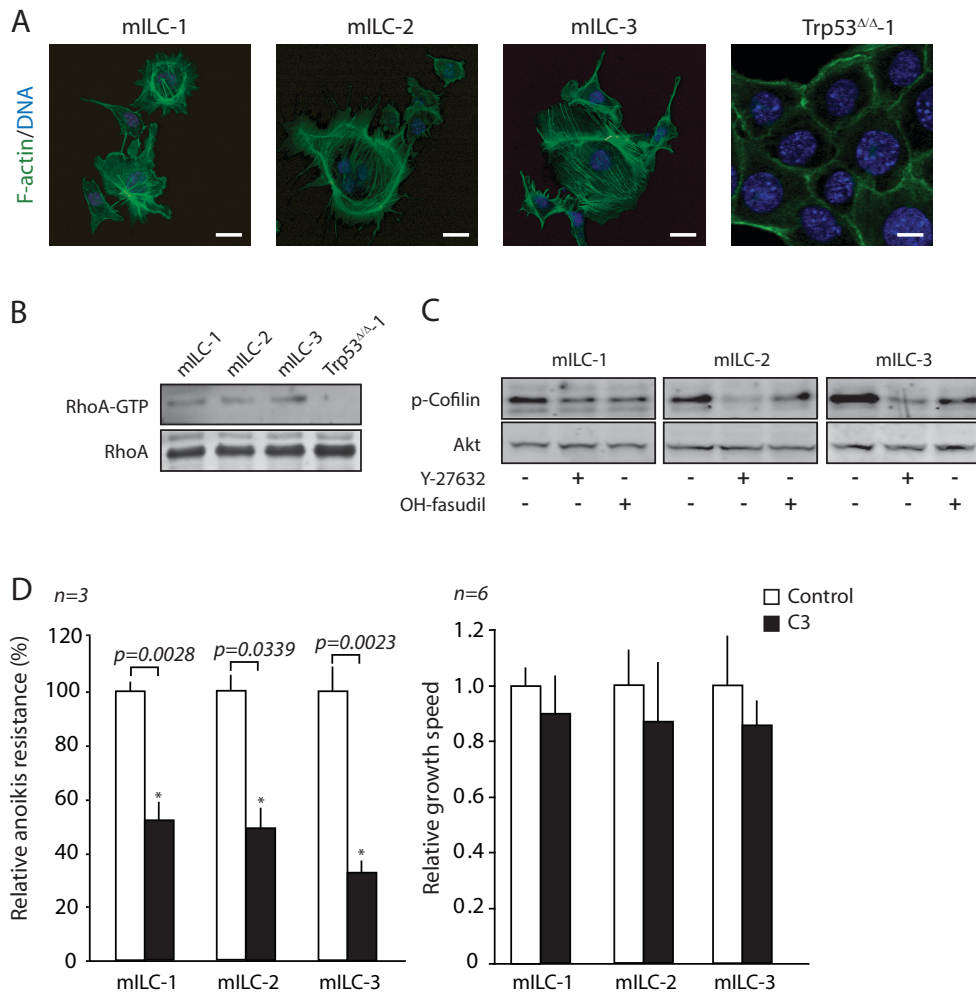
Author Contributions

RCJS and PWBD designed the experiments. RCJS, JHIH, PWBD and EJv executed the in vitro experiments. MA performed all in vivo experiments with help from JMLR. VAH attained and analyzed the mass spectrometry data. JSV carried out the statistical analyses. PG executed the immune histochemistry and PJD and PWBD analyzed the results. EEV and JJ critically reviewed the experiments and paper. RCJS and PWBD wrote the paper.

Supplemental data

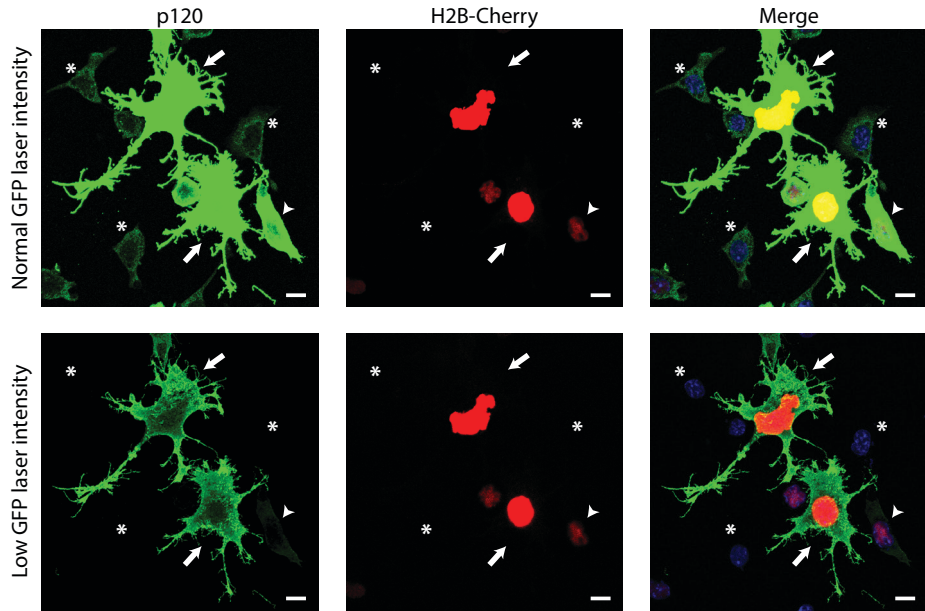


lines. Trp53^{Δ/Δ}-1 (left panel) and mILC-1 cells (right panel) were stained for active β-catenin (red) and DNA was visualized by ToPro3 (blue). Bars, 30 μm. **C**) Canonical Wnt signaling is not induced in mILC cells. mILC and Trp53^{Δ/Δ} cells were transfected with TCF/LEF-luciferase reporter plasmids (TOP) or a scrambled, non responsive version thereof (FOP), and assayed for luminescence (white bars). The TOP/FOP ratio (TOP over FOP luminescence counts) is shown on the Y-axis. Also shown are the effects of administration of exogenous Wnt3a (black bars) or β-catenin transfection (grey bars).



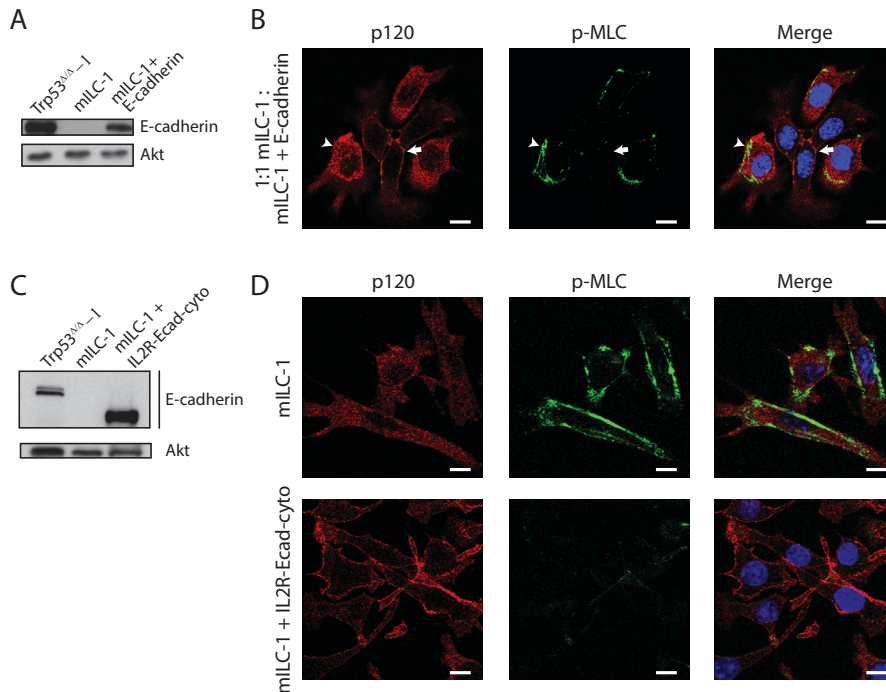
Supplementary Figure S2

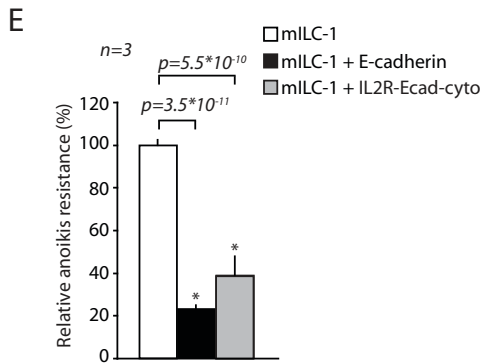
mILC cells show active Rho in the presence of cytosolic p120. **A**) Hallmarks of Rho activity in mILC. Cells were stained for Filamentous (F)-actin using Alexa-488 conjugated phalloidin. Note the presence of F-actin (green) in mILC cells. DNA was visualized by DAPI (blue). Bars, 5 μm. **B**) Rho activity in mILC cells. GTP-bound RhoA levels were determined using a GST-Rhotekin pulldown assay. Total RhoA levels are shown as loading control. **C**) Rock signaling is activated in mILC. mILC cells were treated with the Rho Associated Kinase (Rock) inhibitors Y-27632 or hydroxy (OH-) fasudil and the levels of phosphorylated Cofilin were determined using western blotting. Akt served as a loading control. **D**) Rho signals control anoikis resistance of mILC cells. mILC cells were grown for four days in the presence of the Rho inhibitor C3 (0,02mg/ml) and assayed for anoikis resistance (left graph), or growth speed (right graph). Error bars represent the standard deviation of triplicate measurements.



Supplementary Figure S3

Overexpression of p120 results in a branching phenotype in mILC cells, indicative of RhoA inhibition. mILC-1 cells were transfected with p120-1A and H2B-Cherry expression plasmids. Cells were stained for p120 (green) and DNA using DAPI (blue); H2B-Cherry is depicted in red. The upper panel shows normal GFP laser intensity in order to visualize endogenous p120 in the non-transfected cells; the lower panel shows low GFP laser intensity to visualize high p120 overexpressing cells. Cells with high p120 overexpression (arrows) show a branching phenotype correlated to RhoA inhibition; overexpression of lower amounts of p120 (arrow head) does not result in the branching phenotype; Non-transfected cells are marked with (*) Bars, 5 μ m.

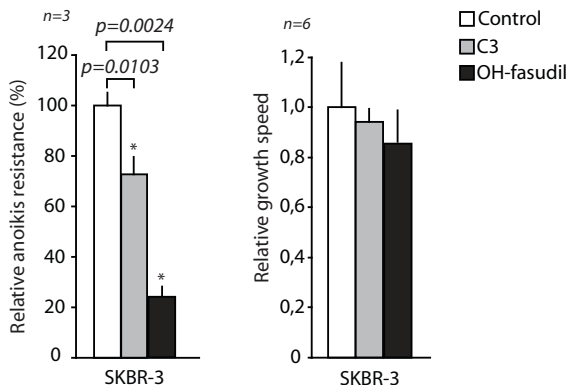




p120-mediated and localization-dependent regulation of Rock signaling. mILC-1 cells were transduced with IL2R-Ecad-cyto lentivirus. Expression levels are shown by western blotting (C). **D**) mILC-1 (upper panels) and IL2R-Ecad-cyto expressing mILC-1 cells were stained for p120 (red), p-MLC (green) and DNA using DAPI (blue) note the decrease of phospho-MLC upon p120 relocalization. Bars, 5µm. **E**) Re-localization of endogenous cytosolic p120 upon expression of E-cadherin restores anoikis sensitivity of mILC. FACS-sorted E-cadherin-expressing cells and IL2R-Ecad-cyto transduced cells were grown in the absence of anchorage after which anoikis resistance was analyzed.

Supplementary Figure S4

Localization of p120 regulates Rock-mediated anoikis resistance in mILC. **A**) mILC-1 cells were transduced with control or E-cadherin-encoding lentivirus and FACS-sorted using antibodies directed against E-cadherin. E-cadherin levels are shown by western blotting. **B**) Restoration of membranous p120 using wild-type E-cadherin leads to inhibition of Rock signaling. FACS-sorted control and E-cadherin expressing mILC-1 cells were mixed 1:1 and stained for p120 (red), p-MLC (green) and DNA using DAPI (blue). Note that cytosolic p120 coincides with expression of phosphorylated MLC (arrow head). In contrast, restoration of membrane-localized p120 leads to inhibition of phospho-MLC (arrow). Bars, 5µm. **C** and **D**) Uncoupling of E-cadherin-controlled cell-cell adhesion from the



Supplementary Figure S5

Rock signaling controls anoikis resistance of the E-cadherin mutant SKBR-3 cell line. SKBR-3 cells were cultured in the absence (left graph) and presence of anchorage (right graph), and inhibitors of Rho (C3) or Rock (OH-fasudil). After 4 days, anoikis resistance (left graph) and growth speed (right graph) were determined. Error bars represent standard deviation of triplicate measurements.



Chapter 5

5

Rock inhibition as a therapeutic alternative in the management of invasive lobular carcinoma

Ron C.J. Schackmann, Romina J. Pagliero, Miranda van Amersfoort, Robert A. van de Ven, Nathaniel I. Martin, David A. Egan and Patrick W.B. Derksen

In preparation

Abstract

Metastatic disease is the most common cause of breast cancer related death. As tumor relapse and metastasis are often accompanied by resistance to chemotherapy, novel treatment regimens are required. Using mouse models of invasive lobular carcinoma (ILC), we recently uncovered that ILC cells depend on active Rho associated kinase (Rock) signaling for metastatic dissemination. Here we extend these findings and show clinical relevance of inducible shRNA-based Rock inhibition on primary tumor growth and metastatic outgrowth of mouse ILC (mILC). We next utilized the pharmacological Rock inhibitor Fasudil to treat mILC. While Fasudil significantly inhibited primary tumor growth, the observed effects were limited. Therefore, we set out to investigate the efficiency of a recently developed and optimized Rock inhibitor GSK-4289286A in reducing mILC anoikis resistance. GSK-4289286A displayed a >60-fold potency in inhibition of Rock signaling and anoikis resistance. Finally, we synthesized GSK-4289286A for usage in future pre-clinical intervention studies.

Introduction

Lobular carcinoma is a breast cancer subtype comprising approximately 15% of all breast cancers cases³¹⁵. Clinical diagnosis of this subtype is difficult due to a characteristic growth pattern that inhibits detection using palpation or standard X-ray mammography⁸. While clinical intervention based on hormone antagonists has proven an effective strategy, hormone receptor negative or nonresponsive disease cannot be treated successfully, indicating the need for alternative curative approaches. In contrast to its well-defined histopathological characteristics, the surface of the underlying biology has only recently been scratched. Nonetheless, recent progress was made in linking loss of E-cadherin and the regulation of prometastatic features by cytosolic p120-catenin (p120)^{122, 171}.

E-cadherin, p120 and beta-catenin are the core components of the adherens junction (AJ), a cell-cell adhesion complex that controls epithelial integrity. Upon loss of E-cadherin, p120 translocates to the cytosol where it controls ILC tumor progression through Mrip-dependent activation of Rho-Rock signaling¹²². Rock activity is crucial for anchorage-independent tumor growth and metastasis of ILC, making this an interesting pharmacological target. In response to active (GTP-loaded) Rho, Rock directly phosphorylates and activates myosin light chain (MLC), and also inactivates MLC phosphatase by phosphorylating MYPT-1, leading to F-actin-dependent contractile forces. Furthermore, Rock activity results in phosphorylation and subsequent inactivation of cofilin through LIM kinases 1 and 2, leading to actin stabilization^{284, 285}. The activity of these Rock effectors, were shown crucial in force-generated ECM remodeling, allowing for single-cell migration and metastasis^{316, 317}. Interestingly, Rock signaling is often found activated in metastatic breast cancers³¹⁸⁻³²⁰, suggesting that inhibition of Rock might be an interesting approach in combined treatment using hormone-based or standard chemotherapeutics to treat metastatic disease.

The only Rock inhibitor currently used for clinical applications, is Fasudil. Fasudil is used in Japan since 1995 to treat vascular diseases related to hypertension such as cerebral vasospasm and ischemic heart disease^{321, 322}. Here, Rock inhibition results in decreased activity of MLC causing relaxation of smooth muscle cells within the blood vessel walls, effectively lowering blood pressure³²³. Aberrant Rock signaling has been observed in many different pathologies ranging from neurodegenerative disease, glaucoma, reno-protection, diabetes and cancer (reviewed in³²⁴). Furthermore, multiple clinical trials are being performed, although their main focus is on the vasodilatory function of Rock inhibition^{325, 326}. In several cancer types the clinical potential of Rock activity has been demonstrated^{122, 327-331}.

We recently demonstrated that Rock controls anchorage-independent tumor growth and metastasis in ILC. Interestingly, dependency on Rock signaling was largely context-dependent, mainly affecting anchorage-independent survival. Although pharmacological or shRNA-based inhibition of Rock did not result in reduced proliferation in 2d culturing, constitutive knockdown of Rock1 prevented outgrowth of orthotopically transplanted mILC cells

Here, we employed an inducible shRNA-mediated Rock knockdown system to study tumor progression in the absence of Rock. Next, we tested pharmacological Rock inhibitors *in vitro* and in mice. Finally, we synthesized the most promising Rock inhibitor, GSK-429286, for pre-clinical *in vivo* experimentation.

Results

Rock1 controls mILC anoikis resistance and in vivo tumor growth

Using cell lines derived from a mouse model of human ILC (mILC), we previously showed that Rock1 signaling controls anoikis resistance and *in vivo* tumor growth of mILC¹²². However, based on the use of a constitutive knockdown system, we could

not exclude the possibility that inhibition of Rock prevented initial colonization and outgrowth of transplanted mILC cells¹²². To address this, we cloned the previously characterized Rock1 shRNA into a lentiviral and doxycycline (Dox)-inducible knock down system (Rock1-iKD)³¹². Successful Rock inhibition was confirmed by culturing mILC-1 cells for 4 days of in the presence of Dox and subsequent western blot analysis (Fig. 1A left panels). Rock1-iKD did not affect expression of Rock2 (Fig. 1A right panels). Next, we assayed anoikis resistance, which we have previously successfully linked to metastatic behavior in mice^{226, 232}. As expected, in the absence of Dox mILC-1 cells showed strong anoikis resistance, whereas Dox-induced Rock1 knockdown caused an identical decrease in anoikis resistance as compared to the constitutive Rock1 knockdown constructs (Fig. 1B and¹²²).

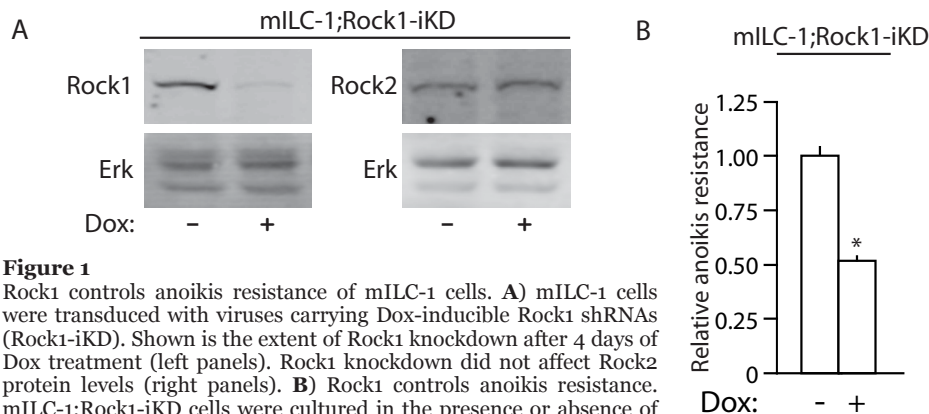


Figure 1

Rock1 controls anoikis resistance of mILC-1 cells. **A)** mILC-1 cells were transduced with viruses carrying Dox-inducible Rock1 shRNAs (Rock1-iKD). Shown is the extent of Rock1 knockdown after 4 days of Dox treatment (left panels). Rock1 knockdown did not affect Rock2 protein levels (right panels). **B)** Rock1 controls anoikis resistance. mILC-1;Rock1-iKD cells were cultured in the presence or absence of Dox for 4 days followed by 4 days of non-adherent culturing after which anoikis resistance was analysed using FACS.

To uncouple the contribution of Rock1 to tumor progression from initial tumor colonization, we orthotopically transplanted 10,000 luciferase-expressing mILC-1;Rock1-iKD cells. Mice were fed Dox-containing chow 2 days prior to transplantation (Fig. 2 dark blue line), two weeks after transplantation to allow initial seeding (Fig. 2 red line), and six weeks after transplantation (after tumors reached a size of 50-100mm³) (Fig. 2 green line). To control for the effect of Dox on tumor development, one cohort of mice was transplanted with control mILC-1 cells and fed Dox-containing chow. We followed tumor growth longitudinally through digital caliper measurements and non-invasive bioluminescence imaging (BLI) (Fig. 2A and 2B). Furthermore, we monitored the presence of lung metastases by measuring bioluminescence of the upper torso (Fig. 2C and 2D). As expected, control mice rapidly developed primary tumors and lung metastases within 10 weeks after transplantation (Fig. 2A-C purple and light blue line). In contrast, transplanted mILC-1;Rock1-iKD cells treatment 2 days prior (dark blue line) or two weeks after transplantation (red line) blocked mILC tumor outgrowth, suggesting that Rock1 is required for tumor outgrowth and subsequent metastasis formation. Intriguingly, removal of Dox after 10 weeks in both groups resulted in tumor outgrowth and subsequent metastasis, suggesting that the -penetrance of- shRNA-mediated Rock1 inhibition was not sufficient to eradicate mILC-1 cells. Finally, we determined whether Rock1 is necessary for metastatic dissemination of mILC. To this end we started Dox treatment upon detectable metastatic foci (>2*10³ photons/s/cm²/sr) (Fig. 2 green line). One week after Dox administration, the BLI signal detected at the primary tumor and lungs was reduced (Fig. 2B and 2D green line, compare week 6 to week 7), indicating a rapid reduction of metabolic activity. Furthermore,

two weeks after Dox treatment, we observed a marked reduction in primary tumor volume (Fig. 2A compare weeks 6-8). Continued treatment reduced tumor size and BLI signals to near-baseline. To determine whether inhibition of Rock1 had resulted

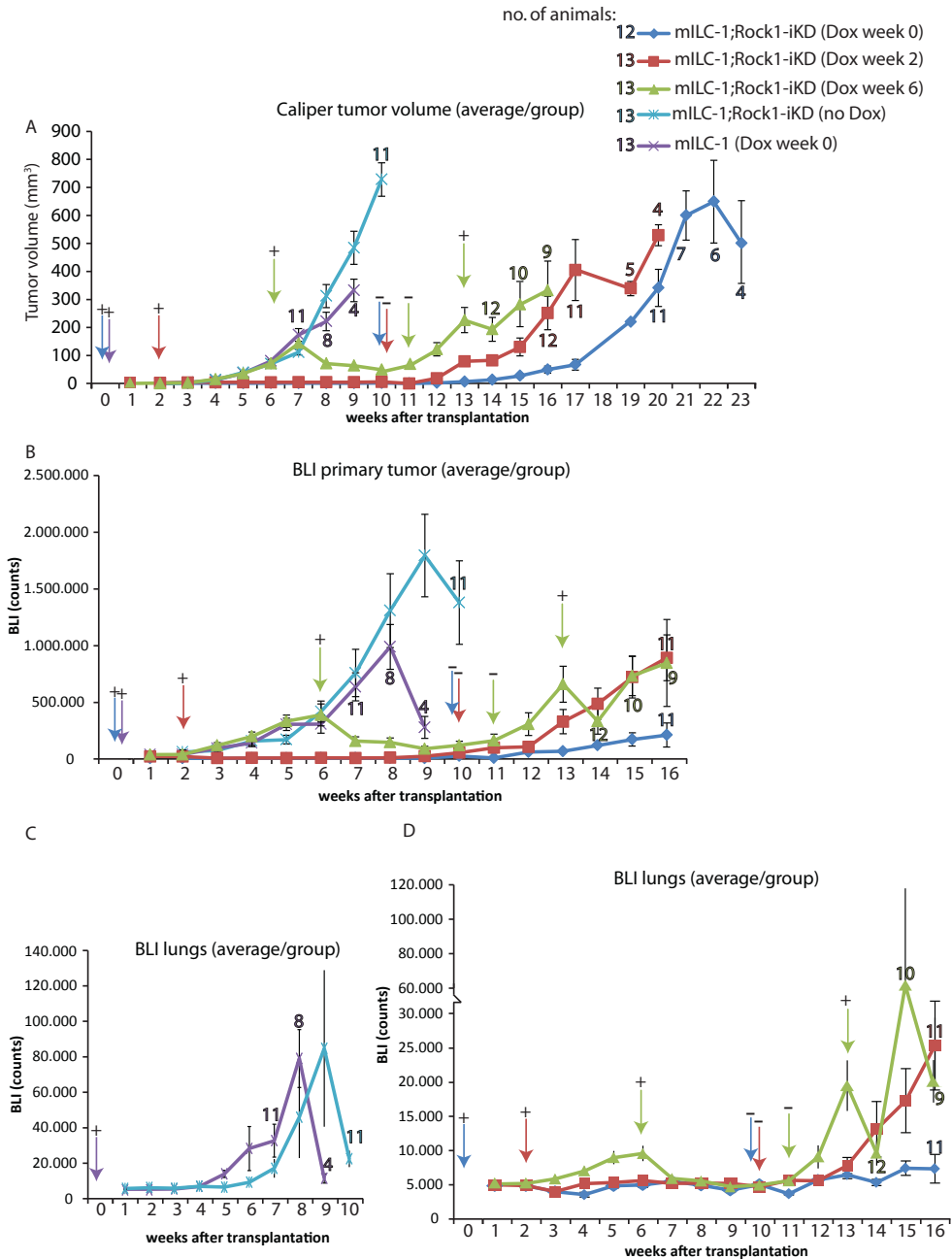


Figure 2 Rock1 controls tumor and metastasis outgrowth. **A-D)** Luciferase-positive mILC-1 (purple line) and mILC-1;Rock1-iKD cells were orthotopically transplanted. At the indicated time points, animals were given Dox-containing or control chow. Tumor volume (A) and BLI of the primary tumor (B) or lungs (C and D) were measured weekly. Numbers in the graph correspond to surviving animals at the indicated time point. All groups start with 13 animals, except for the mILC-1;Rock1-iKD directly onto Dox (blue line) which contain 12 animals. Error bars represent SEM.

in tumor clearance, we removed Dox administration at week 11 and followed tumor growth. After one week of Dox withdrawal, tumors relapsed and BLI signals in the lungs increased, suggesting that, despite the initial decrease in tumor size and BLI signal, viable cells were still present after a persistent period (from week 7 until week 11) of Rock knock-down. Next, Dox administration was again started at week 13 to test responsiveness to Rock inhibition. Although we observed an initial decrease in tumor volume and lung BLI, (Fig. 2B, 2D and 2A respectively), this response was temporary and mice soon had to be euthanized due to the lung metastasis. Overall, these data indicate that Rock1 controls mILC tumor growth and metastasis.

Pharmacological Rock inhibition in mILC

Given the stringent dependency of mILC growth and dissemination on Rock1 using genetic inhibition, we set out to assess whether pharmacological Rock inhibition could be used to as a preclinical too to treat mILC. We therefore employed the clinically approved Rock inhibitor Fasudil (HA1077)³³². Fasudil has a high oral availability (~50%) and needs to be metabolized by the liver to attain the active metabolite hydroxyfasudil³³³. This reversible ATP-competitive inhibitor suppresses Rock1 activity (IC_{50} 10.7 μ M), but also inhibits several other kinases, albeit with lower IC_{50} values (such as PKA, PRK2, MSK1, S6K1 and others^{334,335}). Hydroxyfasudil administration inhibited in vitro anoikis resistance of mILC and E-cadherin mutant human breast cancer cell lines. Four independent human cell lines responded readily to Fasudil treatment –showing a 25-70% decrease in anoikis resistance under non-

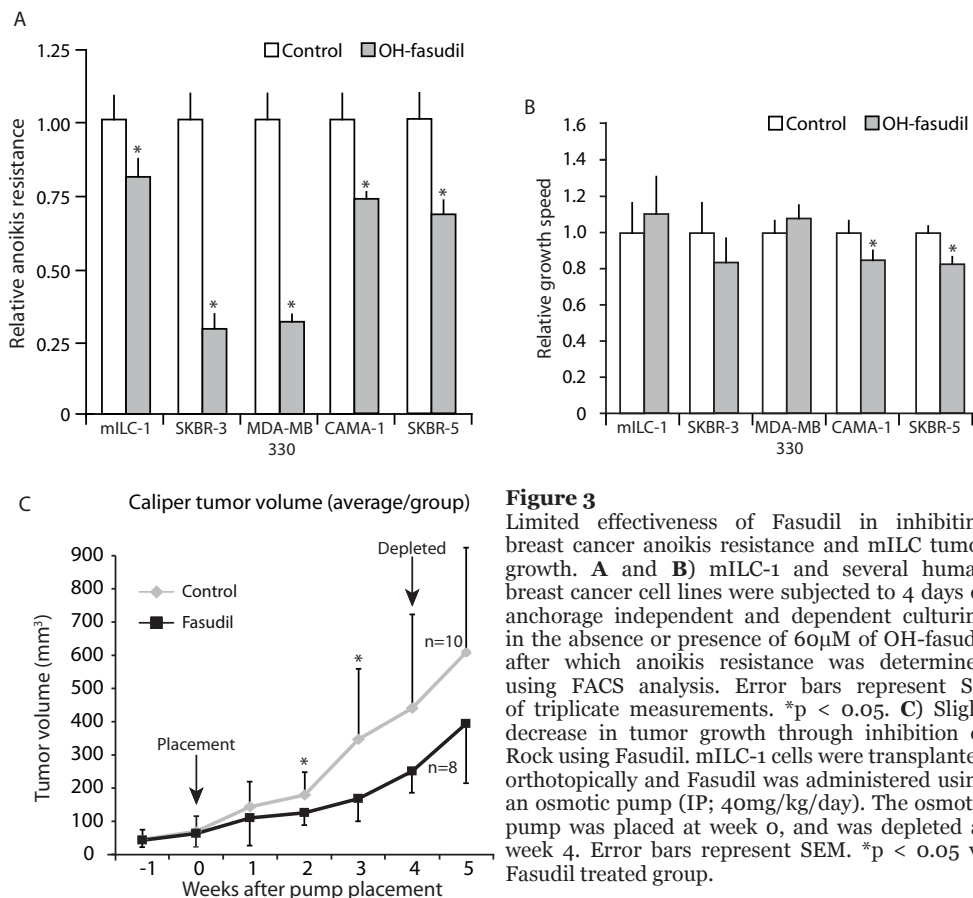


Figure 3

Limited effectiveness of Fasudil in inhibiting breast cancer anoikis resistance and mILC tumor growth. **A** and **B**) mILC-1 and several human breast cancer cell lines were subjected to 4 days of anchorage independent and dependent culturing in the absence or presence of 60 μ M of OH-fasudil after which anoikis resistance was determined using FACS analysis. Error bars represent SD of triplicate measurements. * $p < 0.05$. **C**) Slight decrease in tumor growth through inhibition of Rock using Fasudil. mILC-1 cells were transplanted orthotopically and Fasudil was administered using an osmotic pump (IP; 40mg/kg/day). The osmotic pump was placed at week 0, and was depleted at week 4. Error bars represent SEM. * $p < 0.05$ vs Fasudil treated group.

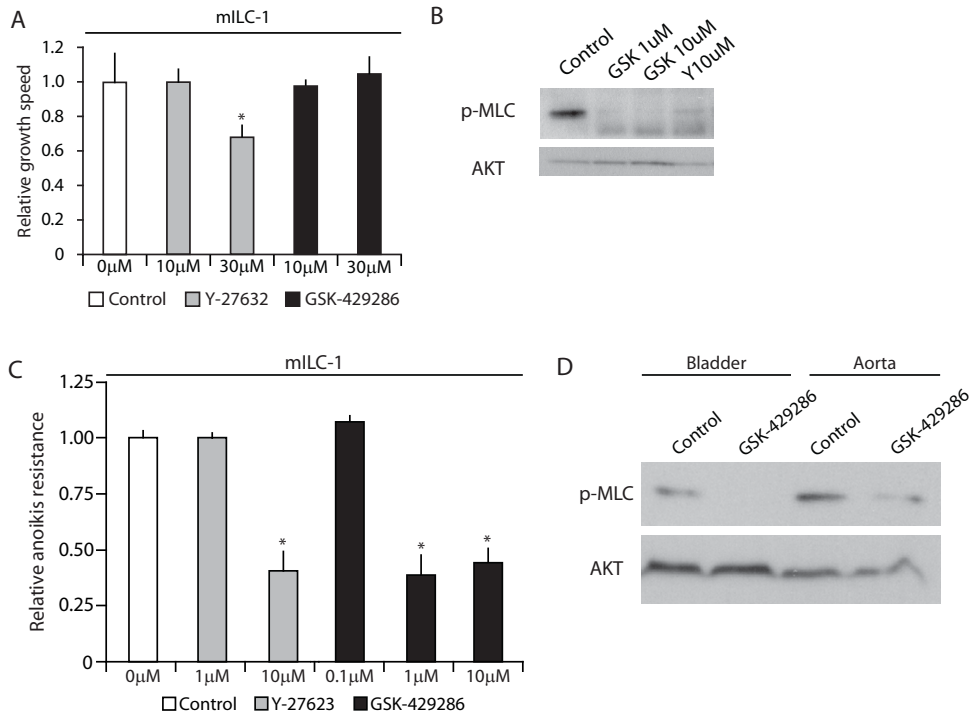


Figure 4

Y-27632 and GSK-429286 are potent inhibitors of Rock signaling in vitro and in vivo. **A**) Rock inhibition does not affect proliferation rate of mILC-1 cells. Cells were grown under adherent conditions in the presence of the indicated inhibitor for 4 days after which growth speed was analyzed. Error bars represent SD of triplicate measurements. * $p < 0.05$. **B**) Rock inhibitors induce potent inhibition of downstream Rock effector MLC phosphorylation. Adherent cells were treated with the indicated inhibitor for 2 hours, and analyzed for phosphorylated MLC by means of western blot. AKT is shown as loading control. **C**) Effective dose of different Rock inhibitors in reducing anoikis resistance. mILC-1 cells were grown under non-adherent conditions for 4 days in the presence of the indicated concentration of inhibitor. Anoikis resistance was determined using FACS analysis. Error bars represent SD of triplicate measurements. * $P < 0.05$. **D**) GSK-429286 strongly reduced MLC phosphorylation levels in vivo. 30mg/kg GSK-429286 was delivered by means of IP injection in a single mouse. One hour after administration, the bladder and aorta were harvested for analysis of MLC phosphorylation by means of western blot. AKT was used as loading control.

adherent culturing- without significantly affecting cellular growth under adherent conditions (Fig. 3A and 3B). However, the overall effectiveness on mILC-1 cells was limited, despite the high (60 μ M) concentration of OH-fasudil used (Fig. 3A and 3B). To test whether Fasudil could be used to inhibit mILC in vivo, we orthotopically transplanted mILC-1 cells in recipient female mice and surgically placed osmotic pumps containing Fasudil (release rate = 40 mg/kg/day, for 4 weeks) when tumors reached an average a volume of 50mm³. While Fasudil treatment modestly but significantly decreased tumor growth (Fig. 3C), postmortem analyses revealed that metastatic dissemination was not prevented. In conclusion, these results suggest that Fasudil did not prevent Rock driven tumor growth and metastasis.

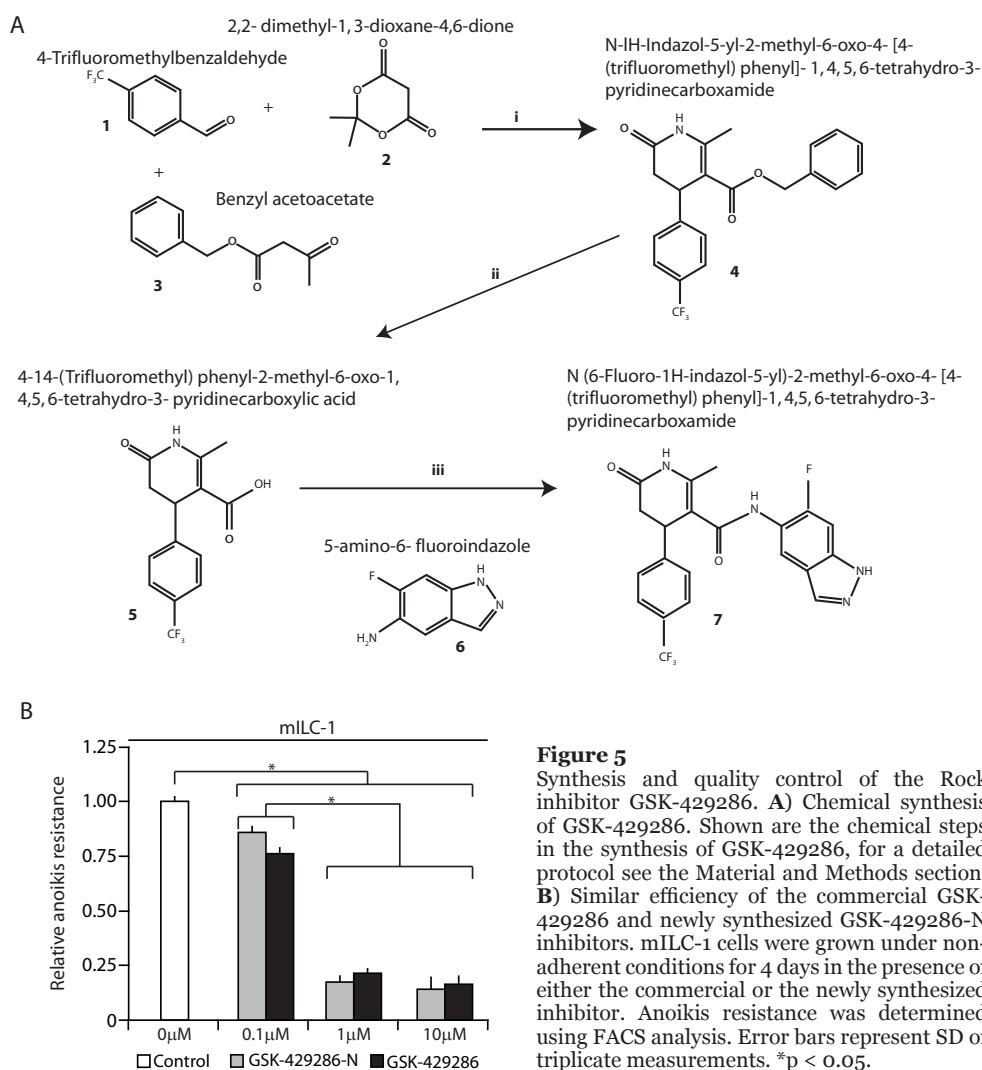
Validation of additional Rock inhibitors

Given the high IC₅₀ value for Fasudil, we set out to test additional, more specific and efficient Rock inhibitors. To this end, we employed the commonly used Rock inhibitor Y-27632 and the recently developed Rock inhibitors GSK-429286^{336,337}. We first determined the effect of high concentrations of both inhibitors on

proliferation under adherent conditions of mILC-1 cells. In contrast to Y27632, 30 μ M of GSK-429286 did not affect proliferation (Fig. 4A). We next explored the ability of both substances to inhibit Rock signaling by means of western blot analysis. Using phosphorylation of MLC as a readout for Rock activity we observed that GSK-429286 inhibited Rock at concentrations as low as 1 μ M (Fig. 4B). In agreement with these inhibitory concentrations, we observed that 1 μ M GSK-429286 induced a strong decrease in anoikis resistance (Fig 4C). In contrast, Y-27632 and OH-fasudil showed 10 and 60-fold less potency in inhibiting anoikis resistance (Fig. 4C).

Large-scale synthesis of GSK-429286

Because GSK-429286 showed more promise as a Rock inhibitor as compared to Y-27632 we decided to validate the Rock inhibitory potential of GSK-429286 *in vivo* by means of a single IP injection of 30mg/kg GSK-429286. Two hours after injection, smooth muscle-containing tissues (bladder and aorta) were harvested for western blot analysis to determine the phosphorylation status of the downstream Rock effector MLC. As expected, IP administration of GSK-429286 resulted in severe



hypotension (data not shown), which was accompanied by a robust decrease of MLC phosphorylation (Fig. 4D).

In order to perform preclinical intervention studies, we developed a strategy for synthesis of GSK-429286, the chemical procedure of which is depicted (Fig. 5A) and described in detail in the material and methods section. In short, 4-Trifluoromethylbenzaldehyde (44.52g) (Fig. 5A; **1**), 2,2-dimethyl-1,3-dioxane-4,6-dione (36.87g) (Fig. 5A; **2**) and Benzyl acetoacetate (49.14g) (Fig. 5A; **3**) were dissolved in acetic acid to generate *N*-1*H*-Indazol-5-yl-2-methyl-6-oxo-4-[4-(trifluoromethyl)phenyl]-1,4,5,6-tetrahydro-3-pyridinecarboxamide (35.5g) (Fig. 5A; **4**). This white solid was dissolved in methanol and treated as described in the material and methods to generate 4-[14-(Trifluoromethyl)phenyl]-2-methyl-6-oxo-1,4,5,6-tetrahydro-3-pyridinecarboxylic acid (Fig. 5A; **5**) (22.0g). This white solid was combined with DMF-dissolved 5-amino-6-fluoroindazole (Fig. 5A; **6**) to generate *N*-(6-Fluoro-1*H*-indazol-5-yl)-2-methyl-6-oxo-4-[4-(trifluoromethyl)phenyl]-1,4,5,6-tetrahydro-3-pyridinecarboxamide (Fig. 5A; **7**) that after repeated purification resulted in 3.89g of a 95-97% pure substance termed GSK-429286-N

To determine the efficiency of the newly synthesized inhibitor, mILC-1 cells were subjected to non-adherent culturing in the presence of either inhibitor. The efficiency of reducing mILC-1 anoikis resistance was identical (Fig. 5B), enabling us to determine the *in vivo* efficacy of Rock inhibition in pre-clinical treatment of mILC.

Discussion

Metastatic disease is the number one cause of cancer related deaths¹. In breast cancer, roughly 30% of patients will relapse with metastatic disease within 5 years after the primary treatment^{13,16}. Metastatic disease is often wide-spread, localized at inoperable sites and resistant to the primary therapeutics. Therefore, therapeutics that target the metastatic cells are required.

We have previously shown in a mouse model of ILC that p120 translocates to the cytosol upon E-cadherin loss. Overall, cytosolic p120 interacts with Mrip, which results in active Rho-Rock signaling and subsequent anoikis resistance¹²². In order to extend our findings and test the applicability of Rock inhibition in the treatment of ILC we employed an inducible Rock1 shRNA-based knockdown system *in vivo*. Our data show that continuous Rock knockdown prevented metastatic dissemination. Tumor cells require anoikis resistance to migrate from the primary tumor into a foreign environment. The induction of anoikis upon loss of Rock expression thus explains the lack of metastasis. However, Rock inhibition also prevented tumor outgrowth seemingly indefinite. In light of recent literature, these findings are surprising, as Rock inhibition was mainly shown to decrease metastatic dissemination and not tumor outgrowth.^{328,338} Several mechanisms might explain the observed reduction in tumor size. For instance, Rock activity is required for efficient cytokinesis in formation of the cleavage furrow and pinching of the contractile ring through myosin-generated contractile forces³³⁹. Furthermore, other studies have shown a dependency of Rock in mediating insulin signaling and subsequent glucose uptake in adipocytes and muscle cells³⁴⁰⁻³⁴². Rock inhibition might thus severely hamper glucose uptake by the tumor. Unable to stop their high proliferative rate, tumor cells would rapidly die. Although Rock inhibition did not result in obvious cell death *in vitro*, this might be caused by the high glucose concentration in normal culture medium as compared to blood (>3000mg/L versus ~800mg/L). Both mechanisms might explain the lack of tumor growth and even the reduction in tumor size and merit additional research on Rock signaling in ILC.

However, even after prolonged knockdown, removal of Dox resulted in tumor outgrowth (Fig. 2 red and dark blue lines), indicating that chronic inhibition of Rock may prevent tumor cell outgrowth. Furthermore, when applying Dox to mice with

large primary and metastasized tumors, tumor size decreased rapidly and metastatic foci regressed to base-line levels based on BLI (Fig. 2 red and green lines).

Discontinuation of Dox administration after the tumor size decreased resulted in rapid outgrowth. Reinstating the Dox treatment (Fig. 2 green line week 13) was insufficient to control tumor and metastasis growth. Although the reason for this is currently unknown, several hypothesis might explain this observation. First, this might reflect the inadequate biodistribution of Dox upon reaching a certain tumor volume. Secondly, some tumor cells might present with an inadequate Rock knockdown, or have acquired resistance to loss of Rock1 expression. Although it is unclear how this might occur in such a short time, it does not appear to be an effect of tumor cell heterogeneity since -directly after transplantation- all cells were and remained sensitive to Rock inhibition (Fig. 2 red and blue lines). Thirdly, the initial inhibition of Rock might have resulted in the induction of necrosis -as suggested by the reduction in tumor volume. Necrotic death results in the release of cellular content into the local environment, facilitating the recruitment of inflammatory cells -tasked to remove the cellular debris and stimulate recovery of the damaged tissue^{343, 344}. Consequentially, the inflammatory cells increased growth factor availability and angiogenesis for the surviving tumor cells, possibly negating the negative effects of Rock inhibition^{343, 345}.

In order to determine the *in vivo* applicability of Rock inhibition in ILC management, we turned to the clinically approved Rock inhibitor Fasudil. Orthotopic transplantation of mILC cells, followed by continuous intra peritoneal (IP) release of Fasudil using osmotic pumps resulted in a slight but significant decrease in tumor outgrowth but did not prevent metastatic dissemination. Several factors may account for this limited effectiveness. First, Fasudil only showed a modest reduction of anoikis resistance of our mILC *in vitro*, possibly insufficient to induce anoikis in metastatic cells. Secondly, we are unacquainted with the stability of Fasudil upon prolonged retainment in osmotic pumps and are unaware of the bioavailability throughout the experiment. Combined with the ambiguous inhibitory nature of Fasudil on kinases besides Rock, this rendered Fasudil insufficient as a clinical intervention modality to treat mILC. We therefore set out to test the established Rock inhibitor Y-27632 and the novel GSK-429289. Although Y-27632 was shown to potently inhibit Rock (IC_{50} 0.14 μ M versus Fasudil IC_{50} 10.7 μ M³³⁶) and potently reduced anoikis resistance (Fig. 4C), Y-27632 was found to have similarly inhibitory potential on leucine-rich repeat protein kinase-2 (LRRK2) -a multi-domain actin, RAS and RhoGTPase regulatory protein³⁴⁶- and protein kinase C-related kinase 2 (PRK2 or PKN2) -a RhoGTPase effector^{347- 334, 335}. Combined with the limited oral availability and short half-life, made Y-27632 unattractive for *in vivo* application³⁴⁸. Overall, we determined GSK-429289 to be most promising for *in vivo* application, with an IC_{50} for Rock of 0.014 μ M, an oral availability of 61% and more selective inhibitory properties³³⁵. We are currently investigating the possibility to determine the presence of GSK-429286 in mouse blood samples, in order to confirm pump efficiency and drug stability over time. Overall, this will result in a more controlled *in vivo* inhibition experiment.

Although Rock inhibition induced anoikis in non-adherent ILC cells, the exact mechanism by which Rock inhibitors might eventually block metastasis remains unclear. Several mechanism may underlie this phenotype. First, our data suggest that Rock inhibition will induce anoikis in cells that migrate from the primary site. Second, there is a strong correlation between primary tumor size and the occurrence of metastatic disease^{349, 350}. As such, the reduced primary tumor size as a result of Rock inhibition might prevent metastatic dissemination. Third, Rock inhibition may prevent single cell migration, as this mode of movement requires active Rock-MLC signaling^{301, 316, 351}. Fourth, Rock inhibition could possibly decrease metastasis size, as shown for genetic Dox-inducible Rock1 inhibition (Fig. 2D green line at week 6), preventing detection. Fifth, Rock inhibition also increases junctional stability

of endothelial cell layers, which in turn can block metastatic cells from entering the bloodstream^{352, 353}. Regardless the exact mode of action, it is clear that Rock inhibition holds promise for therapeutic intervention of metastatic ILC.

In conclusion, we have established a preclinical platform to test the use of Rock inhibition for the treatment of metastatic ILC,

Material and methods

Cell culture, antibodies and inhibitors

Mouse mILC-1 (Cdh1^{Δ/Δ};Trp53^{Δ/Δ}) was derived from a primary mILC tumor that developed in a K14cre;Cdh1^{F/F};Trp53^{F/F} female mice²³². Cells were cultured as described previously²³². Human cell lines SKBR-3, MDA-MB-330, CAMA-1 and SKBR-5 were cultured in DMEM/F12 (Invitrogen) containing 6% fetal calf serum, 100 IU/ml penicillin and 100 μg/ml streptomycin. The following antibodies were used: mouse anti-Rock1 (catalog no. 611136; BD Biosciences), mouse anti-Rock2 (catalog no. 610624, BD Biosciences), rabbit anti-phospho-MLC2 (Ser19) (catalog no. 3671; Cell Signaling Technology), goat anti-Akt1 (C-20) (catalog no. SC-1618; Santa Cruz Biotechnology), rabbit anti-Erk1 (C-16) (catalog no. SC-93; Santa Cruz Biotechnology). Secondary antibodies were HRP-conjugated rabbit anti-goat, goat anti-mouse, (1:2000, Dako), HRP-conjugated goat anti-rabbit (1:2000, Cell Signaling) and Alexa Fluor 488-conjugated anti rabbit (1:600 Sigma-Aldrich). The following inhibitors were used: hydroxy fasudil (60 μM; Sigma-Aldrich), Y-27632 (Sigma-Aldrich) and GSK-429286 (Sigma-Aldrich).

Synthesis of GSK-429286

GSK-429286 was synthesized in a three-step reaction procedure (Fig. 5A), in which each intermediate was subject of extensive purification before proceeding to the next step. During the entire process purity and identity of each intermediate and the final product were checked by Nuclear Magnetic Resonance (NMR). All NMR was performed in a Varian Gemini 300 MHz Spectrometer (300MHz H1, 75Hz C13). All spectra were taken in d6-DMSO (Sigma-Aldrich). 4-Trifluoromethylbenzaldehyde, 2,2-dimethyl-1, 3-dioxane-4,6-dione and Benzyl acetoacetate were purchased (Sigma-Aldrich). 5-amino-6-fluorindazole was purchased (Activate Scientific GmbH). All solvents were from Acros-Organic and were "reagent grade". DMF was dried over molecular sieves before use.

Step1. N-1H-Indazol-5-yl-2-methyl-6-oxo-4-[4-(trifluoromethyl) phenyl]-1, 4, 5, 6-tetrahydro-3-pyridinecarboxamide (4). 4-Trifluoromethylbenzaldehyde (**1**, 43.5mL, 44.52g, 256mmol, 1.00 eq.), 2,2-dimethyl-1, 3-dioxane-4,6-dione (**2**, 36.87g, 256mmol, 1.00 eq.), Benzyl acetoacetate (**3**, 54.6mL, 256mmol, 49.14g, 1.00 eq.), and ammonium acetate (20.5g, 365mmol, 1.07 eq.) were dissolved in acetic acid (450 mL) and heated to reflux. The reflux was maintained for 3 hours with continuous stirring. Afterwards, water (500mL) was added to induce the precipitation of an off-white solid. The residue was recover by filtration and triturated with 50% Aceton/hexane resulting in 87g of an off-white solid. The product was further purified by chromatography on silica gel, eluted with a gradient of Hexane:Ethyl Acetate (4:1 → 2:1). The yellow solid was further washed with Hexane:Ethyl Acetate (1:1) and filtrated to give N-1H-Indazol-5-yl-2-methyl-6-oxo-4-[4-(trifluoromethyl) phenyl]-1, 4, 5, 6-tetrahydro-3-pyridinecarboxamide as a white solid (35.5g, 91.25mmol, 35.6%).

Step2. 4-14-(Trifluoromethyl) phenyl-2-methyl-6-oxo-1, 4,5, 6-tetrahydro-3-pyridinecarboxylic acid (5). The product from Step 1 (35.5g, 91.25mmol, 1.00 eq.) was dissolved in MeOH (500mL) and treated with Pd/Charcoal while stirred under H₂ pressure at room temperature for 1h. The catalyst was removed by celite

filtration and evaporation. This solid was wash with Hexane:Ethyl Acetate (1:1) and recovered by filtration. The 4-(14-(Trifluoromethyl) phenyl)-2-methyl-6-oxo-1, 4,5, 6-tetrahydro-3- pyridinecarboxylic acid was obtained as a white solid (22.0gr, 73.51 mmol, 80.5%).

Step3. *N* (6-Fluoro-1*H*-indazol-5-yl)-2-methyl-6-oxo-4- [4- (trifluoromethyl) phenyl]-1, 4,5, 6-tetrahydro-3-pyridinecarboxamide (7). 5-amino-6- fluorindazole (6, 1.5g, 33.1mmol, 1.0 eq.) was dissolved in 170mL of anhydrous DMF. Immediately after, the product from Step 2 was added (10.96g, 36.6mmol, 1.1 eq.) together with EDC (7.93g, 39.98mmol, 1.2 eq.). Finally, Et₃N (10 mL, 71.4mmol, 1.2 eq.) was added and the solution was stirred at room temperature for 18hs under N₂ atmosphere. The next day DMF and Et₃N were evaporated and the solid residue was dissolved with Ethyl Acetate and 1N HCl. The phases were separated, and the organic phase was washed three times with 1N HCl (3x 200mL), once with a saturated NaHCO₃ (1x 200mL), and once with saturated NaCl (1x 200mL). Next, the substance was dried over Na₂SO₄, filtered and concentrated by vacuum. The residue (13.5g dark-drown solid) was purified by chromatography on silica gel, and eluted with a gradient of Hexane:Ethyl Acetate (4:1→3:1→2:1→1:1→1:2→1:3→pure Ethyl Acetate). Quality of the off-white solid (6.65g, 46.6%) was confirmed by NMR and MS (ES+) m/e 433 [M+H]⁺. compounds were further purified by means of recrystallization. To this end, the product was dissolve in Ethyl Acetate under reflux and cooled to 40°C. Hexane was added until the solution precipitated. The round bottom flask was then place on ice for 15 minutes and subsequently at 4°C overnight. The resulting precipitate was filtrated and dried under high vacuum, resulting in a final product (3.89g (27.2%) of an off-white solid). Purity was estimated by NMR to be 95-97%.

Immunohistochemistry

For immunofluorescence, cells were grown on coverslips and fixed using 1% paraformaldehyde in PBS for 10 minutes. Cells were permeabilized using 0.3% Triton-X 100 in PBS and subsequently blocked using 5% BSA (Roche). Coverslips were incubated with primary antibodies in 1% BSA for 60 minutes, after which cells were incubated in 1% BSA with secondary antibodies for 30 minutes. DNA was stained with DAPI for 5 minutes (Invitrogen), and coverslips were mounted onto object glasses using Vectashield mounting medium (Vector Laboratories). Cells were analyzed by confocal laser microscopy using a Zeiss LSM510 META (Carl Zeiss).

Constructs, viral production and transduction

A previously validated Rock1 hairpin (GACCTTCAAGCACGAATTA)¹²² was cloned into the inducible RNAi system (TaconicArtemis) as described before¹²². Lentiviral particles were produced in Cos-7 cells using third-generation packaging constructs²⁷⁴. Supernatant containing viral particles was harvested 48 hours after transfection, passed through a 0.45-μm filter, and concentrated 10-fold by centrifugation (175,000 g; 150 minutes). mILC-1 cells were transduced overnight in the presence of 4μg/ml polybrene (Sigma-Aldrich). Knockdown was induced by culturing cells in the presence of 0.2μg/ml of Dox for 4 days without refreshing.

Anoikis resistance and Growth speed assay

In order to determine growth speed under adherent conditions, cells were plated at a density of 20,000 cells in a 24-well culture plate, left to adhere for 4 hours, after which the indicated inhibitor was added. After four days, or until cells reached near-confluence, cells were fixed with 100% methanol, stained using 0.2% crystal violet (Sigma-Aldrich) and washed with water. The incorporated crystal violet was eluted using acetic acid 10% (v/v) and quantified with a spectrophotometer at 560 nm (BioRad).

Anoikis resistance was analyzed by seeding cells at a density of 20,000 cells per well

(in 500 μ l) in a 24-well ultra-low cluster polystyrene culture dish (catalog no. 3473, Corning). After 4 days, cells were harvested and resuspended in 75 μ l of Annexin-V buffer supplemented with Annexin-V and Propidium Iodide. The percentage of anoikis resistant cells was determined by FACS analysis as the Annexin-V and Propidium Iodide negative population on a BD FACSCalibur.

Western blotting

Cells were placed on ice, washed twice with ice-cold, magnesium and calcium containing, PBS and lysed directly in sample buffer (50 mM Tris-Cl pH6.8, 0.5% β -mercaptoethanol, 2% SDS, 0.005% bromophenolblue, and 10% glycerol (all Sigma-Aldrich)). Samples were heated for 5 minutes at 100°C, and proteins were separated using standard PAGE protocols and blotting. Mouse tissues were harvested, briefly rinsed with cold PBS and quickly frozen using dry ice. Tissues were weighed, thawed on ice, roughly minced using two scalpel knives and placed into 1,5 ml eppendorf tubes. 1mL of Urea lysis buffer (100mM NaH₂PO₄, 10mM Tris-Cl pH 8.0, 8M Urea adjusted to pH 8.0 directly prior to use) was added per 200mg of tissue. Samples were homogenized using 1ml plastic eppendorf pestles. The homogenized samples were centrifuged for 10 minutes at 14 Krpm and supernatant was transferred to a clean tube. Protein concentration was determined using the Bradford assay (Bio-rad), after which samples were dissolved in sample buffer and treated as described.

Orthotopic transplantations and inhibitor validation

Recipient female nude mice (Hsd:Athymic Nude-Foxn1nu; Harlan) were anaesthetized by intraperitoneal (ip) injection of a mixture containing 25 μ l Hypnorm (0.315mg/ml Fentanyl Citrate, 10mg/ml Fluanisone) (Janssen Pharmaceutica), 25 μ l (5 mg/ml) Dormicum (Roche) and 50 μ l H₂O. The 4th mammary gland was exposed and approximately 10,000 luciferase expressing mILC-1 or mILC-1;Rock1-iKD cells were injected in the 4th mammary gland using a 10 μ l Hamilton syringe. 100 μ l (0.03mg/ml) Temgesic (Buprenorphine) was injected subcutaneous as analgesic treatment. After a recovery period of two weeks, mice were anaesthetized with isoflurane (Janssen Pharmaceutica), injected ip with 225 μ g/g body weight *n*-luciferin (potassium salt; Biosynth AG) and imaged on a Biospace bioluminescence imager (Biospace Lab). Tumor development was measured using a digital caliper (Mitutoyo) on a weekly basis. Doxycycline was administered through the chow (catalog no. S3888 and control-chow S4207, Bio-serve).

For preclinical intervention studies with fasudil, 20,000 mILC cells were injected into the 4th mammary gland of syngeneic female mice. F1 syngeneic hybrids were obtained by crossing 129P2/OlaHsd mice (Harlan) with FVB/NCrl (Charles River). When tumor volume reached approximately 50 mm³, an osmotic pump (catalog no 1004, Alzet) containing the Rock inhibitor fasudil was placed in the peritoneum of recipient mice. Tumor development was measured using a digital caliper on a weekly basis. Mice were sacrificed when tumor volume reached >500 mm³, or if mice presented detectable lung metastases using bioluminescence. All animal experiments were performed in accordance with institutional guidelines and national regulations. In order to validate functionality of the Rock inhibitor GSK-429286 *in vivo*, 30mg/kg inhibitor (dissolved as 5mM in 50% DMSO) was injected intra peritoneal into a female nude mouse. Two hours after administration, the mouse was sacrificed and tissues were harvested for western blot analysis as described.

Statistical analysis

For growth speed and anoikis assays, statistical significance was calculated using 2-tailed Student's t test, showing measurements of at least 3 independent experiments. Statistical significance of the genetic and pharmacological inhibition experiments in mice was calculated using the Mann-Whitney test. Error bars represent SEM. Error

bars in all other experiments represent SD of at least triplicate measurements. P values of less than 0.05 was considered statistically significant.

Acknowledgements

We wish to thank Hilde Rosing for LC-MS analyses. We are also indebted to the UMC biobank.



Chapter 6

Summary and Discussion

6

Summary

Chapter 1 gives a general overview on epithelial homeostasis and the diverse functions p120 fulfills in adherens junction dynamics, RhoGTPase signaling and transcriptional regulation. Chapter 2 reviews the literature on the contribution of p120 in tumor development of different tissues with a focus on breast cancer. In chapter 3 we report on p120 loss in invasive breast cancer and its correlation to several clinicopathological characteristics. To further investigate the significance of p120 loss, we introduced a conditional p120 allele into a nonmetastatic mouse tumor model based on mammary-specific knockout of p53. Although p120 loss did not affect tumor onset, we observed a marked increase in metastatic dissemination. To determine the causal changes of p120 loss, we generated knockdown cell lines of mouse and human origin, and uncovered that p120 inactivation increased growth factor receptor (GFR) sensitivity, which translated into an increase in anoikis resistance - a hallmark of metastatic capacity. Furthermore, loss of p120 induced secretion of inflammatory cytokines, and as such facilitated formation of a prometastatic microenvironment. Chapter 4 reports on the role for cytosolic p120 in ILC tumor growth and metastasis. Here, p120 confers anoikis resistance through binding of Mrip, a known Rho-Rock antagonist, and subsequent activation of Rock signaling. In this setting, active Rock signaling controls anchorage-independent tumor growth and metastasis. Finally, the potential therapeutic ramifications of Rock inhibition in the treatment of ILC are discussed in chapter 5. Using inducible knock-down systems and pharmacological inhibition in a preclinical setting, we started to investigate the applicability of Rock inhibition for preclinical intervention of metastatic ILC.

Discussion

p120-catenin, a metastasis suppressor in breast cancer

Organ system differences

Inactivation of p120 in the mouse mammary gland is not tolerated and results in apoptosis²²⁸. This is in contrast to genetic inactivation of p120 in several other organ systems, where loss induces impaired tissue homeostasis and hyperplasia and can even result in tumor formation^{129, 213, 219, 250, 251}. It is difficult to ascertain what exactly sets the mammary gland apart from the other organ systems when it comes to p120 inactivation. It is well known that loss of cell-cell contact can induce apoptosis. Possibly cell-cell contact of p120 negative cells in the skin and gut can be retained by alternative adhesion complexes -such as desmosomes and tight junctions²⁹. In contrast, these junctions appear to be incapable of maintaining cell-cell contact in the p120-negative mammary gland. Alternatively, the p120 family members (ARVCF, Delta-catenin and p0071) have been shown capable of -partially- restoring E-cadherin membrane localization and AJ formation upon p120 inactivation³⁵. Although the family members are expressed in mammary epithelial cells, they cannot functionally restore the AJ upon conditional ablation of p120²²⁸. From a biological point of view it would be interesting to determine if induction of desmosome or tight junctions in p120-negative breast cancer cells can rescue cell-cell contact and whether this contact is then sufficient to allow membranous E-cadherin and AJ formation to occur. The reason why p120 knockout leads to effects ranging from hyperplasia to actual tumor formation is currently unknown and appears highly tissue specific.

The induction of metastasis through loss of p120-mediated AJ destabilization

In breast cancer, loss of p120 expression is often observed in at least part of the tumor (chapter 3), suggesting a possible tumor suppressor function for p120 in breast cancer. We therefore introduced a conditional p120 allele (*Ctnnd1^F*) into the mammary-specific p53 mouse tumor model (*Wcre;Trp53^{F/F}*), which develops non-metastatic mammary carcinomas. The resulting female compound mice developed

mammary carcinomas with a similar latency as seen for p53 inactivation alone, irrespective of p120 dosage. In contrast to carcinomas that developed in *Wcre;Trp53^{F/F}* and *Wcre;Ctnnd1^{F/+};Trp53^{F/F}* mice tumors from *Wcre;Ctnnd1^{F/F};Trp53^{F/F}* female mice displayed a complete loss of membranous E-cadherin. Furthermore, p120 loss induced a marked increase in metastatic potential, an effect not observed in conditional mice in which p120 knockout was targeted to other organ system^{129, 213, 214}. But what causes this difference in metastatic potential?

The acquisition of metastatic potential relies on the ability of tumor cells to physically detach from the primary site and subsequently resist anoikis as they traverse and colonize foreign environments. Loss of AJ stability, characterized by functional inactivation of E-cadherin, lies at the basis of removing the physical restriction retaining cells at the primary site.

In contrast to conditional knockout in the mammary gland, p120 ablation resulted in residual E-cadherin expression in the salivary gland, intestine and skin. As a result, physical restriction is still present, which might explain the lack of metastatic potential in these models. This is in concurrence with our finding that heterozygous p120 loss was not sufficient to inhibit E-cadherin expression and did not result in an increase in metastasis. Why E-cadherin expression was not retained in the mammary gland upon homozygous knockout of p120 is unclear. p120 family members were expressed in the absence of p120 and E-cadherin, which therefore excludes functional redundancy. Possibly the expression levels of the family members were insufficient to compensate for p120 loss and rescue E-cadherin expression. Alternatively, skin and the gastro-intestinal tract might have a more supportive surrounding tissue, physically aiding the p120-negative cells in the formation of other adhesion complexes -for instance desmosomes-, which in turn facilitate close enough cell-cell proximity to allow the weak AJs to be present. This hypothesis is supported by findings in the colon, where structural integrity is more severely compromised in the free-standing villi of the small intestine as compared to the more tightly packed crypts of the colon upon loss of p120. Alternatively, the lack of metastasis in these p120 knockout models might be due to the inability of detached cells to survive. Despite the presence of residual E-cadherin, some shedding of p120-negative cells was observed in the salivary gland and intestine. However, instead of forming metastasis these cells underwent apoptosis²¹⁵. Why were these cells incapable of metastatic outgrowth? In normal epithelia, AJ formation blocks proliferation whereas it stimulates PI3K and MAPK survival signaling³⁵⁴. Secondly, loss of cell-cell contact releases signaling factors from E-cadherin, which induce apoptosis through induction of p14Arf^{355, 356}. As E-cadherin was partially retained in both the salivary gland and intestine upon p120 loss, these cells might have relied on the AJ formation for sufficient survival signaling. Concomitantly detachment from the primary site might have induced apoptotic signaling. In our model system, the additional loss of p53 results in increased survival and/or reduced apoptotic signaling, allowing survival of detached cells^{357, 358}. However, loss of p53 is insufficient to confer anoikis resistance as demonstrated by the lack of anchorage-independent survival capabilities of our p53^{Δ/Δ} cells. This suggests that p120 loss is not just required for physical detachment from the surrounding cells, but also facilitates additional survival signaling. Overall, in order for metastasis to occur, physical restriction needs to be overcome, and sufficient survival signaling has to be generated to prevent anoikis. The question therefore remains whether induction of additional survival signaling in the other model systems would be sufficient to induce metastatic disease as well.

Additional survival signaling through RTK sensitization

Loss of p120 is sufficient to attenuate mechanical restriction of cell movement -required to allow metastatic dissemination- in our model. Apart from the initial

anoikis resistance attained by combined loss of p120 and p53 -as described above- we uncovered that inactivation of the AJ through loss of p120 led to increased sensitization of GFR signaling. Upon further investigation, we excluded a possible upregulation of EGFR expression or increased EGF binding at the membrane. Membrane receptors like E-cadherin are known to directly influence the activity of unrelated neighboring receptors^{262, 263}, although the outcome of this effect highly depends on cellular context^{77, 257}. Therefore, the observed sensitization of GFR signaling upon loss of p120 may be due to the absence of inhibition through E-cadherin. Alternatively, the AJ might be required to recruit or localize phosphatases to the activated GFRs, rapidly reducing receptor activity. However, the AJ-dependent inhibition of GFR signaling is not specific for a given GFR, and would thus require a non-discriminant phosphatase such as DEP-1³⁵⁹. Comparison of phosphatases associated with GFRs in the presence and absence of p120 might yield which, if any, phosphatase could be responsible. It would be interesting to further determine which components of the AJ are responsible for the observed inhibition of GFR signaling. Is membranous localization of p120 sufficient to inhibit GFR signaling? Could expression of an extracellular-E-cadherin-domain construct result in inhibition of GFR signaling? Or are these effects induced by the mislocalization and degradation of the other catenins upon AJ inactivation?

The development and consequences of a pro-metastatic tumor environment

Over the past years, the tumor microenvironment has received increasing attention for its role in promoting tumor progression. Generation of an inflammatory microenvironment is a hallmark of invasive cancer and facilitates angiogenesis, growth factor production and stimulates metastatic behavior as reviewed in²¹⁶. We uncovered that combined loss of p120 and p53 results in secretion of several cytokines. It is well established that mammary tumor cells may instigate a paracrine signaling loop where secretion of cytokines attracts growth factor producing macrophages, stimulating prometastatic pathways in tumor cells^{269, 270}. Given the induced GFR sensitization upon p120 loss, this signaling loop may underlie regulation of anoikis resistance and tumor dissemination in p120-negative tumors. However, we have yet to determine whether the secreted cytokines are causally linked to recruitment of the observed tumor associated macrophages. Examining whether p120 loss induces influx of macrophages (for instance by means of trans-well assays), would be highly informative. Furthermore, this would allow us to directly validate the hypothesized paracrine signaling loop and investigate whether survival signaling of the p120 negative cells is indeed stimulated. Finally, we have yet to determine how p120 loss induces cytokine production in mammary tumor cells. Possibly, loss of p120 induces activation of NFκB-regulated cytokine production, as shown in the skin and upper GI tract³⁶⁰.

Overall, due to their inability to form intercellular AJs, p120 negative cells gain the ability to migrate from the primary site. Although this would normally result in apoptosis, concomitant loss of p53 prevents an apoptotic signal, thus leading to an overall anoikis resistance. Survival signaling is further stimulated by the induction of a pro-inflammatory tumor environment, where a paracrine signaling loop between macrophages and p120 possibly further stimulates survival signaling. Overall, these findings provide a rationale for the attained metastatic capacity observed in our mouse model and suggest that p120-negative cells -present in a large percentage of human breast tumors- play an important role in metastasis formation.

Cytosolic p120-catenin, an oncogene in ILC

Early inactivation of E-cadherin is causal to the development of the second most prevalent type of breast cancer, invasive lobular carcinoma. Like p120, mammary

specific loss of E-cadherin is not tolerated^{229, 232}. In chapter 4 we used conditional mouse models of human ILC, based on dual inactivation of E-cadherin and p53. E-cadherin is well known for facilitating contact-induced inhibition of cellular growth by regulating survival signaling and cell cycle progression³⁶¹⁻³⁶³, a finding that may underlie the observed decreased latency as compared to inactivation of p53 only. Chapter 4 investigates the underlying mechanism of anoikis resistance and subsequent metastasis of ILC. Interestingly, p120 interacted with Mrip - an inhibitor of Rho-Rock signals and regulator of actin dynamics - resulting in an active Rho-Rock cascade and subsequent anoikis resistance. Knockdown of p120 and the successive release of Mrip inhibition clearly led to a decrease in activity of downstream Rho-Rock activity and anoikis resistance. Although, loss of Mrip was not tolerated and induced rapid cell death, dual knockdown of p120 and Mrip restored Rock signals and rescued this phenotype. We hypothesized that this cell death might be caused by the release of p120 and subsequent inhibition of RhoA by means of its RhoGDI function¹²⁰. However, treatment of cells with the Rho inhibitor C3 did not induce cell death under adherent conditions, contradicting this hypothesis. More likely is a scenario whereby loss of Mrip expression results in aberrant actin dynamics or cause hyper-activation of Rock, both of which are known to induce cell death^{305, 306, 364}.

How does E-cadherin loss lead to activation of Rho-Rock signaling in ILC? While our data indicated that knockdown of p120 results in Mrip-induced inhibition of downstream Rock activity, it did not alter RhoA activity. This suggests that RhoA is activated by means independent from p120 and Mrip. Hypothetically, RhoA activation could be caused by increased activity of a RhoGEF, or decreased activity of a RhoGAP. Alternatively, RhoGAP activity might be misregulated upon E-cadherin loss. Comparing the effect of RhoGAP knockdown on ILC as opposed to E-cadherin proficient cells might yield a specific GAP which only inactivates RhoA in the presence of E-cadherin. Interestingly, AJ inactivation -shown to sensitize EGFR signaling- can also induce RhoA activation^{365, 366}. Furthermore, RhoA activation in ILC might be a result of transcriptional regulation. Although total RhoA levels did not appear to differ upon loss of E-cadherin, RhoGEF or GAP expression might be altered for instance through E-cadherin-loss induced upregulation of the transcription factor Twist³⁵⁶. Finally, cytosolic p120 facilitates nuclear exclusion of the transcriptional repressor Kaiso^{244, 246}. In *Xenopus* this results in the expression of several target genes that can induce an autocrine loop activating RhoA-Rock signaling^{148, 367, 368}. Unpublished data from our laboratory indicate that p120 can relieve Kaiso-dependent transcriptional repression of *Wnt11*, thereby activating RhoA in mILC cells (Van de Ven *et. al.* manuscript in preparation).

Rock as an additional therapeutic target to treat ILC

Regardless of the exact mechanism responsible for RhoA activation in ILC, it is clear that Rho-Rock signaling is crucial in the regulation of anchorage-independent tumor growth and metastasis. In chapter 5 we determined at which stages of tumor progression Rho-Rock signaling is essential. Employing a Dox-inducible Rock knockdown system, we evaluated the effect of Rock inhibition during (i) initial tumor seeding, (ii): shortly after seeding and (iii): after formation of metastatic foci. Inducing Rock knockdown during or shortly after seeding prevented tumor outgrowth and metastatic dissemination. Interestingly, Rock knockdown in established tumors resulted in a strong decrease in tumor size, suggesting a rapid onset of cell death. The inhibition of initial tumor growth and the size reduction of established tumors might be explained by the impaired ability of cells to undergo proper cytokinesis upon Rock knockdown^{339, 369}. Furthermore, Rock knockdown is known to disrupt the actin cytoskeleton, which can result in apoptosis. However, *in vitro* inhibition of Rock had no apparent effect on proliferation or viability. Alternatively, it is well known that tumors often display an increased glucose demand to facilitate their elevated

proliferative rate³⁷⁰⁻³⁷². Although evidence is currently lacking for epithelial cancers, active Rock was shown crucial for the insulin-mediated glucose uptake in adipocytes and muscle cells³⁴⁰⁻³⁴². The high amount of glucose present in normal culture medium as compared to the blood-glucose concentration might explain why Rock knockdown did not impair proliferation or viability *in vitro*, but severely affected tumor growth and viability *in vivo*. However, restoring Rock expression by removal of Dox eventually resulted in tumor outgrowth. Clearly, Rock inhibition prevented *in vivo* tumor formation, although we did not observe effect on proliferation *in vitro*.

Apart from the growth inhibition and induced cell death, removal of Dox-induced knockdown always resulted in tumor progression, indicating a percentage of cells survived. Possibly, the surviving cells underwent autophagy, whereby a reduction of available nutrients -for instance glucose- promotes a state of reversible dormancy^{373, 374}.

p120 in RhoGTPase signaling

p120 is well known for its ability to influence actin dynamics through regulation of the RhoGTPases, particularly RhoA^{119, 120}. However, as shown in both chapters 3 and 4, p120 loss or relocalization did not appear to affect RhoA activity. Possible reasons for these differences lie in the expression levels of different Rho regulating proteins such as Vav2, p190RhoGAP and mesenchymal cadherins, which strongly affect the ability of p120 to influence RhoA activity. Furthermore, the predominant p120 isoform expressed might determine whether RhoA activity is affected. Direct inhibition of RhoA by p120 was shown to dependent on the p120 N-terminal region, solely expressed by isoform 1. However, other studies have shown all p120 isoforms capable of nuclear localization are capable of inhibiting RhoA activity (see chapter 1 for overview). Even within a single cell system p120 can differentially affect RhoA activity, as both overexpression and knockdown induced RhoA activation^{121, 129}. In conclusion, the presence of Rho effectors (GEFs, GAPs, kinases, G proteins and other cadherins), the p120 isoforms expressed are highly dependent on the cell type studied and the tools used.

Clinical perspectives

The relevance of p120-negative breast cancer

In contrast to E-cadherin somatic mutations in p120 are rare. Based on the COSMIC online database, to date only 1 missense (1081C->A (stage III, ER/PR/Her2-negative ductal carcinoma) and 1 nonsense (1963C->T (stage II ER/PR-positive Her2-negative mixed ductal lobular carcinoma)) p120 mutation were found in breast cancer³⁷⁵. This may be caused by a lack of coverage and high tumor heterogeneity. Nonetheless, breast cancer often displays loss of p120 protein expression in part of the tumor^{223, 224, 252} (chapter 3), which suggest that p120 may be downregulated by epigenetic or post-translational processes. Moreover, it implies that inactivation of p120 is probably a late event in breast cancer. Together with the fact that dual inactivation of p120 and p53 does not lead to ILC formation in mice, it suggests that loss of p120-induced tumor progression may be confined to the ductal carcinoma subtype.

We show that p120 loss and subsequent AJ inactivation is a general mechanism to induce indiscriminate sensitization of GFR signaling, without inducing upregulation of GFR expression levels. As described in chapter 3, this induces anchorage independent survival possibly leading to metastasis formation. These findings suggest that treatment of p120-negative tumors by inhibition of GFR signaling would be clinically beneficial in patients lacking overexpression or mutation of a given GFR. However, due to the indiscriminant nature of the GFR sensitization, one would need to identify all GFRs and inhibit their tyrosine kinase activity. While several broad spectrum GFR inhibitors exist (SU6668 which inhibits PDGFR

and FGFR³⁷⁶, sunitinib which inhibit VEGFR PDGFR KIT and FLT3, lapatinib/GW572016 which inhibits Her2 and EGFR³⁷⁷), it is unlikely that a single inhibitor will suffice in inhibiting all expressed GFRs. Therefore, it may be preferred to inhibit GFR signaling through a mutual downstream survival pathway such as the PI3K/Akt and mTOR cascade. Combined Akt and mTOR inhibition might prove beneficial due to positive feedback loops whereby mTOR inhibition can facilitate activation of Akt signaling^{378, 379}. Several promising inhibitors exist, multiple of which are currently evaluated in clinical trials (PI3K/Akt inhibitor: MK-2206 phase I³⁸⁰; BKM120 phase I³⁸¹; Perifosine phase II³⁸²; mTOR inhibitor: Temsirolimus phase II³⁸³ Everolimus clinically approved³⁸⁴) (reviewed in³⁸⁵).

Additionally, the metastatic capacity of p120 negative tumor cells can be further attenuated by inhibiting formation of the prometastatic microenvironment. Use of anti-inflammatory drugs such as COX-^{386, 387} or NFκB-inhibitors³⁶⁰ might impede formation of the prometastatic microenvironment, although we have not yet determined whether these signaling pathways are causative to the p120-loss induced microenvironment. Alternatively, the use of blocking antibodies that specifically target the cytokines released by p120-negative tumors might reduce the influx of inflammatory cells and inhibit tumor progression and metastasis formation.

Rock inhibition to treat ILC

The majority (~80%) of ILCs are estrogen receptor (ER) positive and therefore *suitable* for hormone therapy. Use of the ER antagonist tamoxifen or blocking intrinsic ER production via aromatase inhibitors have proven highly beneficial in reducing tumor recurrence, with a disease-free survival rate of 50% 7 years after primary treatment^{13, 16}. Unfortunately, resistance to the primary therapeutics eventually occurs, resulting in wide-spread dissemination, often localized at inoperable sites^{13, 24-26}. This may indicate the presence of early metastasizing cells, which need to be eliminated before therapeutic resistance and outgrowth can occur. In chapters 4 and 5, we demonstrate that p120-dependent activation of Rho-Rock signaling promotes tumor growth and metastasis of ILC. Rock inhibition might thus hold promise when combined with conventional therapeutics to induce anoikis in anchorage-independent ILC cells.

While shRNA-mediated Rock inhibition showed promising results *in vivo*, we observed that the induction of *in vitro* anoikis by pharmacological inhibition of Rock could be partially overcome by the addition of EGF (unpublished data). Furthermore, alike p120 loss, E-cadherin inactivation leads to sensitized GFR signaling. This suggests that (pre)clinical use of pharmacological Rock inhibitors might be compromised by growth factor signaling. Thus it seems likely that a dual inhibition of Rock and GFR signaling may be required to treat metastatic ILC.

In closing, the work described in this thesis provides mechanistic insight in how functional inactivation of the adherens junction controls breast cancer progression. Using complex conditional mouse models, and a combination of cell biology, biochemistry and clinical data we uncovered novel functions for p120 that provide a mechanistic basis for the development of novel intervention strategies to treat metastatic breast cancer.



Addendum



References

Nederlandse samenvatting

Curriculum Vitae

Publications

Dankwoord

References

1. Jemal, A. *et al.* Global cancer statistics. *CA Cancer J Clin* **61**, 69-90 (2011).
2. Kenemans, P., Verstraeten, R.A. & Verheijen, R.H. Oncogenic pathways in hereditary and sporadic breast cancer. *Maturitas* **61**, 141-150 (2008).
3. O'Malley, F.P. Lobular neoplasia: morphology, biological potential and management in core biopsies. *Modern pathology : an official journal of the United States and Canadian Academy of Pathology, Inc* **23 Suppl 2**, S14-25 (2010).
4. Ozanne, E.M. *et al.* Characterizing the impact of 25 years of DCIS treatment. *Breast cancer research and treatment* **129**, 165-173 (2011).
5. Fisher, E.R. *et al.* Pathologic findings from the National Surgical Adjuvant Breast and Bowel Project: twelve-year observations concerning lobular carcinoma in situ. *Cancer* **100**, 238-244 (2004).
6. Hwang, E.S. *et al.* Clonality of lobular carcinoma in situ and synchronous invasive lobular carcinoma. *Cancer* **100**, 2562-2572 (2004).
7. Schnitt, S.J. Benign breast disease and breast cancer risk: potential role for antiestrogens. *Clinical cancer research : an official journal of the American Association for Cancer Research* **7**, 4419s-4422s; discussion 4411s-4412s (2001).
8. Hilleren, D.J., Andersson, I.T., Lindholm, K. & Linnell, F.S. Invasive lobular carcinoma: mammographic findings in a 10-year experience. *Radiology* **178**, 149-154 (1991).
9. Berx, G. *et al.* E-cadherin is a tumour/invasion suppressor gene mutated in human lobular breast cancers. *EMBO J* **14**, 6107-6115 (1995).
10. Lehr, H.A., Folpe, A., Yaziji, H., Kommoss, F. & Gown, A.M. Cytokeratin 8 immunostaining pattern and E-cadherin expression distinguish lobular from ductal breast carcinoma. *American journal of clinical pathology* **114**, 190-196 (2000).
11. Molland, J.G. *et al.* Infiltrating lobular carcinoma--a comparison of diagnosis, management and outcome with infiltrating duct carcinoma. *Breast* **13**, 389-396 (2004).
12. Tubiana-Hulin, M. *et al.* Response to neoadjuvant chemotherapy in lobular and ductal breast carcinomas: a retrospective study on 860 patients from one institution. *Annals of oncology : official journal of the European Society for Medical Oncology / ESMO* **17**, 1228-1233 (2006).
13. Pestalozzi, B.C. *et al.* Distinct clinical and prognostic features of infiltrating lobular carcinoma of the breast: combined results of 15 International Breast Cancer Study Group clinical trials. *J Clin Oncol* **26**, 3006-3014 (2008).
14. Ferlicot, S. *et al.* Wide metastatic spreading in infiltrating lobular carcinoma of the breast. *European journal of cancer* **40**, 336-341 (2004).
15. Prat, A. & Perou, C.M. Deconstructing the molecular portraits of breast cancer. *Mol Oncol* **5**, 5-23 (2011).
16. Hind, D., Wyld, L. & Reed, M.W. Surgery, with or without tamoxifen, vs tamoxifen alone for older women with operable breast cancer: cochrane review. *British journal of cancer* **96**, 1025-1029 (2007).
17. Perou, C.M. *et al.* Molecular portraits of human breast tumours. *Nature* **406**, 747-752 (2000).
18. Sorlie, T. *et al.* Gene expression patterns of breast carcinomas distinguish tumor subclasses with clinical implications. *Proc Natl Acad Sci U S A* **98**, 10869-10874 (2001).
19. Herschkowitz, J.I. *et al.* Identification of conserved gene expression features between murine mammary carcinoma models and human breast tumors. *Genome Biol* **8**, R76 (2007).
20. Prat, A. *et al.* Phenotypic and molecular characterization of the claudin-low intrinsic subtype of breast cancer. *Breast Cancer Res* **12**, R68 (2010).
21. Deisenroth, C., Thorner, A.R., Enomoto, T., Perou, C.M. & Zhang, Y. Mitochondrial Hep27 is a c-Myb target gene that inhibits Mdm2 and stabilizes p53. *Mol Cell Biol* **30**, 3981-3993 (2010).
22. Gonzalez-Angulo, A.M., Morales-Vasquez, F. & Hortobagyi, G.N. Overview of resistance to systemic therapy in patients with breast cancer. *Adv Exp Med Biol* **608**, 1-22 (2007).
23. Jemal, A. *et al.* Cancer statistics, 2009. *CA Cancer J Clin* **59**, 225-249 (2009).
24. Hoefnagel, L.D. *et al.* Receptor conversion in distant breast cancer metastases. *Breast Cancer Res* **12**, R75 (2010).
25. Clemons, M., Danson, S. & Howell, A. Tamoxifen ("Nolvadex"): a review. *Cancer treatment reviews* **28**, 165-180 (2002).
26. Ali, S. & Coombes, R.C. Endocrine-responsive breast cancer and strategies for combating resistance. *Nature reviews. Cancer* **2**, 101-112 (2002).
27. Garrod, D. & Chidgey, M. Desmosome structure, composition and function. *Biochim Biophys Acta* **1778**, 572-587 (2008).
28. Camilleri, M., Madsen, K., Spiller, R., Greenwood-Van Meerveld, B. & Verne, G.N. Intestinal

- barrier function in health and gastrointestinal disease. *Neurogastroenterology and motility : the official journal of the European Gastrointestinal Motility Society* **24**, 503-512 (2012).
29. Niessen, C.M. Tight junctions/adherens junctions: basic structure and function. *J Invest Dermatol* **127**, 2525-2532 (2007).
 30. Kowalczyk, A.P. & Nanes, B.A. Adherens junction turnover: regulating adhesion through cadherin endocytosis, degradation, and recycling. *Subcell Biochem* **60**, 197-222 (2012).
 31. Hyafil, F., Morello, D., Babinet, C. & Jacob, F. A cell surface glycoprotein involved in the compaction of embryonal carcinoma cells and cleavage stage embryos. *Cell* **21**, 927-934 (1980).
 32. Yoshida-Noro, C., Suzuki, N. & Takeichi, M. Molecular nature of the calcium-dependent cell-cell adhesion system in mouse teratocarcinoma and embryonic cells studied with a monoclonal antibody. *Developmental biology* **101**, 19-27 (1984).
 33. Nagafuchi, A., Shirayoshi, Y., Okazaki, K., Yasuda, K. & Takeichi, M. Transformation of cell adhesion properties by exogenously introduced E-cadherin cDNA. *Nature* **329**, 341-343 (1987).
 34. Ratheesh, A. & Yap, A.S. A bigger picture: classical cadherins and the dynamic actin cytoskeleton. *Nat Rev Mol Cell Biol* **13**, 673-679 (2012).
 35. Davis, M.A., Ireton, R.C. & Reynolds, A.B. A core function for p120-catenin in cadherin turnover. *J Cell Biol* **163**, 525-534 (2003).
 36. Reynolds, A.B., Kanner, S.B., Wang, H.C. & Parsons, J.T. Stable association of activated pp60src with two tyrosine-phosphorylated cellular proteins. *Mol Cell Biol* **9**, 3951-3958 (1989).
 37. Kanner, S.B., Reynolds, A.B. & Parsons, J.T. Tyrosine phosphorylation of a 120-kilodalton pp60src substrate upon epidermal growth factor and platelet-derived growth factor receptor stimulation and in polyomavirus middle-T-antigen-transformed cells. *Mol Cell Biol* **11**, 713-720 (1991).
 38. Downing, J.R. & Reynolds, A.B. PDGF, CSF-1, and EGF induce tyrosine phosphorylation of p120, a pp60src transformation-associated substrate. *Oncogene* **6**, 607-613 (1991).
 39. Reynolds, A.B., Herbert, L., Cleveland, J.L., Berg, S.T. & Gaut, J.R. p120, a novel substrate of protein tyrosine kinase receptors and of p60v-src, is related to cadherin-binding factors beta-catenin, plakoglobin and armadillo. *Oncogene* **7**, 2439-2445 (1992).
 40. Peifer, M., Berg, S. & Reynolds, A.B. A repeating amino acid motif shared by proteins with diverse cellular roles. *Cell* **76**, 789-791 (1994).
 41. Tewari, R., Bailes, E., Bunting, K.A. & Coates, J.C. Armadillo-repeat protein functions: questions for little creatures. *Trends Cell Biol* **20**, 470-481 (2010).
 42. Anastasiadis, P.Z. & Reynolds, A.B. The p120 catenin family: complex roles in adhesion, signaling and cancer. *J Cell Sci* **113** (Pt 8), 1319-1334 (2000).
 43. Sakai, R. *et al.* A novel signaling molecule, p130, forms stable complexes in vivo with v-Crk and v-Src in a tyrosine phosphorylation-dependent manner. *EMBO J* **13**, 3748-3756 (1994).
 44. Yap, A.S., Niessen, C.M. & Gumbiner, B.M. The juxtamembrane region of the cadherin cytoplasmic tail supports lateral clustering, adhesive strengthening, and interaction with p120ctn. *J Cell Biol* **141**, 779-789 (1998).
 45. Thoreson, M.A. *et al.* Selective uncoupling of p120(ctn) from E-cadherin disrupts strong adhesion. *J Cell Biol* **148**, 189-202 (2000).
 46. Ozawa, M. & Kemler, R. The membrane-proximal region of the E-cadherin cytoplasmic domain prevents dimerization and negatively regulates adhesion activity. *J Cell Biol* **142**, 1605-1613 (1998).
 47. Perez-Moreno, M. & Fuchs, E. Catenins: keeping cells from getting their signals crossed. *Dev Cell* **11**, 601-612 (2006).
 48. Carnahan, R.H., Rokas, A., Gaucher, E.A. & Reynolds, A.B. The molecular evolution of the p120-catenin subfamily and its functional associations. *PLoS One* **5**, e15747 (2010).
 49. Kosik, K.S., Donahue, C.P., Israely, I., Liu, X. & Ochiishi, T. Delta-catenin at the synaptic-adherens junction. *Trends Cell Biol* **15**, 172-178 (2005).
 50. Hatzfeld, M. The p120 family of cell adhesion molecules. *European journal of cell biology* **84**, 205-214 (2005).
 51. Hatzfeld, M. Plakophilins: Multifunctional proteins or just regulators of desmosomal adhesion? *Biochim Biophys Acta* **1773**, 69-77 (2007).
 52. Roczniak-Ferguson, A. & Reynolds, A.B. Regulation of p120-catenin nucleocytoplasmic shuttling activity. *J Cell Sci* **116**, 4201-4212 (2003).
 53. Mo, Y.Y. & Reynolds, A.B. Identification of murine p120 isoforms and heterogeneous expression of p120cas isoforms in human tumor cell lines. *Cancer Res* **56**, 2633-2640 (1996).
 54. Slorach, E.M., Chou, J. & Werb, Z. Zeppo1 is a novel metastasis promoter that represses E-cadherin expression and regulates p120-catenin isoform expression and localization. *Genes Dev* **25**, 471-484 (2011).

55. Montonen, O., Aho, M., Uitto, J. & Aho, S. Tissue distribution and cell type-specific expression of p120ctn isoforms. *J Histochem Cytochem* **49**, 1487-1496 (2001).
56. Keirsebilck, A. *et al.* Molecular cloning of the human p120ctn catenin gene (CTNND1): expression of multiple alternatively spliced isoforms. *Genomics* **50**, 129-146 (1998).
57. Aho, S. *et al.* Specific sequences in p120ctn determine subcellular distribution of its multiple isoforms involved in cellular adhesion of normal and malignant epithelial cells. *J Cell Sci* **115**, 1391-1402 (2002).
58. Hinck, L., Nathke, I.S., Papkoff, J. & Nelson, W.J. Dynamics of cadherin/catenin complex formation: novel protein interactions and pathways of complex assembly. *J Cell Biol* **125**, 1327-1340 (1994).
59. Chen, Y.T., Stewart, D.B. & Nelson, W.J. Coupling assembly of the E-cadherin/beta-catenin complex to efficient endoplasmic reticulum exit and basal-lateral membrane targeting of E-cadherin in polarized MDCK cells. *J Cell Biol* **144**, 687-699 (1999).
60. Jou, T.S., Stewart, D.B., Stappert, J., Nelson, W.J. & MARRS, J.A. Genetic and biochemical dissection of protein linkages in the cadherin-catenin complex. *Proc Natl Acad Sci U S A* **92**, 5067-5071 (1995).
61. Miranda, K.C., Joseph, S.R., Yap, A.S., Teasdale, R.D. & Stow, J.L. Contextual binding of p120ctn to E-cadherin at the basolateral plasma membrane in polarized epithelia. *J Biol Chem* **278**, 43480-43488 (2003).
62. Wahl, J.K., 3rd, Kim, Y.J., Cullen, J.M., Johnson, K.R. & Wheelock, M.J. N-cadherin-catenin complexes form prior to cleavage of the proregion and transport to the plasma membrane. *J Biol Chem* **278**, 17269-17276 (2003).
63. Chen, X., Kojima, S., Borisy, G.G. & Green, K.J. p120 catenin associates with kinesin and facilitates the transport of cadherin-catenin complexes to intercellular junctions. *J Cell Biol* **163**, 547-557 (2003).
64. Wu, Y., Vendome, J., Shapiro, L., Ben-Shaul, A. & Honig, B. Transforming binding affinities from three dimensions to two with application to cadherin clustering. *Nature* **475**, 510-513 (2011).
65. Wu, Y. *et al.* Cooperativity between trans and cis interactions in cadherin-mediated junction formation. *Proc Natl Acad Sci U S A* **107**, 17592-17597 (2010).
66. Brasch, J., Harrison, O.J., Honig, B. & Shapiro, L. Thinking outside the cell: how cadherins drive adhesion. *Trends Cell Biol* **22**, 299-310 (2012).
67. Ireton, R.C. *et al.* A novel role for p120 catenin in E-cadherin function. *J Cell Biol* **159**, 465-476 (2002).
68. Ishiyama, N. *et al.* Dynamic and static interactions between p120 catenin and E-cadherin regulate the stability of cell-cell adhesion. *Cell* **141**, 117-128 (2010).
69. Daniel, J.M. & Reynolds, A.B. The tyrosine kinase substrate p120cas binds directly to E-cadherin but not to the adenomatous polyposis coli protein or alpha-catenin. *Mol Cell Biol* **15**, 4819-4824 (1995).
70. Peifer, M. & Yap, A.S. Traffic control: p120-catenin acts as a gatekeeper to control the fate of classical cadherins in mammalian cells. *J Cell Biol* **163**, 437-440 (2003).
71. Yu, J. *et al.* N-terminal 1-54 amino acid sequence and Armadillo repeat domain are indispensable for P120-catenin isoform 1A in regulating E-cadherin. *PLoS One* **7**, e37008 (2012).
72. Eagle, H. & Levine, E.M. Growth regulatory effects of cellular interaction. *Nature* **213**, 1102-1106 (1967).
73. Motti, M.L. *et al.* Reduced E-cadherin expression contributes to the loss of p27kip1-mediated mechanism of contact inhibition in thyroid anaplastic carcinomas. *Carcinogenesis* **26**, 1021-1034 (2005).
74. McClatchey, A.I. & Yap, A.S. Contact inhibition (of proliferation) redux. *Curr Opin Cell Biol* **24**, 685-694 (2012).
75. Takahashi, K. & Suzuki, K. Density-dependent inhibition of growth involves prevention of EGF receptor activation by E-cadherin-mediated cell-cell adhesion. *Exp Cell Res* **226**, 214-222 (1996).
76. Mellman, I. & Nelson, W.J. Coordinated protein sorting, targeting and distribution in polarized cells. *Nat Rev Mol Cell Biol* **9**, 833-845 (2008).
77. Qian, X., Karpova, T., Sheppard, A.M., McNally, J. & Lowy, D.R. E-cadherin-mediated adhesion inhibits ligand-dependent activation of diverse receptor tyrosine kinases. *EMBO J* **23**, 1739-1748 (2004).
78. Nanes, B.A. *et al.* p120-catenin binding masks an endocytic signal conserved in classical cadherins. *J Cell Biol* **199**, 365-380 (2012).
79. Miyashita, Y. & Ozawa, M. Increased internalization of p120-uncoupled E-cadherin and a requirement for a dileucine motif in the cytoplasmic domain for endocytosis of the protein. *J*

- Biol Chem* **282**, 11540-11548 (2007).
80. Fujita, Y. *et al.* Hakai, a c-Cbl-like protein, ubiquitinates and induces endocytosis of the E-cadherin complex. *Nat Cell Biol* **4**, 222-231 (2002).
 81. Palacios, F., Tushir, J.S., Fujita, Y. & D'Souza-Schorey, C. Lysosomal targeting of E-cadherin: a unique mechanism for the down-regulation of cell-cell adhesion during epithelial to mesenchymal transitions. *Mol Cell Biol* **25**, 389-402 (2005).
 82. Nishimura, T. & Kaibuchi, K. Numb controls integrin endocytosis for directional cell migration with aPKC and PAR-3. *Dev Cell* **13**, 15-28 (2007).
 83. Gulino, A., Di Marcotullio, L. & Screpanti, I. The multiple functions of Numb. *Exp Cell Res* **316**, 900-906 (2010).
 84. Sato, K. *et al.* Numb controls E-cadherin endocytosis through p120 catenin with aPKC. *Mol Biol Cell* **22**, 3103-3119 (2011).
 85. Wang, Z. & Li, S.S. Numb: A new player in EMT. *Cell Adh Migr* **4**, 176-179 (2010).
 86. Wang, Z., Sandiford, S., Wu, C. & Li, S.S. Numb regulates cell-cell adhesion and polarity in response to tyrosine kinase signalling. *EMBO J* **28**, 2360-2373 (2009).
 87. Baki, L. *et al.* Presenilin-1 binds cytoplasmic epithelial cadherin, inhibits cadherin/p120 association, and regulates stability and function of the cadherin/catenin adhesion complex. *Proc Natl Acad Sci U S A* **98**, 2381-2386 (2001).
 88. Marambaud, P. *et al.* A presenilin-1/gamma-secretase cleavage releases the E-cadherin intracellular domain and regulates disassembly of adherens junctions. *EMBO J* **21**, 1948-1956 (2002).
 89. Spasic, D. & Annaert, W. Building gamma-secretase: the bits and pieces. *J Cell Sci* **121**, 413-420 (2008).
 90. Kouchi, Z. *et al.* p120 catenin recruits cadherins to gamma-secretase and inhibits production of Abeta peptide. *J Biol Chem* **284**, 1954-1961 (2009).
 91. Kiss, A., Troyanovsky, R.B. & Troyanovsky, S.M. p120-catenin is a key component of the cadherin-gamma-secretase supercomplex. *Mol Biol Cell* **19**, 4042-4050 (2008).
 92. Fortini, M.E. Gamma-secretase-mediated proteolysis in cell-surface-receptor signalling. *Nat Rev Mol Cell Biol* **3**, 673-684 (2002).
 93. Vale, R.D., Malik, F. & Brown, D. Directional instability of microtubule transport in the presence of kinesin and dynein, two opposite polarity motor proteins. *J Cell Biol* **119**, 1589-1596 (1992).
 94. Vasioukhin, V., Bauer, C., Yin, M. & Fuchs, E. Directed actin polymerization is the driving force for epithelial cell-cell adhesion. *Cell* **100**, 209-219 (2000).
 95. Ivanov, A.I., Nusrat, A. & Parkos, C.A. Endocytosis of the apical junctional complex: mechanisms and possible roles in regulation of epithelial barriers. *Bioessays* **27**, 356-365 (2005).
 96. Stehbens, S.J. *et al.* Dynamic microtubules regulate the local concentration of E-cadherin at cell-cell contacts. *J Cell Sci* **119**, 1801-1811 (2006).
 97. Yanagisawa, M. *et al.* A novel interaction between kinesin and p120 modulates p120 localization and function. *J Biol Chem* **279**, 9512-9521 (2004).
 98. Sumigray, K.D., Foote, H.P. & Lechler, T. Noncentrosomal microtubules and type II myosins potentiate epidermal cell adhesion and barrier formation. *J Cell Biol* **199**, 513-525 (2012).
 99. Yamada, S. & Nelson, W.J. Localized zones of Rho and Rac activities drive initiation and expansion of epithelial cell-cell adhesion. *J Cell Biol* **178**, 517-527 (2007).
 100. Meng, W., Mushika, Y., Ichii, T. & Takeichi, M. Anchorage of microtubule minus ends to adherens junctions regulates epithelial cell-cell contacts. *Cell* **135**, 948-959 (2008).
 101. Rimm, D.L., Koslov, E.R., Kebriaei, P., Cianci, C.D. & Morrow, J.S. Alpha 1(E)-catenin is an actin-binding and -bundling protein mediating the attachment of F-actin to the membrane adhesion complex. *Proc Natl Acad Sci U S A* **92**, 8813-8817 (1995).
 102. Yamada, S., Pokutta, S., Drees, F., Weis, W.I. & Nelson, W.J. Deconstructing the cadherin-catenin-actin complex. *Cell* **123**, 889-901 (2005).
 103. Drees, F., Pokutta, S., Yamada, S., Nelson, W.J. & Weis, W.I. Alpha-catenin is a molecular switch that binds E-cadherin-beta-catenin and regulates actin-filament assembly. *Cell* **123**, 903-915 (2005).
 104. Abe, K. & Takeichi, M. EPLIN mediates linkage of the cadherin catenin complex to F-actin and stabilizes the circumferential actin belt. *Proc Natl Acad Sci U S A* **105**, 13-19 (2008).
 105. Knudsen, K.A., Soler, A.P., Johnson, K.R. & Wheelock, M.J. Interaction of alpha-actinin with the cadherin/catenin cell-cell adhesion complex via alpha-catenin. *J Cell Biol* **130**, 67-77 (1995).
 106. Weiss, E.E., Kroemker, M., Rudiger, A.H., Jockusch, B.M. & Rudiger, M. Vinculin is part of the cadherin-catenin junctional complex: complex formation between alpha-catenin and vinculin. *J Cell Biol* **141**, 755-764 (1998).
 107. le Duc, Q. *et al.* Vinculin potentiates E-cadherin mechanosensing and is recruited to actin-

- anchored sites within adherens junctions in a myosin II-dependent manner. *J Cell Biol* **189**, 1107-1115 (2010).
108. Yonemura, S., Wada, Y., Watanabe, T., Nagafuchi, A. & Shibata, M. alpha-Catenin as a tension transducer that induces adherens junction development. *Nat Cell Biol* **12**, 533-542 (2010).
109. Taguchi, K., Ishiuchi, T. & Takeichi, M. Mechanosensitive EPLIN-dependent remodeling of adherens junctions regulates epithelial reshaping. *J Cell Biol* **194**, 643-656 (2011).
110. Menke, A. & Giehl, K. Regulation of adherens junctions by Rho GTPases and p120-catenin. *Arch Biochem Biophys* **524**, 48-55 (2012).
111. DeMali, K.A. & Burridge, K. Coupling membrane protrusion and cell adhesion. *J Cell Sci* **116**, 2389-2397 (2003).
112. Kraemer, A., Goodwin, M., Verma, S., Yap, A.S. & Ali, R.G. Rac is a dominant regulator of cadherin-directed actin assembly that is activated by adhesive ligation independently of Tiam1. *Am J Physiol Cell Physiol* **292**, C1061-1069 (2007).
113. Mege, R.M., Gavard, J. & Lambert, M. Regulation of cell-cell junctions by the cytoskeleton. *Curr Opin Cell Biol* **18**, 541-548 (2006).
114. Kitt, K.N. & Nelson, W.J. Rapid suppression of activated Rac1 by cadherins and nectins during de novo cell-cell adhesion. *PLoS One* **6**, e17841 (2011).
115. Leung, T., Chen, X.Q., Manser, E. & Lim, L. The p160 RhoA-binding kinase ROK alpha is a member of a kinase family and is involved in the reorganization of the cytoskeleton. *Mol Cell Biol* **16**, 5313-5327 (1996).
116. Kher, S.S. & Worthylake, R.A. Nuanced junctional RhoA activity. *Nat Cell Biol* **14**, 784-786 (2012).
117. Ratheesh, A. *et al.* Centralspindlin and alpha-catenin regulate Rho signalling at the epithelial zonula adherens. *Nat Cell Biol* **14**, 818-828 (2012).
118. Gomez, G.A., McLachlan, R.W. & Yap, A.S. Productive tension: force-sensing and homeostasis of cell-cell junctions. *Trends Cell Biol* **21**, 499-505 (2011).
119. Yanagisawa, M. *et al.* A p120 catenin isoform switch affects Rho activity, induces tumor cell invasion, and predicts metastatic disease. *J Biol Chem* **283**, 18344-18354 (2008).
120. Anastasiadis, P.Z. *et al.* Inhibition of RhoA by p120 catenin. *Nat Cell Biol* **2**, 637-644 (2000).
121. Cozzolino, M. *et al.* p120 Catenin is required for growth factor-dependent cell motility and scattering in epithelial cells. *Mol Biol Cell* **14**, 1964-1977 (2003).
122. Schackmann, R.C. *et al.* Cytosolic p120-catenin regulates growth of metastatic lobular carcinoma through Rock1-mediated anoikis resistance. *J Clin Invest* **121**, 3176-3188 (2011).
123. Alcaide, P. *et al.* p120-Catenin prevents neutrophil transmigration independently of RhoA inhibition by impairing Src dependent VE-cadherin phosphorylation. *Am J Physiol Cell Physiol* **303**, C385-395 (2012).
124. Wong, L.E., Reynolds, A.B., Dissanayaka, N.T. & Minden, A. p120-catenin is a binding partner and substrate for Group B Pak kinases. *J Cell Biochem* **110**, 1244-1254 (2010).
125. Castano, J. *et al.* Specific phosphorylation of p120-catenin regulatory domain differently modulates its binding to RhoA. *Mol Cell Biol* **27**, 1745-1757 (2007).
126. Fukuhara, S., Chikumi, H. & Gutkind, J.S. RGS-containing RhoGEFs: the missing link between transforming G proteins and Rho? *Oncogene* **20**, 1661-1668 (2001).
127. Wang, E.H. *et al.* Abnormal expression and clinicopathologic significance of p120-catenin in lung cancer. *Histol Histopathol* **21**, 841-847 (2006).
128. Liu, Y. *et al.* Reduction of p120(ctn) isoforms 1 and 3 is significantly associated with metastatic progression of human lung cancer. *APMIS* **115**, 848-856 (2007).
129. Perez-Moreno, M. *et al.* p120-catenin mediates inflammatory responses in the skin. *Cell* **124**, 631-644 (2006).
130. Sander, E.E., ten Klooster, J.P., van Delft, S., van der Kammen, R.A. & Collard, J.G. Rac downregulates Rho activity: reciprocal balance between both GTPases determines cellular morphology and migratory behavior. *J Cell Biol* **147**, 1009-1022 (1999).
131. Schnelzer, A. *et al.* Rac1 in human breast cancer: overexpression, mutation analysis, and characterization of a new isoform, Rac1b. *Oncogene* **19**, 3013-3020 (2000).
132. Orlichenko, L. *et al.* The 19-amino acid insertion in the tumor-associated splice isoform Rac1b confers specific binding to p120 catenin. *J Biol Chem* **285**, 19153-19161 (2010).
133. Valls, G. *et al.* Rac1 activation upon Wnt stimulation requires Rac1 and Vav2 binding to p120-catenin. *J Cell Sci* (2012).
134. Tamas, P. *et al.* Mechanism of epidermal growth factor regulation of Vav2, a guanine nucleotide exchange factor for Rac. *J Biol Chem* **278**, 5163-5171 (2003).
135. Nieman, M.T., Prudoff, R.S., Johnson, K.R. & Wheelock, M.J. N-cadherin promotes motility in human breast cancer cells regardless of their E-cadherin expression. *J Cell Biol* **147**, 631-644 (1999).

136. Pishvaian, M.J. *et al.* Cadherin-11 is expressed in invasive breast cancer cell lines. *Cancer Res* **59**, 947-952 (1999).
137. Yanagisawa, M. & Anastasiadis, P.Z. p120 catenin is essential for mesenchymal cadherin-mediated regulation of cell motility and invasiveness. *J Cell Biol* **174**, 1087-1096 (2006).
138. Noren, N.K., Liu, B.P., Burrridge, K. & Kreft, B. p120 catenin regulates the actin cytoskeleton via Rho family GTPases. *J Cell Biol* **150**, 567-580 (2000).
139. Franz, C.M. & Ridley, A.J. p120 catenin associates with microtubules: inverse relationship between microtubule binding and Rho GTPase regulation. *J Biol Chem* **279**, 6588-6594 (2004).
140. Thompson, A.J. *et al.* Characterization of protein phosphorylation by mass spectrometry using immobilized metal ion affinity chromatography with on-resin beta-elimination and Michael addition. *Anal Chem* **75**, 3232-3243 (2003).
141. Vasanth, S., ZeRuth, G., Kang, H.S. & Jetten, A.M. Identification of nuclear localization, DNA binding, and transactivating mechanisms of Kruppel-like zinc finger protein Gli-similar 2 (Glis2). *J Biol Chem* **286**, 4749-4759 (2011).
142. Hosking, C.R. *et al.* The transcriptional repressor Glis2 is a novel binding partner for p120 catenin. *Mol Biol Cell* **18**, 1918-1927 (2007).
143. Wegiel, J., Gong, C.X. & Hwang, Y.W. The role of DYRK1A in neurodegenerative diseases. *The FEBS journal* **278**, 236-245 (2011).
144. Hong, J.Y. *et al.* Down's-syndrome-related kinase Dyrk1A modulates the p120-catenin-Kaiso trajectory of the Wnt signaling pathway. *J Cell Sci* **125**, 561-569 (2012).
145. Daniel, J.M. & Reynolds, A.B. The catenin p120(ctn) interacts with Kaiso, a novel BTB/POZ domain zinc finger transcription factor. *Mol Cell Biol* **19**, 3614-3623 (1999).
146. Prokhortchouk, A. *et al.* The p120 catenin partner Kaiso is a DNA methylation-dependent transcriptional repressor. *Genes Dev* **15**, 1613-1618 (2001).
147. Daniel, J.M., Spring, C.M., Crawford, H.C., Reynolds, A.B. & Baig, A. The p120(ctn)-binding partner Kaiso is a bi-modal DNA-binding protein that recognizes both a sequence-specific consensus and methylated CpG dinucleotides. *Nucleic Acids Res* **30**, 2911-2919 (2002).
148. Kim, S.W. *et al.* Non-canonical Wnt signals are modulated by the Kaiso transcriptional repressor and p120-catenin. *Nat Cell Biol* **6**, 1212-1220 (2004).
149. Ogden, S.R. *et al.* p120 and Kaiso regulate Helicobacter pylori-induced expression of matrix metalloproteinase-7. *Mol Biol Cell* **19**, 4110-4121 (2008).
150. Kelly, K.F., Spring, C.M., Otchere, A.A. & Daniel, J.M. NLS-dependent nuclear localization of p120ctn is necessary to relieve Kaiso-mediated transcriptional repression. *J Cell Sci* **117**, 2675-2686 (2004).
151. Ferber, E.C. *et al.* A role for the cleaved cytoplasmic domain of E-cadherin in the nucleus. *J Biol Chem* **283**, 12691-12700 (2008).
152. Kouros-Mehr, H. & Werb, Z. Candidate regulators of mammary branching morphogenesis identified by genome-wide transcript analysis. *Developmental dynamics : an official publication of the American Association of Anatomists* **235**, 3404-3412 (2006).
153. Zhang, D.L. *et al.* Effect of Wnt signaling pathway on wound healing. *Biochemical and biophysical research communications* **378**, 149-151 (2009).
154. Logan, C.Y. & Nusse, R. The Wnt signaling pathway in development and disease. *Annual review of cell and developmental biology* **20**, 781-810 (2004).
155. Clevers, H. & Nusse, R. Wnt/beta-catenin signaling and disease. *Cell* **149**, 1192-1205 (2012).
156. Del Valle-Perez, B. *et al.* Wnt controls the transcriptional activity of Kaiso through CK1epsilon-dependent phosphorylation of p120-catenin. *J Cell Sci* **124**, 2298-2309 (2011).
157. Ruzov, A. *et al.* The interaction of xKaiso with xTcf3: a revised model for integration of epigenetic and Wnt signalling pathways. *Development* **136**, 723-727 (2009).
158. Casagolda, D. *et al.* A p120-catenin-CK1epsilon complex regulates Wnt signaling. *J Cell Sci* **123**, 2621-2631 (2010).
159. Del Valle-Perez, B., Arques, O., Vinyoles, M., de Herreros, A.G. & Dunach, M. Coordinated action of CK1 isoforms in canonical Wnt signaling. *Mol Cell Biol* **31**, 2877-2888 (2011).
160. Markham, N.O. *et al.* Monoclonal antibodies to DIPA: a novel binding partner of p120-catenin isoform 1. *Hybridoma (Larchmt)* **31**, 246-254 (2012).
161. Iwai, A. *et al.* Coiled-coil domain containing 85B suppresses the beta-catenin activity in a p53-dependent manner. *Oncogene* **27**, 1520-1526 (2008).
162. Whyte, J.L., Smith, A.A. & Helms, J.A. Wnt signaling and injury repair. *Cold Spring Harbor perspectives in biology* **4**, a008078 (2012).
163. Congdon, K.L. *et al.* Activation of Wnt signaling in hematopoietic regeneration. *Stem cells* **26**, 1202-1210 (2008).
164. Mortazavi, F., An, J., Dubinett, S. & Rettig, M. p120-catenin is transcriptionally downregulated by FOXC2 in non-small cell lung cancer cells. *Mol Cancer Res* **8**, 762-774 (2010).

165. Mani, S.A. *et al.* Mesenchyme Forkhead 1 (FOXC2) plays a key role in metastasis and is associated with aggressive basal-like breast cancers. *Proc Natl Acad Sci U S A* **104**, 10069-10074 (2007).
166. Mortazavi, F., Dubinett, S. & Rettig, M. c-Crk proto-oncogene contributes to transcriptional repression of p120-catenin in non-small cell lung cancer cells. *Clin Exp Metastasis* **28**, 391-404 (2011).
167. Rettig, M. *et al.* PAK1 kinase promotes cell motility and invasiveness through CRK-II serine phosphorylation in non-small cell lung cancer cells. *PLoS One* **7**, e42012 (2012).
168. Bartel, D.P. MicroRNAs: target recognition and regulatory functions. *Cell* **136**, 215-233 (2009).
169. Hamada, S. *et al.* MiR-197 induces epithelial-mesenchymal transition in pancreatic cancer cells by targeting p120 catenin. *J Cell Physiol* (2012).
170. Ohkubo, T. & Ozawa, M. The transcription factor Snail downregulates the tight junction components independently of E-cadherin downregulation. *J Cell Sci* **117**, 1675-1685 (2004).
171. Sarrio, D. *et al.* Cytoplasmic localization of p120ctn and E-cadherin loss characterize lobular breast carcinoma from preinvasive to metastatic lesions. *Oncogene* **23**, 3272-3283 (2004).
172. Warzecha, C.C., Sato, T.K., Nabet, B., Hogenesch, J.B. & Carstens, R.P. ESRP1 and ESRP2 are epithelial cell-type-specific regulators of FGFR2 splicing. *Mol Cell* **33**, 591-601 (2009).
173. Warzecha, C.C., Shen, S., Xing, Y. & Carstens, R.P. The epithelial splicing factors ESRP1 and ESRP2 positively and negatively regulate diverse types of alternative splicing events. *RNA Biol* **6**, 546-562 (2009).
174. Gemmill, R.M. *et al.* ZEB1-responsive genes in non-small cell lung cancer. *Cancer Lett* **300**, 66-78 (2011).
175. Horiguchi, K. *et al.* TGF-beta drives epithelial-mesenchymal transition through deltaEF1-mediated downregulation of ESRP. *Oncogene* **31**, 3190-3201 (2012).
176. Reinke, L.M., Xu, Y. & Cheng, C. Snail represses the splicing regulator epithelial splicing regulatory protein 1 to promote epithelial-mesenchymal transition. *J Biol Chem* **287**, 36435-36442 (2012).
177. Bertocchi, C., Vaman Rao, M. & Zaidel-Bar, R. Regulation of adherens junction dynamics by phosphorylation switches. *J Signal Transduct* **2012**, 125295 (2012).
178. Xia, X., Carnahan, R.H., Vaughan, M.H., Wildenberg, G.A. & Reynolds, A.B. p120 serine and threonine phosphorylation is controlled by multiple ligand-receptor pathways but not cadherin ligation. *Exp Cell Res* **312**, 3336-3348 (2006).
179. Zhang, P.X. *et al.* p120-catenin isoform 3 regulates subcellular localization of Kaiso and promotes invasion in lung cancer cells via a phosphorylation-dependent mechanism. *Int J Oncol* **38**, 1625-1635 (2011).
180. Frame, M.C. Newest findings on the oldest oncogene; how activated src does it. *J Cell Sci* **117**, 989-998 (2004).
181. Piedra, J. *et al.* p120 Catenin-associated Fer and Fyn tyrosine kinases regulate beta-catenin Tyr-142 phosphorylation and beta-catenin-alpha-catenin Interaction. *Mol Cell Biol* **23**, 2287-2297 (2003).
182. Kim, L. & Wong, T.W. The cytoplasmic tyrosine kinase FER is associated with the catenin-like substrate pp120 and is activated by growth factors. *Mol Cell Biol* **15**, 4553-4561 (1995).
183. Calautti, E. *et al.* Tyrosine phosphorylation and src family kinases control keratinocyte cell-cell adhesion. *J Cell Biol* **141**, 1449-1465 (1998).
184. Kinch, M.S., Clark, G.J., Der, C.J. & Burridge, K. Tyrosine phosphorylation regulates the adhesions of ras-transformed breast epithelia. *J Cell Biol* **130**, 461-471 (1995).
185. Ozawa, M. & Ohkubo, T. Tyrosine phosphorylation of p120(ctn) in v-Src transfected L cells depends on its association with E-cadherin and reduces adhesion activity. *J Cell Sci* **114**, 503-512 (2001).
186. Avizienyte, E., Fincham, V.J., Brunton, V.G. & Frame, M.C. Src SH3/2 domain-mediated peripheral accumulation of Src and phospho-myosin is linked to deregulation of E-cadherin and the epithelial-mesenchymal transition. *Mol Biol Cell* **15**, 2794-2803 (2004).
187. Owens, D.W. *et al.* The catalytic activity of the Src family kinases is required to disrupt cadherin-dependent cell-cell contacts. *Mol Biol Cell* **11**, 51-64 (2000).
188. Papkoff, J. Regulation of complexed and free catenin pools by distinct mechanisms. Differential effects of Wnt-1 and v-Src. *J Biol Chem* **272**, 4536-4543 (1997).
189. Pang, J.H., Kraemer, A., Stehens, S.J., Frame, M.C. & Yap, A.S. Recruitment of phosphoinositide 3-kinase defines a positive contribution of tyrosine kinase signaling to E-cadherin function. *J Biol Chem* **280**, 3043-3050 (2005).
190. Fukuyama, T., Ogita, H., Kawakatsu, T., Inagaki, M. & Takai, Y. Activation of Rac by cadherin through the c-Src-Rap1-phosphatidylinositol 3-kinase-Vav2 pathway. *Oncogene* **25**, 8-19 (2006).

191. Lillien, J. & Balsamo, J. The regulation of cadherin-mediated adhesion by tyrosine phosphorylation/dephosphorylation of beta-catenin. *Curr Opin Cell Biol* **17**, 459-465 (2005).
192. Alema, S. & Salvatore, A.M. p120 catenin and phosphorylation: Mechanisms and traits of an unresolved issue. *Biochim Biophys Acta* **1773**, 47-58 (2007).
193. Mariner, D.J., Davis, M.A. & Reynolds, A.B. EGFR signaling to p120-catenin through phosphorylation at Y228. *J Cell Sci* **117**, 1339-1350 (2004).
194. Mariner, D.J. *et al.* Identification of Src phosphorylation sites in the catenin p120ctn. *J Biol Chem* **276**, 28006-28013 (2001).
195. Smyth, D., Leung, G., Fernando, M. & McKay, D.M. Reduced surface expression of epithelial E-cadherin evoked by interferon-gamma is Fyn kinase-dependent. *PLoS One* **7**, e38441 (2012).
196. Frank, C. *et al.* Effective dephosphorylation of Src substrates by SHP-1. *J Biol Chem* **279**, 11375-11383 (2004).
197. Keilhack, H. *et al.* The protein-tyrosine phosphatase SHP-1 binds to and dephosphorylates p120 catenin. *J Biol Chem* **275**, 26376-26384 (2000).
198. Palka, H.L., Park, M. & Tonks, N.K. Hepatocyte growth factor receptor tyrosine kinase met is a substrate of the receptor protein-tyrosine phosphatase DEP-1. *J Biol Chem* **278**, 5728-5735 (2003).
199. Holsinger, L.J., Ward, K., Duffield, B., Zachwieja, J. & Jallal, B. The transmembrane receptor protein tyrosine phosphatase DEP1 interacts with p120(ctn). *Oncogene* **21**, 7067-7076 (2002).
200. Kim, W.K. *et al.* RPTPmu tyrosine phosphatase promotes adipogenic differentiation via modulation of p120 catenin phosphorylation. *Mol Biol Cell* **22**, 4883-4891 (2011).
201. Wang, T. *et al.* FERM-containing protein FRMD5 is a p120-catenin interacting protein that regulates tumor progression. *FEBS Lett* **586**, 3044-3050 (2012).
202. Strumane, K. *et al.* E-cadherin regulates human Nanos1, which interacts with p120ctn and induces tumor cell migration and invasion. *Cancer Res* **66**, 10007-10015 (2006).
203. Smith, A.L., Friedman, D.B., Yu, H., Carnahan, R.H. & Reynolds, A.B. ReCLIP (reversible cross-link immuno-precipitation): an efficient method for interrogation of labile protein complexes. *PLoS One* **6**, e16206 (2011).
204. Smith, A.L., Dohn, M.R., Brown, M.V. & Reynolds, A.B. Association of Rho-associated protein kinase 1 with E-cadherin complexes is mediated by p120-catenin. *Mol Biol Cell* **23**, 99-110 (2012).
205. Hirako, Y. & Owaribe, K. Hemidesmosomes and their unique transmembrane protein BP180. *Microsc Res Tech* **43**, 207-217 (1998).
206. Aho, S., Rothenberger, K. & Uitto, J. Human p120ctn catenin: tissue-specific expression of isoforms and molecular interactions with BP180/type XVII collagen. *J Cell Biochem* **73**, 390-399 (1999).
207. Claudepierre, T. *et al.* Collagen XVII and BPAG1 expression in the retina: evidence for an anchoring complex in the central nervous system. *J Comp Neurol* **487**, 190-203 (2005).
208. Reynolds, A.B. *et al.* Identification of a new catenin: the tyrosine kinase substrate p120cas associates with E-cadherin complexes. *Mol Cell Biol* **14**, 8333-8342 (1994).
209. Shibamoto, S. *et al.* Association of p120, a tyrosine kinase substrate, with E-cadherin/catenin complexes. *J Cell Biol* **128**, 949-957 (1995).
210. Hartsock, A. & Nelson, W.J. Competitive regulation of E-cadherin juxtamembrane domain degradation by p120-catenin binding and Hakai-mediated ubiquitination. *PLoS One* **7**, e37476 (2012).
211. Wildenberg, G.A. *et al.* p120-catenin and p190RhoGAP regulate cell-cell adhesion by coordinating antagonism between Rac and Rho. *Cell* **127**, 1027-1039 (2006).
212. Park, J.I. *et al.* Frodo links Dishevelled to the p120-catenin/Kaiso pathway: distinct catenin subfamilies promote Wnt signals. *Dev Cell* **11**, 683-695 (2006).
213. Davis, M.A. & Reynolds, A.B. Blocked acinar development, E-cadherin reduction, and intraepithelial neoplasia upon ablation of p120-catenin in the mouse salivary gland. *Dev Cell* **10**, 21-31 (2006).
214. Smalley-Freed, W.G. *et al.* p120-catenin is essential for maintenance of barrier function and intestinal homeostasis in mice. *J Clin Invest* **120**, 1824-1835 (2010).
215. Smalley-Freed, W.G. *et al.* Adenoma formation following limited ablation of p120-catenin in the mouse intestine. *PLoS One* **6**, e19880 (2011).
216. Hanahan, D. & Weinberg, R.A. Hallmarks of cancer: the next generation. *Cell* **144**, 646-674 (2011).
217. Perez-Moreno, M., Song, W., Pasolli, H.A., Williams, S.E. & Fuchs, E. Loss of p120 catenin and links to mitotic alterations, inflammation, and skin cancer. *Proc Natl Acad Sci U S A* **105**, 15399-15404 (2008).
218. Ishizaki, Y. *et al.* Reduced expression and aberrant localization of p120catenin in human

- squamous cell carcinoma of the skin. *Journal of dermatological science* **34**, 99-108 (2004).
219. Stairs, D.B. *et al.* Deletion of p120-catenin results in a tumor microenvironment with inflammation and cancer that establishes it as a tumor suppressor gene. *Cancer Cell* **19**, 470-483 (2011).
220. van Hengel, J. & van Roy, F. Diverse functions of p120ctn in tumors. *Biochim Biophys Acta* **1773**, 78-88 (2007).
221. Macpherson, I.R. *et al.* p120-catenin is required for the collective invasion of squamous cell carcinoma cells via a phosphorylation-independent mechanism. *Oncogene* **26**, 5214-5228 (2007).
222. Dabbs, D.J., Bhargava, R. & Chivukula, M. Lobular versus ductal breast neoplasms: the diagnostic utility of p120 catenin. *The American journal of surgical pathology* **31**, 427-437 (2007).
223. Dillon, D.A., D'Aquila, T., Reynolds, A.B., Fearon, E.R. & Rimm, D.L. The expression of p120ctn protein in breast cancer is independent of alpha- and beta-catenin and E-cadherin. *The American journal of pathology* **152**, 75-82 (1998).
224. Talvinen, K. *et al.* Altered expression of p120catenin predicts poor outcome in invasive breast cancer. *Journal of cancer research and clinical oncology* **136**, 1377-1387 (2010).
225. Thoreson, M.A. & Reynolds, A.B. Altered expression of the catenin p120 in human cancer: implications for tumor progression. *Differentiation; research in biological diversity* **70**, 583-589 (2002).
226. Derksen, P.W. *et al.* Mammary-specific inactivation of E-cadherin and p53 impairs functional gland development and leads to pleomorphic invasive lobular carcinoma in mice. *Disease models & mechanisms* **4**, 347-358 (2011).
227. Soto, E. *et al.* p120 catenin induces opposing effects on tumor cell growth depending on E-cadherin expression. *J Cell Biol* **183**, 737-749 (2008).
228. Kurley, S.J. *et al.* p120-catenin is essential for terminal end bud function and mammary morphogenesis. *Development* **139**, 1754-1764 (2012).
229. Boussadia, O., Kutsch, S., Hierholzer, A., Delmas, V. & Kemler, R. E-cadherin is a survival factor for the lactating mouse mammary gland. *Mechanisms of development* **115**, 53-62 (2002).
230. Qian, B. *et al.* A distinct macrophage population mediates metastatic breast cancer cell extravasation, establishment and growth. *PLoS One* **4**, e6562 (2009).
231. Guilford, P.J. *et al.* E-cadherin germline mutations define an inherited cancer syndrome dominated by diffuse gastric cancer. *Human mutation* **14**, 249-255 (1999).
232. Derksen, P.W. *et al.* Somatic inactivation of E-cadherin and p53 in mice leads to metastatic lobular mammary carcinoma through induction of anoikis resistance and angiogenesis. *Cancer Cell* **10**, 437-449 (2006).
233. Ceteci, F. *et al.* Disruption of tumor cell adhesion promotes angiogenic switch and progression to micrometastasis in RAF-driven murine lung cancer. *Cancer Cell* **12**, 145-159 (2007).
234. Shibata, T., Kokubu, A., Sekine, S., Kanai, Y. & Hirohashi, S. Cytoplasmic p120ctn regulates the invasive phenotypes of E-cadherin-deficient breast cancer. *The American journal of pathology* **164**, 2269-2278 (2004).
235. Bellovin, D.I., Bates, R.C., Muzikansky, A., Rimm, D.L. & Mercurio, A.M. Altered localization of p120 catenin during epithelial to mesenchymal transition of colon carcinoma is prognostic for aggressive disease. *Cancer Res* **65**, 10938-10945 (2005).
236. Dohn, M.R., Brown, M.V. & Reynolds, A.B. An essential role for p120-catenin in Src- and Rac1-mediated anchorage-independent cell growth. *J Cell Biol* **184**, 437-450 (2009).
237. Cheung, L.W., Leung, P.C. & Wong, A.S. Cadherin switching and activation of p120 catenin signaling are mediators of gonadotropin-releasing hormone to promote tumor cell migration and invasion in ovarian cancer. *Oncogene* **29**, 2427-2440 (2010).
238. Taniuchi, K. *et al.* Overexpressed P-cadherin/CDH3 promotes motility of pancreatic cancer cells by interacting with p120ctn and activating rho-family GTPases. *Cancer Res* **65**, 3092-3099 (2005).
239. Miao, Y. *et al.* p120ctn isoform 1 expression significantly correlates with abnormal expression of E-cadherin and poor survival of lung cancer patients. *Medical oncology* **27**, 880-886 (2010).
240. Soubry, A. *et al.* Expression and nuclear location of the transcriptional repressor Kaiso is regulated by the tumor microenvironment. *Cancer Res* **65**, 2224-2233 (2005).
241. Prokhortchouk, A. *et al.* Kaiso-deficient mice show resistance to intestinal cancer. *Mol Cell Biol* **26**, 199-208 (2006).
242. Park, J.I. *et al.* Kaiso/p120-catenin and TCF/beta-catenin complexes coordinately regulate canonical Wnt gene targets. *Dev Cell* **8**, 843-854 (2005).
243. Jones, J. *et al.* Nuclear Kaiso indicates aggressive prostate cancers and promotes migration and invasiveness of prostate cancer cells. *The American journal of pathology* **181**, 1836-1846

- (2012).
244. Vermeulen, J.F. *et al.* Nuclear Kaiso expression is associated with high grade and triple-negative invasive breast cancer. *PLoS One* **7**, e37864 (2012).
 245. Pokutta, S. & Weis, W.I. Structure and mechanism of cadherins and catenins in cell-cell contacts. *Annual review of cell and developmental biology* **23**, 237-261 (2007).
 246. Jeanes, A., Gottardi, C.J. & Yap, A.S. Cadherins and cancer: how does cadherin dysfunction promote tumor progression? *Oncogene* **27**, 6920-6929 (2008).
 247. Gould Rothberg, B.E. & Bracken, M.B. E-cadherin immunohistochemical expression as a prognostic factor in infiltrating ductal carcinoma of the breast: a systematic review and meta-analysis. *Breast cancer research and treatment* **100**, 139-148 (2006).
 248. Kalluri, R. & Weinberg, R.A. The basics of epithelial-mesenchymal transition. *J Clin Invest* **119**, 1420-1428 (2009).
 249. Reynolds, A.B. p120-catenin: Past and present. *Biochim Biophys Acta* **1773**, 2-7 (2007).
 250. Bartlett, J.D. *et al.* Targeted p120-catenin ablation disrupts dental enamel development. *PLoS One* **5** (2010).
 251. Tian, H., Sanders, E., Reynolds, A., van Roy, F. & van Hengel, J. Ocular anterior segment dysgenesis upon ablation of p120 catenin in neural crest cells. *Invest Ophthalmol Vis Sci* **53**, 5139-5153 (2012).
 252. Nakopoulou, L. *et al.* Abnormal alpha-catenin expression in invasive breast cancer correlates with poor patient survival. *Histopathology* **40**, 536-546 (2002).
 253. Paredes, J. *et al.* Breast carcinomas that co-express E- and P-cadherin are associated with p120-catenin cytoplasmic localisation and poor patient survival. *Journal of clinical pathology* **61**, 856-862 (2008).
 254. Birchmeier, W., Hulsken, J. & Behrens, J. E-cadherin as an invasion suppressor. *Ciba Foundation symposium* **189**, 124-136; discussion 136-141, 174-126 (1995).
 255. Douma, S. *et al.* Suppression of anoikis and induction of metastasis by the neurotrophic receptor TrkB. *Nature* **430**, 1034-1039 (2004).
 256. Frisch, S.M. & Francis, H. Disruption of epithelial cell-matrix interactions induces apoptosis. *J Cell Biol* **124**, 619-626 (1994).
 257. Reddy, P. *et al.* Formation of E-cadherin-mediated cell-cell adhesion activates AKT and mitogen activated protein kinase via phosphatidylinositol 3 kinase and ligand-independent activation of epidermal growth factor receptor in ovarian cancer cells. *Mol Endocrinol* **19**, 2564-2578 (2005).
 258. Pollard, J.W. Macrophages define the invasive microenvironment in breast cancer. *Journal of leukocyte biology* **84**, 623-630 (2008).
 259. Rossi, D.L., Vicari, A.P., Franz-Bacon, K., McClanahan, T.K. & Zlotnik, A. Identification through bioinformatics of two new macrophage proinflammatory human chemokines: MIP-3alpha and MIP-3beta. *Journal of immunology* **158**, 1033-1036 (1997).
 260. Yang, J. & Weinberg, R.A. Epithelial-mesenchymal transition: at the crossroads of development and tumor metastasis. *Dev Cell* **14**, 818-829 (2008).
 261. Fujimoto, H. *et al.* Stromal MCP-1 in mammary tumors induces tumor-associated macrophage infiltration and contributes to tumor progression. *International journal of cancer. Journal international du cancer* **125**, 1276-1284 (2009).
 262. Chen, X. & Gumbiner, B.M. Crosstalk between different adhesion molecules. *Curr Opin Cell Biol* **18**, 572-578 (2006).
 263. Sakamoto, Y. *et al.* Interaction of integrin alpha(v)beta3 with nectin. Implication in cross-talk between cell-matrix and cell-cell junctions. *J Biol Chem* **281**, 19631-19644 (2006).
 264. Bremm, A. *et al.* Enhanced activation of epidermal growth factor receptor caused by tumor-derived E-cadherin mutations. *Cancer Res* **68**, 707-714 (2008).
 265. Mateus, A.R. *et al.* EGFR regulates RhoA-GTP dependent cell motility in E-cadherin mutant cells. *Human molecular genetics* **16**, 1639-1647 (2007).
 266. Balkwill, F., Charles, K.A. & Mantovani, A. Smoldering and polarized inflammation in the initiation and promotion of malignant disease. *Cancer Cell* **7**, 211-217 (2005).
 267. Murri, A.M. *et al.* The relationship between the systemic inflammatory response, tumour proliferative activity, T-lymphocytic and macrophage infiltration, microvessel density and survival in patients with primary operable breast cancer. *British journal of cancer* **99**, 1013-1019 (2008).
 268. Ueno, T. *et al.* Significance of macrophage chemoattractant protein-1 in macrophage recruitment, angiogenesis, and survival in human breast cancer. *Clinical cancer research : an official journal of the American Association for Cancer Research* **6**, 3282-3289 (2000).
 269. Condeelis, J. & Pollard, J.W. Macrophages: obligate partners for tumor cell migration, invasion, and metastasis. *Cell* **124**, 263-266 (2006).

270. Qian, B.Z. & Pollard, J.W. Macrophage diversity enhances tumor progression and metastasis. *Cell* **141**, 39-51 (2010).
271. Batlle, E. *et al.* The transcription factor snail is a repressor of E-cadherin gene expression in epithelial tumour cells. *Nat Cell Biol* **2**, 84-89 (2000).
272. Graff, J.R. *et al.* E-cadherin expression is silenced by DNA hypermethylation in human breast and prostate carcinomas. *Cancer Res* **55**, 5195-5199 (1995).
273. Hajra, K.M., Chen, D.Y. & Fearon, E.R. The SLUG zinc-finger protein represses E-cadherin in breast cancer. *Cancer Res* **62**, 1613-1618 (2002).
274. Dull, T. *et al.* A third-generation lentivirus vector with a conditional packaging system. *Journal of virology* **72**, 8463-8471 (1998).
275. Reid, T. *et al.* Rhotekin, a new putative target for Rho bearing homology to a serine/threonine kinase, PKN, and rhophilin in the rho-binding domain. *J Biol Chem* **271**, 13556-13560 (1996).
276. Derksen, P.W. *et al.* Illegitimate WNT signaling promotes proliferation of multiple myeloma cells. *Proc Natl Acad Sci U S A* **101**, 6122-6127 (2004).
277. van der Groep, P. *et al.* Distinction between hereditary and sporadic breast cancer on the basis of clinicopathological data. *Journal of clinical pathology* **59**, 611-617 (2006).
278. Packeisen, J., Korsching, E., Herbst, H., Boecker, W. & Buerger, H. Demystified...tissue microarray technology. *Molecular pathology : MP* **56**, 198-204 (2003).
279. van Diest, P.J. No consent should be needed for using leftover body material for scientific purposes. *For. Bmj* **325**, 648-651 (2002).
280. Klein, S.C. *et al.* An improved, sensitive, non-radioactive in situ hybridization method for the detection of cytokine mRNAs. *APMIS* **103**, 345-353 (1995).
281. Perez-Moreno, M., Jamora, C. & Fuchs, E. Sticky business: orchestrating cellular signals at adherens junctions. *Cell* **112**, 535-548 (2003).
282. Vos, C.B. *et al.* E-cadherin inactivation in lobular carcinoma in situ of the breast: an early event in tumorigenesis. *British journal of cancer* **76**, 1131-1133 (1997).
283. Etienne-Manneville, S. & Hall, A. Rho GTPases in cell biology. *Nature* **420**, 629-635 (2002).
284. Kimura, K. *et al.* Regulation of myosin phosphatase by Rho and Rho-associated kinase (Rho-kinase). *Science* **273**, 245-248 (1996).
285. Maekawa, M. *et al.* Signaling from Rho to the actin cytoskeleton through protein kinases ROCK and LIM-kinase. *Science* **285**, 895-898 (1999).
286. Totsukawa, G. *et al.* Distinct roles of ROCK (Rho-kinase) and MLCK in spatial regulation of MLC phosphorylation for assembly of stress fibers and focal adhesions in 3T3 fibroblasts. *J Cell Biol* **150**, 797-806 (2000).
287. Kamai, T. *et al.* Significant association of Rho/ROCK pathway with invasion and metastasis of bladder cancer. *Clinical cancer research : an official journal of the American Association for Cancer Research* **9**, 2632-2641 (2003).
288. Sahai, E. & Marshall, C.J. RHO-GTPases and cancer. *Nature reviews. Cancer* **2**, 133-142 (2002).
289. Zhou, J. *et al.* Gene expression profiles at different stages of human esophageal squamous cell carcinoma. *World journal of gastroenterology : WJG* **9**, 9-15 (2003).
290. Kaneko, K., Satoh, K., Masamune, A., Satoh, A. & Shimosegawa, T. Expression of ROCK-1 in human pancreatic cancer: its down-regulation by morpholino oligo antisense can reduce the migration of pancreatic cancer cells in vitro. *Pancreas* **24**, 251-257 (2002).
291. Gebbink, M.F. *et al.* Identification of a novel, putative Rho-specific GDP/GTP exchange factor and a RhoA-binding protein: control of neuronal morphology. *J Cell Biol* **137**, 1603-1613 (1997).
292. Surks, H.K., Richards, C.T. & Mendelsohn, M.E. Myosin phosphatase-Rho interacting protein. A new member of the myosin phosphatase complex that directly binds RhoA. *J Biol Chem* **278**, 51484-51493 (2003).
293. Riddick, N., Ohtani, K. & Surks, H.K. Targeting by myosin phosphatase-RhoA interacting protein mediates RhoA/ROCK regulation of myosin phosphatase. *J Cell Biochem* **103**, 1158-1170 (2008).
294. Mulder, J., Ariaens, A., van den Boomen, D. & Moolenaar, W.H. p116Rip targets myosin phosphatase to the actin cytoskeleton and is essential for RhoA/ROCK-regulated neuriteogenesis. *Mol Biol Cell* **15**, 5516-5527 (2004).
295. De Leeuw, W.J. *et al.* Simultaneous loss of E-cadherin and catenins in invasive lobular breast cancer and lobular carcinoma in situ. *J Pathol* **183**, 404-411 (1997).
296. van de Wetering, M. *et al.* Mutant E-cadherin breast cancer cells do not display constitutive Wnt signaling. *Cancer Res* **61**, 278-284 (2001).
297. Gottardi, C.J., Wong, E. & Gumbiner, B.M. E-cadherin suppresses cellular transformation by inhibiting beta-catenin signaling in an adhesion-independent manner. *J Cell Biol* **153**, 1049-1060 (2001).

298. Egles, C. *et al.* Denatured collagen modulates the phenotype of normal and wounded human skin equivalents. *J Invest Dermatol* **128**, 1830-1837 (2008).
299. Hein, T.W. *et al.* Integrin-binding peptides containing RGD produce coronary arteriolar dilation via cyclooxygenase activation. *American journal of physiology. Heart and circulatory physiology* **281**, H2378-2384 (2001).
300. Taubenberger, A.V., Woodruff, M.A., Bai, H., Muller, D.J. & Hutmacher, D.W. The effect of unlocking RGD-motifs in collagen I on pre-osteoblast adhesion and differentiation. *Biomaterials* **31**, 2827-2835 (2010).
301. Sahai, E. & Marshall, C.J. Differing modes of tumour cell invasion have distinct requirements for Rho/ROCK signalling and extracellular proteolysis. *Nat Cell Biol* **5**, 711-719 (2003).
302. Liu, B.P. & Burridge, K. Vav2 activates Rac1, Cdc42, and RhoA downstream from growth factor receptors but not beta1 integrins. *Mol Cell Biol* **20**, 7160-7169 (2000).
303. He, M. *et al.* Vascular endothelial growth factor C promotes cervical cancer metastasis via up-regulation and activation of RhoA/ROCK-2/moesin cascade. *BMC cancer* **10**, 170 (2010).
304. Lai, J.M., Hsieh, C.L. & Chang, Z.F. Caspase activation during phorbol ester-induced apoptosis requires ROCK-dependent myosin-mediated contraction. *J Cell Sci* **116**, 3491-3501 (2003).
305. Minambres, R., Guasch, R.M., Perez-Arago, A. & Guerri, C. The RhoA/ROCK-I/MLC pathway is involved in the ethanol-induced apoptosis by anoikis in astrocytes. *J Cell Sci* **119**, 271-282 (2006).
306. Coleman, M.L. *et al.* Membrane blebbing during apoptosis results from caspase-mediated activation of ROCK I. *Nat Cell Biol* **3**, 339-345 (2001).
307. Sebbagh, M. *et al.* Caspase-3-mediated cleavage of ROCK I induces MLC phosphorylation and apoptotic membrane blebbing. *Nat Cell Biol* **3**, 346-352 (2001).
308. Croft, D.R. *et al.* Actin-myosin-based contraction is responsible for apoptotic nuclear disintegration. *J Cell Biol* **168**, 245-255 (2005).
309. Koga, Y. & Ikebe, M. p116Rip decreases myosin II phosphorylation by activating myosin light chain phosphatase and by inactivating RhoA. *J Biol Chem* **280**, 4983-4991 (2005).
310. Brummelkamp, T.R., Bernards, R. & Agami, R. A system for stable expression of short interfering RNAs in mammalian cells. *Science* **296**, 550-553 (2002).
311. Wiznerowicz, M. & Trono, D. Conditional suppression of cellular genes: lentivirus vector-mediated drug-inducible RNA interference. *Journal of virology* **77**, 8957-8961 (2003).
312. Herold, M.J., van den Brandt, J., Seibler, J. & Reichardt, H.M. Inducible and reversible gene silencing by stable integration of an shRNA-encoding lentivirus in transgenic rats. *Proc Natl Acad Sci U S A* **105**, 18507-18512 (2008).
313. Hendriksen, J. *et al.* Plasma membrane recruitment of dephosphorylated beta-catenin upon activation of the Wnt pathway. *J Cell Sci* **121**, 1793-1802 (2008).
314. Pinkse, M.W. *et al.* Highly robust, automated, and sensitive online TiO₂-based phosphoproteomics applied to study endogenous phosphorylation in *Drosophila melanogaster*. *Journal of proteome research* **7**, 687-697 (2008).
315. Arpino, G., Bardou, V.J., Clark, G.M. & Elledge, R.M. Infiltrating lobular carcinoma of the breast: tumor characteristics and clinical outcome. *Breast Cancer Res* **6**, R149-156 (2004).
316. Wyckoff, J.B., Pinner, S.E., Gschmeissner, S., Condeelis, J.S. & Sahai, E. ROCK- and myosin-dependent matrix deformation enables protease-independent tumor-cell invasion in vivo. *Current biology : CB* **16**, 1515-1523 (2006).
317. Olson, M.F. & Sahai, E. The actin cytoskeleton in cancer cell motility. *Clin Exp Metastasis* **26**, 273-287 (2009).
318. Fritz, G., Just, I. & Kaina, B. Rho GTPases are over-expressed in human tumors. *International journal of cancer. Journal international du cancer* **81**, 682-687 (1999).
319. Lane, J., Martin, T.A., Watkins, G., Mansel, R.E. & Jiang, W.G. The expression and prognostic value of ROCK I and ROCK II and their role in human breast cancer. *Int J Oncol* **33**, 585-593 (2008).
320. Jiang, W.G. *et al.* Prognostic value of rho GTPases and rho guanine nucleotide dissociation inhibitors in human breast cancers. *Clinical cancer research : an official journal of the American Association for Cancer Research* **9**, 6432-6440 (2003).
321. Zhao, J. *et al.* Effect of fasudil hydrochloride, a protein kinase inhibitor, on cerebral vasospasm and delayed cerebral ischemic symptoms after aneurysmal subarachnoid hemorrhage. *Neurologia medico-chirurgica* **46**, 421-428 (2006).
322. Suzuki, Y., Shibuya, M., Satoh, S., Sugimoto, Y. & Takakura, K. A postmarketing surveillance study of fasudil treatment after aneurysmal subarachnoid hemorrhage. *Surgical neurology* **68**, 126-131; discussion 131-122 (2007).
323. Mukai, Y. *et al.* Involvement of Rho-kinase in hypertensive vascular disease: a novel therapeutic target in hypertension. *FASEB journal : official publication of the Federation of American*

- Societies for Experimental Biology* **15**, 1062-1064 (2001).
324. Hahmann, C. & Schroeter, T. Rho-kinase inhibitors as therapeutics: from pan inhibition to isoform selectivity. *Cellular and molecular life sciences : CMLS* **67**, 171-177 (2010).
325. Williams, R.D., Novack, G.D., van Haarlem, T., Kopczynski, C. & Group, A.R.P.A.S. Ocular hypotensive effect of the Rho kinase inhibitor AR-12286 in patients with glaucoma and ocular hypertension. *American journal of ophthalmology* **152**, 834-841 e831 (2011).
326. Fava, A. *et al.* Efficacy of Rho kinase inhibitor fasudil in secondary Raynaud's phenomenon. *Arthritis care & research* **64**, 925-929 (2012).
327. Croft, D.R. *et al.* Conditional ROCK activation in vivo induces tumor cell dissemination and angiogenesis. *Cancer Res* **64**, 8994-9001 (2004).
328. Liu, S., Goldstein, R.H., Scepanky, E.M. & Rosenblatt, M. Inhibition of rho-associated kinase signaling prevents breast cancer metastasis to human bone. *Cancer Res* **69**, 8742-8751 (2009).
329. Patel, R.A. *et al.* RKI-1447 Is a Potent Inhibitor of the Rho-Associated ROCK Kinases with Anti-Invasive and Antitumor Activities in Breast Cancer. *Cancer Res* **72**, 5025-5034 (2012).
330. de Toledo, M., Anguille, C., Roger, L., Roux, P. & Gadea, G. Cooperative Anti-Invasive Effect of Cdc42/Rac1 Activation and ROCK Inhibition in SW620 Colorectal Cancer Cells with Elevated Blebbing Activity. *PLoS One* **7**, e48344 (2012).
331. Vigil, D. *et al.* ROCK1 and ROCK2 Are Required for Non-Small Cell Lung Cancer Anchorage-Independent Growth and Invasion. *Cancer Res* **72**, 5338-5347 (2012).
332. Ono-Saito, N., Niki, I. & Hidaka, H. H-series protein kinase inhibitors and potential clinical applications. *Pharmacology & therapeutics* **82**, 123-131 (1999).
333. Shimokawa, H. *et al.* Rho-kinase-mediated pathway induces enhanced myosin light chain phosphorylations in a swine model of coronary artery spasm. *Cardiovascular research* **43**, 1029-1039 (1999).
334. Davies, S.P., Reddy, H., Caivano, M. & Cohen, P. Specificity and mechanism of action of some commonly used protein kinase inhibitors. *Biochem J* **351**, 95-105 (2000).
335. Nichols, R.J. *et al.* Substrate specificity and inhibitors of LRRK2, a protein kinase mutated in Parkinson's disease. *Biochem J* **424**, 47-60 (2009).
336. Uehata, M. *et al.* Calcium sensitization of smooth muscle mediated by a Rho-associated protein kinase in hypertension. *Nature* **389**, 990-994 (1997).
337. Goodman, K.B. *et al.* Development of dihydropyridone indazole amides as selective Rho-kinase inhibitors. *Journal of medicinal chemistry* **50**, 6-9 (2007).
338. Ying, H. *et al.* The Rho kinase inhibitor fasudil inhibits tumor progression in human and rat tumor models. *Molecular cancer therapeutics* **5**, 2158-2164 (2006).
339. Amano, M., Nakayama, M. & Kaibuchi, K. Rho-kinase/ROCK: A key regulator of the cytoskeleton and cell polarity. *Cytoskeleton* **67**, 545-554 (2010).
340. Furukawa, N. *et al.* Role of Rho-kinase in regulation of insulin action and glucose homeostasis. *Cell metabolism* **2**, 119-129 (2005).
341. Lee, D.H. *et al.* Targeted disruption of ROCK1 causes insulin resistance in vivo. *J Biol Chem* **284**, 11776-11780 (2009).
342. Chun, K.H. *et al.* Regulation of glucose transport by ROCK1 differs from that of ROCK2 and is controlled by actin polymerization. *Endocrinology* **153**, 1649-1662 (2012).
343. Grivennikov, S.I., Greten, F.R. & Karin, M. Immunity, inflammation, and cancer. *Cell* **140**, 883-899 (2010).
344. Kuraishy, A., Karin, M. & Grivennikov, S.I. Tumor promotion via injury- and death-induced inflammation. *Immunity* **35**, 467-477 (2011).
345. Nijkamp, M.W. *et al.* Accelerated perinecrotic outgrowth of colorectal liver metastases following radiofrequency ablation is a hypoxia-driven phenomenon. *Annals of surgery* **249**, 814-823 (2009).
346. Li, C. & Beal, M.F. Leucine-rich repeat kinase 2: a new player with a familiar theme for Parkinson's disease pathogenesis. *Proc Natl Acad Sci U S A* **102**, 16535-16536 (2005).
347. Bauer, A.F. *et al.* Regulation of protein kinase C-related protein kinase 2 (PRK2) by an intermolecular PRK2-PRK2 interaction mediated by Its N-terminal domain. *J Biol Chem* **287**, 20590-20602 (2012).
348. Nagaoka, T. *et al.* Inhaled Rho kinase inhibitors are potent and selective vasodilators in rat pulmonary hypertension. *American journal of respiratory and critical care medicine* **171**, 494-499 (2005).
349. Carter, C.L., Allen, C. & Henson, D.E. Relation of tumor size, lymph node status, and survival in 24,740 breast cancer cases. *Cancer* **63**, 181-187 (1989).
350. Li, C.I., Uribe, D.J. & Daling, J.R. Clinical characteristics of different histologic types of breast cancer. *British journal of cancer* **93**, 1046-1052 (2005).
351. Sahai, E. Mechanisms of cancer cell invasion. *Current opinion in genetics & development* **15**,

- 87-96 (2005).
352. Wojciak-Stothard, B., Potempa, S., Eichholtz, T. & Ridley, A.J. Rho and Rac but not Cdc42 regulate endothelial cell permeability. *J Cell Sci* **114**, 1343-1355 (2001).
353. Nakajima, M. *et al.* WF-536 inhibits metastatic invasion by enhancing the host cell barrier and inhibiting tumour cell motility. *Clinical and experimental pharmacology & physiology* **30**, 457-463 (2003).
354. Laprise, P. *et al.* Phosphatidylinositol 3-kinase controls human intestinal epithelial cell differentiation by promoting adherens junction assembly and p38 MAPK activation. *J Biol Chem* **277**, 8226-8234 (2002).
355. Kumar, S. *et al.* A pathway for the control of anoikis sensitivity by E-cadherin and epithelial-to-mesenchymal transition. *Mol Cell Biol* **31**, 4036-4051 (2011).
356. Onder, T.T. *et al.* Loss of E-cadherin promotes metastasis via multiple downstream transcriptional pathways. *Cancer Res* **68**, 3645-3654 (2008).
357. Bates, S. & Vousden, K.H. Mechanisms of p53-mediated apoptosis. *Cellular and molecular life sciences : CMLS* **55**, 28-37 (1999).
358. Ilic, D. *et al.* Extracellular matrix survival signals transduced by focal adhesion kinase suppress p53-mediated apoptosis. *J Cell Biol* **143**, 547-560 (1998).
359. Tarcic, G. *et al.* An unbiased screen identifies DEP-1 tumor suppressor as a phosphatase controlling EGFR endocytosis. *Current biology : CB* **19**, 1788-1798 (2009).
360. Tak, P.P. & Firestein, G.S. NF-kappaB: a key role in inflammatory diseases. *J Clin Invest* **107**, 7-11 (2001).
361. Kandikonda, S., Oda, D., Niederman, R. & Sorkin, B.C. Cadherin-mediated adhesion is required for normal growth regulation of human gingival epithelial cells. *Cell adhesion and communication* **4**, 13-24 (1996).
362. Fournier, M.V., Fata, J.E., Martin, K.J., Yaswen, P. & Bissell, M.J. Interaction of E-cadherin and PTEN regulates morphogenesis and growth arrest in human mammary epithelial cells. *Cancer Res* **69**, 4545-4552 (2009).
363. St Croix, B. *et al.* E-Cadherin-dependent growth suppression is mediated by the cyclin-dependent kinase inhibitor p27(KIP1). *J Cell Biol* **142**, 557-571 (1998).
364. Desouza, M., Gunning, P.W. & Stehn, J.R. The actin cytoskeleton as a sensor and mediator of apoptosis. *Bioarchitecture* **2**, 75-87 (2012).
365. Casteel, D.E. *et al.* Rho Isoform-specific Interaction with IQGAP1 Promotes Breast Cancer Cell Proliferation and Migration. *J Biol Chem* **287**, 38367-38378 (2012).
366. Gilcrease, M.Z. *et al.* Alpha6beta4 integrin crosslinking induces EGFR clustering and promotes EGF-mediated Rho activation in breast cancer. *Journal of experimental & clinical cancer research : CR* **28**, 67 (2009).
367. Toyama, T., Lee, H.C., Koga, H., Wands, J.R. & Kim, M. Noncanonical Wnt11 inhibits hepatocellular carcinoma cell proliferation and migration. *Mol Cancer Res* **8**, 254-265 (2010).
368. Uysal-Onganer, P. & Kypta, R.M. Wnt11 in 2011 - the regulation and function of a non-canonical Wnt. *Acta physiologica* **204**, 52-64 (2012).
369. Kosako, H. *et al.* Rho-kinase/ROCK is involved in cytokinesis through the phosphorylation of myosin light chain and not ezrin/radixin/moesin proteins at the cleavage furrow. *Oncogene* **19**, 6059-6064 (2000).
370. Hsu, P.P. & Sabatini, D.M. Cancer cell metabolism: Warburg and beyond. *Cell* **134**, 703-707 (2008).
371. Papa, V. *et al.* Elevated insulin receptor content in human breast cancer. *J Clin Invest* **86**, 1503-1510 (1990).
372. Macheda, M.L., Rogers, S. & Best, J.D. Molecular and cellular regulation of glucose transporter (GLUT) proteins in cancer. *J Cell Physiol* **202**, 654-662 (2005).
373. Levine, B. & Kroemer, G. Autophagy in the pathogenesis of disease. *Cell* **132**, 27-42 (2008).
374. White, E. & DiPaola, R.S. The double-edged sword of autophagy modulation in cancer. *Clinical cancer research : an official journal of the American Association for Cancer Research* **15**, 5308-5316 (2009).
375. Stephens, P.J. *et al.* The landscape of cancer genes and mutational processes in breast cancer. *Nature* **486**, 400-404 (2012).
376. Laird, A.D. *et al.* SU6668 is a potent antiangiogenic and antitumor agent that induces regression of established tumors. *Cancer Res* **60**, 4152-4160 (2000).
377. Xia, W. *et al.* Anti-tumor activity of GW572016: a dual tyrosine kinase inhibitor blocks EGF activation of EGFR/erbB2 and downstream Erk1/2 and AKT pathways. *Oncogene* **21**, 6255-6263 (2002).
378. O'Reilly, K.E. *et al.* mTOR inhibition induces upstream receptor tyrosine kinase signaling and activates Akt. *Cancer Res* **66**, 1500-1508 (2006).

379. Breuleux, M. *et al.* Increased AKT S473 phosphorylation after mTORC1 inhibition is rictor dependent and does not predict tumor cell response to PI3K/mTOR inhibition. *Molecular cancer therapeutics* **8**, 742-753 (2009).
380. Yap, T.A. *et al.* First-in-man clinical trial of the oral pan-AKT inhibitor MK-2206 in patients with advanced solid tumors. *J Clin Oncol* **29**, 4688-4695 (2011).
381. Bendell, J.C. *et al.* Phase I, dose-escalation study of BKM120, an oral pan-Class I PI3K inhibitor, in patients with advanced solid tumors. *J Clin Oncol* **30**, 282-290 (2012).
382. Leighl, N.B. *et al.* A Phase 2 study of perifosine in advanced or metastatic breast cancer. *Breast cancer research and treatment* **108**, 87-92 (2008).
383. Reungwetwattana, T. *et al.* Brief report: a phase II “window-of-opportunity” frontline study of the MTOR inhibitor, temsirolimus given as a single agent in patients with advanced NSCLC, an NCCTG study. *Journal of thoracic oncology : official publication of the International Association for the Study of Lung Cancer* **7**, 919-922 (2012).
384. Motzer, R.J. *et al.* Efficacy of everolimus in advanced renal cell carcinoma: a double-blind, randomised, placebo-controlled phase III trial. *Lancet* **372**, 449-456 (2008).
385. Pal, S.K., Reckamp, K., Yu, H. & Figlin, R.A. Akt inhibitors in clinical development for the treatment of cancer. *Expert opinion on investigational drugs* **19**, 1355-1366 (2010).
386. Dannhardt, G. & Kiefer, W. Cyclooxygenase inhibitors--current status and future prospects. *European journal of medicinal chemistry* **36**, 109-126 (2001).
387. Mohammed, S.I. *et al.* Cyclooxygenase inhibitors in urinary bladder cancer: in vitro and in vivo effects. *Molecular cancer therapeutics* **5**, 329-336 (2006).

#

Nederlandse samenvatting

Een menselijk lichaam is opgebouwd uit miljoenen cellen die aan elkaar vast zitten. Deze grote clusters van cellen vormen zo onze organen. Verschillende organen moeten verschillende functies uitvoeren (we ruiken met onze neus, maar onze ogen kunnen niet ruiken). Daarom zitten de cellen waaruit ze bestaan vol met eiwitten, kleine machines die nagenoeg alle functies vervullen die de cellen uniek maken. De plaats waar een specifiek eiwit in de cel zit, bepaalt mede zijn functie. Zo bevinden er zich eiwitten op de buitenkant van de cel, welke plakken aan dezelfde eiwitten op een andere cel, zodat de cellen aan elkaar vast blijven zitten. Dit eiwit heet E-cadherine. Andere eiwitten zijn nodig om te zorgen dat E-cadherine op de buitenkant kan blijven zitten; ze stabiliseren E-cadherine. Het eiwit 'p120' is hier cruciaal voor. Haal je p120 weg, dan kan E-cadherine niet meer stabiel op de buitenkant van de cel blijven zitten, en valt er af. Als gevolg hiervan kan deze cel niet meer aan zijn buur-cellen vast blijven zitten. Dit is voor de meeste cel types dodelijk, behalve bijvoorbeeld voor rode bloed cellen die in de bloedvaten blijven leven zonder daarbij vast te hoeven zitten aan andere cellen. Ook sommige kanker cellen kunnen zonder aan andere cellen vast te zitten in leven blijven.

Met meer dan 1.3 miljoen nieuwe gevallen per jaar, is borstkanker wereldwijd het meest voorkomende type kanker bij vrouwen. Dit resulteert in ongeveer 450.000 dodelijke slachtoffers per jaar, wat borstkanker op de nummer 1 positie zet wat betreft kanker-gerelateerde dood.

Er bestaan vele verschillende subtypes borstkanker, gebaseerd op pathologische kenmerken zoals; hoe cellen in een tumor groeien, de vorm van de cellen en welke eiwitten er in welke mate op welke plek in deze cellen zitten. In de meeste gevallen komen mensen niet te overlijden aan de kanker, de primaire tumor, die wordt ontdekt in de borst. Deze primaire tumor kan namelijk vaak chirurgisch worden verwijderd. Echter, cellen van deze primaire tumor kunnen los raken en door het lichaam beginnen te zwerven. Vele jaren nadat de primaire tumor is verwijderd, kunnen de rondzwervende cellen zich nestelen in andere organen, zoals de longen, eierstokken, hersenen of waar dan ook, en daar weer beginnen te groeien (metastaseren). Een aantal mogelijke antwoorden op de vragen hoe de cellen losraken van elkaar en op welke manier we de vorming van metastasen kunnen voorkomen, worden in dit proefschrift beschreven.

In hoofdstuk 1 wordt een algemene introductie gegeven over borstkanker, de eiwitten die verantwoordelijk zijn voor de hechting tussen cellen (door middel van onder andere E-cadherine en p120) en wat de verdere functies zijn van deze eiwitten, met een focus op p120. In hoofdstuk 2 wordt de literatuur besproken over hoe p120 betrokken is bij de ontwikkeling van kanker in verschillende weefsels, maar vooral in de borst. In hoofdstuk 3 tonen wij aan dat het verlies van p120 correleert met verschillende klinische kenmerken van agressieve borstkanker. Om de klinische relevantie van deze bevinding te bevestigen, is een muismodel gemaakt, waarin p120 specifiek wordt verwijderd in het borstweefsel, in combinatie met de tumor suppressor p53. Verlies van p53 alleen leidt tot niet-metastaserende tumoren. Echter, verlies van zowel p53 als p120 zorgt voor de vorming van tumoren die wel in staat zijn om te metastaseren. Om te achterhalen wat de effecten van p120-verlies zijn die resulteren in metastase vorming, hebben we gebruik gemaakt van muis- en humane tumor-cellijnen, in welke we op een reguleerbare manier p120 eiwit expressie kunnen reduceren. Reductie van p120 expressie maakt de cellen gevoeliger voor groeifactoren, wat correleert met de mogelijkheid van deze cellen om te overleven in de afwezigheid van aanhechting (zoals ook wordt ondergaan door tumorcellen die zich los maken van de primaire tumor). Verder resulteert p120 verlies in productie van inflammatoire cytokines, stoffen die door de cellen worden

#

uitgescheiden en zorgen voor een tumor-stimulerende ontstekingsreactie. Een van de effecten hiervan is dat er in de omgeving van de tumor meer groeifactoren worden geproduceerd, welke de tumor stimuleren om te groeien en te metastaseren. In hoofdstuk 4 laten we zien dat het verlies van p53 gecombineerd met E-cadherine verlies leidt tot vorming van metastaserende kanker. We tonen aan dat dit komt doordat er een relocalisatie van p120 plaatsvindt. In plaats van vast geplakt aan de wand van de cel, bevindt p120 zich verspreid door de cel. Hierdoor gaat p120 een remmende interactie aan met Mrip, bekend om zijn remmende werking op Rho-Rock signalering. Dit resulteert in actief Rho-Rock en geeft de cellen het vermogen om te overleven zonder aanhechting, wat indicatief is voor het metastaserend vermogen van tumorcellen. Verder laten we zien dat actief Rho-Rock cruciaal is voor tumoren om uit te groeien. Hoewel de modellen in hoofdstuk 3 en 4 op elkaar lijken, resulteert verlies van p120 of E-cadherine in sterk verschillende typen borstkanker en brengen ze verschillende effecten teweeg in de cellen. Wij zijn dan ook bezig om deze tumoren met verschillende medicijnen te behandelen in onze muismodellen.

Om de mogelijke klinische toepasbaarheid van Rock inhibitie te onderzoeken om metastaserende borstkanker te behandelen, maken we in hoofdstuk 5 gebruik van een induceerbaar systeem om Rock te remmen en testen we verschillende farmacologische remmers om te bepalen of we de vorming van metastases kunnen tegen gaan. In conclusie beschrijft dit proefschrift dat p120 een belangrijke rol speelt in het remmen van metastases, maar ook dat het de tumorgroei en metastase vorming stimuleert, afhankelijk van waar in de cel p120 zich bevindt. Al met al toont dit proefschrift de context afhankelijke rol van p120 in de vorming en metastasering van borstkanker aan.

#

Curriculum Vitae

Ronald Cornelis Johannes Schackmann werd geboren op 15 juli 1984 te Amsterdam. In 2002 behaalde hij zijn VWO diploma aan het Sint Michaël-College te Zaandam. In hetzelfde jaar startte hij met de opleiding Bio-Medische Wetenschappen aan de Vrije Universiteit (VU) van Amsterdam, die hij in 2007 afrondde met de master Bio-Molecular Sciences. Gedurende deze master liep hij stage bij de afdeling Structuur Biologie van de VU, onder begeleiding van Dr. Dirk Bald. Hier onderzocht hij de mogelijkheid om een Kinesin-F₁ nanomachine te produceren met behulp van laser-tweezer microscopie. Tijdens zijn tweede stage op de afdeling Moleculaire Biologie van het Nederlands Kanker Instituut, onder begeleiding van Eva Wielders, genereerde hij specifieke puntmutaties in de MSH2/MSH6 mismatch reparatie genen in muisstamcellen. In 2007 begon hij zijn promotieonderzoek, beschreven in dit proefschrift, bij de afdeling Medische Oncologie van het Universitair Medisch Centrum Utrecht onder begeleiding van Dr. Patrick Derksen. Sinds november 2012 is hij werkzaam als post-doc op de afdeling Pathologie van het Universitair Medisch Centrum Utrecht waar hij dit onderzoek voortzet.



Publications

Schackmann RC, van Amersfoort M, Haarhuis JH, Vlug EJ, Halim VA, Roodhart JM, Vermaat JS, Voest EE, van der Groep P, van Diest PJ, Jonkers J, Derksen PW. *Cytosolic p120-catenin regulates growth of metastatic lobular carcinoma through Rock1-mediated anoikis resistance*. J Clin Invest. 2011 Aug;121(8):3176-88. doi: 10.1172/JCI41695. Epub 2011 Jul 11.

Hoogwater FJ, Nijkamp MW, Smakman N, Steller EJ, Emmink BL, Westendorp BF, Raats DA, Sprick MR, Schaefer U, Van Houdt WJ, De Bruijn MT, **Schackmann RC**, Derksen PW, Medema JP, Walczak H, Borel Rinkes IH, Kranenburg O. *Oncogenic K-Ras turns death receptors into metastasis-promoting receptors in human and mouse colorectal cancer cells*. Gastroenterology. 2010 Jun;138(7):2357-67. doi: 10.1053/j.gastro.2010.02.046. Epub 2010 Feb 23.

#

Ron C.J. Schackmann*, Sjoerd Klarenbeek*, Eva J. Vlug, Suzan Stelloo, Miranda van Amersfoort, Milou Tenhagen, Tanya M. Braumuller, Jeroen F. Vermeulen, Petra van der Groep, Ton Peeters, Elsken van der Wall, Paul J. van Diest, Jos Jonkers, Patrick W.B. Derksen
Loss of p120-catenin Induces Metastatic Mammary Carcinoma through Induction of Anoikis Resistance and Sensitization of Growth Factor Receptor Signaling. Manuscript under consideration.

Ron C.J. Schackmann, Milou Tenhagen, Robert A. H. van de Ven and Patrick W.B. Derksen
p120-catenin in Cancer; Models, Mechanisms, and Opportunities for Intervention. Manuscript in preparation.

Ron C.J. Schackmann, Romina J. Pagliero, Miranda van Amersfoort, Robert A. van de Ven, Nathaniel I. Martin, David A. Egan and Patrick W.B. Derksen
Rock inhibition as a therapeutic alternative in the management of invasive lobular carcinoma. Manuscript in preparation.

Dankwoord

Even een lijstje met namen maken voor het dankwoord, dat is makkelijker gezegd dan gedaan. Wederom blijkt dat, net als alles tijdens het AIO traject, dit meer tijd kost dan verwacht. Zoals denk ik voor iedere AIO geldt, voelt het een beetje onwerkelijk nu dit monster eindelijk af begint te komen. Om te beginnen wil ik iedereen die dit graag zou willen horen, geluk wensen met hun proeven/studies/opstarten-van-eigen-groepen en iedereen hartelijk danken voor hun steun tijdens de afgelopen promotie jaren (zo, dan hoeft ik dat niet meer per persoon te doen).

Patrick, onvoorstelbaar hoe verschillend wij zijn. Best wel handig, want als jij weer eens laaiend enthousiast over een film was, wist ik meteen dat ik die niet hoefde te kijken. Gelukkig denken we meestal wel hetzelfde over proeven, anders hadden de afgelopen jaren erg lang geduurd. Ik kan me nog herinneren hoe een van onze eerste gesprekken ging; ik zou verder werken aan het project dat jij als postdoc bij Jos had opgestart. Even een paar gaatjes dicht timmeren en binnen een jaar m'n eerste stuk af... 3,5 jaar later was het paper dan eindelijk af (voor de niet-ingewijden, dat is hoofdstuk 4 geworden). Gelukkig verloopt het publiceren van het 2^e paper (hoofdstuk 3) een stuk soepeler... Vaak verzandde ik in het eindeloos herhalen om er zeker van te zijn dat de proef toch echt wel klopte, ik denk dat ik daar nu meer balans in heb gevonden. Ik baal nog altijd dat er niet meer gepubliceerde hoofdstukken in dit boekje staan, maar als het goed is volgen er "snel" 2 publicaties. En dan nu nog even wat extra projectjes opzetten voor m'n vervolgonderzoek. Dank dat ik al deze tijd ben betaald (ik weet maar al te goed hoe ongebruikelijk dat is).

Mijn promotor, **René**, wat fijn dat jij mijn promotor bent (en dus geen vragen kan stellen tijdens mijn verdediging). Sinds jij naar het NKI bent verhuisd, heeft de snoepspot het nog nooit zo lang volgehouden. Zonder iets te zeggen kwam je binnen lopen om een snoepje te pakken en vervolgens zonder ook maar 1 woord te zeggen weer terug te gaan naar je kantoor. Zelfs toen onze kamer aan de andere kant van de brug was (en je dus een flink stuk om moest lopen).

Mijn paranimfen, **Martin**, broeder, wat was de kans dat we allebei het onderzoek in gingen? En dat we dan ook nog beiden gaan promoveren? Ergens had ik toch verwacht dat in ieder geval één van ons wel iets met computers zou gaan doen. Ik ben echt wel van plan nog iets met die piano te gaan doen die in de woonkamer staat; eerst nog even promoveren, dat ene paper publiceren en dan heb ik er wel tijd voor... Dank voor het me met rust laten tijdens het schrijven en de verzorgingsstaat waar ik de afgelopen maanden in heb geleefd. Nog even volhouden, dan wonen er 2 Dr.'s op de Otterstraat 78. En natuurlijk **Miranda**, ik kwam in het begin misschien over als een ongezellige nerd; ik denk dat jouw beeld van mij wel wat is veranderd in de jaren na onze eerste ontmoeting. Gelukkig had Patrick haast en geen keuze uit verschillende AIO kandidaten, anders vraag ik me af of ik wel was aangenomen. Eens kijken of ik straks bij m'n promotie net zo wit weg trek als die ene keer bij de KWF meeting... Bedankt voor het blijven zeuren of ik alles voor de receptie en het feest al geregeld had. Bij jou had ik een 2^e thuis als ik dat nodig had.

Eva, Hihhi ow Vera, ik heet Ron, niet Rob, niet Roy, RON! Uniek hoe jij dingen vaak net even anders inziet dan anderen, dat houdt het wel interessant. Ik vond het nog wel mee vallen met hoe dronken je was na die ene cocktail. Ik stel voor dat we het nog eens met wat meer alcohol proberen... **Robert**, de jongen met de perfecte tanden (en vergeet nooit dat je tanden de belangrijkste reden waren dat je bent aangenomen!). Eindelijk wat echte mannelijke versterking in onze groep; Patrick begon het zat te worden dat hij met niemand over voetbal en "goede films" kon ouwehoeren. Hopelijk

#

kom je snel van je Wnt verhaal af (hm.. was er tegen je gezegd dat je alleen nog even wat kleine gaten moest dicht en je vervolgens snel kon submitten? ...klinkt bekend). **Milou**, en weer iemand die niet drinkt op onze kamer; maar toch altijd tot het einde blijft bij de borrels. Wat zal jij een interessant dankwoord kunnen schrijven in je boekje... (1 tip, begin nu alvast met schrijven, dat scheelt je later veel moeite) Dank voor het overnemen van m'n proeven toen ik thuis zat te schrijven (en nu hopen dat die cellijnen het net zo goed doen als we hopen). **Iordanka**, it's good to have you as a postdoc in our group (also because our work discussions have to be in English now!). I hope you'll get the option to stay in our group; at least until the Fer fishing expedition is finished. **Jolien**, de eerste geneeskundige die zowaar liever onderzoeker wordt dan arts... Leuk dat jij verder gaat met het p120-werk, ik ben benieuwd wat er allemaal uit gaat komen (en hoe snel mijn artikelen toch incorrect/onvolledig gaan blijken te zijn). **Jeske**, Hardrock Jan ON! Excuus als ik je zo af en toe een beetje zit aan te staren (ik kijk dan naar je T-shirt, echt waar!!). **Mijanou**, ik heb m'n best gedaan, zie onderaan. Heb je nou eindelijk al eens het celkweeklab van plastics voorzien?

#

En dan de Vromans groep, **Martijn**, Martijntjeuhh. Als je weer eens een slaapplaats nodig hebt, m'n zolder is ingericht (maar niet in de hoek plassen hè!). Wonderbaarlijk dat je met zulke korte beentjes nog zo hard over die squashbaan kan rennen. Ik hoop nog vaak een zeepje voor je te kunnen laten vallen onder de douche. Zodra ik m'n eigen groep ga beginnen, kom ik je halen om de hele zoi op te zetten! **Rutger**, ruttie, trutget, Gordon, de blonde god. Jaja, ik heb de primers besteld, ik ga d'r nu echt aan beginnen... en dat heeft maar driekwart jaar geduurd. **Arianne**, een grote mond vanaf dag 1; dat belooft veel goeds. **Amanda**, ga je nou echt aan borstkanker werken? Of zijn die cellijnen toch te lastig te kweken... **Armando**, bedankt voor de espresso machine tip, hij bevalt erg goed (en die S brandt nu al bijna een jaar probleemloos). **Michael**, weer zo'n fanatiekeling in het Lens lab, waar haalt Susanne ze toch allemaal vandaan? Super stimulerend om kleine zijprojectjes met jou te bespreken, en dan straks hopelijk af van de virale beperkingen. Wat me wel is opgevallen is dat jullie verdraaid vaak koekjes hebben; en 's middags koffie zitten te drinken (als Susanne er niet is), ik vraag me af wie daar verantwoordelijk voor is... **Sanne**? En natuurlijk **Susanne** bedankt dat je deze groep mensen bij elkaar hebt gebracht, het zijn zeer prettige burens.

Sander, roomie (in de slaapkamer zin van het woord, niet de werkkamer). Één van de eerste gesprekken die we hadden, ging over het vrijuit flatuleren op onze gedeelde slaapkamer op de retraite in Twello (ja Patrick, "fucking Twello"). Menig uur terrashangen en uiteten, waren zeer vermakelijk. Ik hoop snel jouw boekje tegemoet te zien!

Paul van Diest, we moeten toch eens kijken of we niet iets aan die ochtendbesprekingen kunnen doen; om 8:30 ben ik nog niet wakker. Dank voor het lezen van mijn proefschrift! **Willy**, bedankt dat je ervoor hebt helpen zorgen dat ik vanaf afgelopen oktober toch nog salaris kreeg. Je staat altijd klaar om te helpen de UMC regelgeving te doorgronden en dat bewonder ik ten zeerste. **Jeroen**, toch zonde dat je er niet bij zat toen ik literatuur bespreking had met die SUMMA studenten. Dank voor de hulp met het statistische geneuzel. **Çiğdem**, good luck with the new job (although I still don't understand what it exactly is you are going to do). **Petra**, nog 1 setje IHC stainings en dan zal ik niks meer van je vragen... Nou ja, nog 2 dan, of toch nog wat meer. **Cathy**, alé zeg, pas eene echte Belg als er flink wat bier in zit; Mallorca was leuk (maar kijk uit voor die piraten schepen)! Hej **Laurien**, geldt die 100 euro voor het lepeltje-lepeltje nog steeds? Ik heb Robert bijna zo ver. **Aram**, blij dat jij het op je hebt genomen om de werkbesprekingen te regelen (ik was heel even

bang dat ik het moest gaan doen..)

Elsken, wat leuk dat je mijn boekje wilde lezen en ook tijd kon maken om 18 april deel te nemen in mijn verdediging. Als vraag zou ik graag willen voorstellen: “Wat is de klinische relevantie van dit onderzoek?”.

Niels Bovenschen, bedankt voor jouw ongeëvenaarde interesse in ons virus werk (of was je soms opzettelijk bezig mij aan Stefanie te koppelen?). Bewonderenswaardig hoe jij iedere maandagochtend weer vragen weet te verzinnen, terwijl het merendeel van de zaal nog ligt te slapen.

Onze oud collega's de NKI-ers, onder leiding van **Rob**; jouw vertrek naar het NKI heeft toch wel iets van een machts-vacuüm gecreëerd. Zodra René het NKI zat is en banketbakker gaat worden, kom je dan terug naar het Stratenum? Of ga je ook dan met hem mee (dan kom ik voortaan Medema-Klompmaker gebakjes bij jullie halen voor m'n verjaardag). **Aniek**, jij straalt altijd een soort van onvoorstelbaar enthousiasme uit. Bedankt voor het beantwoorden van al m'n vragen over het promoveren de afgelopen maanden. Veel succes in SF met Coen! **Marvin**, je hebt helemaal gelijk, je krijgt je boekje nooit zo als je het zou willen hebben. **Melinda**, I've got a couple of beers ready for you the 18th of April; could you bring a ladder so I don't have to get down on my knees to talk to you? Good to see you stuck around after Monica left the lab! **Lenno**, eerst als student, later als AIO; het leven was altijd een grote borrel met jou, ik verwacht wel dat je los gaat op m'n feest! **Indra**, met stipt één van de meest bijzondere mensen die ik ooit ben tegengekomen; fijn om te weten dat je zaad pas gaat zwemmen als je er PBS bij doet. **Claudio**, it's good to see you back in Utrecht; I hope I can find you to give you one of these. **Anneloes**, jaja eigenlijk hoor je niet meer bij de Klompmaker groep, maar toch. **Jonne**, wat leuk dat je ons nog mailt als jullie een paper borrel hebben, maar zou je het misschien meer dan een paar uur vantevoren kunnen laten weten? **Wytse**, **Roy** en al degene die ik nu vergeet; jullie worden gemist!

Onno, immer kritisch, nog bedankt dat jij vroeger aan p116^{RIP}/MRIP/MPRIP hebt gewerkt, ik weet niet hoe hoofdstuk 4 er anders uit had gezien. Maar het lijkt toch alsof er in verhouding steeds minder artsen in je groep komen, begin je het soms zat te worden om ze te vertellen dat dat blauwe ding niet het beschermkapje van de pipet is? Je krijgt het p116Rip boekje van Mulder nog van me terug! **Daniëlle**, de stille kracht achter het Kranenburg lab. Nou ja tot er een paar wijntjes in zitten (ik stel voor dat iedereen mee helpt Daniëlle dronken te krijgen op m'n feestje!). **Benjamin**, Pappa Bear, blijf jij maar lekker in die darmen grutten, ik hou het toch liever bij borsten. **Lutske**, heb je je telefoon nog? Of ligt ie weer ergens in de gracht? Als iemand zich nog afvroeg waarom het tegenwoordig zo duur is je nieuwe telefoon te verzekeren... **Ernst**, Hi, my name is Urnst. Ik dacht dat ik het zwaar had met het schrijven van dit proefschrift, ik kan me niet voorstellen hoe het moet zijn als er dan 's nachts ook nog een kleintje is die je wakker houdt en je van de ene nachtdienst de andere in rolt. Gelukkig heb je Daniëlle om je proeven af te maken. **Maarten** en **Frederik**, oud collega's, jullie duo presentatie was memorabel (met een lekker hoog cabaret gehalte). And **Jamila**, I'm still not sure whether to speak Dutch or English with you.. En dan nog **Nikol**, hier eindelijk m'n boekje, krijg ik er dan ook meteen eentje van jou?

De Bos en Burgering groep (ik weet nooit wie bij welke groep hoort, dus dan maar allemaal tegelijk); **Boudewijn Burgering**, alvast bedankt dat je tijd kon maken om te opponeren, eens kijken of ik daar na jouw vragen nog zo over denk... **Marten**, met hoe vaak je bij ons op de kamer staat vraag ik me toch iets af... Heeft Patrick je

#

nou wel of niet aangenomen? **On Ying**, idd jammer dat het gezamenlijke projectje nooit van de grond is gekomen. **David**, als we Patrick weer eens niet kunnen vinden, gaan we voortaan jou bellen (of meteen langs het Micaffee lopen). Dr. **Pannekoek**, jij had echt een van de beste proefschrift voorkant foto's die ik ooit heb gezien. Eens kijken wie er langer bij z'n oude baas blijft hangen. Ja **Fried**, ik vind de koffie uit dat apparaat beneden ook beter dan het spul uit die grote machines. **Tobias**, ik stel voor dat de Image Processing course verplicht wordt gesteld, een van de meest leerzame cursussen die ik in de afgelopen 5 jaar heb gevolgd! **Ingrid**, en nu dan toch weer naar de 2^e verdieping voor het viruswerk? Nee **Patricia**, ik kom niets jatten; deze keer kom ik iets brengen. **Hester, Astrid, Marrit**, dank voor de randome labgesprekken en borrels.

En natuurlijk onze nieuwste verdiepingsgenoten vanuit het WKZ; **Daniëlle** weer terug van weg geweest, we moeten toch nog weer eens meer ons best doen om wat borrels te regelen! **Ismayil**, dank voor de uitleg over de western imager, ik zou willen dat dat apparaat er 5 jaar geleden was; dat had me heel wat DOKA-gerelateerde depressies kunnen schelen. **Ellen**, d'r staat boven een Seahorse, jij hebt niet toevallig tijd om eens uit te zoeken hoe dat ding werkt (of zit jij officieel weer niet bij de groep die dat ding heeft gekocht)?

Johan de Rooij, dank dat je wil opponeren. Is het al opgevallen dat jouw HGF steeds sneller oprakte het afgelopen jaar? **Emma and Sarah**, it's been too long since we've been out to lunch... Maine was a lot of fun, thanks for keeping me company during the long drive back to Boston. Enne Emma, heb je nog wat HGF voor me??

Jos Jonkers, dank voor het vele samenwerken op de verschillende projecten. Jouw commentaar is altijd scherp en kritisch, ik zie nu al uit naar m'n verdediging... **Sjoerd** en **Tanya**, dank voor de p120 muizen! En aan alle andere NKI-ers, voor Patrick werken gaat prima hoor, waarom blijf ik die vraag steeds krijgen?

De Kops groep, onder leiding van **Geert**, de beurzen blijven maar binnen vliegen, volgend jaar een 3 miljoen dollar 'Life Sciences' prijs? **Nannette**, één van de weinigen die er al was toen ik begon en er nog steeds is. Mooi om te zien hoe enthousiast jij kan worden van andermans onderzoek, dank voor het glucosevrij medium (waarvan ik de resultaten nog niet bepaald begrijp). Ook fijn om te zien dat er meer mensen het belang van muizenonderzoek gaan inzien, daar wens ik jou en **Ajit**, veel succes mee. Laat je niet aansteken door het soms wat humeurige gedrag van sommige collega's. **Wilco**, work hard, play hard en laat de lunch maar zitten toch? **Timo**, die zuurkast is een bende, ben jij soms weer bezig geweest? **Tale**, tijdens jouw stukje moeten denk ik alle mannen in vrouwenkleren. **Livio**, jouw telefoonnummer zit onder speed-dial 1; hoe vaak het wel niet gebeurde dat de confocal niet deed wat ik wilde of dat de FACS er weer eens totaal mee kapte (gelukkig kan ik die laatste tegenwoordig zelf redelijk goed fiksen). Maar mensen draai in vredesnaam die buitennaald er weer op als je klaar bent (nee Livio, ik ben niet meer de enige die dat dingetje eraf haalt, en ik zet em er altijd weer terug op zodra ik klaar ben, echt waar!). And of course thanks to all the other members of the Kops lab for their borrels. Maar uhm **Antoinette**, maak je geen zorgen, die competente bacteriën staan al bijna in onze eigen -80°C.

De Van Rheenen groep, **Jacco**, altijd aanstekelijk enthousiast, en je harem blijft maar groeien! **Laila**, het was leuk op het NKI, achteraan gaan zitten en dan zo snel en vaak mogelijk antwoord geven op vragen van de docenten (daar was de eerste keer dat een docent tegen me zei dat ik niet hoefde te antwoorden terwijl het mijn beurt was).

Emile Voest en al zijn vrouwen (afgezien van **Marco** natuurlijk); wel apart dat je altijd naar het Stratenum komt als je weer een interview of photoshoot hebt (komt zeker door onze mooie koffiehoeke). **Jeanine**, wat leuk dat ik op je bruiloft mocht komen; samen met **Marlies** het dreamteam van Emile. Sinds jullie weg zijn, wordt er niet half zo veel bloed meer afgedraaid bij ons. **Laura**, het viel me toch tegen dat je dat infuus niet wilde zetten bij me. En **Julia** als opvolger, gaat Emile nu dan toch breken met de alleen maar artsen-AIO's traditie? **Marijn**, eens kijken wat de mensen van de 'Rubicon' gaan zeggen als je ze afwijst. Best wel een unieke situatie zo, hou me op de hoogte! **Martijn Lolkema**, met jou in de buurt valt er altijd wat te lachen. Misschien wordt het alleen wel tijd voor een 2^e (en 3^e?) telefoonlijn; en misschien een goede headset, zodat wij van je conference-calls af zijn... Voor mij blijf jij toch die gast die op de bar stond bij Dorus z'n promotie (en dat kon doen zonder z'n hoofd te stoten aan het plafond). Gelukkig heb je **Ilse** gevonden om op gelijk niveau mee te kunnen praten!

Verder wil ik de nog niet genoemde leden van mijn commissie, **Paul Coffe**, **Marc Vooijs** en **René Bernards** bedanken voor het lezen van mijn proefschrift en het opponeren tijdens mijn verdediging.

Huub, ongetwijfeld één van de meest relaxte veiligheidsfunctionarissen die er bestaat. Altijd bereid om mee te werken en te denken. Het zal mij benieuwen wat er nu weer met het viruslab gaat gebeuren. We zijn gegaan van een aggenebbis kast naar 2 kasten, nu weer één, en dan straks 3 werkplekken (in 2 kasten...). En dan over een half jaar verhuizen naar een grotere ruimte omdat het dan echt te druk wordt in dat miniatuurlabje?

Het IT gepeupel, onder leiding van **Wim**; je mag dan je eigen kantoor hebben, mijn eerste e-mail zal toch altijd naar jou gaan. Dat profiel van Eva is eindelijk weer in vorm, helaas is de mijne nog steeds veel te groot... Enne, kan iemand mij uitleggen waarom m'n e-mailadres direct wordt afgesloten op het moment dat ik uit dienst ga?

Mijn ex-studente **Judith**, nu veilig onder Benjamin's vleugel. Fijn te zien dat je goed terecht bent gekomen. Vat alles niet te persoonlijk op. Ik heb nog wel een paar CFA's die gedaan moeten worden als je tijd hebt.... **Suzan**, de ultieme student; je wist alles al, je kon alles al; menig jaloerse AIO's hebben mij nagestaard. wat leuk om jouw laudatio te mogen doen! Ik hoop snel ons stuk te hebben gepubliceerd. **Tamara**, Je hebt nooit aan mijn project gewerkt en toch voel je een beetje als mijn student...

VU-ers, **Jelle**, **Emilie**, **Ruben**, **Vicky** en **Viola**. Legendarische cocktailavondjes, kansloze disco-bowling nachten en dat achterlijke konijnen-hameren. Pukkelpop was onvergetelijk!

Arianne, Arie, ex-buuf; dank voor de avonden bankhangen, zeiken over onze projecten en de flessen wijn die er doorheen zijn gegaan in onze eerste jaren. We hebben er beiden exact even lang over gedaan om die titel te krijgen (en ook nog eens betaald gekregen tijdens het hele traject). Veel plezier met Arie en tot le Clochard.

Mijn verwaarloosde vrienden, **Amrish**, **Daan**, **Tim**, **Eelco**, **Laurens**, **Rolita**, **Danny** en al degene die ik nu vergeet; velen ben ik ondertussen uit het oog verloren, wat eeuwig zonde is. Toch hoop ik jullie nog weer eens tegen te komen. Even een update: ik heb een huis gekocht, m'n vriendin heet Stefanie en, owja, ik ben bijna gepromoveerd.

Laurie, **Yvonne**, **Martijn**, **Jan** en **Colinde**. Fijn dat jullie mij geadopteerd hebben

#

(denk dat Stefanie best wel boos was geworden als jullie dat niet hadden gedaan). Hoewel ik het als bovensloter toch wel apart vond om op mijn 28^e naar de Efteling te gaan (daar was ik sinds mijn 2^e al niet meer geweest), komend jaar weer? En dan weer dresscode: 'Black'?

Lieve **Stefanie**, ik zet jou expres niet onderaan omdat ik het altijd kotsbaar vind, van die slijmstukjes over hoe geweldig je geliefde wel niet is (en zo er tussendoor valt dan wat minder op). Je bent voor mij echt precies op tijd gekomen. Sorry voor de verwaarlozing van de afgelopen maanden, ik hoop dat ik dat nog goed kan maken, voordat jij fulltime moet gaan schrijven... Misschien kunnen we eens gaan schaatsen? Of naar de film (mag jij een leuke uitzoeken). Het lijkt me geweldig om samen met jou (voor een tijdje) naar het buitenland te gaan. **Harrie** en **Nanny**, dank dat jullie een dochter hebben gekregen! Ik moet echt eens langskomen om die Drunense duinen te zien. **Maarten**, jou wil ik ook bijzonder bedanken dat je Stefanie van jongs af aan aan computerspellen hebt laten wennen (dat scheelde mij weer een hoop moeite!). Het ergste is misschien nog wel dat zij de afgelopen tijd meer speel-uren heeft dan ik.

#

En dan nog een paar woorden voor mijn familie, de Schapen. Ik weet dat het hele "ge-ome" niet meer mag, maar het staat zo vreemd als ik het niet doe, dus daar gaan we. (**Ome** **Johan**, dank dat ik nu eindelijk een stopcontact uit elkaar durf te draaien (had ik dat niet op school horen te leren?). Ik zal m'n mond dicht houden over die elektriciteitskabel die het net niet overleefde in de woonkamer. **Ger**, nooit gedacht dat een perilex kabel door die kabelgoot getrokken kon worden. Dank voor het leren tegelen, hoewel zelfs de expert wel eens op de verkeerde plek begint... **Ome René** en **Ernst**, de feestlocatie is speciaal voor jullie uitgezocht; te herkennen aan de regenboogvlag. Mijn nichtjes **Nikki** en **Lisanne**, wat leuk dat jullie naar Utrecht zijn gekomen om de Dom te beklimmen; de plantjes doen het nog altijd goed (maar ja, vetplantjes dood laten gaan, is ook best wel moeilijk). Alle andere Schapen en Schaa-gerelateerden, ook al noem ik jullie niet allemaal (dan zou dit dankwoord nog weer 3 pagina's langer worden), jullie worden wel allemaal op 18 april verwacht in Utrecht!

Lieve **opa en oma**, wat leuk dat jullie er zijn om dit moment met mij mee te maken, sorry dat het al zo vroeg begint.

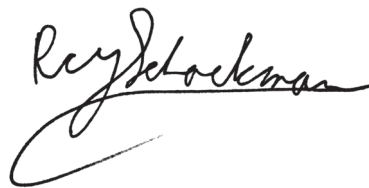
Hoi **pap en mam**, de eerste jaren dat ik met mijn promotie bezig was, leek het voor jullie net alsof ik nog thuis woonde. Niet vreemd, aangezien ik ieder weekend nog thuis kwam. Nu hebben we een huis gekocht (en er geen moment spijt van). Ik zie jullie, zoals wel meer mensen, echt niet vaak genoeg; dat schijnt bij dit werk te horen... Ik zal proberen een mooie plek uit te zoeken om te postdocen, zodat jullie meteen een vakantie adresje hebben.

Verder zou ik iedereen willen bedanken die ik nog niet heb genoemd (niks persoonlijks hoor, maar op een gegeven moment weet je echt niet meer wat je in zo'n dankwoord moet schrijven),

#

Ron Schackmann

*AKA de Schackmeister;
AKA the Shagmann;
AKA the Shagilator;
AKA Ronnie;
AKA Lonnie;
AKA lange;
etc. etc.*

A handwritten signature in black ink that reads "Ron Schackmann". The signature is written in a cursive style with a large, sweeping underline that extends to the left and then curves back under the name.